



UNIVERSITY OF  
BIRMINGHAM

**CONTROLLING DIESEL NO<sub>x</sub> & PM EMISSIONS USING  
FUEL COMPONENTS AND ENHANCED  
AFTERTREATMENT TECHNIQUES**

**DEVELOPING THE NEXT GENERATION EMISSION  
CONTROL SYSTEM**

by

**SIMARANJIT SINGH GILL**

A thesis submitted to  
The University of Birmingham  
for the degree of

**DOCTOR OF PHILOSOPHY**

School of Mechanical Engineering  
The University of Birmingham  
June 2012

UNIVERSITY OF  
BIRMINGHAM

**University of Birmingham Research Archive**

**e-theses repository**

This unpublished thesis/dissertation is copyright of the author and/or third parties. The intellectual property rights of the author or third parties in respect of this work are as defined by The Copyright Designs and Patents Act 1988 or as modified by any successor legislation.

Any use made of information contained in this thesis/dissertation must be in accordance with that legislation and must be properly acknowledged. Further distribution or reproduction in any format is prohibited without the permission of the copyright holder.

## ABSTRACT

The following research thesis focuses on methods of controlling nitrogen oxides ( $\text{NO}_x$ ) and particulate matter (PM) emissions emitted from a low temperature diesel exhaust. This involves studying the influence of hydrogen ( $\text{H}_2$ ) on various aftertreatment devices such as hydrocarbon selective catalytic reduction (HC-SCR) over silver-alumina ( $\text{Ag-Al}_2\text{O}_3$ ) catalysts for lean  $\text{NO}_x$  reduction, platinum diesel oxidation catalysts (DOC) for nitrogen dioxide ( $\text{NO}_2$ ) production and passive regeneration methods for the diesel particulate filter (DPF).

$\text{H}_2$  was implemented on-board either through diesel exhaust gas fuel reforming or via the simulation of ammonia ( $\text{NH}_3$ ) dissociation. Both methods showed to be very effective in enhancing the activity of a silver HC-SCR catalyst for the reduction of  $\text{NO}_x$  with conversions reaching 90% with the aid of an upstream DPF.

A combined DOC and catalysed DPF (cDPF) configuration proved promising for passive regeneration in the presence of reformed exhaust gas recirculation (REGR). The addition of  $\text{H}_2$  over the DOC led to an improved catalyst light-off temperature and increased rate of oxidation for  $\text{NO}_2$  production.

Implementing filtered EGR (FEGR) removes the hydrocarbon (HC) and soot recirculation penalty, thus minimising particulate growth which results in a significantly reduced engine-out soot emission during exhaust gas recirculation (EGR) and hence, an improved  $\text{NO}_x$ /soot ratio.

Introducing fuel components which enhance the cetane number and oxygenate the diesel fuel allow better control of the  $\text{NO}_x$ /soot trade-off with improved soot oxidation properties.

## **ACKNOWLEDGEMENTS**

The following thesis would have not been possible without the help, support and contribution of a number of individuals throughout the course of my study.

I would like to express my sincerest gratitude to my supervisor, Dr. Athanasios Tsolakis, for believing in my ability and providing invaluable advice, guidance and support. I would also like to thank Dr. Karl Dearn, for his advice and contribution to the publication of my review article.

Special thanks go to my fellow colleagues (friends) of the Future Power System Group, as well as Dr. Kampanart Theinnoi and Dr. Jose Martin Herreros, for their technical and moral support.

I am grateful to our colleagues at Johnson Matthey Technology Centre, Reading-UK, for the supply of the catalysts used in this research and also for their useful suggestions, advice and technical expertise throughout the experimental work. I also thank Shell Global Solutions UK, for the supply of the fuels used in this research.

I gratefully thank The University of Birmingham for the provision of a PhD scholarship and maintenance grant for the duration of my study.

Finally, and most importantly, to my family; thank you for the support, encouragement and motivation to get me through my PhD.

**Simaranjit Singh Gill**

**June 2012**

# TABLE OF CONTENTS

CHAPTER 1 .....	1
INTRODUCTION .....	1
1.1 Overview .....	1
1.2 Research Objectives and Focus .....	2
1.3 Thesis Outline.....	4
CHAPTER 2 .....	7
LITERATURE REVIEW: DIESEL ENGINE OPERATION AND EMISSIONS REDUCTION STRATEGIES .....	7
2.1 Diesel Engine Operation – Introduction.....	7
2.1.1 Compression Ignition Process .....	8
2.1.2 Overview of Diesel Emissions and Current Situation.....	11
2.2 Emission Standards – Transport Sector.....	14
2.3 Emission formation .....	16
2.3.1 CO Formation.....	16
2.3.2 NO <sub>x</sub> Formation .....	17
2.3.3 PM Formation .....	18
2.4 Emission Control Technologies .....	20
2.4.1 Exhaust Gas Recirculation .....	20
2.4.2 Aftertreatment Technologies.....	23
2.4.2.1 Diesel Oxidation Catalysts.....	24
2.4.2.2 Diesel PM Control and Regeneration Techniques.....	26
2.4.2.3 Diesel NO <sub>x</sub> Removal Catalyst Technology.....	30
2.5 On-board H <sub>2</sub> Production .....	40
2.5.1 Ammonia for High Density Hydrogen Storage and its Dissociation.....	40
2.5.1.1 On-board Storage and Supply.....	41
2.5.1.2 Effects of Ammonia on IC Engines.....	42
2.5.2 Fuel Reforming .....	44

2.5.3	Improving Diesel Emissions with H <sub>2</sub> Addition.....	47
2.6	Alternative fuels .....	50
2.6.1	Biodiesel Fuels .....	51
2.6.2	Fischer-Tropsch Diesel Fuels.....	53
2.6.2.1	Effect of Fuel Properties with F-T fuel on Engine Emissions.....	58
2.7	Additives.....	60
2.8	Summary.....	65
CHAPTER 3.....		67
EXPERIMENTAL SETUP .....		67
3.1	Test Bench Engine & Instrumentation .....	67
3.2	Data Processing .....	70
3.3	Catalysts .....	72
3.4	Liquid and Gaseous Fuels .....	74
3.5	Exhaust Gas Analysing and Measuring Equipment .....	75
3.6	Other Parameters and Equipment.....	79
CHAPTER 4.....		80
ENHANCING THE PERFORMANCE OF AN Ag-Al <sub>2</sub> O <sub>3</sub> CATALYST FOR LEAN NO <sub>x</sub> REDUCTION IN DIESEL ENGINE EXHAUSTS .....		80
4.1	Introduction .....	80
4.2	Results and Discussion .....	82
4.2.1	The effect of a DPF on the overall passive-SCR activity and NO <sub>x</sub> reduction performance .....	82
4.2.2	Active mode HC-SCR in the presence of H <sub>2</sub> and a DPF .....	85
4.2.3	The influence of NH <sub>3</sub> on the activity of an Ag-Al <sub>2</sub> O <sub>3</sub> catalyst in H <sub>2</sub> and DPF assisted conditions .....	90
4.3	Summary.....	99
CHAPTER 5.....		100
ENHANCING THE PERFORMANCE OF AN Ag-Al <sub>2</sub> O <sub>3</sub> LEAN NO <sub>x</sub> CATALYST USING ON-BOARD DIESEL EXHAUST GAS FUEL REFORMING .....		100
5.1	Introduction .....	100

5.2	Results and Discussion .....	102
5.2.1	Performance of a HC-SCR with an on-board fuel reformer .....	102
5.2.2	High load HC-SCR catalyst performance – Engine load of 5.3 bar IMEP .....	104
5.2.2.1	On-board Reforming Tests .....	104
5.2.2.2	Simulated Reforming Tests .....	115
5.2.3	Low load HC-SCR catalyst performance – Engine load of 3 bar IMEP.....	118
5.2.4	Reformer Activity .....	121
5.3	Summary.....	125
CHAPTER 6.....		127
ANALYSIS OF REFORMED EGR ON THE PERFORMANCE OF A DIESEL PARTICULATE FILTER .....		127
6.1	Introduction .....	127
6.2	Results and Discussion .....	131
6.2.1	Combustion Performance.....	132
6.2.1.1	Effects of EGR.....	132
6.2.1.2	Effects of REGR .....	132
6.2.2	Aftertreatment System Performance .....	135
6.2.2.1	Reformate Utilisation.....	135
6.2.2.2	Effects of EGR on the NO <sub>2</sub> /NO <sub>x</sub> ratio.....	137
6.2.2.3	Effects of REGR on NO <sub>2</sub> .....	139
6.2.2.4	Effect of the DOC .....	139
6.2.2.5	DPF and cDPF comparison.....	141
6.2.2.6	Pressure drop and soot loading .....	142
6.3	Extended Work – The effect of H <sub>2</sub> over the DOC.....	146
6.4	Summary.....	153
CHAPTER 7.....		155
CONTROLLING SOOT FORMATION WITH FILTERED EGR FOR DIESEL AND BIODIESEL FUELLED ENGINES.....		155
7.1	Introduction .....	155
7.2	Filtered EGR – Filtering the EGR Loop.....	155

7.2.1	Results and Discussion.....	157
7.2.1.1	Combustion and emissions performance of diesel and biodiesel (RME).....	157
7.2.1.2	Effect of filtered EGR on engine-out emissions.....	160
7.3	Full Scale Filtered EGR – Taking the EGR Loop Downstream the Aftertreatment System .....	167
7.3.1	The Effectiveness of Combining a DOC and DPF for FEGR.....	168
7.3.2	Assessing the Potential of FEGR .....	171
7.4	Summary.....	174
CHAPTER 8.....		177
DIESEL EMISSIONS IMPROVEMENTS THROUGH THE USE OF BIODIESEL OR OXYGENATED BLENDING COMPONENTS .....		177
8.1	Introduction .....	177
8.2	Results and Discussion .....	180
8.3	Summary.....	195
CHAPTER 9.....		197
CONCLUSIONS .....		197
9.1	Concluding Remarks .....	197
9.2	Future Work.....	203
LIST OF REFERENCES .....		205
APPENDICES .....		222
Appendix A: Measuring Equipment Technical Data .....		222
Appendix B: Publications and Awards to Date .....		224
	Author Publications .....	224
	Awards .....	225

## LIST OF FIGURES

Figure 1: Diesel Combustion Phases - Typical Direct Injection Heat-Release Rate Diagram ..	8
Figure 2: Overall Compression Ignition Process.....	9
Figure 3: Dec's Conceptual Model of DI Combustion during the Quasi-Steady Phase .....	11
Figure 4: European Emission Standards Comparison for, a) Diesel Passenger Cars b) Heavy-Duty Diesel Engines .....	16
Figure 5: Equivalence Ratio - Temperature Region of Diesel Soot Precursor Formation .....	23
Figure 6: Diesel Particulate Filter (Wall-Flow Monolith) [Courtesy Corning <sup>®</sup> ] .....	28
Figure 7: The Effect of Temperature on Soot Oxidation with NO <sub>2</sub> and O <sub>2</sub> [Courtesy of Johnson Matthey Plc] .....	29
Figure 8: Schematic of NAC Process, a) Lean Exhaust Gas Operation (Trapping) and b) Rich Exhaust Gas Operation (Regeneration and Reduction) [Courtesy of Johnson Matthey Plc]...	33
Figure 9: Mechanism for both H <sub>2</sub> assisted HC-SCR and NH <sub>3</sub> -SCR .....	39
Figure 10: The Transesterification Process of Triglycerides into Esters .....	52
Figure 11: F-T Technology .....	56
Figure 12: Single Cylinder Diesel Engine Test Rig .....	68
Figure 13: a) Honeycomb Monolith Substrate with the Catalyst Formulation Coated onto the Channel Walls, b) Diesel Particulate Filter .....	74
Figure 14: Example of a Mini Reactor Configuration.....	74
Figure 15: Filter Set.....	78
Figure 16: Schematic of Dissociated NH <sub>3</sub> with HC-SCR System .....	81
Figure 17: Enhancing Catalyst Performance with 8000ppm H <sub>2</sub> .....	83
Figure 18: Generalised Emission Conversion over a DPF-SCR System .....	84
Figure 19: Enhancing Catalyst Performance with 8000ppm H <sub>2</sub> and Upstream DPF.....	85
Figure 20: The Effect of HC:NO <sub>x</sub> Ratio on Catalyst Activity with 8000ppm H <sub>2</sub> .....	87
Figure 21: Catalyst NO <sub>x</sub> Reduction Activity at HC:NO <sub>x</sub> = 3 with 8000ppm H <sub>2</sub> .....	88
Figure 22: Temperature Effect on the Catalyst NO <sub>x</sub> Reduction Activity .....	89
Figure 23: The Effect of 1%NH <sub>3</sub> Mixture over the Ag-Al <sub>2</sub> O <sub>3</sub> Catalyst .....	90
Figure 24: The Effect of 2%NH <sub>3</sub> Mixture over the Ag-Al <sub>2</sub> O <sub>3</sub> Catalyst .....	91

Figure 25: Combustion Characteristics under EGR and Dissociated NH <sub>3</sub> Conditions .....	93
Figure 26: The Influence of Dissociated NH <sub>3</sub> over an Ag-Al <sub>2</sub> O <sub>3</sub> Catalyst .....	94
Figure 27: Composition of Exhaust Emission during the Addition of, a) Dissociated Mixture and            b) Dissociated Mixture with EGR .....	95
Figure 28: Observing the Influence of EGR and GHSV during the Addition of Dissociated NH <sub>3</sub> .....	97
Figure 29: Catalyst Performance during a Stop-Start Sequence .....	98
Figure 30: Schematic of an Integrated On-board Exhaust Gas Fuel Reformer with Aftertreatment Reactor .....	102
Figure 31: The Effect of Reformate Addition on the Catalyst Performance.....	107
Figure 32: The Effect of GHSV on the Catalyst NO <sub>x</sub> Conversion Performance.....	108
Figure 33: Lean NO <sub>x</sub> Catalyst Performance with On-board Integrated Fuel Reformer .....	109
Figure 34: Hydrocarbon Concentration Downstream the Lean NO <sub>x</sub> Catalyst.....	110
Figure 35: Measurable Non-active Hydrocarbon Species.....	110
Figure 36: NH <sub>3</sub> Slip Downstream Lean NO <sub>x</sub> Catalyst.....	111
Figure 37: Lean NO <sub>x</sub> Catalyst Performance over a Wide Diesel Exhaust Gas Temperature Window .....	113
Figure 38: The Effect of a Start-Stop Sequence on the Activity of a Lean NO <sub>x</sub> Catalyst .....	114
Figure 39: The Effect of a Start-Stop Sequence on the Activity of a Lean NO <sub>x</sub> Catalyst without a DPF.....	115
Figure 40: The Effect of Pure H <sub>2</sub> on the Activity of a Lean NO <sub>x</sub> Catalyst during a Start-Stop Sequence.....	116
Figure 41: The Effect of Pure H <sub>2</sub> and CO on the Activity of a Lean NO <sub>x</sub> Catalyst during a Start-Stop Sequence.....	117
Figure 42: The Effect of Pure H <sub>2</sub> and HC on the Activity of a Lean NO <sub>x</sub> Catalyst during a Start-Stop Sequence.....	118
Figure 43: The Effect of a Start-Stop Sequence during Low Load Operation on the Activity of a Lean NO <sub>x</sub> Catalyst.....	121
Figure 44: On-board Fuel Reformer Affecting the Lean NO <sub>x</sub> Catalyst Performance during 3 bar IMEP .....	122
Figure 45: Reformer Coking Affecting Lean NO <sub>x</sub> Catalyst Performance during 5.3 bar IMEP .....	123

Figure 46: Schematic of Passive DPF Regeneration with Simulated Reformate.....	130
Figure 47: DOC, DPF and cDPF Systems with overall Emission Conversions .....	131
Figure 48: The Effect of REGR on Diesel Combustion.....	134
Figure 49: Indicated Specific Fuel Consumption .....	135
Figure 50: Indicated Engine Thermal Efficiency .....	135
Figure 51: Reformate Oxidation during Combustion and over the DOC and cDPF: Reformate added to the a) Exhaust, b) Intake .....	136
Figure 52: Exhaust NO and NO <sub>2</sub> Concentrations in the Presence of a DOC .....	137
Figure 53: Exhaust NO and NO <sub>2</sub> Concentrations without a DOC .....	138
Figure 54: The Effect of the NO <sub>2</sub> /NO <sub>x</sub> Ratio in the Presence of a DOC .....	138
Figure 55: The Effect of the NO <sub>2</sub> /NO <sub>x</sub> Ratio without a DOC .....	139
Figure 56: Filter Soot Loading for each Configuration Tested .....	142
Figure 57: Pressure Drop across DOC-DPF and DPF Configurations.....	143
Figure 58: Pressure Drop across DOC-cDPF and cDPF Configurations .....	144
Figure 59: NO <sub>2</sub> Formation Over DOC: a) Effect of H <sub>2</sub> over Catalyst A, b) Effect of EGR and H <sub>2</sub> over Catalyst A and c) Effect of GHSV .....	149
Figure 60: CO and HC Oxidation - Catalyst A .....	150
Figure 61: N <sub>2</sub> O Formation over DOC - Catalyst A.....	150
Figure 62: Influence of Temperature on the Oxidation Ability of PM - Catalyst A.....	152
Figure 63: The Effect of a DOC on the Particulate Matter .....	152
Figure 64: Schematic of FEGR Setup and Sampling Locations .....	157
Figure 65: Combustion Characteristics of Diesel and Biodiesel Fuel (RME) .....	159
Figure 66: The Effect of Fuel Types and EGR/FEGR on the NO <sub>x</sub> /Soot Trade-off.....	160
Figure 67: The Effect of EGR and FEGR on Engine-out Total PM Emissions with a) Diesel and b) RME .....	161
Figure 68: The Effect of EGR and FEGR on the Engine-out Specific Emissions with a) Diesel and b) RME .....	163
Figure 69: FEGR Schematic with Emission Control .....	168
Figure 70: Effect of NO <sub>x</sub> Emissions during EGR and FEGR Compared to Pure N <sub>2</sub> EGR....	170
Figure 71: Effect of Soot Emissions during EGR and FEGR Compared to Pure N <sub>2</sub> EGR....	171

Figure 72: Particulate Mass Distribution: a) EGR and b) FEGR with DOC.....	172
Figure 73: a) Indicated Specific Fuel Consumption and b) Indicated Engine Thermal Efficiency.....	181
Figure 74: Combustion Characteristics of Neat and Blended Fuels - 3 bar IMEP.....	182
Figure 75: Engine-out Specific Emissions of Neat and Blended Fuels.....	184
Figure 76: The Effect of the NO <sub>x</sub> /Soot Trade-off: a) 3Bar IMEP, b) 5Bar IMEP.....	186
Figure 77: Particulate Size Distributions at 3 bar IMEP: a) Particulate Number, b) Particulate Mass.....	188
Figure 78: Particulate Size Distributions at 5 bar IMEP: a) Particulate Number, b) Particulate Mass.....	189
Figure 79: a) Total particle Number, b) Mean Diameter and c) Total Particle Mass.....	191
Figure 80: Correlation between VOF and SOF.....	192
Figure 81: TGA Analysis from a Loaded Filter Paper at 5 bar IMEP.....	194
Figure 82: Peak Soot Oxidation Temperature at 5 bar IMEP.....	194
Figure 83: Ag-Al <sub>2</sub> O <sub>3</sub> Optimisation Methods: In the Presence of a DPF at 250°C, GHSV of 30,000 h <sup>-1</sup> .....	198
Figure 84: Optimising the Aftertreatment System.....	201
Figure 85: Optimised Aftertreatment System 1.....	202
Figure 86: Optimised Aftertreatment System 2.....	202

## LIST OF TABLES

Table 1: Effect of EGR on NO <sub>x</sub> and PM Emissions .....	21
Table 2: Functionality of Catalyst Systems used for Diesel Oxidation Catalysts and Diesel Filters .....	26
Table 3: Lean NO <sub>x</sub> Catalysts.....	35
Table 4: Summary of Fuel Additives .....	63
Table 5: Test Engine Specifications .....	69
Table 6: Diesel and RME Fuel Properties .....	75
Table 7: TGA Heating Programme .....	78
Table 8: Exhaust Gas Composition during Dissociated NH <sub>3</sub> Addition and/or EGR.....	94
Table 9: On-board Fuel Reformer Conditions and H <sub>2</sub> Production .....	103
Table 10: Summary of Test Conditions under an Engine Load of 5.3 bar IMEP .....	104
Table 11: Average Engine-out Emissions and On-board Reformer Product Gas - Engine Load of 5.3 bar IMEP .....	105
Table 12: Summary of Test Conditions under an Engine Load of 3 bar IMEP .....	119
Table 13: Average Engine-out Emissions and On-board Reformer Product Gas - Engine Load of 3 bar IMEP .....	120
Table 14: Operating Conditions and Engine-out NO <sub>2</sub> Concentrations.....	147
Table 15: Calculated Mass per Cycle of Soot (Under Diesel Combustion).....	166
Table 16: Calculated Mass per Cycle of Soot (FEGR with DOC).....	173
Table 17: Fuel Properties.....	179
Table 18: Technical data for Horiba MEXA 7100 Analyser.....	222
Table 19: Other technical data for Horiba MEXA 7100 Analyser.....	222
Table 20: Measurements Specifications for MKS Type MultiGas Analyser.....	223
Table 21: Technical data for Horiba MEXA 1230PM Real-time Analyser .....	223
Table 22: Perkin Elmer Pyris 1 TGA Instrument Technical Data.....	224

## LIST OF NOTATIONS

<b>Symbol</b>	<b>Unit</b>	
$\dot{m}_p$	kg/s	Mass flow rate of the combustion products
$\dot{m}_r$	kg/s	Mass flow rate of the combustion reactants
$\dot{V}_i$	cm <sup>3</sup> /s	Measured intake air volumetric flow rate with EGR
$\dot{V}_o$	cm <sup>3</sup> /s	Measured intake air volumetric flow rate without EGR
$\dot{m}_{fuel}$	kg/s	Mass flow rate of the combustion fuel
$LCV_{fuel}$	MJ/kg	Lower calorific value of the combustion fuel
$LCV_p$	MJ/kg	Lower calorific value of the products
$LCV_r$	MJ/kg	Lower calorific value of the reactants
$P_b$	kW	Engine brake power
$P_{ind}$	kW	Engine Indicated Power
GHSV	h <sup>-1</sup>	Gas Hourly Space Velocity
$V_d$	m <sup>3</sup>	Displaced Cylinder Volume
N	rps	Engine Speed
$\eta_c$	%	Engine combustion efficiency
$\eta_{th}$	%	Engine thermal efficiency

## LIST OF ABBREVIATIONS

A/F	Air to Fuel Ratio
Ag-Al <sub>2</sub> O <sub>3</sub>	Silver Supported on Alumina
AgNO <sub>3</sub>	Silver Nitrate
Ag-ZSM5	Silver Supported on Zeolite
Al <sub>2</sub> TiO <sub>5</sub>	Aluminium Titanate
ATR	Auto-Thermal Reforming
bTDC	Before Top Dead Centre
BaCO <sub>3</sub>	Barium carbonate
BDC	Bottom Dead Centre
BOC	British Oxygen Company
BSFC	Brake Specific Fuel Consumption
BTE	Brake Thermal Efficiency
BTL	Biomass-to-Liquid
C	Atomic Carbon
CAD	Crank Angle Degree
CCRT <sup>®</sup>	Catalysed Continuously Regenerating Trap
cDPF	Catalysed Diesel Particulate Filter
CeO <sub>2</sub> -ZrO <sub>2</sub>	Ceria-Zirconia
CH <sub>3</sub> COO <sup>-</sup>	Acetate Anion
CH <sub>3</sub> NO <sub>2</sub>	Nitromethanes
CH <sub>4</sub>	Methane
CI	Compression Ignition
CLD	Chemiluminescence Detection
CN	Cetane Number
CO	Carbon Monoxide
CO <sub>2</sub>	Carbon Dioxide

Co-Al <sub>2</sub> O <sub>3</sub>	Cobalt Supported on Alumina
CO(NH <sub>2</sub> ) <sub>2</sub>	Urea
COV	Coefficient of Variation
CPC	Condensation Particle Counter
CPSI	Cells per Square Inch
CRT <sup>®</sup>	Continuously Regenerating Trap
CTL	Coal-to-Liquid
Cu-ZSM5	Copper Supported on Zeolite
DC	Diffusion Charging
DGM	Diglyme
DI	Direct Injection
DMA	Differential Mobility Analyser
DOC	Diesel Oxidation Catalyst
DPF	Diesel Particulate Filter
EGR	Exhaust Gas Recirculation
EOC	End of Combustion
EOI	End of Injection
EU	European Union
FAME	Fatty Acid Methyl Ester
FEGR	Filtered Exhaust Gas Recirculation
FID	Flame Ionisation Detection
F-T	Fischer-Tropsch
GC	Gas Chromatograph
GHG	Greenhouse Gas
GTL	Gas-to-Liquid
GWP	Global Warming Potential
H <sub>2</sub>	Hydrogen
H <sub>2</sub> O	Water

H <sub>2</sub> S	Hydrogen Sulphide
HC	Hydrocarbon
HC:NO <sub>x</sub>	Hydrocarbon to NO <sub>x</sub> ratio
HC-SCR	Hydrocarbon Selective Catalytic Reduction
HPL	High Pressure Loop
HTFT	High-Temperature Fischer-Tropsch
HO <sub>2</sub>	Hydroperoxyl Radicals
IC	Internal Combustion
IETE	Indicated Engine Thermal Efficiency
IMEP	Indicated Mean Effective Pressure
ISF	Insoluble Organic Fraction
ISFC	Indicated Specific Fuel Consumption
LNT	Lean NO <sub>x</sub> Trap
LPL	Low Pressure Loop
LTFT	Low-Temperature Fischer-Tropsch
MK1	Swedish Low Sulphur Environmental Classified Diesel Fuel
N <sub>2</sub>	Nitrogen
N <sub>2</sub> O	Nitrous Oxide
NAC	NO <sub>x</sub> Adsorber Catalyst
NaOH	Sodium Hydroxide
NCO	Isocyanate
NDIR	Non-Dispersive Infra-Red
NH <sub>3</sub>	Ammonia
NH <sub>3</sub> -SCR	Ammonia Selective Catalytic Reduction
NMHC's	Non-Methane Hydrocarbons
NO	Nitric Oxide or Nitrogen Monoxide
NO <sub>2</sub>	Nitrogen Dioxide
NO <sub>x</sub>	Nitrogen Oxides

O	Atomic Oxygen
O <sub>2</sub>	Oxygen
O <sub>2</sub> <sup>-</sup>	Oxygen Species
OH	Hydroxyl Radicals
PAH	Polycyclic Aromatic Hydrocarbon
PGM	Platinum Group Metal
PM	Particulate Matter
PO <sub>x</sub>	Partial Oxidation
PPM	Parts Per Million
Pt	Platinum
Pt-Al <sub>2</sub> O <sub>3</sub>	Platinum Supported on Alumina
REGR	Reformed Exhaust Gas Recirculation
Rh	Rhodium
Rh(NO <sub>3</sub> ) <sub>3</sub>	Rhodium Nitrate
RME	Rapeseed Methyl Ester
ROHR	Rate of Heat Release
SCR	Selective Catalytic Reduction
SI	Spark Ignition
SiC	Silicon Carbide
SME	Soybean Methyl Ester
SMPS	Scanning Mobility Particle Sizer
SO <sub>2</sub>	Sulphur Dioxide
SOC	Start of Combustion
SOF	Soluble Organic Fraction
SOI	Start of Injection
SOM	Soluble Organic Material
SR	Steam Reforming
TCD	Thermal Conductivity Detector

TDC	Top Dead Centre
TGA	Themogravimetric Analyser
THC	Total Hydrocarbon
TWC	Three Way Catalyst
ULSD	Ultra Low Sulphur Diesel
V <sub>2</sub> O <sub>5</sub>	Vanadium Oxide
VOF	Volatile Organic Fraction
VOM	Volatile Organic Material
WGS	Water Gas Shift

## LIST OF DEFINITIONS

Adsorption	Accumulation (attracting and retaining) of molecules and atoms of a substance on the surface of a liquid or solid
Agglomeration	The process in which primary soot particles stick together to form large groups of primary particles (agglomerates)
Air-fuel Ratio	Mass ratio of air to fuel present in an internal combustion engine
Amorphous	Solid which does not exhibit crystalline structure
Anhydrous	Substance containing no water
Aqueous Suspension	A mixture of insoluble particles in water
Auto-ignition Temperature	Temperature a fixed volume of air/fuel mixture must be heated to before an explosion will take place without an external ignition source
Calcining	To heat a substance to a high temperature below the melting point to oxidise, reduce or remove water
Catalyst	Compounds or elements that take part in speeding up the rate of a chemical reaction and lowering the activation energy
Chemiluminescence	Quantitative measurement technique to determine a substance or chemical constituent concentration emission from energised molecules
Coagulation/Coalescence	Collisions between particles during their random motions resulting in decreasing the number of particles, holding the combined mass of the two particles and larger sized particles

Condensation Particle Counter	Measures particle number concentration
Coking	The formation of hydrocarbon deposits on the catalyst surface
De-alumination	Chemical removal of alumina from a material
Decarbonisation	Remove carbon from an internal combustion engine
Decomposition	Separation of a substance into simpler substances or basic elements
Differential Mobility Analyser	Classify particles depending on electrical mobility which can be related to the particle size
Diffusion Charging Method	Method to calculate soot concentration by measuring the electrical current of ions attached to the surface of charged particles
Diffusion Membrane	Transfer of atoms or molecules through random motion from one part of a medium to another. The membrane controls what molecules can and cannot pass through
Dissociation	A reversible chemical change of the molecules of a single compound into two or more other molecules
Equivalence Ratio	Ratio of fuel to oxidiser divided by the same ratio at stoichiometric conditions
Flame Ionisation Detection	To measure concentrations of hydrocarbons within a sampled gas by burning it in an air-hydrogen flame, producing high levels of ionisation which is proportional to the number of single carbon atoms within the sample
Gas Chromatograph	Technique used to separate and analyse volatile compounds without decomposition

Lambda	Ratio of actual air-fuel ratio to stoichiometric for a given mixture
Magnetopneumatic Method	Method to measure the oxygen concentration, where the oxygen is attracted to a pulsed magnetic field creating a pressure imbalance in the flow
Non-Dispersive Infrared	Technique used to measure the volumetric concentration of specific gasses based on infra red absorption at particular frequencies
Particle Inception	Formation of particles from gas-phase reactants. Chemical and physical growth of soot precursors resulting in the formation of particle nuclei with diameters around 1-2nm
Permeability	The ability of a substance to allow another substance to pass through it
Porosity	A measure of the void (empty) space in a material
Pyrolysis	Process of thermal decomposition of organic material
Quenching Distance	The distance from the cylinder wall that the flame extinguishes due to heat losses
Reforming	To change the molecular structure of a hydrocarbon to make it suitable as a combustion fuel by heat, pressure and the action of catalysts
Regeneration (DPF)	Process of removing accumulated soot from a diesel particulate filter, either passively or actively
Sintering	Process of forming a solid or porous mass by heating a metallic powdered material without melting

Soot Precursors	Fuel pyrolysis reactions result in the formation of these compounds (e.g. acetylene 'C <sub>2</sub> H <sub>2</sub> ', polycyclic aromatic hydrocarbons 'PAH') further forming the first soot particle
Substrate	Consisting of multiple compounds that need to react together – Are essentially chemical reactants
Surfactants	Compounds which lower the surface tension of a liquid or the interfacial tension between two liquids
Thermal Conductivity Detector	A detector in a gas chromatograph that senses an increase in heat conduction ability when a gas emerges from a column

# CHAPTER 1

## INTRODUCTION

### 1.1 Overview

Interest in diesel engines has risen substantially over the past decade, with considerable focus on improved fuel-efficient vehicles with reduced carbon dioxide (CO<sub>2</sub>) emissions. Although the oxidation of HC and carbon monoxide (CO) emissions are fairly straightforward, the control of the NO<sub>x</sub> emissions during lean exhaust conditions are much more difficult, especially under low exhaust gas temperatures typical for diesel engines. Currently the legislative NO<sub>x</sub> emissions of diesel vehicles have been met through engine control methods alone. However, with future legislation limits becoming more stringent, aftertreatment NO<sub>x</sub> control will be required. There are two distinct approaches being developed. These include NO<sub>x</sub> trapping with periodic reductive regeneration and selective catalytic reduction (SCR) with ammonia or hydrocarbon.

Due to the nature of the combustion process, some carbonaceous particulate material (PM) is also formed and emitted into the exhaust. The control of such emission involves a combined strategy of engine modification (e.g. high pressure pumps, increased number of smaller injector nozzles and multiple injections) and the introduction of a diesel particulate filter to the exhaust system (Twigg, 2007). Although this has been successfully introduced, controlled filter regeneration methods are still being developed to maintain their long-term operation. As a result, further development and optimisation of the aftertreatment system is necessary to comply with future stringent emission legislation.

## **1.2 Research Objectives and Focus**

The overall aim of this work is to illustrate a strategic emission control system for a diesel engine that can effectively reduce NO<sub>x</sub>, PM, CO and HC exhaust emissions. This involves investigating methods of increasing the efficiency of low temperature diesel aftertreatment technologies that are currently available and which will be used widely in the foreseeable future. The research work presented here was undertaken to understand how the diesel oxidation catalyst, lean NO<sub>x</sub> catalyst and the diesel particulate filter could be simultaneously manipulated to control the more difficult NO<sub>x</sub> and PM emissions under lean, low temperature conditions. This knowledge should aid in developing a more effective and robust exhaust aftertreatment system for diesel engines.

The focus will be on enhancing the low temperature performance of an Ag-Al<sub>2</sub>O<sub>3</sub> HC-SCR system, a less-well-developed technique for NO<sub>x</sub> control. This considers a 2wt. % Ag on an alumina support which has been reported widely as being the most active and selective catalysts for selective catalytic reduction of NO by HC's and for having a good SCR activity at higher exhaust gas temperature. However, in this work the catalyst performance will be examined at low exhaust gas temperatures (< 300°C) in the presence of a DPF while implementing methods such as diesel exhaust gas fuel reforming to produce on-board H<sub>2</sub> rich gas to enhance the NO<sub>x</sub> reduction efficiency. Currently the DPF technology is at a stage of optimisation and cost reduction. For PM control, better catalysts and improved management methods are required. Better understanding of the catalyst-support-soot-gas interaction will lead to a more effective DPF catalyst. It is well known that a catalysed filter system will 'passively' regenerate from the reaction of NO<sub>2</sub> with carbon and is limited by the exhaust gas temperature and NO<sub>2</sub> availability. Therefore a low temperature (< 300°C) combined DOC and catalysed DPF system will be examined in the presence of H<sub>2</sub>, with the focus primarily on the

production of NO<sub>2</sub>. Further work will also be carried out to understand the ‘hydrogen effect’ over a DOC. Although various conclusions have been previously reported, it is still unclear whether the reaction mechanisms are influenced through a chemical interaction with H<sub>2</sub> or an increased rate of reaction as a result of the localised thermal effect of the H<sub>2</sub> gas (i.e. heat produced from the oxidation of H<sub>2</sub>). Overall the final result of this work will endeavour to show the most effective diesel aftertreatment system.

As the majority of the work focuses on enhancing the diesel aftertreatment catalysts and filters, techniques which introduce cleaner EGR and enhance diesel combustion will also be considered. The key objectives of this work can be broken down as follows:

- Explore options to enhance the individual aftertreatment devices under a low temperature window (i.e. < 300°C):
  - Lean NO<sub>x</sub> reduction through HC-SCR (Ag-Al<sub>2</sub>O<sub>3</sub> catalyst)
    - Feasibility of the reductant to be fuel-derived while producing on-board H<sub>2</sub> rich gas to enhance NO<sub>x</sub> reduction activity
      - The concept of reforming diesel fuel
      - Introduction of NH<sub>3</sub> dissociation
    - Minimise or control catalyst deactivation
      - Requirement of DPF to prevent carbon (soot) deposition on catalyst surface
  - DOC (platinum catalyst)/ Catalysed DPF (PGM coated)
    - Enhancing the oxidation reactions with H<sub>2</sub> through reformed EGR
      - Understanding the ‘Hydrogen Effect’
    - Promoting NO<sub>2</sub> for Passive DPF regeneration

- Explore alternative options that can reduce the stress placed on the aftertreatment systems
  - Maximising or extending the practical EGR limit
    - The impact of soot recirculation on the overall NO<sub>x</sub>/soot trade-off
  - The addition of fuel components to conventional diesel
    - Improving the properties of diesel fuel by increasing the cetane number (CN) and introducing oxygen into the fuel molecule

### **1.3 Thesis Outline**

This thesis is divided into nine chapters and a brief description of their contents is given below:

#### **Chapter 2 – Literature Review: Diesel Engine Operation and Emissions Reduction Strategies**

A concise overview of diesel emission control technologies with particular attention given to the control of NO<sub>x</sub> and PM emissions. Methods for on-board H<sub>2</sub> production as well as the use of alternative fuels and additives for improved combustion are also described.

#### **Chapter 3 – Experimental Setup**

A detailed description of the experimental engine, instrumentation and exhaust gas analysing equipment, including the type of catalysts and filters used as part of this research, is given.

#### **Chapter 4 – Enhancing the Performance of an Ag-Al<sub>2</sub>O<sub>3</sub> Catalyst for Lean NO<sub>x</sub> Reduction in Diesel Engine Exhausts**

Low temperature (< 300°C) lean NO<sub>x</sub> reduction over a Ag-Al<sub>2</sub>O<sub>3</sub> catalyst is investigated under passive control (i.e. no externally added hydrocarbons) in the presence of a simulated mixture of dissociated ammonia (1-2% NH<sub>3</sub> + 75% H<sub>2</sub> + 23-24% N<sub>2</sub>). NH<sub>3</sub> dissociation is an alternative method for on-board H<sub>2</sub> production as opposed to typical exhaust gas fuel

reforming techniques. The focus is primarily on the effect of the residual  $\text{NH}_3$  in the  $\text{H}_2$  feed and whether this could be used as a co-reductant in the HC-SCR reaction.

**Chapter 5 – Enhancing the Low Temperature Performance of HC-SCR over a  $\text{Ag-Al}_2\text{O}_3$  Catalyst using On-Board Diesel Exhaust Gas Fuel Reforming**

An integrated on-board exhaust gas fuel reformer is coupled to an  $\text{Ag-Al}_2\text{O}_3$  catalyst for lean  $\text{NO}_x$  reduction, providing a source of  $\text{H}_2$  to enhance the HC-SCR reactions. The fuel reformer is able to run effectively under diesel fuelling using the existing fuel infrastructure and waste heat of the exhaust during operation.

**Chapter 6 – Analysis of Reformed EGR on the Performance of a Diesel Particulate Filter**

The effect of REGR is investigated on the performance of passive DPF regeneration and soot deposition (i.e. pressure drop across the DPF and soot loading). This involves promoting the  $\text{NO}_2$  fraction either through combustion or catalyst interaction.

**Chapter 7 – Controlling Soot Formation with Filtered EGR for Diesel and Biodiesel Fuelled Engines**

Although EGR is an effective strategy for controlling the levels of  $\text{NO}_x$  emitted from a diesel engine, the full potential of EGR in  $\text{NO}_x/\text{PM}$  trade-off and engine performance (i.e. fuel economy) has not fully been exploited. It has previously been reported that engine operation with oxygenated fuels (e.g. biodiesel) reduces the PM emissions and extends the engine tolerance to EGR before it reaches smoke limited conditions. This work however looks into the potential of extending the EGR limits by controlling the soot and HC recirculation penalty and improving the overall  $\text{NO}_x/\text{soot}$  ratio for passive DPF regeneration.

## **Chapter 8 – Diesel Emissions Improvements Through the use of Biodiesel or Oxygenated Blending Components**

A direct comparison between biodiesel (i.e. Rapeseed Methyl Ester, RME) and a high cetane number, oxygenated fuel component referred to as diglyme (DGM) is investigated, based on their inherent oxygen availability. The primary focus is to enhance the soot oxidation properties as well as improve the combustion of diesel fuel, reducing engine-out carbon-containing species while minimising any associated NO<sub>x</sub> penalty.

## **Chapter 9 – Conclusions**

A summary of the core findings of the research are presented here, including a proposed diesel emission control system. Future research recommendations are also given.

## CHAPTER 2

# LITERATURE REVIEW: DIESEL ENGINE OPERATION AND EMISSIONS REDUCTION STRATEGIES

### 2.1 Diesel Engine Operation – Introduction

Due to its high efficiency, the diesel engine has become the most popular power-train in heavy and light duty vehicles. The realisation of high-pressure direct injection (DI) combined with modern turbo-charging techniques has completely revolutionised diesel engine technology. Over the past decade, demand for diesel passenger cars has risen significantly as a result of their high power output and high low-end torque combined with excellent fuel economy and significant noise reduction (Baumgarten, 2006). Diesel engines have inherently high thermal efficiencies, resulting from their high compression ratios and fuel lean operation. A high compression ratio is desirable, enabling the engine to extract more mechanical energy from a given mass of air/fuel (A/F) mixture due to its higher thermal efficiency. Higher ratios tend to result in better mixing and evaporation of fuel droplets by having the available oxygen ( $O_2$ ) and fuel in a reduced space along with the adiabatic heat of compression. The high compression ratio produces the high temperatures required to achieve auto-ignition and the resulting high expansion ratio minimises the thermal energy discharged to the exhaust (Heywood, 1988, Borman and Ragland, 1998, Stone, 1999). The excess  $O_2$  in the cylinders facilitates complete combustion as well as compensates for the non-homogeneity in the fuel distribution. However the predominating high flame temperatures in the presence of abundant  $O_2$  and nitrogen ( $N_2$ ) subsequently generate a large amount of  $NO_x$ . Due to the short time

available for mixture formation, the A/F mixture always consists of fuel-rich and lean regions, and thus it is strongly heterogeneous (Borman and Ragland, 1998).

### 2.1.1 Compression Ignition Process

Due to the increasing gas temperature during compression, the combustion process is initiated by auto-ignition. The start of combustion is controlled by the injection timing, and the desired engine torque is adjusted by the amount of fuel injected per cycle. The rate of heat release (ROHR) analysis presented in Figure 1 shows the typical diesel combustion phases of a 4-stroke cycle compression ignition (CI) engine.

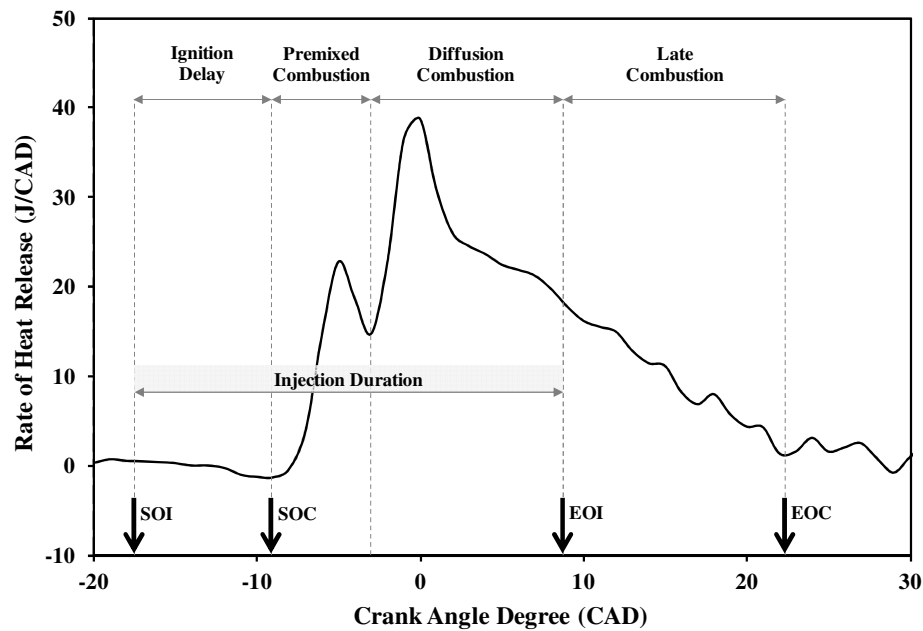


**Figure 1: Diesel Combustion Phases - Typical Direct Injection Heat-Release Rate Diagram**

As the piston moves towards top dead centre (TDC), the compression increases the in-cylinder pressure and as a result heats up the air charge to a temperature above the fuel ignition point. In a DI diesel engine, the fuel is injected into the hot compressed air inside the combustion chamber. At the start of conventional single injection (near the end of the compression stroke), the fuel begins to penetrate into the combustion chamber where high

temperature air is entrained into the spray. The first step towards ignition involves transitioning from a liquid to a gas phase. The time required for this transition is the ‘physical delay’ in ignition, which includes the time required for a droplet of fuel to heat, vaporise and mix with hot air in the cylinder. For ignition to occur, the fuel must be heated to a temperature sufficient to break the weaker bonds and form radicals. The finite rate of these radical forming oxidation reactions is responsible for the chemical delay in compression ignition engines. Once sufficient concentration of free radicals is reached, rapid oxidation occurs (ignition). The role of physical and chemical fuel properties in the compression ignition process is summarised in Figure 2 [adapted from (Murphy et al., 2004)].

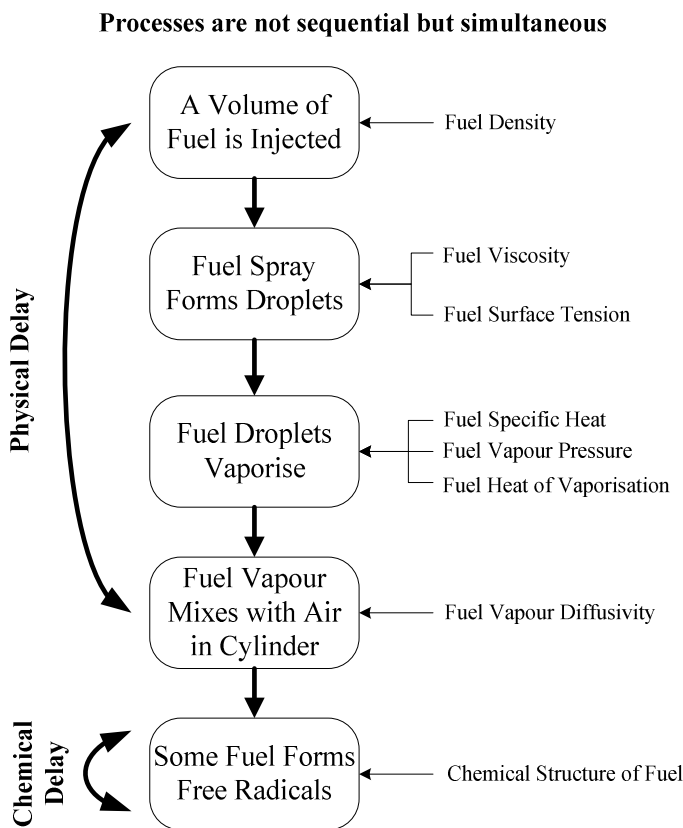


**Figure 2: Overall Compression Ignition Process**

As the piston continues to move closer to TDC, the A/F mixture temperature reaches the fuel’s ignition temperature and begins spontaneously to auto-ignite, causing ignition of some

premixed quantity of fuel and air. The balance of fuel that had not participated in the premixed combustion is consumed in the rate-controlled diffusion combustion which extends into the expansion stroke (i.e. late combustion). The initial part of the fuel oxidation process occurs in the fuel-rich mixture region beyond the lift-off length. The products of the rich combustion then pass downstream and diffuse radially outward until reaching the surrounding cylinder gases. The final oxidation process takes place around the periphery of the jet as a diffusion flame illustrated by Dec's conceptual model in Figure 3 [adapted from refs; (Argachoy and Pimenta, 2005, Dec, 1997, Mueller et al., 2003)]. The diffusion flame surrounds the jet in a thin turbulent sheet extending upstream towards the nozzle. Nitric oxide (NO) forms on the lean side of the diffusion flame, while soot forms throughout the jet cross-section, primarily due to the products of rich-ignition (Kitamura et al., 2002, Argachoy and Pimenta, 2005).

The ignition delay can be defined as the start of fuel injection (SOI) in the combustion chamber until the A/F mixture is on the verge of auto-igniting (i.e. start of combustion – SOC). During this phase the fuel absorbs part of the heat release, resulting in an endothermic process before combusting. The end of injection (EOI) defines the end of the diffusion phase and the beginning of late combustion. Once the heat release rate falls towards zero, the combustion process can be said to be completed (i.e. end of combustion – EOC). The heat released during late combustion may be the result of any remaining unburnt fuel and/or combustion of by-products (i.e. from incomplete combustion) allowing for more complete combustion. Although the in-cylinder temperature is successively reducing, the expansion stroke can result in mixing within the cylinder. Before bottom dead centre (BDC) is reached the gasses are then expelled from the combustion chamber.

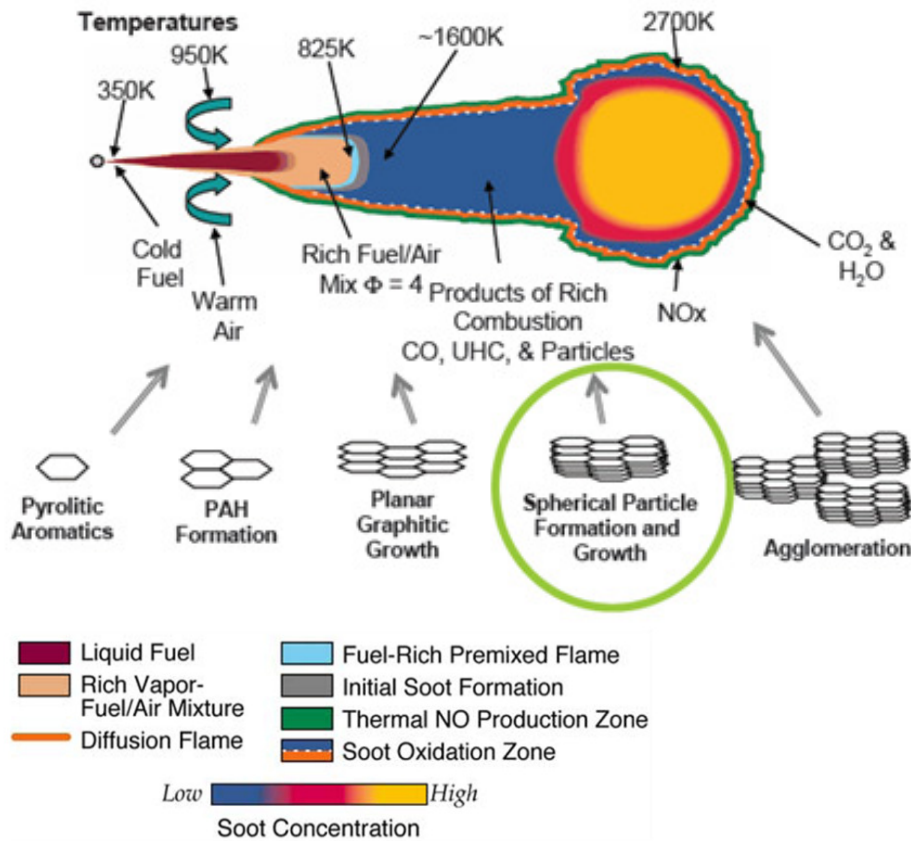


Figure 3: Dec's Conceptual Model of DI Combustion during the Quasi-Steady Phase

### 2.1.2 Overview of Diesel Emissions and Current Situation

The challenge for CI diesel engines lies primarily on the control of the three pollutant phases emitted from the exhaust. This is much more complicated than the control of gas phase emissions from spark ignition (SI) gasoline engines. In a diesel engine, the resulting exhaust gas contains a large amount of  $O_2$ , thus three-way catalysts (TWC), which rely primarily on a stoichiometric mixture cannot be employed as a balance of pollutants is required in the exhaust in order to carry out both oxidation and reduction reactions (York et al., 2010). The emissions from a diesel engine are composed of gaseous pollutants and PM. The particulates are a combination of soot and other liquid or solid phase materials that are collected once exhaust gases are passed through a filter medium below  $52^\circ C$  (EPA) or  $47^\circ C$  (EC) and are responsible for the black smoke associated with diesel powered vehicles. Soot (referred to as

the insoluble dry fraction), mostly clusters of solid carbon particles are formed from the unburned fuel, nucleating from the vapour to solid phases in the fuel-rich regions during combustion (Ganesan, 2008). Depending on the local conditions, the hydrocarbons may then condense on or be adsorbed by the soot forming soluble liquid or solid phase materials. The liquid HC (i.e. the heavier component of the HC emission) present in the PM are a combination of unburned diesel fuel and evaporated lubricating oil which appear as soluble (soluble organic fraction, SOF) or volatile organic compounds (volatile organic fractions, VOF) in the exhaust which tend to adsorb onto the dry carbon particles (Tree and Svensson, 2007, Kennedy, 1997).

The main constituents which make up the gaseous phase are the HC (i.e. the lighter component of the HC emission), CO, oxides of nitrogen (NO, NO<sub>2</sub>; etc) and sulphur dioxide (SO<sub>2</sub>) (Farrauto and Voss, 1996, Vaaraslahti et al., 2006). SO<sub>2</sub> emissions from internal combustion engines are solely a result of fuel-bound sulphur and are readily reduced by limiting sulphur in the fuel. HC's are divided into reactive and nonreactive categories, based upon their role in photochemical smog formation. The simplest such breakdown is categorising HC's as methane (CH<sub>4</sub>) and non-methane hydrocarbons (NMHC's), since all HC's except for CH<sub>4</sub> will react given sufficient time. Actual emissions vary greatly on engine design, fuels combusted, and combustion and post-combustion controls involved. Few of the factors affecting air pollutant emissions include: ignition and valve timing, fuel types and additives combusted, lubricants employed in the engine, and exhaust gas treatments employed.

Although the diesel engine is an attractive solution for CO<sub>2</sub> reduction, there remains a challenge to control simultaneously NO<sub>x</sub> and PM emissions to a level required by prevailing regulations (Kitano et al., 2005, Abu-Jrai et al., 2006). Unfortunately, if the diesel combustion

system is not well controlled, it can produce higher levels of PM and/or NO<sub>x</sub>. PM, which is composed of soot and sulphate bound with water and unburned oil and fuel, can have associated health issues. NO<sub>x</sub>, which is formed by oxidation of atmospheric and/or fuel contained nitrogen at high temperatures in the power cylinder, is capable of producing smog and acid rain, therefore polluting waterways and crops (McGeehan et al., 2005).

Since NO<sub>x</sub> and PM emissions from current diesel technologies are close to the limits permitted by regulations and both limits will become more stringent in the near future; these two emissions will be critical factors in the development of new diesel engines. An improved knowledge of the potential to reduce these types of emissions could help engine manufacturers adapt their engines to the use of biofuels and to optimise them. This can be done by readjusting the compromise between efficiency, costs and emissions within the regulation limits (Lapuerta et al., 2008a). However as engines are currently calibrated to be as efficient as possible while complying with the emission standards, there still stands a trade-off between the emissions performance and efficiency. Among other solutions to reduce both NO<sub>x</sub> and PM such as REGR, SCR catalysts, and DPF's, alternative fuels like bio-fuels and designed fuels such as Fischer-Tropsch (F-T) diesel fuels appear to be the feasible short term solution (Abu-Jrai et al., 2006). There are two strands to the European Legislation which promote the use of biofuels, namely article 7bis of the Fuels Quality Directive and the Renewable Energy Directive. The European directive 2009/30/EC was adopted to revise the Fuel Quality Directive 98/70/EC. Apart from establishing the target aiming to satisfy 10% of its transport fuel needs from renewable sources, it introduces a requirement of fuel suppliers to reduce the greenhouse gas (GHG) intensity of energy supplied for road transport in article 7bis (EC 2009a). The European Union (EU) Renewable Energy Directive sets out a path targeting 15% of energy from renewable sources by 2020 (RES 2009).

With ongoing improvements aimed at enhancing performance and reducing noise and emissions, the diesel engine has become an increasingly attractive option for passenger car applications. Over the past years, stringent emission legislations have been imposed to regulate emissions such as NO<sub>x</sub>, smoke and PM emitted from automotive diesel engines worldwide.

## **2.2 Emission Standards – Transport Sector**

The geographical focus of regulatory development is now the EU, where Euro 6 regulations for light duty vehicles have been finalised for implementation in 2014. Under the framework of the European Climate Change Programme, the European Commission set a goal of reducing CO<sub>2</sub> emissions from new passenger cars and light commercial vehicles. A fleet-average CO<sub>2</sub> emission target of 130g/km for new passenger cars must be reached by each vehicle manufacturer by 2015, using vehicle technology under the Regulation 443/2009/EC. However to meet the EU CO<sub>2</sub> target of 120g/km, a further 10g/km is to be provided through additional measures such as biofuels (EC 2009c). The proposed legislation to reduce the CO<sub>2</sub> emissions from light commercial vehicles [COM (2009) 593] introduces a fleet-average CO<sub>2</sub> emission target of 175g/km fully phased-in by 2016. This regulation is applicable to vehicles category N<sub>1</sub> (light commercial vehicles) with a reference mass not exceeding 2610kg (EC 2009b).

Euro 6 stage has been adopted at the same time as Euro 5, but will lay down significantly lower limits for NO<sub>x</sub> emissions from diesel cars (2009b). The Euro 6 Stage European emission regulations for light passenger and commercial vehicles were introduced by Regulation (EC) No. 715/2007 later amended by the Commission regulation (EC) No. 692/2008 of July 2008. All vehicles equipped with a diesel engine will be required to reduce

substantially their emissions of NO<sub>x</sub> for the Euro 6 regulation to be introduced on 1<sup>st</sup> September 2014 for the approval of vehicles, and from 1<sup>st</sup> January 2015 for the registration and sale of new types of cars. The NO<sub>x</sub> emissions from passenger cars and light commercial vehicles (category N<sub>1</sub>, class I) intended to be used for transport will be capped at 80mg/km, an additional reduction of more than 50% compared to the Euro 5 standard (2009a). Other regulated emissions, such as the control of CO and total hydrocarbon (THC), although not in engines, will probably be required to meet future limits as a result of developments in aftertreatment systems. This is especially the case if low-temperature combustion modes are used (for example late/early injection, high EGR ratios etc), reducing the high peak temperature regions in the combustion chamber therefore resulting in more homogeneous burning. In the case of PM, Euro 6 will not reduce the emissions compared to the levels imposed by Euro 5, but the latter has already forced manufacturers to introduce DPF in vehicles. Inversely, the NO<sub>x</sub> aftertreatment techniques associated with heavy-duty diesel have already been implemented in order to meet the Euro V limits, while Euro VI will mainly imply an effort to reduce PM emissions. European emission regulations for new heavy-duty engines, which generally include trucks and buses, were introduced by Regulation 595/2009, published in July 2009.

It is worth noting that for passenger and light commercial vehicles, the standards are defined in mg/km, while for heavy duty vehicles they are defined by engine power, mg/kWh, and are therefore not directly comparable. Figure 4 gives an overview of the European emission standards which stage the progressive introduction of increasingly stringent standards (Rodríguez-Fernández et al., 2009a, Gill et al., 2011b).

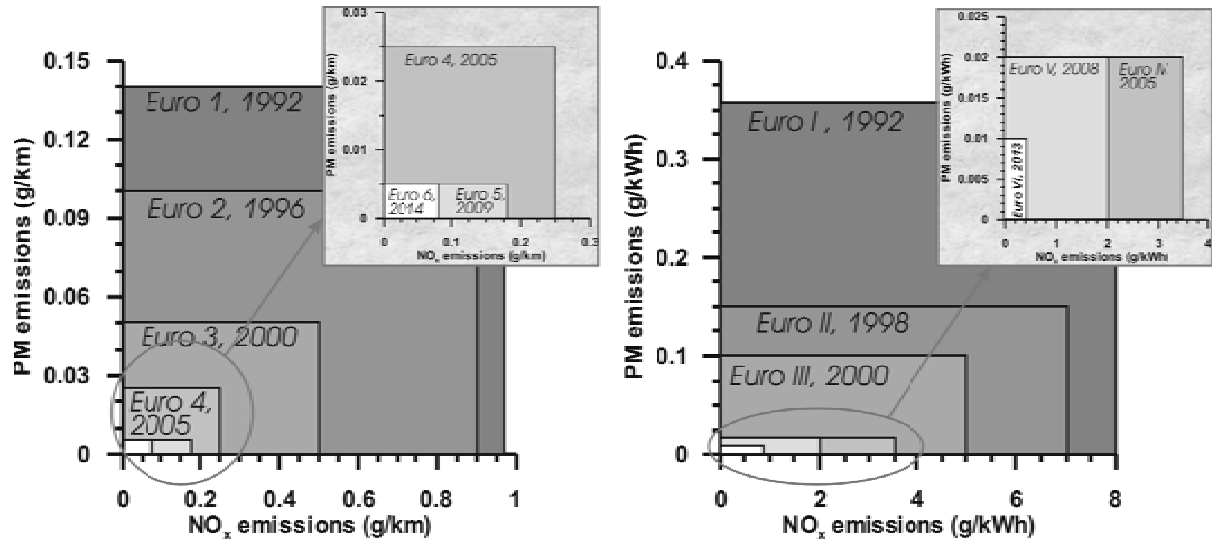


Figure 4: European Emission Standards Comparison for, a) Diesel Passenger Cars b) Heavy-Duty Diesel Engines

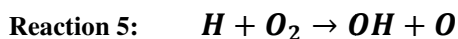
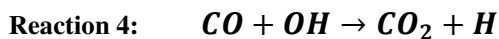
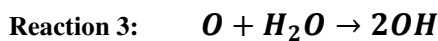
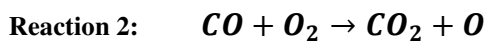
## 2.3 Emission formation

### 2.3.1 CO Formation

The formation of CO emissions from the combustion of a hydrocarbon radical, R, is as follows (Bowman, 1975):



Once CO has formed, it is slow to oxidise to CO<sub>2</sub> through the following steps:

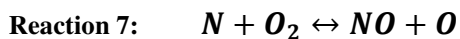
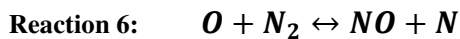


It should be noted that water provides one of the primary oxidant sources for the reaction. As Reaction 2 is slow the primary oxidation of CO occurs through Reaction 4, while Reaction 5 continuously produces the hydroxyl radicals (OH) for this to take place.

### 2.3.2 NO<sub>x</sub> Formation

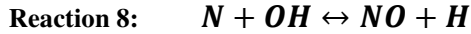
NO<sub>x</sub> is referred to here as mixtures of NO and NO<sub>2</sub>. These specific emissions need to be controlled because of their contribution to the formation chemistry of low-level ozone, or smog, an environmental and human health hazard. Both gases are considered toxic; but NO<sub>2</sub> has a level of toxicity five times greater than that of NO and is also directly of concern as a human lung irritant. While NO and NO<sub>2</sub> are lumped together as NO<sub>x</sub>, there are some distinctive differences between these two pollutants. NO is a colourless and odourless gas, while NO<sub>2</sub> is a reddish brown gas with pungent odour (Levendis et al., 1994). NO<sub>x</sub> can also be defined to include other oxides of nitrogen, including nitrous oxide (N<sub>2</sub>O). These nitrogen oxide species have a lower global warming potential (GWP), are insignificant in the emissions from internal combustion engines, and readily react to form NO and NO<sub>2</sub>. NO generally accounts for over 90% of the total NO<sub>x</sub> emissions from fossil fuel combustion, with the remainder being NO<sub>2</sub>. The formation of NO can be explained through the following mechanisms and can take place during both the premixed and diffusion phases (Heywood, 1988, Turns, 2000):

The Extended Zeldovich mechanism (or thermal NO) in which the atomic oxygen, hydroxyl radicals and N<sub>2</sub> are in equilibrium concentrations. The primary pathway for NO formation is oxidation of atmospheric molecular N<sub>2</sub>:

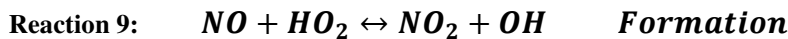


The NO formation chain reactions are initiated by the atomic oxygen, which forms from the dissociation of O<sub>2</sub> molecules at the high temperatures reached during the combustion

process. Extending the thermal NO formation mechanism to include the hydroxyl radical reaction with nitrogen was proposed by Lavoie et al. (1970):



Thermal NO formation rate is slow relative to combustion and is considered unimportant below 1800K. Thermal NO formation attributed to Reaction 6 through Reaction 8 is considered to be formed in the post-combustion exhaust gases. The final reaction mechanism considered here for NO<sub>x</sub> formation is the production of NO<sub>2</sub> in the flame zone. Reactions contributing to the formation and destruction of NO<sub>2</sub> are as follows:



The hydroperoxyl (HO<sub>2</sub>) radicals form in the low temperature regions, leading to NO<sub>2</sub> formation through Reaction 9. However, at high temperatures the NO<sub>2</sub> destruction can proceed via the reactions described in Reaction 10 and Reaction 11 with active H and O radicals. Thus during high temperatures, the majority of the NO<sub>x</sub> emitted from internal combustion engines is in the form of NO.

### 2.3.3 PM Formation

Diesel particulates have bimodal distribution, a mixture of ‘nuclei’ and ‘accumulation’ mode particles. The nuclei mode particles are commonly referred to as nanoparticles, defined as particles below 50nm and are usually volatile precursors as the exhaust gas dilutes and cools. The accumulation mode particles are formed by agglomeration of primary carbon

particles with adsorbed gasses (condensed heavy hydrocarbons) and are defined as particles in the range of 50nm and 1000nm (Kittelson, 1998).

Primary particles are formed during the early stages of soot formation and can grow by two mechanisms, either by collision coagulation (physical process) or by surface growth (chemical process) during the diffusion phase combustion. After the growth of the primary particles, they will undergo collisions which will result in the agglomeration process (formation of clusters), thus resulting in the final soot agglomerate (Kennedy, 1997). The processes of soot growth are illustrated alongside Dec's model in Figure 3. It is evident that the fuel goes through two oxidation processes, with the first at the fuel-rich premixed zone and the second at the diffusion flame at the periphery. PAH's, considered as the main soot precursors, are formed in the fuel-rich premixed zone, growing in the centre due to surface growth with a portion being oxidised in the diffusion flame.

The formation of soot as described in the work of Richter and Howard (2000) begins with the formation of the first aromatic ring structure (i.e. from the decomposition of the fuel molecule) followed by subsequent polycyclic aromatic hydrocarbon (PAH) growth (i.e. molecular precursors) and particle inception/nucleation steps. The bulk of the soot yield is generated by surface growth processes which proceed directly after nucleation. This process involves the attachment of gas phase species (i.e. acetylene and PAH) to the surface of the particles increasing the overall mass but not affecting the number of soot particles. The elementary particles serve as nuclei while the heavy hydrocarbons can be chemically or physical adsorbed either during diffusion combustion or in the exhaust stroke. This is then followed by particle coagulation, where there are collisions between the particles resulting in an increase in the average particle size (through the increase in the number of primary particles which forms the aggregates) and decreased particle number without increasing the

total mass of soot (Richter and Howard, 2000). However during pyrolytic conditions in the post-flame zone, the amorphous soot material will progressively convert to a more graphitic carbon material as shown in the work of Richter and Howard (2000), resulting in a small decrease in particle mass but no change in particle number. The oxidation of the PAH and soot particles is also limited as it is always competing with the formation of these particular species.

## **2.4 Emission Control Technologies**

Technologies such as EGR, soot traps and exhaust gas aftertreatment are essential to cater to the challenges posed by increasingly stringent environmental emission legislations.

### **2.4.1 Exhaust Gas Recirculation**

EGR has been a key strategy in controlling  $\text{NO}_x$  formation, influencing the thermodynamic properties and the oxygen concentration of the cylinder charge whilst keeping minimum degradations in power and efficiency. Apart from the reduction in  $\text{O}_2$  availability, the effect of adding  $\text{CO}_2$ , water vapour ( $\text{H}_2\text{O}$ ) and  $\text{N}_2$  through the use of EGR reduces the flame temperature while increasing the overall heat capacity of the cylinder charge (Zheng et al., 2004, Abd-Alla, 2002). Thus EGR decreases the temperature rise for the same heat release in the combustion chamber. For a given torque and power output, the amount of fuel injected into the cylinder must stay constant and as a result the engine operates at a lower effective A/F ratio, substantially affecting the exhaust emissions (Ladommatos et al., 2000).

In the work of Ladommatos (1996a) and Zhao (2000), it was concluded that the majority of the  $\text{NO}_x$  reduction from  $\text{CO}_2$  was primarily the result of the dilution effect (i.e. a reduction in oxygen mass fraction) with a minor contribution due to a chemical and thermal effect (i.e. heat consumed during endothermic reactions such as the dissociation of  $\text{CO}_2$  and

H<sub>2</sub>O). Table 1 gives a general overview of the dilution, chemical and thermal effects of EGR (Ladommatos et al., 2000).

**Table 1: Effect of EGR on NO<sub>x</sub> and PM Emissions**

EGR Effect	Species	Result of....	Effect on NO <sub>x</sub>	Effect on PM
Dilution	O <sub>2</sub>	Reduction in O <sub>2</sub> availability	Decrease 80-90%	Increase 80-90%
Chemical	CO <sub>2</sub>	Thermal dissociation and its products participate in combustion	Decrease 5-10% <sup>*1</sup>	Decrease 5-10% <sup>*1</sup>
	H <sub>2</sub> O			Increase 5-10% <sup>*1</sup>
Thermal	CO <sub>2</sub>	Higher specific heat capacity than O <sub>2</sub> and N <sub>2</sub>	Decrease < 5% <sup>*1</sup>	Minor
	H <sub>2</sub> O			
Inlet Temperature <sup>*2</sup> (Hot EGR)	-	Increased inlet charge temperature and reduced volumetric efficiency	Increase <sup>*3</sup>	Increase <sup>*3</sup>

\*1 Dependant on engine mode

\*2 At constant charge mass flow rate and charge composition

\*3 Proportional to inlet charge temperature

Employing EGR, although effective in reducing NO<sub>x</sub> formation aggravates the prevailing PM/NO<sub>x</sub> trade-off, especially under higher load where diesel combustion tends to generate more smoke because of the fuel rich pockets struggling to find oxygen at the late stages of combustion (Zheng et al., 2004). The formation of soot appears in the diffusion flame following sequential growth and coagulation steps. Earlier studies have demonstrated that uncharged radicals and molecules are the flame nucleation precursors (Hall-Roberts et al., 2000), with surface growth promoted by the addition of gaseous carbonaceous species. Thus the particles are subjected to collision and sticking mechanisms coagulating into aggregates as the combustion gas is cooled (Stanmore et al., 2001). Others have also reported that the coagulation of metallic ash particles, and heterogeneous nucleation of PAH and carbon soot on the metallic ash particles may also have a minor influence on PM formation with EGR (Graskow et al., 1998, Ristovski et al., 2000). It is also well known that the presence of soot

can actually promote the heat transfer rates of the combustion system (i.e. radiative heat transfer) during the formation and oxidation processes (Farias et al., 1998, Chang and Rhee, 1983). As a result this will reduce the gas temperatures and hence soot burn-up.

Soot derived from oxygenated fuels such as biodiesel carries some surface oxygen functionality and thereby possesses higher reactivity than soot from conventional diesel fuel (Song et al., 2006). In addition it has been reported that combustion of oxygenate fuels, such as biodiesel, allow a greater engine tolerance to EGR as a result of the oxygen enrichment which leads to reduced PM/smoke recycled back into combustion chamber (Tsolakis, 2006). The corresponding increase in PM introduced by EGR calls for further emission controls to be introduced to meet forthcoming stricter regulations, especially as a result of their environmental and human health effects.

$\text{NO}_x$  and soot formation in hydrocarbon combustion depends strongly on the equivalence ratio (fuel/air ratio) and temperature (Pickett et al., 2006). Figure 5 [adapted from refs; (Johnson, 2008, Kamimoto and Bae, 1988, Kitamura et al., 2002)] shows the equivalence ratio-versus-temperature plot for a diesel-like fuel with contours indicating the regions of high soot formation in fuel-rich mixtures and regions of high  $\text{NO}_x$  formation at high temperature. The soot contours are soot yield, the percentage of fuel carbon formed into soot. The arrow shows the predicted path, after ignition, of a typical diesel fuel spray moving from fuel-rich regions to a near-stoichiometric diffusion flame.

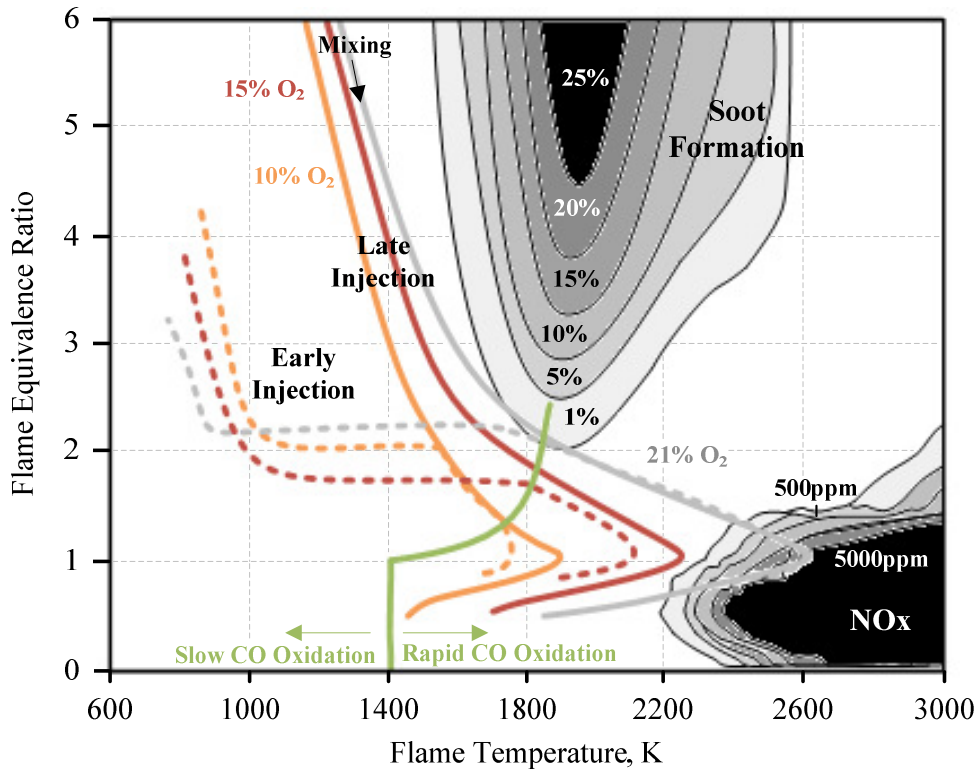


**Figure 5: Equivalence Ratio - Temperature Region of Diesel Soot Precursor Formation**

The reduced  $O_2$  concentrations simulate the effect of various levels of EGR in an engine. Soot and  $NO_x$  are inhibited using high EGR levels with either early (highly premixed) fuel injection or late injection. In early injection strategies, much of the fuel charge is mixed with gas before ignition, hence avoiding the conditions for soot formation. However the  $NO_x$  formation regime is avoided by implementing high levels of EGR, which keeps the flame temperature lower. With late injection strategies, the charge is mixed and simultaneously burned. Thus the combination of good mixing and high EGR helps the charge avoid the soot and  $NO_x$  regimes (Johnson, 2008).

#### 2.4.2 Aftertreatment Technologies

Aftertreatment technologies including SCR, lean  $NO_x$  trap (LNT), DOC and DPF have been introduced in order to reduce significantly both  $NO_x$  and PM emissions to meet new regulations. Usually a combination of catalysts is required for the simultaneous removal of all

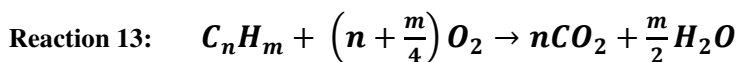
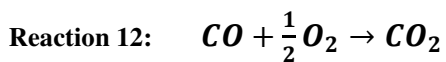
pollutants. Diesel exhaust gas aftertreatment can be divided into three categories (York et al., 2010):

1. Oxidation catalysts – HC and CO oxidation
2. Catalysts and filters – Trapping of PM including soot oxidation strategies
3. Catalysts for NO<sub>x</sub> abatement

The most common catalyst structure makes use of a ceramic monolith honeycomb with a thin layer (high surface area typically about 100m<sup>2</sup>/g) of catalytically active material to the channel walls. The monoliths are often formed from a ceramic material known as cordierite (2MgO.2Al<sub>2</sub>O<sub>3</sub>.5SiO<sub>2</sub>) with a typical 400 channels in<sup>2</sup>. Cordierite has a low coefficient of thermal expansion and as a result can withstand the high heating rates of the exhaust gas (Twigg, 2007, York et al., 2010). Platinum group metals for instance are compatible with cordierite and can be directly applied to the ceramic monolith without the need of a transition metal oxide carrier or washcoat layer.

#### 2.4.2.1 Diesel Oxidation Catalysts

CO, gas phase HC and the organic fraction of diesel particulates can be controlled over the catalyst to form harmless products through the following reactions. This includes the HC derived emissions of aldehydes and PAH's:



Additionally oxidation of NO to NO<sub>2</sub> as shown in Reaction 14 is another reaction which occurs over the DOC. Interest in NO<sub>2</sub> has been attributed to facilitate passive DPF regenerations as well as enhance the performance of some SCR catalysts.



The active catalytic sites have the function of adsorbing  $O_2$ , thus are the key to the reaction mechanism. In general the catalytic oxidation mechanism consists of oxygen being bonded to the catalytic sites; reactants of CO and HC diffuse and react with the surface oxygen forming reaction products of  $CO_2$  and  $H_2O$ . The DOC can also participate in small  $NO_x$  reductions, however as this is typically low and occurs within a very narrow temperature window it is suggested that some of the engine-out  $NO_2$  may be utilised for the oxidation of the accumulated soot within the catalyst itself (York et al., 2010). Table 2 [adapted from refs; (Majewski, Revised 2010.04, Twigg, 2007, Johansen et al., 2007)] gives an overview of some of the catalytic components that have been reported in literature. With increased availability in low sulphur fuels, platinum (Pt) has become the catalyst of choice for commercial filters (i.e. catalysed DPF's) as well as DOC's. However the level of  $NO_2$  formation over platinum has called for research into alternative coatings, especially as  $NO_2$  is more toxic than NO. Currently novel base metal-palladium catalytic coatings have proven to be comparable to current platinum-based coatings at a lower cost while also having the ability to remove  $NO_2$  within a wide temperature range and limit the overall formation of  $NO_2$  (Johansen et al., 2007).

**Table 2: Functionality of Catalyst Systems used for Diesel Oxidation Catalysts and Diesel Filters**

Functionality	Catalytic Components	Comments
Oxidation of gases and SOF	Noble Metals (e.g. Pt, Pt/Pd)	<ul style="list-style-type: none"> <li>• High Pt loading at typical diesel exhaust temperatures to promote CO and HC oxidation</li> <li>• Production of sulphate particulates</li> <li>• Increased levels of NO<sub>2</sub></li> </ul>
Cracking and/or oxidation of SOF	Base Metals (e.g. Ceria)	<ul style="list-style-type: none"> <li>• Often include low loaded Pt</li> <li>• Can be used for PM emission control</li> <li>• Low activity for the oxidation of CO and HC</li> <li>• Produce little sulphate particulates and/or NO<sub>2</sub></li> </ul>
Washcoat Storage of HC's	Zeolite	<ul style="list-style-type: none"> <li>• Used for HC trapping</li> <li>• Added to DOC washcoat for cold start improvement</li> </ul>
Lean NO <sub>x</sub> Activity	Platinum	<ul style="list-style-type: none"> <li>• Limiting low temperature range</li> <li>• Not commercially available</li> </ul>
NO <sub>2</sub> Emission Control at Low Temperatures	Novel Base Metal-Palladium Coatings	<ul style="list-style-type: none"> <li>• Ability to react NO<sub>2</sub> with soot or carbon monoxide under a temperature window of 180-330°C</li> <li>• Limited NO<sub>2</sub> formation above 330°C</li> <li>• Soot combustion with HC/CO conversion properties comparable to Pt-based coatings</li> </ul>

#### 2.4.2.2 Diesel PM Control and Regeneration Techniques

In the case of diesel engines, the control of soot emissions is based on a filtration system. Currently the most successful and widely used PM emission control device is the wall flow filter, also known as a DPF. They are typically constructed from cordierite, silicon carbide (SiC), or aluminium titanate (Al<sub>2</sub>TiO<sub>5</sub>) (York et al., 2010). This is a honeycomb

structured device (i.e. similar to a catalyst substrate but with the channels blocked at alternate ends) consisting of ordered square channels through which the diesel exhaust gas permeates into the walls as shown in Figure 6, trapping the soot particles within the porous wall as well as over the inlet channel surfaces (Matti Maricq, 2007). The DPF is the most effective way of reducing not only the mass but also the number of emitted particles with filtration efficiencies as high as 95-98% once a layer of soot begins to stabilise within the monolithic channels (Johansen et al., 2007).

The filters can either be bare or have a platinum catalyst coat added onto the walls of the monolith material in the form of a washcoat, leading to a thin, porous catalyst layer (30-150 $\mu$ m); this is the basis of the Catalysed Continuous Regenerating Trap (CCRT<sup>®</sup>) (York et al., 2010). The main purpose of the catalyst coating is to assist soot burning, either by promoting NO<sub>2</sub> formation or by catalysing the oxidation of soot, thus lowering the soot combustion temperature and allowing the filter to self-regenerate at moderate exhaust temperatures, minimising the fuel penalty (Johansen et al., 2007). Although catalysts have been proposed for the oxidation of soot, there still stands a major problem with regards to the interaction between the soot and the catalysed monolith channel. A poor contact between the soot and the catalyst (commonly referred to as 'loose contact') results in a low oxidation activity and thus limits the soot reduction efficiency (Neeft et al., 1997). It is believed that catalysts such as copper (Cu), potassium (K) and molybdenum (Mo) contain mobile catalytic species that are likely to resemble 'tight contact' (an increased contact between the soot and catalyst). Although platinum based catalysts do not contain mobile catalytic species, it has been reported that they are active under a different mechanism promoting NO<sub>2</sub> for low temperature soot oxidation (Cooper and Thoss, 1989, Neeft et al., 1997).

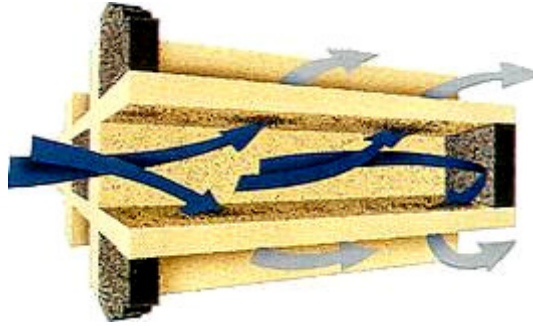


**Figure 6: Diesel Particulate Filter (Wall-Flow Monolith) [Courtesy Corning<sup>®</sup>]**

To maintain the long-term operation of the filters, an efficient process to remove the filtered PM is required to prevent an increased back pressure which can lead to a higher fuel penalty, reduction of available torque and incomplete regeneration during stop-start journeys (Yamamoto et al., 2009). There are subsequently two types of regeneration processes, commonly referred to as passive regeneration, a continuous process or periodic active regeneration. However both approaches can be simultaneously implemented. In a passive system, under a temperature range of 200-450°C, small amounts of NO<sub>2</sub> will promote the continuous oxidation of the deposited carbon particulates. This is the basis of the Continuously Regenerating Trap (CRT<sup>®</sup>) which uses exhaust NO<sub>2</sub> (enhanced by the DOC by oxidising NO) continuously to oxidise soot within relatively low temperatures over a DPF (York et al., 2007, Allansson et al., 2002). However the performance of this system (i.e. the amount of NO to NO<sub>2</sub> conversion) depends highly on the available NO<sub>x</sub>, the hydrocarbon fuels as well as the exhaust gas temperature (Hori et al., 2002). If the available NO<sub>x</sub> and exhaust temperature is too low, active regeneration can be periodically applied to the system in which trapped soot is removed through a controlled oxidation with O<sub>2</sub> at 550°C or higher (Jeguirim et al., 2005). However, the temperature required is far above that observed in a typical diesel exhaust. Therefore extra heat needs to be provided, usually by injecting hydrocarbons (i.e. fuel) into the exhaust upstream of the DOC (York et al., 2010).

The possibility of high temperatures and uncontrolled regeneration from excessive soot loading or injected fuel can cause irreversible damage to the DPF due to cyclic thermal stresses (Martirosyan et al., 2010, Bensaid et al., 2009). As a result of the problems encountered with DPF's at high temperatures, it is suggested that a low temperature regeneration technique be more advantageous. NO<sub>2</sub> based systems are greatly favoured because the reaction takes place at temperatures seen in most diesel exhausts as illustrated in Figure 7.

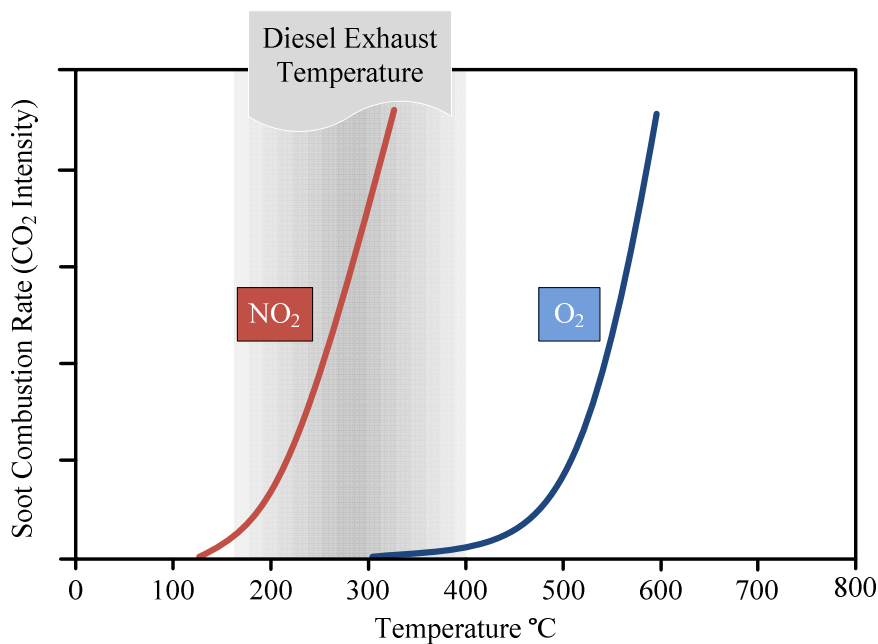


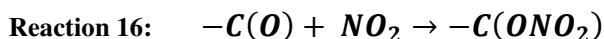
**Figure 7: The Effect of Temperature on Soot Oxidation with NO<sub>2</sub> and O<sub>2</sub> [Courtesy of Johnson Matthey Plc]**

NO<sub>2</sub> will promote the continuous oxidation of the deposited carbon particulates in the temperature range of 200-450°C. The following reaction mechanism was proposed for the evolution of CO<sub>2</sub> and CO (Ehrburger et al., 2002):

O<sub>2</sub> chemisorption on the carbon surface (-C\* is a carbon active site):



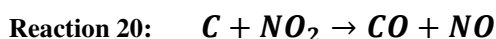
$\text{NO}_2$  promotes the decomposition of the intermediate C-O complex:



The following reactions lead to the regeneration of active sites on the carbon surface:



Therefore the overall oxidation reactions are:

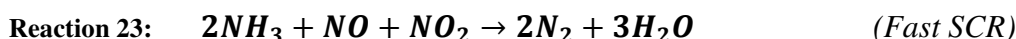
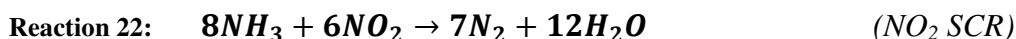
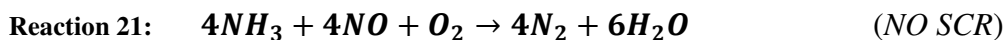


Water vapour can increase the overall oxidation rate of the above reactions; however it does not modify the global mechanism. A platinum catalyst can act to increase the formation of key component species of soot.  $\text{O}_2$  is adsorbed on the platinum and then spillovered to active carbon sites to produce  $-\text{C}(\text{O})$ . The  $-\text{C}(\text{O})$  is then destabilised by  $\text{NO}_2$  to  $-\text{C}(\text{ONO}_2)$  intermediate complex as shown in Reaction 16, decomposing to CO and  $\text{NO}_2$  or  $\text{CO}_2$  and NO.

#### 2.4.2.3 Diesel $\text{NO}_x$ Removal Catalyst Technology

The most common diesel  $\text{NO}_x$  removal catalyst technology is the urea/ammonia SCR. This is a process in which  $\text{NO}_x$  is reduced by  $\text{NH}_3$ , typically introduced into the exhaust stream as a urea solution upstream a catalyst. Common catalysts include supported vanadium oxide ( $\text{V}_2\text{O}_5$ ) and iron or copper supported on zeolite. The  $\text{NH}_3$ -SCR process over vanadium catalysts has demonstrated good selectivity for the conversion of NO to  $\text{N}_2$  with moderate formation of  $\text{N}_2\text{O}$  at temperatures typical of a heavy-duty diesel engine exhaust gas (Twigg, 2007).

The following reactions occur once the urea has been decomposed and hydrolysed (York et al., 2010):



The reaction of NH<sub>3</sub> and NO<sub>x</sub> occurs at a temperature range of around 200-450°C with achievable reduction efficiencies of 90% or greater. It was reported in the work of Kass et al. (2003) that ‘urea-SCR was one of the few catalyst methods capable of reducing diesel NO<sub>x</sub> emissions to the 2007 NO<sub>x</sub> limit’.

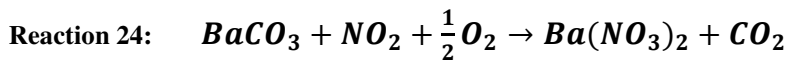
The other catalyst technology available for NO<sub>x</sub> removal is the LNT or referred to as the NO<sub>x</sub> adsorber catalyst (NAC). The concept of a NAC involves the storage of NO<sub>x</sub> on the catalyst washcoat during lean exhaust operation which is then reduced and released during rich operation. The washcoat consists of three active components, namely (Epling et al., 2004):

- An oxidation catalyst
- An adsorbent, commonly combined with alkali metals
- A reduction catalyst

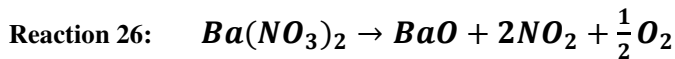
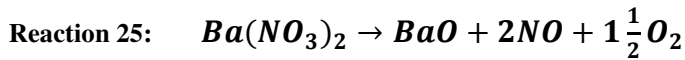
Common catalysts comprise of platinum and rhodium (Rh) supported on γ-Al<sub>2</sub>O<sub>3</sub> and a NO<sub>x</sub> storage component such as barium carbonate (BaCO<sub>3</sub>). Ceria in the catalyst washcoat is also used to promote the water gas shift reaction (WGS), inhibit platinum sintering and slow sulphur poisoning of the barium sites. However the most common role of ceria is to provide an O<sub>2</sub> storage capacity.

The key reaction steps are summarised as follows (Epling et al., 2004, Majewski and Khair, 2006, Brogan et al., 1998):

1. Under lean conditions the NO<sub>x</sub>, mainly NO, is oxidised over the platinum active sites to form NO<sub>2</sub> (Reaction 14)
2. The NO<sub>2</sub> is then adsorbed by the storage material in the form of barium nitrate:



3. Once the adsorption capacity becomes saturated, the exhaust is switched to rich conditions (i.e. elevated exhaust temperatures) to initiate the regeneration process. During this stage the O<sub>2</sub> is replaced by reducing species such as HC's, CO and H<sub>2</sub>. Under these conditions the stored nitrate species become thermodynamically unstable and decompose forming NO and NO<sub>2</sub> (Brogan et al., 1998):



4. The released NO<sub>x</sub> is then further reduced over the reducing catalyst in the presence of CO, HC and H<sub>2</sub> to form N<sub>2</sub> in a conventional three-way catalyst process:

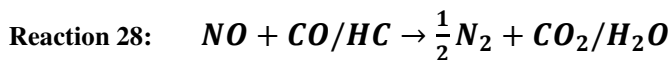
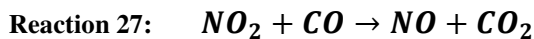
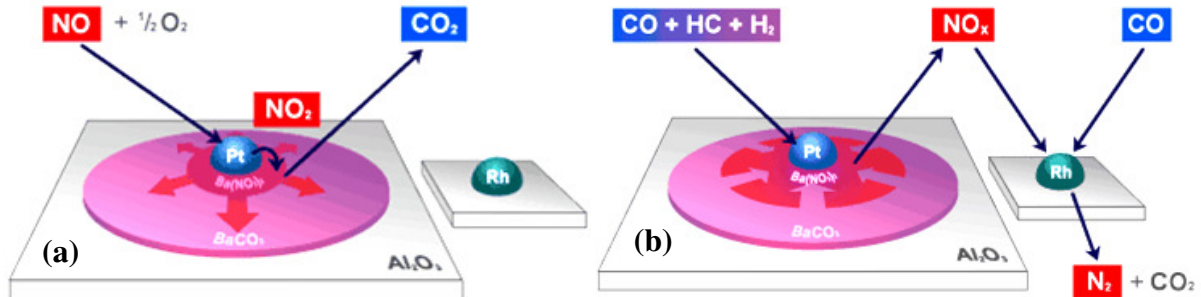


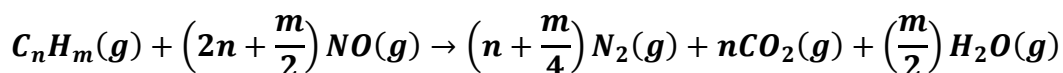
Figure 8 shows the principle operation of a Pt/BaCO<sub>3</sub>-Al<sub>2</sub>O<sub>3</sub> NAC with an Rh-based reducing catalyst (Gill et al., 2004). There are a number of ways in which a fuel rich exhaust atmosphere can be achieved and these include the injection of additional diesel or H<sub>2</sub> into the cylinder called in-cylinder generation (West et al., 2004) or direct injection of fuel into the

exhaust upstream the NAC (Schenk et al., 2001). Implementing an additional fuel injection to enrich the exhaust will lead to an increase in fuel penalty.



**Figure 8: Schematic of NAC Process, a) Lean Exhaust Gas Operation (Trapping) and b) Rich Exhaust Gas Operation (Regeneration and Reduction) [Courtesy of Johnson Matthey Plc]**

Nevertheless, research into applying urea-based SCR and NO<sub>x</sub> adsorber catalysts to on-road vehicles have exposed a number of concerns. For example, with urea-SCR there is a risk of residue build-up from unwanted urea and formation of urea decomposition products. Further, it was reported by Johnson (2012) that the low temperature control of NO<sub>x</sub> emissions using urea-SCR is difficult, because urea cannot be properly evaporated and decomposed to form NH<sub>3</sub>. Similarly the lean NO<sub>x</sub> trap technology requires complex controls to produce the required frequency of calibrated fuel-rich pulses and as a result the fuel penalty may prove to be excessive as well as the concern for the cost of the precious metal loadings (Thomas et al., 2005). Although the NAC systems are capable of providing high NO<sub>x</sub> conversions over a wide temperature window, there a number of drawbacks, especially at low exhaust gas temperatures. The most challenging has been the development of efficient desulphation strategies. Other issues include the control of secondary unregulated emissions such as NH<sub>3</sub>, N<sub>2</sub>O and hydrogen sulphide (H<sub>2</sub>S). An alternative less-developed technology for NO<sub>x</sub> control is HC-SCR over an Ag-Al<sub>2</sub>O<sub>3</sub> catalyst. This is where NO<sub>x</sub> is converted under lean exhaust conditions to N<sub>2</sub>. Reaction 29 describes the basic pathway.

**Reaction 29:**

Silver-loaded alumina is amongst the most active and selective catalyst for selective catalytic reduction of NO by HC's (Shimizu and Satsuma, 2007, Shimizu et al., 2007). The use of unburned hydrocarbons present in the exhaust as the reductant is the main advantage of the HC-SCR system. The oxidative activation of hydrocarbons is the key step for obtaining high SCR activity at lower temperatures. It has become clear that Ag-Al<sub>2</sub>O<sub>3</sub> catalysts have several key advantages over other potential diesel-SCR catalysts (i.e. Cu supported on zeolite – Cu-ZSM5 and platinum supported on alumina). Such advantages include low activity for SO<sub>2</sub> oxidation, relatively high thermal and hydrothermal durability (compared to Cu-ZSM5) and high selectivity to N<sub>2</sub> (contrasting platinum-based catalysts which form considerable quantities of N<sub>2</sub>O). Some of the common catalytic components have been collated in Table 3 (Shibata et al., 2002, Houel et al., 2007a, Schmiege et al., 2008, Kass et al., 2003, Kim et al., 2005, Iliopoulou et al., 2004).

The major disadvantage with Ag-Al<sub>2</sub>O<sub>3</sub> catalysts is its relatively low activity under the low-temperature window (< 300°C) representative of a typical diesel exhaust. The reasons for such low activity has been linked to the silver catalyst self-poisoning itself by forming stable surface nitrates and the gaseous hydrocarbons transforming into carbon-rich surface species, thus restricting the access to the active sites (Theinnoi et al., 2008). Although the catalyst is highly influenced by the nature of the fuel as well as severely deactivating by sulphur ageing, most of the activity can be recovered by treatment at high temperature in the presence of the fuel, despite the exhaust gas being oxygen rich (Houel et al., 2007a).

**Table 3: Lean NO<sub>x</sub> Catalysts**

Catalytic Components	Comments
Noble Metals (Platinum Group Metals – PGM), e.g. Pt-Al <sub>2</sub> O <sub>3</sub>	<ul style="list-style-type: none"> <li>• Stable and highly active for NO<sub>x</sub> removal</li> <li>• Narrow temperature window (approx. 175-250°C)</li> <li>• Poor selectivity for NO<sub>x</sub> reduction to N<sub>2</sub></li> <li>• Highly selective to N<sub>2</sub>O production</li> <li>• H<sub>2</sub> is easily oxidised by O<sub>2</sub> over PGM metals</li> </ul>
Zeolite, e.g. Cu-ZSM5	<ul style="list-style-type: none"> <li>• Stable and highly active for NO<sub>x</sub> removal</li> <li>• Zeolite dealumination</li> <li>• Hydrothermally unstable</li> <li>• Cu sintering (reduced porosity) when using Cu-ZSM5</li> </ul>
Metal Oxide, (Ag-Al <sub>2</sub> O <sub>3</sub> )	<ul style="list-style-type: none"> <li>• Highly selectivity to N<sub>2</sub> and stable</li> <li>• Less active than Zeolite</li> <li>• Ag-Al<sub>2</sub>O<sub>3</sub> in particular shows good resistance/durability to both H<sub>2</sub>O and SO<sub>2</sub> inhibition</li> </ul>

The study by Houel et al. (2007a) showed fouling of the silver catalyst by coking at low temperatures, while at higher temperatures (> 290°C) the oxidation of soot is faster than its formation. It was concluded that the coking was dependant on the nature of the hydrocarbons present in the fuel and as a result control of the HC:NO<sub>x</sub> ratio is required. Therefore, to promote the NO<sub>x</sub> reduction activity, it was suggested simply to keep the HC:NO<sub>x</sub> ratio low at lower temperatures and then increase as a function of temperature compensating for the loss of hydrocarbons through oxidation (Houel et al., 2007a). Several papers have examined the influence of various hydrocarbon fuels as possible reducing agents, with the general consensus being heavy hydrocarbons (e.g. decane) and diesel fuel enable NO<sub>x</sub> conversion at lower temperatures (Shimizu et al., 2000, Shimizu et al., 2001, Eränen et al., 2004,

Wichterlová et al., 2005, Thomas et al., 2005, Sazama et al., 2005), while the light hydrocarbon fuels (e.g. propane) tend to result in combustion products yielding NO<sub>x</sub> conversion only at high temperatures (Schmieg et al., 2008, Satokawa et al., 2003, Richter et al., 2004a).

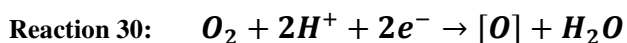
Light alcohols (e.g. ethanol, butanol) for instance have shown to be very reactive over a broad temperature window and is believed to be the result of them having a low molecular weight, promoting the diffusion rates and highly polar (and water soluble) compounds which compete successfully with water for the catalyst surface sites (Thomas et al., 2005). However drawbacks still arise especially with safety/flammability issues and therefore the important question now is the feasibility of the successful reductant to be fuel-borne or fuel derived/reformed. Such examples include ethanol which can be easily incorporated into diesel fuel using an emulsifying agent and mixtures of ethanol-diesel (E-diesel – containing up to 15% ethanol) have shown themselves to be relatively stable during engine operation (Kass et al., 2003, Thomas et al., 2005, Lapuerta et al., 2009).

To date, H<sub>2</sub> has been found to have a positive effect in the activity of Ag-Al<sub>2</sub>O<sub>3</sub> by promoting the HC-SCR and NH<sub>3</sub>-SCR reactions. Although there have been numerous studies published over the last few years showing the ‘hydrogen effect’, there have been vastly different conclusions documented with no general consensus being agreed. Research carried out by Richter et al. (2004a) concluded the role of H<sub>2</sub> was essentially the activation of molecular O<sub>2</sub>, while Shimizu et al. (2007) concluded H<sub>2</sub> lowered the activation energy for the reaction of O<sub>2</sub> into reactive O<sub>2</sub><sup>-</sup> species which are reactive toward the C-H bonds of the hydrocarbon. Brosius et al. (2005) proposed H<sub>2</sub> can effectively remove the strongly adsorbed nitrates from the Ag sites as well as the nitrates on the alumina support. Houel et al. (2007b) suggested that the H<sub>2</sub> promotes the formation of NO<sub>2</sub> which effectively oxidises the carbon

deposits at low temperature, thus removing the carbon-rich surfaces that poison the SCR reaction. However, Sazama et al. (2005) suggested that the acceleration of the SCR-NO<sub>x</sub> reaction by H<sub>2</sub> is mainly the result of an increased rate of oxidation of the HC's, but not from the increased rate of the NO-NO<sub>2</sub> reaction. It must be noted that H<sub>2</sub> does not act as a reducing agent of NO since Ag-Al<sub>2</sub>O<sub>3</sub> does not catalyse the NO selective reduction by H<sub>2</sub> in excess oxygen (Satokawa et al., 2003). Schmieg et al. (2008) concluded that H<sub>2</sub> addition can actually improve the high temperature CO oxidation capability of the catalyst as well as improve the selectivity to N<sub>2</sub>. However, H<sub>2</sub> addition at temperatures above 500°C can accelerate the HC oxidation reaction relative to the NO<sub>x</sub> reduction reaction, which in turn will hinder the catalyst performance. The 'hydrogen effect' was also observed by Shibata et al. (2004a, 2004b) over an Ag-ZSM5 catalyst, while the study of Satokawa et al. (2003) showed there to be no effect on Ag supported on carriers such as silica, zirconia and titania. Similarly the enhancing effect of H<sub>2</sub> on the HC-SCR reaction was not observed over metals such as cobalt (Co-Al<sub>2</sub>O<sub>3</sub>) and platinum (Pt-Al<sub>2</sub>O<sub>3</sub>) as H<sub>2</sub> was easily oxidised (Backman et al., 2006). In general at lower catalyst temperatures, more H<sub>2</sub> and lesser amounts of fuel are required and vice versa at higher catalyst temperatures (Schmieg et al., 2008).

In addition to H<sub>2</sub>, it was concluded by Sazama et al. (2005) that the presence of water vapour is valuable to prevent the formation of deposits (olefin-type intermediates) being adsorbed to the silver catalyst surface. Further investigations with Ag-Al<sub>2</sub>O<sub>3</sub> catalysts have shown that the formation of sulphate on the silver surfaces can actually improve the overall NO<sub>x</sub> conversion with some reductants. It was suggested that the sulphates influenced the selectivity towards NO<sub>x</sub> reduction, thus increasing HC slip as well as reducing the formation of N<sub>2</sub>O (Kass et al., 2003).

The mechanism of H<sub>2</sub> promoting HC-SCR and NH<sub>3</sub>-SCR consists of numerous key reactions defined in the work by Shimizu and Satsuma (2007). Firstly the H<sub>2</sub> dissociates on the Ag sites, with an H atom forming a proton on the alumina base. This is followed by aggregation of Ag<sup>+</sup> species to form Ag clusters. The O<sub>2</sub> is then reduced in the presence of the Ag cluster and proton (H<sup>+</sup>) to yield oxygen species (O<sub>2</sub><sup>-</sup>) and H<sub>2</sub>O. The following reaction gives a general representation of the ‘reductive oxidation’ process, where [O] stands for the reactive oxygen species.



The C-H activation of the HC and N-H activation of NH<sub>3</sub> by O<sub>2</sub><sup>-</sup> yields HC radicals and NH<sub>x</sub> species respectively. The hydrocarbon radicals then further convert to acetate ions, while NO goes through the process of oxidation in the presence of O<sub>2</sub><sup>-</sup> species to form NO<sub>2</sub>. In the case of HC-SCR, the acetate anion (CH<sub>3</sub>COO<sup>-</sup>) reacts with NO<sub>2</sub> producing nitromethanes (CH<sub>3</sub>NO<sub>2</sub>), which are then converted to NH<sub>3</sub> via species such as isocyanate (NCO). It is the surface reaction (i.e. over the unsulphated silver-alumina) between nitrates and oxygenates that leads to the formation of NCO and cyanide species, which finally leads to the formation of N<sub>2</sub> through oxidation or hydrolysis of these nitrogen-containing species (Meunier et al., 2000). According to Sazama et al. (2005) the most enhanced reaction step during the addition of H<sub>2</sub> is the transformation of the intermediate cyanide species to NCO and the oxidation of the HC to formates (e.g. HCOO<sup>-</sup>).

The work of Gang et al. (2001) was one of the earlier studies which looked into the effect of silver catalysts, focusing primarily on the NH<sub>3</sub> oxidation mechanism. The study revealed NH<sub>3</sub> dissociating and adsorbing as NH<sub>x</sub> species on the oxidised silver surface with one or two atomic hydrogen being removed from the surface oxygen. The work of Shimizu

and Satsuma (2007) follows on from the work of Gang et al. (2001), showing H<sub>2</sub> addition promoting the oxidative hydrogen abstraction of NH<sub>3</sub> by surface oxygen on Ag-Al<sub>2</sub>O<sub>3</sub> catalysts. Figure 9 gives a clear picture of how the presence of H<sub>2</sub> promotes the reaction of molecular O<sub>2</sub> into reactive O<sub>2</sub><sup>-</sup> species (Shimizu and Satsuma, 2007, Shimizu et al., 2007). In addition, it is also possible to see how the C-H activation of HC and N-H activation of NH<sub>3</sub> occurs through the presence of such species. Although many studies show the HC-SCR reaction taking place on the surface of the catalyst, it is understood that this reaction can also take place in the gas phase (Eränen et al., 2003).

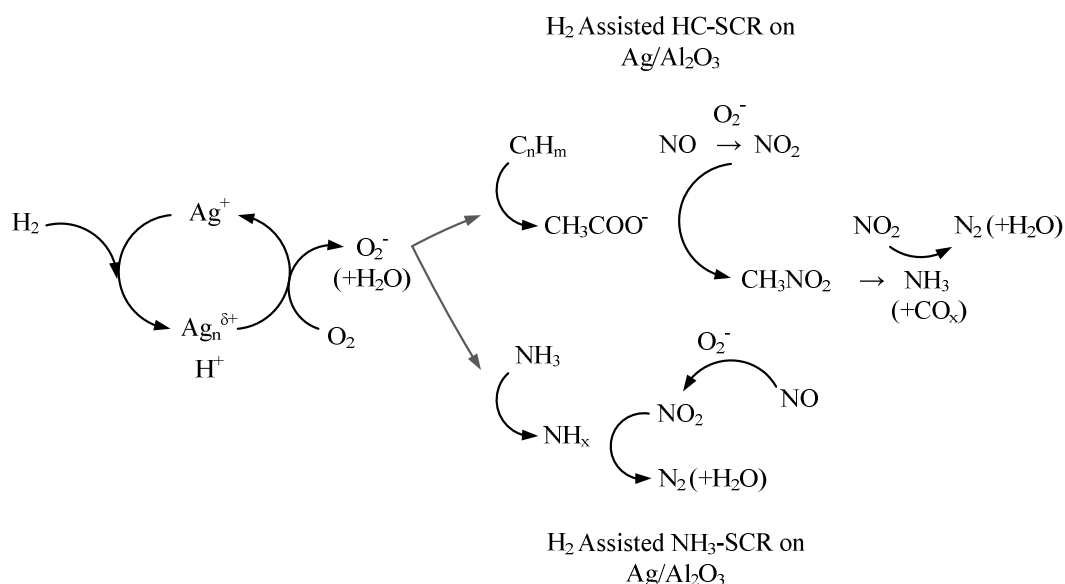


**Figure 9: Mechanism for both H<sub>2</sub> assisted HC-SCR and NH<sub>3</sub>-SCR**

While there have been many advances in diesel aftertreatment, the focus has also been on the production of on-board H<sub>2</sub>, particularly for catalyst enhancement as well as part replacement (i.e. dual fuel combustion or diesel pilot-ignited hydrogen combustion) of diesel fuel with a carbon-free alternative for CO<sub>2</sub> reductions.

## 2.5 On-board H<sub>2</sub> Production

Over the past decade many researchers have reported the benefits of H<sub>2</sub> (Verhelst and Wallner, 2009, Abu-Jrai et al., 2007, Bika et al., 2008, Lilik et al., 2010), but one of the major obstacles at the present time is the storage of H<sub>2</sub> on-board the vehicle for on-demand supply. Rather than having an external H<sub>2</sub> storage tank on-board the vehicle, techniques such as exhaust gas fuel reforming of diesel type fuels and NH<sub>3</sub> dissociation (i.e. resulting in a mixture of H<sub>2</sub> and N<sub>2</sub>) can be applied for on-board H<sub>2</sub> production, with the latter being in its early stages of development.

### 2.5.1 Ammonia for High Density Hydrogen Storage and its Dissociation

Although molecular H<sub>2</sub> is the most obvious choice, there are still challenges relating mainly to its distribution and on-board storage (Zuttel et al., 2010). By comparison, NH<sub>3</sub> is surprisingly overlooked, and yet the technology and facilities for its production, storage, handling and distribution are well established and extensive. By comparison, in recent years there has been a great deal more research into the use of H<sub>2</sub>, particularly for dual-fuelling of CI engines (Szwaja and Grab-Rogalinski, 2009, Abu-Jrai et al., 2007, Saravanan and Nagarajan, 2010). Although NH<sub>3</sub> can be used as a source of dilute H<sub>2</sub>, the volumetric energy density of liquid NH<sub>3</sub> is 45% higher than that of liquid H<sub>2</sub> (Kroch, 1945), arising from strong H<sub>2</sub> bonding between NH<sub>3</sub> molecules in the condensed phase (Gray et al., 1966, Jorgensen and Ibrahim, 1980). One of the major concerns about NH<sub>3</sub> is its high apparent toxicity, which is a combined measure of its volatility and intrinsic toxicity. This has been addressed in a detailed hazard assessment of each step in the distribution and storage of liquid NH<sub>3</sub>, carried out by the Risø National Laboratory in Denmark (Duijm et al., 2005), which has defined the required control measures for its safe public use as a vehicle fuel. The study emphasises the similarity in physical properties between liquid NH<sub>3</sub> and liquefied petroleum gas (LPG), and

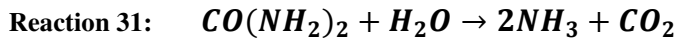
recommends that the failsafe fuel-tank design (lightweight porous carbon-fibre shell with polymer lining) developed for LPG is used for ammonia-fuelled vehicles.

NH<sub>3</sub> is neither a greenhouse gas nor a direct emitter of CO<sub>2</sub> but the route by which it is currently manufactured generates CO<sub>2</sub> as a by-product. The first step in the route (steam reforming or auto-thermal reforming of hydrocarbon to produce syngas) is common to the manufacture of H<sub>2</sub> but requires a subsequent synthesis step (the Haber process) in which the H<sub>2</sub> combines with N<sub>2</sub>. Although the synthesis step is exothermic, it nevertheless incurs additional (though relatively small) energy and carbon penalties. However, as pointed out by Klerke et al. (2008), NH<sub>3</sub> production lends itself to permanent carbon-capture because CO<sub>2</sub> has to be removed from the feed-gas in the synthesis step to avoid poisoning the catalyst. Furthermore, when the energy requirement for liquefaction is factored in, the efficiency of liquid H<sub>2</sub> storage is only 54%, while the overall efficiency for NH<sub>3</sub> synthesis followed by liquefaction and storage of the liquid is 85%, assuming the same starting point of high pressure H<sub>2</sub> (Klerke et al., 2008). In the future, either dissociation or hydrolysis of catabolically-formed urea could provide the most sustainable route for the large-scale manufacture of NH<sub>3</sub> (Rollinson et al., 2011).

### **2.5.1.1 On-board Storage and Supply**

Urea has been widely evaluated as an on-board source of NH<sub>3</sub> for catalytic SCR aftertreatment systems, where the role of NH<sub>3</sub> is to reduce NO<sub>x</sub> to nitrogen. Some of the advantages of urea include its low volatility and toxicity in its solid form, and the fact that it can be injected as an aqueous solution (Lambert et al., 2004, Rollinson et al., 2011). On the other hand, the disadvantages of aqueous urea include a high freezing point and the possible formation of isocyanic acid as a by-product during reaction with exhaust gases (Koebel et al., 2000). In addition, as liquid NH<sub>3</sub> has a gravimetric H<sub>2</sub> content of 17.6wt.% compared to

7.95wt.% for aqueous urea, using neat NH<sub>3</sub> is a much more weight-efficient option, especially for large scale application as a supplementary fuel (Rollinson et al., 2011). However, in the context of the progressive decarbonisation of IC engines, the most compelling disadvantage of urea is that it forms CO<sub>2</sub> during the hydrolysis reaction that releases NH<sub>3</sub>, as shown below:



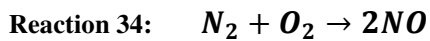
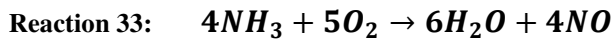
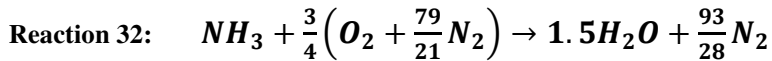
Overall, liquid NH<sub>3</sub> is seen as a better option for improving light-duty combustion and for enabling advanced aftertreatment technologies (e.g. HC-SCR) which require promotion by H<sub>2</sub> (Abu-Jrai and Tsolakis, 2007, Houel et al., 2007b).

#### 2.5.1.2 Effects of Ammonia on IC Engines

The feasibility of using NH<sub>3</sub> as an alternative to hydrocarbon fuels was demonstrated on fleet scale in Europe during World War II, when it was used to fuel buses in Belgium during a shortage of conventional fossil fuels (Kroch, 1945). Later, in the 1960s, the U.S Army carried out more systematic studies of NH<sub>3</sub> as a substitute for hydrocarbons in SI and CI engines (Gray et al., 1966, Pearsall and Garabedian, 1967). These studies highlighted the effectiveness of dual fuelling CI engines with diesel and NH<sub>3</sub>. On its own, NH<sub>3</sub> has a high ignition resistance, which can be overcome by injecting enough diesel fuel directly into the cylinder to initiate combustion (Pearsall and Garabedian, 1967). Another perceived disadvantage of NH<sub>3</sub> is its low heating value but this is largely compensated for by the low A/F ratio at stoichiometry, which means that the energy content per unit mass of a stoichiometric mixture is only 7% lower than that of a comparable diesel/air mixture.

Despite its long history as an alternative or supplementary fuel, our understanding of the effects of NH<sub>3</sub> on thermal combustion efficiency and emission quality is still in its infancy. In the most detailed study of NH<sub>3</sub> addition reported to date, Reiter and Kong (2008, 2011) have

investigated the combustion and emissions characteristics of a dual-fuelled turbocharged diesel engine. They have shown that CO<sub>2</sub> and soot emissions can be reduced without sacrificing engine power when 40-60% of the fuel energy delivered to the engine is provided by NH<sub>3</sub>. The major issue, however, relates to the emissions directly resulting from the NH<sub>3</sub>. Although the predominant reaction of NH<sub>3</sub> in the engine is its clean combustion to produce only N<sub>2</sub> and H<sub>2</sub>O (Reaction 32), there is a persistent slip of unconverted NH<sub>3</sub> that results in a concentration of 1000-3000 ppm in the exhaust. Additionally, when most of the fuel energy is provided by NH<sub>3</sub>, some of the NH<sub>3</sub> can undergo over-oxidation (Reaction 33), resulting in very high rates of NO<sub>x</sub> emissions. However, Reiter and Kong (2008, 2011) have also shown that when < 40% of the fuel energy is provided by NH<sub>3</sub>, NO<sub>x</sub> emissions are lower than for a diesel engine running entirely on hydrocarbon fuel because substitution by NH<sub>3</sub> lowers the combustion temperature, and hence reduces the thermally-induced formation of NO<sub>x</sub> (Reaction 34).



Further, in forming H<sub>2</sub> from NH<sub>3</sub>, the minimum ignition energy is lowered from 8 mJ to 0.018 mJ, while the laminar burning velocity is increased from 0.015 ms<sup>-1</sup> to 3.51 ms<sup>-1</sup> (Saika et al., 2006). At the same time, although the proportion of unburnt NH<sub>3</sub> may remain the same, the substantially lower concentration being fed to the engine should result in much lower slip of NH<sub>3</sub> through to the exhaust.

In a practical on-board H<sub>2</sub> production system, it is believed that liquid NH<sub>3</sub> will be released from a storage tank into an evaporator where it will undergo a phase change to form

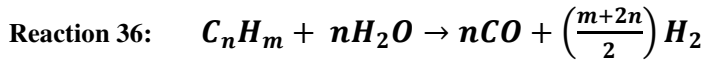
gas phase  $\text{NH}_3$ , which can then be catalytically dissociated to  $\text{H}_2$  and  $\text{N}_2$ . The dissociation of  $\text{NH}_3$  (Reaction 35) is limited by a chemical equilibrium between the forward and reverse reactions, which results in a small percent of  $\text{NH}_3$  in the product stream at temperatures below  $700^\circ\text{C}$  (at 1 atm) (Faleschini et al., 2000). However, a temperature of  $400^\circ\text{C}$  or higher will promote stable dissociation (Saika et al., 2006). It can be assumed that a dissociated gas stream containing 1-2% unconverted  $\text{NH}_3$  can be produced in a catalytic reactor, where the endothermic heat of dissociation can be provided by the combustion of some of the  $\text{NH}_3$  over the catalyst and through the recovery of waste heat from the engine exhaust. In a further adaptation of the same concept, a diffusion membrane can be implemented to separate the  $\text{H}_2$  from the  $\text{N}_2$  and unreacted  $\text{NH}_3$  in the exit stream from the catalytic reactor. In this scenario, the function of the  $\text{NH}_3$  is as a  $\text{H}_2$  carrier and as a heat recovery medium.



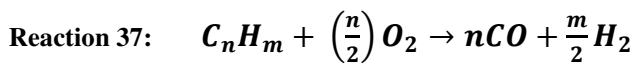
### 2.5.2 Fuel Reforming

Currently there has been extensive research in developing fuel reforming to produce  $\text{H}_2$ -rich synthetic gas for various applications such as fuel cells, IC engines and exhaust gas aftertreatment systems. The most common techniques are partial oxidation ( $\text{PO}_x$ ), steam reforming (SR) and auto-thermal reforming (ATR) producing  $\text{H}_2$  from reforming of hydrocarbon fuels. The following section breaks down the several techniques that are already available for  $\text{H}_2$  production and have been summarised from the work of Tsolakis and Megaritis (2004b):

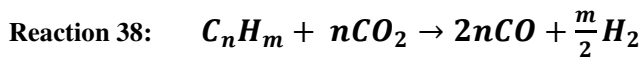
- In hydrocarbon SR, high temperature steam separates the H<sub>2</sub> from the carbon atoms. Although productive, the reaction is highly endothermic resulting in a high loss of energy:



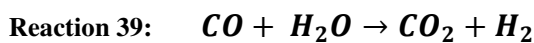
- PO<sub>x</sub> is an exothermic process and the resulting H<sub>2</sub> containing fuel has a lower calorific value than that of the original feedstock. Therefore PO<sub>x</sub> is considered to be inefficient:



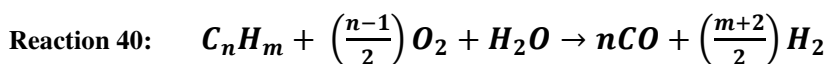
- The endothermic dry reforming reaction takes place at temperatures > 800°C, utilising some of the fuel and CO<sub>2</sub> to produce more H<sub>2</sub>:



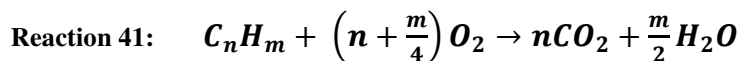
- The WGS reaction is commonly referred to as a secondary reaction taking place due to the presence of CO and excess steam, producing additional H<sub>2</sub> under temperatures below 750°C:



- ATR is a combination of PO<sub>x</sub> and SR requiring fuel, H<sub>2</sub>O and O<sub>2</sub> (or air) to be fed into a reactor simultaneously. It has been reported that ATR is well suited for heavier hydrocarbons such as diesel with relatively high reforming efficiencies and fuel conversion (Ahmed and Krumpelt, 2001):



- The most undesirable reaction in terms of H<sub>2</sub> production which can also take place is complete oxidation of the fuel:



Since the focus of this thesis is on diesel emissions, the primary focus for fuel reforming is H<sub>2</sub> production to enhance combustion as well as the aftertreatment devices. Instead of having an external H<sub>2</sub> storage tank on-board the vehicle, which has many issues such as a relatively high compression cost, high volatility and low volumetric energy density (Tsolakis et al., 2007a), it is believed exhaust gas fuel reforming could be utilised. Using heavier hydrocarbon fuels such as diesel, with its well-established infrastructure, not only makes it practical for on-board fuel reforming but gives the advantage of a high H<sub>2</sub> density. Exhaust gas fuel reforming, which is a combination of all the basic reforming processes, is similar to that of ATR and involves a process essentially involving the catalytic cracking of the source feed or more specifically direct catalytic interaction of fuel with the engine exhaust gases (i.e. O<sub>2</sub>, H<sub>2</sub>O and CO<sub>2</sub>) to produce a synthesis gas that mainly contains H<sub>2</sub>, CO, H<sub>2</sub>O, CO<sub>2</sub> and N<sub>2</sub> (Tsolakis et al., 2004). However, the composition of this gas is controlled by the reactor inlet feed ratios (O<sub>2</sub>/C and H<sub>2</sub>O/C) and the exhaust gas temperature (Abu-Jrai et al., 2008). The main reactions which occur consecutively during exhaust gas fuel reforming are the exothermic complete oxidation of part of the fuel (Reaction 41), the endothermic SR (Reaction 36), WGS (Reaction 39) and sometimes dry reforming (Reaction 38) (Tsolakis and Golunski, 2006).

The advantage of implementing exhaust gas fuel reforming is that there is no need for the storage and supply of H<sub>2</sub>O and O<sub>2</sub>. The waste heat of the exhaust can be utilised to light-off the reforming catalyst and evaporate the liquid fuel, while the H<sub>2</sub>O in the exhaust is

already in the form of steam so therefore no extra heat is required for its evaporation (Tsolakis and Megaritis, 2004b, Tsolakis et al., 2004). On-board fuel reforming of liquid hydrocarbon fuels is a way to supply on-demand  $H_2$  on-board a vehicle by using the existing fuel infrastructure. Renewable biodiesel fuels (e.g. RME, bio-ethanol etc) can also be used for reforming under temperatures typical of diesel exhaust temperatures operating at part load. This is promising; especially as interest in renewable and alternative combustion fuels have grown increasingly, primarily to improve engine performance and emissions but also to ensure the sustainability of the fuel supplies.

Among the most promising technologies for conventional vehicles are a combination of reforming and EGR, commonly referred to as REGR, which allows the fuel/air feed to be enriched with reformat. Despite the advantages, diesel reforming is still challenging, especially with issues that affect its long term performance and operation. These include sulphur poisoning and carbon deposition, which with time degrade the reforming performance (Yoon et al., 2008). Using low O/C ratios, which are ideal for high efficiency reformer operation, can result in catalyst poisoning by coke formation (Tsolakis et al., 2007a).

### **2.5.3 Improving Diesel Emissions with $H_2$ Addition**

Earlier studies (Abu-Jrai et al., 2009, Tsolakis et al., 2004) have shown the benefits of  $H_2$  through the use of REGR, i.e. reforming reactor product from diesel exhaust gas fuel reforming. It was observed greater REGR levels improved the emissions of smoke and  $NO_x$ , especially under low load conditions. However, there was a penalty in  $NO_x$  emissions at high load with high REGR levels. Other studies have found that the addition of pure  $H_2$  (i.e. simulated using bottles gases) to a diesel-fuelled engine can substantially lower the emissions of HC, CO and  $CO_2$  simultaneously (Saravanan and Nagarajan, 2010). However, this came with an engine-out  $NO_x$  emission penalty as a result of an increased in-cylinder flame

temperature when H<sub>2</sub> was present under normal diesel operation (Saravanan and Nagarajan, 2010, Abu-Jrai et al., 2007, Abu-Jrai and Tsolakis, 2007, Lee et al., 1995). The addition of H<sub>2</sub> also promoted the oxidation of NO by increasing the production of the HO<sub>2</sub> radical which is active in the conversion of NO to NO<sub>2</sub> (Chong et al., 2010), hence substantially increasing the NO<sub>2</sub> fraction of NO<sub>x</sub>.

A recent study by Shin et al. (2011) demonstrated the effectiveness of introducing H<sub>2</sub> into the combustion chamber through the intake manifold. It was concluded that low temperature NO<sub>x</sub> reduction improved as a result of H<sub>2</sub> addition under high EGR ratios. It was observed that by replacing part of the intake charge with H<sub>2</sub> (i.e. reducing the O<sub>2</sub> concentration) there was an increased content of inert gasses in the exhaust stream and as this was part of an EGR loop it influenced the intake manifold gas concentrations. Overall it was suggested that H<sub>2</sub> promoted diesel combustion, reducing the engine-out emissions of unburned HC and CO emissions as a result of its higher combustion temperatures and high flame velocity. The smaller quenching distance of H<sub>2</sub> compared to hydrocarbon fuels also allowed the flame to propagate closer to the combustion chamber walls where HC's would otherwise be left unburned. Although H<sub>2</sub> substitution of diesel fuel reduces the amount of carbon available to form soot, higher levels of H<sub>2</sub> substitution can result in reduced air present in the intake charge, thus leaving less O<sub>2</sub> to be entrained into the diesel fuel (Lilik et al., 2010). As a result it was suggested by Lilik et al. (2010) that this richer stoichiometry in the spray flame will offset the reduced amount of carbon available to form soot.

Compared to diesel fuel, H<sub>2</sub> has a greater heating value, lower density and requires a higher auto-ignition temperature, thus once ignited H<sub>2</sub> is highly reactive. Although the auto-ignition temperature of H<sub>2</sub> is higher than that of diesel, the ignition energy for a H<sub>2</sub>/air mixture is lower when compared to that of many hydrocarbon fuel/air mixtures (Heywood, 1988).

Thus a reduction of the diesel ignition delay occurs due to either the ignition of diesel fuel causing the ignition of H<sub>2</sub> or the enriched H<sub>2</sub>/air mixture self-igniting as a result of the high in-cylinder temperatures. Evidence of the latter type of H<sub>2</sub> auto-ignition has also been observed in recent studies (Szwaja and Grab-Rogalinski, 2009, Abu-Jrai et al., 2007). The combustion characteristics of H<sub>2</sub> include higher energy content and flame speed than diesel, leading to an increased ROHR.

Many papers have reported the effects of H<sub>2</sub> on the thermal efficiency with vastly different conclusions, and no general consensus being agreed as to whether H<sub>2</sub> has a negative or beneficial influence. Possible reasons for the drop in thermal efficiency with H<sub>2</sub> dual-fuel modes include increased heat loss from the combustion chamber (Shudo, 2007, Shudo et al., 2001), changes to combustion characteristics and changes to the efficiency of H<sub>2</sub> combustion under different loads and concentrations (Liew et al., 2010). Several studies (Varde and Frame, 1983, Liew et al., 2010) have found that a reduction in H<sub>2</sub> thermal combustion efficiency occurs when it is added in relatively small amounts as a result of a very lean H<sub>2</sub>-air mixture. The work by Shudo (2007) explains how the characteristics of H<sub>2</sub> combustion can influence the engine thermal efficiency. This includes the higher flame velocity, smaller quenching distance (approx. 0.64mm) and higher thermal conductivity of H<sub>2</sub> compared with hydrocarbon fuels (Lewis and von Elbe, 1961, Verhelst and Wallner, 2009). The higher flame velocity allows for a larger convection of burning gas and subsequently a greater transfer of heat loss to the combustion chamber walls (Shudo, 2007). A smaller quenching distance allows the combustion flames to propagate nearer to the chamber walls thus transferring more heat, and a higher thermal conductivity results in greater heat transfer to the walls from the unburned mixture (Shudo, 2007).

## **2.6 Alternative fuels**

The world is presently confronted with the twin crises of fossil fuel depletion and environmental degradation. Excessive use of fossil fuels has major local, regional and global environmental impacts (Agarwal, 2007):

1. Local – Air pollution
2. Regional – Acid rain and airborne pathogens (i.e. infections, particles and chemicals)
3. Global – Greenhouse effect

Projections for the 30-year period from 1990 to 2020 indicate that vehicle travel, and consequently fossil-fuel demand, will almost triple and the resulting emissions will pose a serious problem. The main reason for increased pollution levels, in spite of the stringent emission standards that have been enforced, is the increased demand for energy in all sectors and most significantly the increased use of automobiles (Agarwal, 2007). Due to the concern about the limited future oil resources and requirement of CO<sub>2</sub> reduction, interests in renewable and alternative fuels have grown increasingly. New diesel fuels are necessary not only to improve engine performance and emissions but also to ensure the sustainability of the fuel supplies.

The quality specifications for diesel fuels are given in the standard EN-590 which all fuel suppliers in Europe must follow. Currently there are two sets of standards which establish the specifications for biodiesel fuels in the EU (2010):

- EN 14214 includes specifications for fatty acid methyl ester (FAME) fuel for diesel engines. B100 (100% Vol. biodiesel) that meets this standard could be used unblended in a diesel engine (if the engine has been adapted to operate on B100) or blended with petroleum diesel fuel.

- EN 590, the European diesel fuel specification, is also applicable to biodiesel blends up to 7% of FAME (as regulated by Directive 2009/30/EC).

Over the years, the standards are periodically updated to reflect the changes in specification (e.g. a minimum cetane number specified by Directive 98/70/EC) which are subject to environmental regulations such as the mandatory reduction in sulphur content to a limit of 10ppm ('sulphur free').

### **2.6.1 Biodiesel Fuels**

Biodiesel is defined as alkyl esters of fatty acids produced from the transesterification of triglycerides (e.g. oils or fats), from plants or animals; with short-chain alcohols such as methanol or ethanol (Monyem and H. Van Gerpen, 2001). The transesterification process is outlined in Figure 10 (Kim et al., 2004). The main aim of transesterification is to lower the viscosity and reduce fuel degradation, thus producing a diesel fuel with high oxygen content, high cetane number, no sulphur/aromatic content, good lubricity, improved stability and enhanced cold flow properties. Transesterification involves using an alcohol in the presence of a catalyst (e.g. sodium hydroxide, NaOH) to break chemically the molecule of the raw renewable oil (e.g. rapeseed oil) into methyl/ethyl esters with glycerol as the by-product, which reduces the viscosity (Babu and Devaradjane, 2003). In Europe, RME is the most common biodiesel available; while in the U.S. soybean methyl ester (SME) predominates.

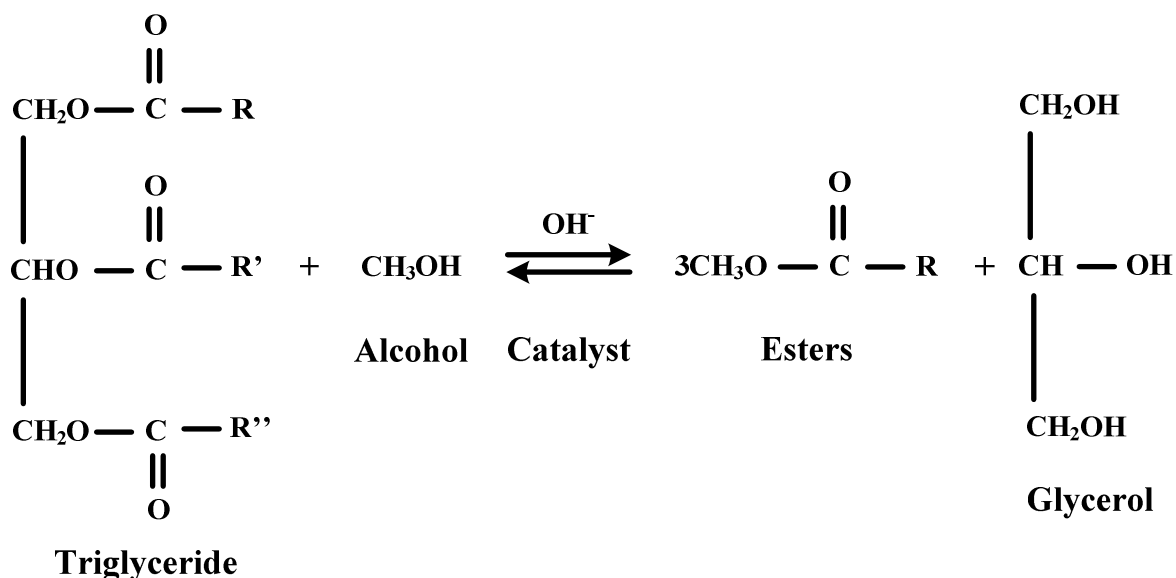


**Figure 10: The Transesterification Process of Triglycerides into Esters**

Biodiesel has a number of well known advantages and disadvantages as summarised below (Ribeiro et al., 2007, Lapuerta et al., 2008a, Monyem and H. Van Gerpen, 2001, Yamane et al., 2001, Graboski and McCormick, 1998):

- The esters of unsaturated fatty acids are unstable with respect to light, catalytic systems and atmospheric oxygen, resulting in poor oxidation stability resulting from the structural carbon double bonds. However, biodiesels which are composed of primarily saturated methyl esters exhibit good oxidation stability, while having poor low temperature flow properties.
- Although biodiesels have better lubricant properties than conventional diesels, they contribute to the formation of deposits. This, however, is dependent on the quality specifications of the fuel such as the degradability, glycerol content and cold flow properties.
- Comparable engine efficiency to that of conventional diesel and can be used as either pure or blended with diesel. However, the lower heating value of biodiesel would result in

proportionally higher fuel consumption compared to conventional diesel for the same output power.

- The combustion of biodiesel provides a reduction of many regulated harmful exhaust emissions which include THC, CO and PM while also including a significant reduction in sulphur oxides and PAH (i.e. soot precursors) emissions. The oxygen content of the biodiesel molecule promotes more complete combustion (reducing HC and CO emissions), especially in regions of fuel-rich diffusion flames, thus promoting the oxidation of the formed soot and its precursors.
- The combustion of biodiesel tends to result in increased NO<sub>x</sub> exhaust emissions which have been reported widely to be related to the injection process being advanced. The pressure rise produced in a pump-line-nozzle injection system is quicker as a consequence of its lower compressibility (higher bulk modulus), thus propagating more quickly towards the injectors due to its higher sound velocity.

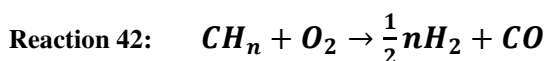
### **2.6.2 Fischer-Tropsch Diesel Fuels**

Ultra-clean, high cetane number fuels (facilitating lower combustion temperatures and pressures) derived from an F–T process (final liquid fuel to be obtained from renewable sources) is a promising alternative (Abu-Jrai et al., 2006, Rodríguez-Fernández et al., 2009b). They are virtually free of sulphur and aromatic hydrocarbons, can facilitate further reduction of engine-out emissions, and improve the performance of the catalytic aftertreatment systems and fuel reformers (Abu-Jrai et al., 2006). These fuels show a very high potential for realising a much more favourable NO<sub>x</sub>/PM trade-off without the commonly observed associated penalties in fuel efficiency (Rounce et al., 2009). The raw material can either be natural gas (the final liquid fuel being GTL), coal (CTL) or residual biomass (BTL). The fuel feedstock for BTL comprises of lignocellulosic biomass mainly from forest and agricultural residues,

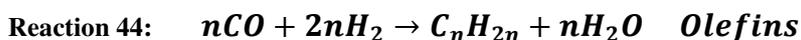
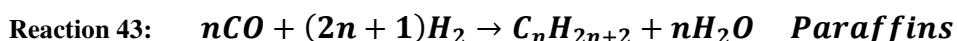
such as tree barks, tops and branches, demolition wood, tall grasses, and crop residues facilitated in the use of low cost, non-edible feedstock (Zhang, 2009, Nigam and Singh, 2010).

The basic technology is known as the Fischer-Tropsch process and a number of companies have developed this synthetic process using catalytic technology. The resulting synthesised straight-chain HC have good compression ignitability and are suitable for use with automobiles as diesel engine fuel. For this reason, many reports have been published concerning the influence of F-T diesel fuel properties on diesel emissions characteristics (Kitano et al., 2007). Franz Fischer and Hans Tropsch developed the process that bears their names in the 1920's. The production of diesel fuels using the F-T process is a set of chemical reactions in the presence of a catalyst (Höök and Aleklett, 2009):

- Synthesis Gas (Syngas) Formation:



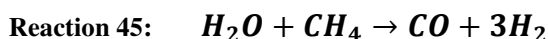
- F-T Synthesis Process:



Several reactions are required to obtain the gaseous reactants required for F-T catalysis. Reactant gases entering an F-T reactor must first be desulphurised to protect the catalysts that are readily poisoned. The following major sets of reactions are employed to adjust the H<sub>2</sub>/CO ratio:

- WGS Reaction (Reaction 39) – Provides a source of H<sub>2</sub>

- SR is important for those F-T plants that start with methane:



Several routes are possible for the formation of synthesis gas from natural gas; including ATR, SR as shown in Reaction 45, and  $PO_x$ . The formation of synthesis gas from coal or biomass is called gasification, wherein the feedstock is reacted with steam and  $O_2$ . The next step in the F-T production process is the conversion of synthesis gas into HC. This begins with  $H_2$  and CO molecules being formed into  $-CH_2-$  alkyl radicals and  $H_2O$  in an exothermic reaction. The  $-CH_2-$  radicals then immediately combine in an iron or cobalt catalytic reaction to make synthetic olefin and/or paraffin HC of various chain-lengths (high boiling point wax and olefinic naphtha) as shown by Reaction 43 and Reaction 44. The selectivity (the amount of desired product obtained per unit consumed reactant) is influenced by parameters such as temperature,  $H_2/CO$  ratio in the feed gas, pressure and the catalyst type.

The F-T product can be upgraded to high quality diesel fuel through post-processing and any oxygenates formed during the F-T process are often removed during this step. Addition of  $H_2$  and a catalyst causes hydro-cracking, rupturing long carbon chains into shorter, liquid parts to produce cuts that correspond to a range of conventional refinery products. Regardless of feedstock or process, F-T diesel fuels typically have a number of very desirable properties (Alleman and McCormick, 2003). Figure 11 gives a simple overview of the F-T technology. Adaptation of the F-T synthesis to syngas of different origins revolves around purity, cleanliness and the  $H_2/CO$  ratio of the gas (EU, 2006, Lawrence, 2006). It is important to note that the distillation range of F-T diesel can be customised by F-T synthesis conditions and by the distillation cut after synthesis occurs. Therefore this is not an inherent property of the F-T diesel.

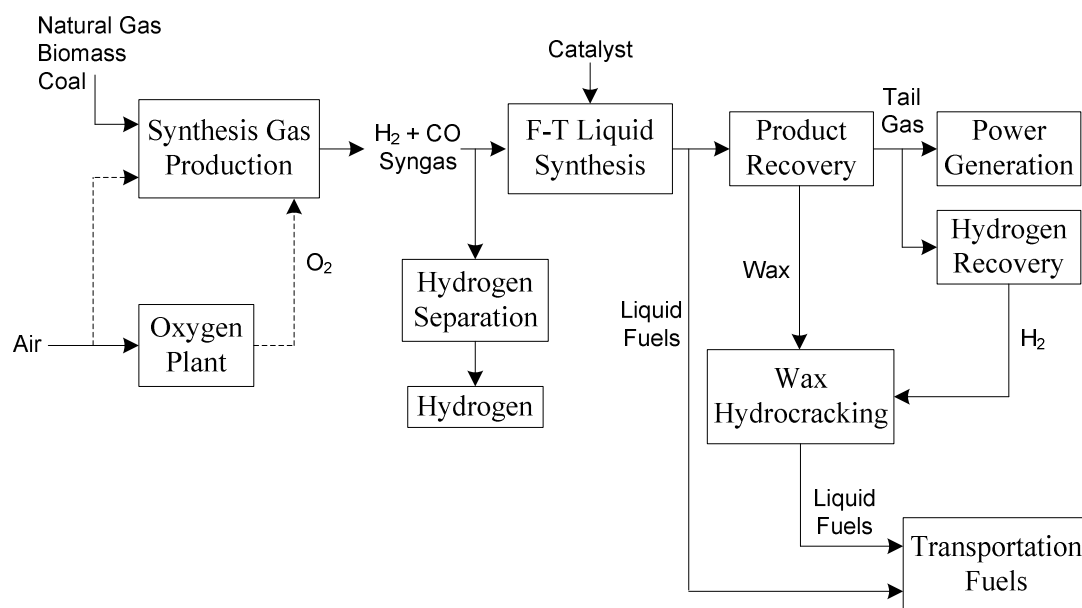


**Figure 11: F-T Technology**

F-T synthesis is technically classified into two categories: the high-temperature Fischer-Tropsch (HTFT) and the low-temperature Fischer-Tropsch (LTFT) processes. The criterion for this classification is the operating temperature of the synthesis, which ranges between 310-340°C for the HTFT process and 210-260°C for the LTFT process (Leckel, 2009, Dry, 2002). HTFT is mainly composed of aromatics and olefins and LTFT of paraffin's. As a consequence, HTFT is apparently more suitable as a gasoline fuel due to the high octane number of aromatics, whereas LTFT is used for diesel fuels (high cetane number of paraffinic compounds, but with a density usually below the diesel standards) (Leckel, 2009). The good ignitability (i.e. high cetane number) and low aromatic content are crucial for a diesel fuel, and constitutes the feature that reinforces the introduction of F-T derived fuels in the market, while density issues do not introduce severe limitations (at least in the typical ranges).

F-T diesel fuels can be designed to have a high cetane number, low aromatics, thus low C/H ratio and relatively low specific gravity. These fuels are also extremely low in sulphur (often less than 1ppm) when derived from natural gas. These particular fuels are a strong

candidate for fuel blending and as a neat fuel in transportation markets. Their impact on aftertreatment catalyst development and particulate abatement is attractive due to their low sulphur content and the absence of aromatic HC (McMillian and Gautam, 2001, Kitano et al., 2005). However, some properties of F-T diesel fuels are still to be improved. Poly-aromatic and sulphur compounds contribute to the lubricity of diesel fuels, although sulphur content in diesel fuels is being virtually eliminated. The very low aromatic content of F-T diesel fuel combined with the near zero sulphur content results in a fuel with poor lubricity properties. Lubricity tests with neat F-T diesel fuels reveal results well below accepted lubricity standards, but not significantly below the US8, EU and MK1 diesel fuels (i.e. before additive addition) which consist of sulphur content below 10ppm. The lubricity of F-T diesel fuels can be improved to acceptable levels using commercial additives. FAME (i.e. biodiesel) can also be used to improve the lubricity of F-T diesel fuel (Alleman and McCormick, 2003). Density is an important factor for fuel consumption, whereas the other properties mentioned have an effect on emissions. Although density is not a problem for aromatic-containing HTFT diesel, LTFT diesel contains virtually no aromatics and the resulting density of 770-780kg/m<sup>3</sup> poses a refining challenge. However, synthetic LTFT distillate is increasingly blended into top quality diesel fuels to reduce emissions in modern high performance diesel engines (Leckel, 2009).

Ideally, a CI fuel would be renewable, produce useable power to current diesel standards, run in both existing and newly manufactured engines and require no engine modifications. In addition, its combustion should produce fewer emissions which would enhance the efficiency of exhaust gas aftertreatment systems primarily by increasing the availability of active catalytic sites. In a modern diesel engine, synthetic fuels can satisfy many of the above ideal fuel requirements. Recent studies have shown that synthetic fuels

have emission benefits in the reduction of HC, CO, NO<sub>x</sub> and PM. However, the density of synthetic fuels such as GTL is lower than that of the standard European specifications for diesel. As a result the volumetric energy density is also lower and the injection system hardware and injection strategy may need to be reconfigured (Larsson and Denbratt, 2007, Rounce et al., 2009).

### **2.6.2.1 Effect of Fuel Properties with F-T fuel on Engine Emissions**

Some of the physical and chemical properties of the F-T fuels are behind their potential to reduce engine-out emissions. Among these properties, the higher cetane number is the most cited to justify the trends (Abu-Jrai et al., 2006, Rounce et al., 2009, Kitano et al., 2007), but others such as the differences in aromatic content or the adiabatic flame temperature play a role as well. Sulphur content or volatility, which could affect emissions, is a marginal consideration as sulphur content is being eradicated from all types of diesel fuels (Lapuerta et al., 2008a). Differences in volatility are uncertain, since this property is strongly affected by the oil-fraction that is used in the manufacturing process of both conventional and F-T diesel fuels.

The cetane number affects engine performance and emissions through the chemical ignition delay. The higher the cetane number, the lower this delay, thus the fraction of injected fuel that is burnt under premixed conditions is reduced. Premixed combustion is associated with higher pressures, pressure gradients and temperatures in the chamber, all of which increase NO<sub>x</sub> formation. Aromatic compounds are suspected of directly influencing the first steps of soot particle formation (for example, soot inception). The chemical pathway involves especially polycyclic aromatic compounds but this is a subject under continuous investigation (Roesler et al., 2003, Marchal et al., 2009). Adiabatic flame temperatures of fuels may be calculated from thermodynamic properties, and are directly related to the

thermal formation of NO<sub>x</sub>. Aromatic compounds are reported to have higher adiabatic flame temperatures than paraffinic ones (Glaude et al., 2010). Regarding the sulphur content in fuels, which when oxidised to form sulphur oxides, combine with H<sub>2</sub>O to produce sulphates, a component of the insoluble organic fraction (ISF) of the PM emitted. However, sulphur reduction in recent years has been related to its effect on catalysts (i.e. deactivation, poisoning) rather than increases in particulate.

Kidoguchi et al. (2000) were one of many research groups who studied the effect of fuel properties on DI diesel combustion. The study revealed that by reducing the cetane number, there was an increase in NO<sub>x</sub> and decrease in PM emissions at high load. This effect was thought to be due to the low cetane number fuel having a long ignition delay, causing a high maximum heat release rate and shortened combustion duration. However, for low loads, lower cetane fuels produced higher THC due to local over lean mixtures caused by the ignition delay, hence resulting in an incomplete combustion. The work of McMillian and Gautam (2001) supported this and concluded THC brake specific emissions were reduced for F-T diesel fuels as a direct result of higher cetane number and hence the expected ignition delay. Szybist et al. (2005) found a similar relationship between NO<sub>x</sub> and cetane number, however only when the injection timing was advanced. The reductions were thought to be coupled to the lower C/H ratio in the fuel which in turn reduced the flame temperature and hence the ability to produce NO<sub>x</sub>.

When the cetane number was kept constant, changing the aromatic content had little effect on the combustion characteristics, although increasing the aromatic content resulted in high NO<sub>x</sub> and PM emissions. This was assumed by Kidoguchi et al. (2000) to be associated with the locally rich and high temperature region formed due to various factors. These may include the high adiabatic flame temperature, the difficulty in pyrolysis of HC containing

aromatics as well as the slow physical process such as evaporation and turbulent mixing. However as the injection pressure was raised, the effects of cetane number and aromatic content on particulate emissions become less significant. It was concluded by Nishiumi et al. (2004) that the narrow distillation characteristics using paraffinic fuels simulating F-T diesel fuel (which eliminates heavy HC fraction) could reduce the SOF in PM emissions. The higher cetane number can result in less PM produced as there is a shorter ignition delay and consequently more time for complete combustion and particle oxidation. However, this will compete with the formation of soot resulting from the reduced premixed and increased diffusion phase (Ying et al., 2006, Gill et al., 2011b).

## **2.7 Additives**

As legislation to reduce harmful exhaust emissions and improve fuel economy becomes ever stricter, focus into enhancing fuel properties and engine system designs have been given considerable interest. It is commonly accepted that clean combustion of diesel engines can be fulfilled only if engine development is coupled with catalytic aftertreatment, diesel fuel reformulation or additive introduction (Ulrich and Wichser, 2003). A range of fuel additives are currently used in the automotive industry to enhance the quality of the fuel. The beneficial effects of fuel additives include increased transportability (handling properties, stability and storage), improved viscosity index (reducing the rate of viscosity change with temperature), reduced wear (agents adsorb on to the metal surface providing chemical-chemical contact rather than metal-metal contact), increased temperature range performance of fuels, improved ignition and combustion efficiency and reduced emissions from the combustion fuel. Table 4 outlines the favourable features of fuel additives available in the market today (Infineum, 2012). Generally, additives added to concentrations less than 1% are called functional additives; more than 1% called blending components and much smaller concentrations called

performance additives. Blending components are mainly oxygenates and petroleum fractions, whereas functional and performance additives are mainly mixtures of chemical compounds dissolved in solvents (Infineum, 2012).

In terms of diesel combustion and emissions, the most studied additives are oxygenated and cetane improvers. Although metal additives are also used, their purpose extends to the efficiency of the aftertreatment devices. Catalytic filters (e.g. DPF) for example need to regenerate in order to maintain their effectiveness and to help regenerate the filters metal additives are introduced to lower the soot oxidation temperature and thus enable effective filter regeneration (Ulrich and Wichser, 2003). Additives such as platinum and cerium are commonly used in low concentrations (0.25ppm and 5ppm respectively) for the catalytic oxidation of diesel particulates, where the platinum accumulates onto the filter, oxidising NO to NO<sub>2</sub>, and the cerium catalyses the oxidation of particulates with NO<sub>2</sub> and O<sub>2</sub> (Jelles et al., 2001). Manganese (Mn) is another which is effective in reducing PAH emissions and commonly referred to as a smoke-suppressant additive (Yang et al., 1998). By introducing Mn and magnesium (Mg) metallic additives, fuel properties such as viscosity, cloud point and flash point can be simultaneously improved (Keskin et al., 2011). Metal additives must also be added in fuels along with detergent and lubricity additives to prevent excessive wear from metal contamination of fuel injection and combustion components.

Oxygenated additives have become one of the most promising approaches in improving diesel emissions as well as reducing the ignition temperature of particulates, since addition of these additives to diesel fuel require no modifications to the engine. It has been found in previous studies that the reduction of PM emissions by introducing oxygenated compounds depends on the molecular structure and oxygen content of the fuel, as well as the local oxygen availability in the fuel plume (Miyamoto et al., 1998, Ribeiro et al., 2007). It has been

reported that to reduce PM emissions fuel-compatible oxygen-bearing compounds should be blended with diesel producing a blend containing 10-25% v/v of oxygenate (Marchetti et al., 2003). Although promising, properties such as density, viscosity, volatility, low temperature behaviour and the cetane number will be affected and would require further attention (Ribeiro et al., 2007). However, the presence of some oxygenated additives (e.g. FAME, N-octyl nitramine) result in the formation of a lubricant film with antiwear properties and can be beneficial when using diesel fuel with a low sulphur content ( $< 0.05\%$ ) (Ribeiro et al., 2007).

The cetane number is a critical parameter of the diesel fuel and is used as a measure of ignitability. This parameter is a function of the composition and the structure of the hydrocarbons present in the diesel fuel, decreasing with an increase in aromatic hydrocarbon presence and vice versa with an increase in the n-paraffin and olefin content (Suppes et al., 2000).

The following factors are generally considered when selecting cetane improvers:

- Efficiency towards improving the ignition properties of the fuel
- The hazards associated with storage, handling and transport
- Nitrogen content
- Cost of diluting cetane improvers to allow their safe transport

Out of the commonly used additives listed in Table 4, an effective oxygenate additive has been diglyme (Ren et al., 2008). Apart from gaining a benefit from the oxygen within the fuel, the high cetane number improves the ignition of diesel, decreasing its ignition delay (measured as the time between the start of fuel injection and detectable ignition) resulting in benefits such as a faster start-up in cold weather and reduced  $\text{NO}_x$  emissions.

Table 4: Summary of Fuel Additives

Fuel Additive Types	Function	Typical Concentrations	Examples
<i>Anti-corrosion</i>	Inhibits corrosion of engine, fuel delivery lines and storage tanks.	10 – 20 ppm	Compounds such as surfactants: E.g. Alkenyl succinic acid ester and dimmers from fatty acid phosphoric acid
<i>Antifoaming Agent</i>	Reduces the tendency of the fuel to foam in fuel delivery systems and during re-fuelling.	1 – 10 ppm	Fluorosilicone Silicone co-polymers
<i>Cetane Improver</i>	Improves the fuel's ignitability and thus enhances combustion and reduces emissions.	0.01 – 0.1 %	2-Ethylhexyl nitrate (EHN) Di-tert-butyl peroxide (DTBP) Di-nitrate of the oleic acid methyl ester (MODN)
<i>Cold Flow Improver</i>	Reduces the risk of wax crystals forming when fuels are cooled to temperatures below their cloud points. Additional advantages can also be seen: - Improved low temperature vehicle operation, maintaining maximum power - Decreased risk of clogging fuel lines and filters within engine	50 ppm – 0.1 %	Acrylate or methacrylate-maleic anhydride copolymers: E.g. Ethylene-vinyl acetate (EVA) co-polymer based
<i>De-icer</i>	Prevents the fuel from 'icing' when contaminated by water and subjected to cold conditions.	50 ppm – 0.01 %	–
<i>Demulsibility</i>	These additives are used to prevent water contamination within the fuel.	60 – 80 ppm	Polyglycols Polyamines Alkoxyated phenols

<i>Detergency</i>	<p>These types of additives prevent the build-up of carbonaceous waste products on fuel injector nozzles and in the combustion chamber leading to the following benefits:</p> <ul style="list-style-type: none"> <li>- No loss in power</li> <li>- Avoids increase in emissions</li> <li>- Ensures the correct fuel injection spray pattern occurs</li> </ul>	-	Based on polyisobutylene succinimide (PIBSI)
<i>Fuel Stabilisation (Anti-Oxidation)</i>	<p>These additives prevent the oxidative degradation of fuels, and thus allow the fuel to be stored for longer without a compromise in quality.</p>	10 – 15 ppm	<p>Butylated hydroxytoluene (BHT)</p> <p>Tert-Butylhydroquinone (TBHQ)</p> <p>Propyl gallate</p> <p>Pyrogallol</p>
<i>Lubricity Improvement</i>	<p>To protect fuel injection and combustion components from excessive wear.</p> <p>Although naturally occurring lubricity elements can be found in sulphur, alternatives will need to be considered as regulations are in place limiting sulphur in diesel fuel.</p>	25 ppm – 0.05 %	<p>FAME, monoacylglycerols and glycerol</p> <p><i>Chemical Groups:</i></p> <p>Carboxylic acid, Carboxylic acid ester, Carboxylic acid amide</p>
<i>Metal Based</i>	<p>Some metal additives are effective in reducing diesel emissions (Yang et al., 1998). This can occur either by:</p> <ul style="list-style-type: none"> <li>- The metals reacting with H<sub>2</sub>O to produce hydroxyl radicals enhancing soot oxidation (Kasper et al., 1999)</li> <li>- The metals reacting directly with carbon atoms in the soot lowering the oxidation temperature (Miyamoto et al., 1987)</li> </ul>	10 ppm	<p>Manganese, iron, copper, barium, cerium, calcium and platinum</p>

<i>Oxygenates</i>	Used to reduce smoke, CO and HC emissions by ensuring a more complete combustion of fuel occurs. This is achieved by using an additive with large oxygen content.	–	Dimethoxymethane (DMM), Diglyme (DGM), Dimethyl carbonate (DMC), Diethyl carbonate (DEC) and Diethyl adipate (DEA)
-------------------	---	---	--

## 2.8 Summary

Although there have been significant advances as described in this chapter for the control of diesel exhaust gas emissions, more advanced systems will need to be developed to meet the long-term emission targets. Better control of the NO<sub>x</sub>/PM trade-off, especially during EGR, will need to be developed either through individual or a combination of engine calibration, cleaner fuels and exhaust gas aftertreatment. Cold start behaviour of not only the fuels but also the catalysts will push for faster light-off systems that are capable of working under low exhaust gas temperatures while keeping a good compromise between efficiency, cost and emissions. Current aftertreatment systems are at a stage of optimisation and cost reduction, with the aim of minimising fuel penalty and the need for precious metal catalysts.

Silver-alumina for instance has been and is currently one of the most widely researched catalysts for lean NO<sub>x</sub> reduction, however there are still many obstacles that need to be solved before such systems are made commercially available. For example, poor low temperature activity and coking of the catalyst are two of the main problems currently faced with silver catalysts. Although there have been numerous studies showing hydrogen promoting the catalyst activity and various reductants being active over the catalyst, the methods to implement these on-board the vehicle need to be made practical.

Diesel particulate filters have proven to be highly effective with significantly high trapping efficiencies; however the regeneration strategies are still a major concern. Better controlled regeneration methods are required to ensure minimal effect on exhaust back pressure and long-term damage to the filters. Possible solutions will involve looking further into passive mode and continuous regeneration systems while trying to gain better control of the NO<sub>x</sub> and PM emissions from combustion and EGR.

Many studies have shown comprehensively that there is a very large, still unexploited potential for improvements in road fuels. These will provide major reductions in pollutant emissions both in vehicles already on the road as well as in future vehicles. High cetane (i.e. purely paraffinic), clean fuels improve combustion and reduce emissions drastically in modern diesel engines without impairing engine performance (noise, fuel consumption and power). The challenge therefore is to increase substantially the production of biofuels by using innovative feedstock, processes and technologies, which are both competitive and sustainable. Further, substituting hydrocarbons by carbon-free fuels (e.g. H<sub>2</sub>, NH<sub>3</sub>) could provide an effective strategy for the progressive decarbonisation of internal combustion (IC) engines during the long transition to electric powertrains. However, their implementation as a transportation fuel continues to be fraught with technical and economic challenges, relating mainly to its distribution and on-board storage. Although significant efforts are being made to make renewable energy economically viable as well as use cleaner fuels, additives will always play an important role due to their wide range of attributes.

## CHAPTER 3

### EXPERIMENTAL SETUP

The equipment that was used during the experimental stage of this research thesis is introduced in this chapter. This includes the diesel test engine, emission analysers, the catalysts and filters as well as the reactors to accommodate them.

#### 3.1 Test Bench Engine & Instrumentation

The experimental engine test rig as shown in Figure 12 consists of an air cooled Thring Titan thyristor-type DC electric dynamometer coupled to a load cell to load and motor the engine. The engine is a single cylinder, direct injection diesel engine equipped with an externally cooled EGR system. The standard injection timing is 22 Crank Angle Degree (CAD) Before Top Dead Centre (bTDC) as set by the manufacturer. The technical data and engine characteristics are given in Table 5. It is important to note that the experimental engine used in this study uses a pump-line-nozzle fuel injection system, where the physical properties of the fuel (such as density or compressibility) are expected to affect the injection process to a greater extent than under other more modern systems (e.g. common rail). This is because the injectors remain closed until the pressure wave generated in the high pressure pump propagates along the fuel lines and reaches the injectors. The propagation of the wave depends directly on those fuel properties. A Romet rotary airflow meter combined with a shaft encoder and a tachometer were introduced to measure the air flow into the engine. Thermocouples (given range of 0-1250°C with an accuracy of  $\pm 2.2^\circ\text{C}$ ) and pressure transducers are positioned around the engine to monitor the engine inlet, exhaust and oil conditions. To ensure consistency between tests the engine was warmed up prior to testing

with the atmospheric conditions such as temperature and pressure within the test cell monitored for the duration of each test. In addition the temperature of the air intake supply was controlled to approximately 22-25°C.

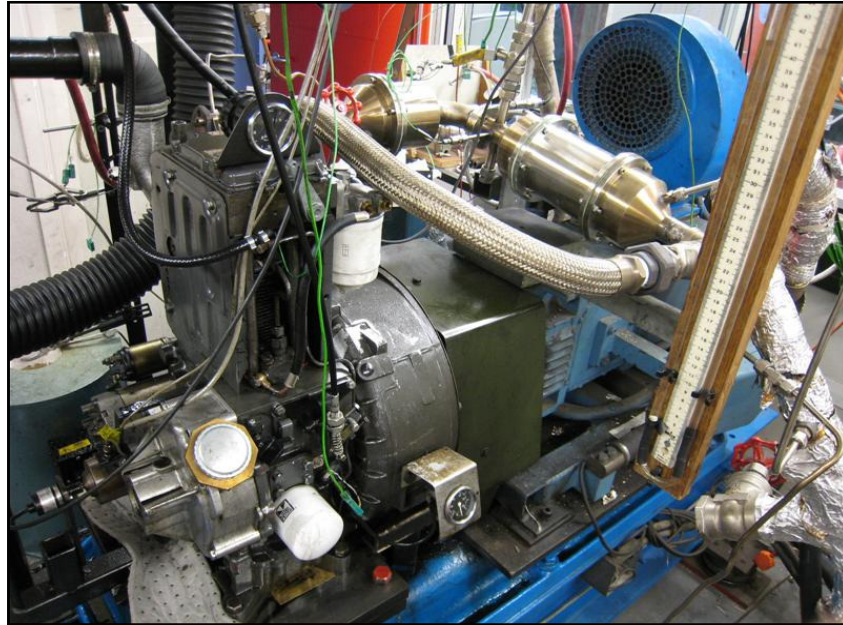


Figure 12: Single Cylinder Diesel Engine Test Rig

The exhaust gas was recycled from the engine exhaust to the inlet (external cooled EGR), with the EGR ratio determined volumetrically as a percentage reduction in volume flow rate of air at a fixed engine operating point, as defined by Equation 1:

$$\text{Equation 1: } \mathbf{EGR (\%Vol.) = \left( \frac{\dot{V}_o - \dot{V}_i}{\dot{V}_o} \right) \times 100}$$

Where  $\dot{V}_i$  and  $\dot{V}_o$  are the measured intake air volume flow rates with and without EGR respectively. According to Ladommatos et al. (2000), implementing cool EGR tends to ameliorate the reduction in engine volumetric efficiency and the associated reduction in the inlet charge mass rate. Hence this stops the increase in PM emissions.

Table 5: Test Engine Specifications

Engine Specification	Data
Number of Cylinders	1
Bore/Stroke	98.4mm/101.6mm
Connecting Rod Length	165mm
Displacement Volume	733cm <sup>3</sup>
Compression Ratio	15.5:1
Rated Power (kW)	8.6@2500rpm
Peak Torque (Nm)	39.2@1800rpm
Injection System	Three holes pump-line-nozzle
Injection Timing (°bTDC)	22
Maximum Injection Pressure (bar)	180
Engine Piston	Bowl-in-piston

The in-cylinder pressure traces were acquired using a Kistler 6125B quartz type pressure transducer with a Kistler 5011 charge amplifier at crank shaft positions determined using a 360-ppr incremental shaft encoder (Baumer BDK 1605A360-5-4). The data acquisition and combustion analysis were carried out using in-house (University of Birmingham) developed LabVIEW software running a National Instruments (PCI-MIO-16E-4) data acquisition board. Output from the analysis of engine cycles included the in-cylinder pressure, indicated mean effective pressure (IMEP), percentage coefficient of variation (COV) of IMEP values and percentage COV of peak cylinder pressures, average crank angle for ignition delay, and other combustion characteristic information. To help eliminate the problems caused by random events and noise in the data signals and acquisition system, the data is collected for a number of cycles (i.e. 100) and then averaged. The COVs of IMEP and peak cylinder pressure were used as criteria for combustion stability (cyclic variability). The COV defines the cyclic variability in indicated work per cycle. There are many phenomena

which cause cycle to cycle fluctuations in the combustion heat and among the many these include frictional losses, adiabatic imperfections and turbulence in the working fluid (Heywood, 1988). Therefore these variations in cylinder pressure can affect the vehicle driveability.

### 3.2 Data Processing

The apparent heat release rate  $\frac{dQ}{d\theta}$  was calculated using the following equation (Heywood, 1988):

**Equation 2:** 
$$\frac{dQ}{d\theta} = \frac{\gamma}{\gamma-1} p \frac{dV}{d\theta} + \frac{1}{\gamma-1} V \frac{dp}{d\theta}$$

Where,  $\gamma$  is the ratio of specific heats ( $C_p/C_v$ ),  $p$  is the instantaneous in-cylinder pressure and  $V$  is the instantaneous engine cylinder volume. The values of  $\gamma$  are calculated by interpolation based on the actual p-V diagrams.

In this study the emissions have been calculated using the indicated power ( $P_{Ind}$ ) based on the IMEP, rather than using the brake power ( $P_b$ ) measured with the dynamometer:

**Equation 3:** 
$$P_{Ind}(kW) = \frac{IMEP \times V_d \times N \times k}{1000}$$

Where  $N$  is the engine speed in revolutions per second (rps) and  $k$  is a constant ( $\frac{1}{2}$  for a 4-stroke engine).  $V_d$  ( $m^3$ ) is the displaced volume and can be calculated as follows:

**Equation 4:** 
$$V_d = A \times L \times n$$

Where  $A$  ( $m^2$ ) is the piston area,  $L$  (m) is the stroke length and  $n$  is the number of cylinders.

The IMEP is the ideal average output pressure over a cycle of the engine calculated only from the cylinder pressure and can be determined using the following equation, where  $p$  and  $V$  represent the in-cylinder pressure and corresponding cylinder volume respectively:

**Equation 5:** 
$$IMEP = \frac{\text{Indicated Work per Cycle}}{\text{Displaced Volume}} = \frac{\oint p dV}{V_d}$$

The indicated specific fuel consumption (ISFC, in g/ikWh) is the mass fuel flow rate ( $\dot{m}_{\text{Fuel}}$ ) per unit power output and can be calculated using the following equation:

**Equation 6:** 
$$ISFC (g/ikWh) = \frac{\dot{m}_{\text{Fuel}}}{P_{\text{Ind}}}$$

In practice the exhaust gas of an internal combustion engine consists of both complete (e.g. CO<sub>2</sub> and H<sub>2</sub>O) and incomplete (e.g. CO, unburned HC's, soot) combustion products. Although the incomplete combustion products in a lean combustion engine are small, it is useful to define the combustion efficiency ( $\eta_c$ ). This can be defined as the actual heat produced during combustion as a fraction of the total heat potential of the fuel supplied:

**Equation 7:** 
$$\eta_c = (\dot{m}_{\text{Fuel}} \times LCV_{\text{Fuel}} - \dot{m}_p \times LCV_p) / (\dot{m}_{\text{Fuel}} \times LCV_{\text{Fuel}})$$

Where  $\dot{m}_r$  and  $\dot{m}_p$  (kg/s) represent the mass flow rates of the reactants (fuel) and products, respectively; while  $LCV_r$  and  $LCV_p$  (MJ/kg) represent the lower calorific values of the reactants and products, respectively.

Another important parameter is the engine thermal efficiency ( $\eta_{th}$ ), defined as a measure of how much heat energy released from the fuel is converted into mechanical work. Thus the greater the thermal efficiency the more power the engine is able to deliver for a given amount of fuel flow rate and is usually expressed by the following equation:

$$\text{Equation 8: } \eta_{th} = P_{Ind}/(\dot{m}_{Fuel} \times LCV_{Fuel})$$

### 3.3 Catalysts

The following section describes the catalysts and filters that were used as part of this research study, which were provided by Johnson Matthey Plc. The gas hourly space velocity (GHSV) is defined as the volumetric flow rate of the reactant feed (i.e. exhaust gas) divided by the external volume of the monolith catalyst (Equation 9). As a result the unit for GHSV is the reciprocal of time expressed as  $h^{-1}$ .

$$\text{Equation 9: } GHSV (h^{-1}) = \frac{\text{Gas flowrate over catalyst } \left(\frac{m^3}{h}\right)}{\text{Catalyst volume } (m^3)}$$

The HC-SCR catalyst was a silver catalyst (2wt.%) prepared by impregnating  $\gamma$ -alumina (surface area  $\sim 150m^2/g$ ) with aqueous silver nitrate ( $AgNO_3$ ) before drying and calcining in air for 2h at  $500^\circ C$ . The catalyst was made into an aqueous suspension, which was then uniformly coated onto ceramic monolith substrates ( $\varnothing = 115mm$ ,  $L = 75mm$ ) with a high cell density (600cps). Among the SCR catalysts available, the  $Ag-Al_2O_3$  catalyst with a 2wt.% Ag loading has been proposed as the most promising for the reduction of  $NO_x$  based on its high activity and selectivity (Masuda et al., 1996, Burch et al., 2004, Lindfors et al., 2004). The following equation shows how the  $NO_x$  reduction activity over the HC-SCR catalyst was determined:

$$\text{Equation 10: } NO_x \text{ Conversion} = \left( \frac{inNO_x - outNO_x}{inNO_x} \right) \times 100$$

The DOC was prepared by impregnating a low loading supported platinum based catalyst coated onto a cordierite honeycomb monolith substrate ( $\varnothing = 115mm$ ,  $L = 75mm$ ) with a high cell density (600cps). The precious metal formulated catalyst is designed to

oxidise CO, gas phase hydrocarbons and the SOM fraction of the diesel particulate matter to CO<sub>2</sub> and H<sub>2</sub>O.

A reforming catalyst with a nominal composition of 1wt.%Rh/CeO<sub>2</sub>-ZrO<sub>2</sub> (by weight) was prepared by impregnating 50g of 50:50 (mole basis) ceria-zirconia (CeO<sub>2</sub>-ZrO<sub>2</sub>) powder with 30cm<sup>3</sup> of an aqueous solution of rhodium nitrate (Rh(NO<sub>3</sub>)<sub>3</sub>) containing 0.5g Rh. The impregnated powder formed a slurry, which was dried at 120°C for 8 hours, before being calcined in static air at 500°C for 2 hours. The reforming catalyst was made into an aqueous suspension, which was uniformly coated onto ceramic monolith substrates with a high cell density (900cps). The catalyst is a Johnson Matthey proprietary formulation designed to promote the main reactions such as oxidation, SR and WGS as shown in earlier research publications (Tsolakis et al., 2007a, Sitshebo et al., 2009). Further, Rh-based monolithic catalysts have proven to be very active for ATR of diesel fuel, showing high selectivity and good durability (Nilsson et al., 2008) while Ceria has also been reported to be a promoter of the WGS and SR reactions (Whittington et al., 1995). Two ceramic honeycomb diesel particulate filters were used (Ø = 58mm, L = 153mm with a channel cell density of 300cps), with one coated with platinum group metals (PGM) and denoted as a cDPF in this study. Figure 13 shows an example of a catalysed flow-through monolith and a wall-flow DPF.

During each of the tests, the filters and monolith catalysts were retained in the exhaust/mini reactor using an intumescent mat. The vermiculite in the mat exfoliates when heated and permanently retains the monolith in place. Figure 14 shows a typical mini reactor designed to test catalyst activity under controlled real diesel exhaust gas compositions. The mini reactor is positioned inside and heated by a tubular furnace, whose temperature is set to simulate that of the engine-out exhaust and controlled by means of a thermocouple positioned at the inlet of the reactor, 5mm upstream the catalyst inlet.

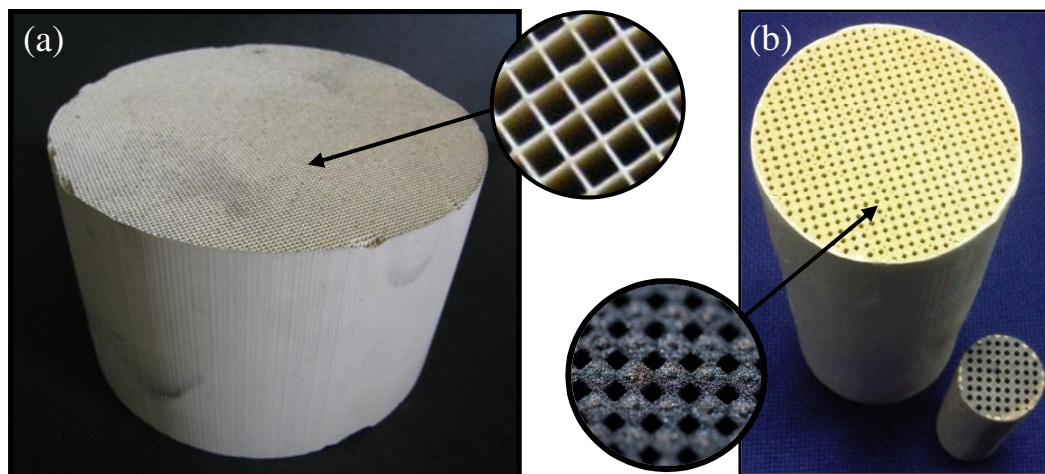


**Figure 13: a) Honeycomb Monolith Substrate with the Catalyst Formulation Coated onto the Channel Walls, b) Diesel Particulate Filter**

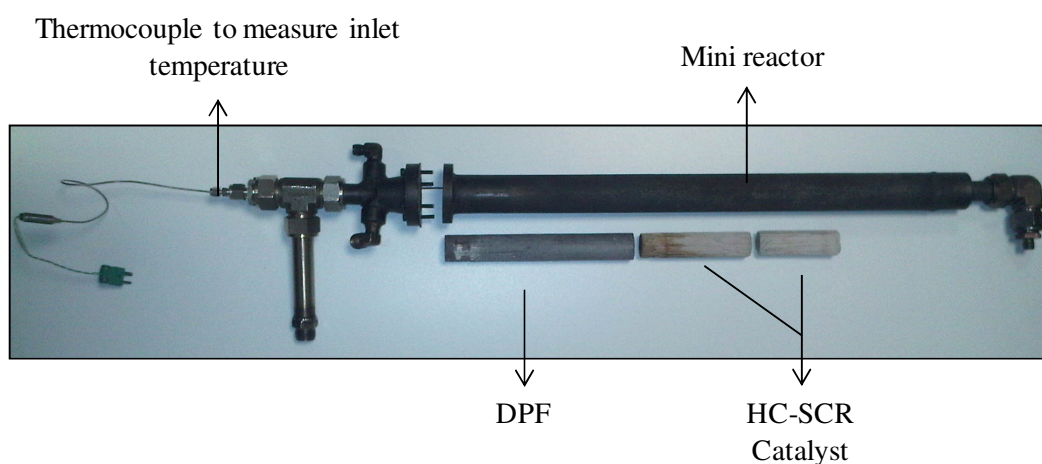


**Figure 14: Example of a Mini Reactor Configuration**

### 3.4 Liquid and Gaseous Fuels

The base fuels used in the following studies were Ultra Low Sulphur Diesel (ULSD) and RME provided by Shell Global Solutions UK. The fuel component Bis (2-methoxyethyl) ether commonly known as Diglyme (DGM) was obtained from Sigma-Aldrich, an anhydrous component with purity of 99.5%. Diglyme is synthesised commonly from ethylene oxide and methanol with production of over a million pounds per year in the United States. It has high  $O_2$  content, good intersolubility with diesel fuel, high cetane number, a freezing point of -

68°C and a boiling point of 162°C. Diglyme is used primarily as a reaction solvent or process chemical (2003). The fuels specifications and properties are listed in Table 6. The gaseous fuels (i.e. H<sub>2</sub> and the dissociated NH<sub>3</sub> mixtures) used in this study were provided by BOC with certified purity levels of  $\geq 95\%$ .

**Table 6: Diesel and RME Fuel Properties**

Fuel Analysis	Diesel (ULSD)	Biodiesel (RME)	Diglyme (DGM)
Chemical Formula	C <sub>14</sub> H <sub>26.18</sub>	C <sub>18.96</sub> H <sub>35.29</sub> O <sub>2</sub>	C <sub>6</sub> H <sub>14</sub> O <sub>3</sub>
Cetane Number	53.9	54.7	126
Density at 15°C (kg/m <sup>3</sup> )	827.1	882.54	937.0
Viscosity at 40°C (cSt)	2.467	4.478	-
LCV (MJ/kg)	43.3	37.4	26.4
Sulphur (mg/kg)	46	5	-
Total Aromatics (% wt)	24.4	-	-
C (wt.%)	86.44	77.12	53.71
H (wt.%)	13.56	12.04	10.52
O (wt.%)	0	10.84	35.77

### 3.5 Exhaust Gas Analysing and Measuring Equipment

A Horiba MEXA 7100DEGR gas analyser was used to take measurements of CO<sub>2</sub> and CO by Non-Dispersive Infrared (NDIR), O<sub>2</sub> by a magnetopneumatic method, NO<sub>x</sub> by chemiluminescence detection (CLD) and HC by flame ionisation detection (FID). For the measuring range, resolution and accuracy of the equipment refer to Appendix A: Table 18 and Table 19.

A MultiGas 2030 FTIR spectroscopic analyser was used to measure the other major gas phase species, including H<sub>2</sub>O, N<sub>2</sub>O, NH<sub>3</sub> and diesel emissions already measured with the

Horiba MEXA 7100DEGR to remove experimental bias. For the measurement specifications refer to Appendix A: Table 20.

A Real-time Horiba MEXA 1230PM was used to measure soot by a diffusion charging (DC) method and soluble organic material (SOM) by a dual FID method equipped with a 47mm diameter Teflon (PTFE)-coated (PALLFLEX) glass fibre filter. The soot concentration is calculated by diluting the sample with an ejector pump and measuring the electrical current of ions attached onto the surface of charged particles. Hot dilution was considered to prevent nuclei mode, with the dilution ratio of the soot diluter set to approximately 40. The SOM concentration is based on the amount of gaseous HC compounds that vaporise and is calculated as the difference between the signals of the FIDs, with one FID using a sample line of 47°C and the other FID with a sample line 191°C. The final result is expressed in terms of SOM as the equipment is pre-calibrated to soluble organic material using a soxhlet extraction method (Fukushima et al., 2000). For the performance of the equipment refer to Appendix A: Table 21. The SOF can be expressed in the following way:

**Equation 11:** 
$$SOF = \frac{SOM}{(Soot + SOM)}$$

The total particulate mass and number concentration measurements were carried out using a TSI Scanning Mobility Particle Sizer (SMPS). This is comprised of an electrostatic classifier series 3080, a 3081 Differential Mobility Analyser (DMA) and a model 3775 Condensation Particle Counter (CPC). The CPC that forms part of the SMPS system has a particle count accuracy of  $\pm 10\%$  for particle concentrations lower than  $5 \times 10^4$  particles/cm<sup>3</sup> and  $\pm 20\%$  for particle concentrations lower than 107 particles/cm<sup>3</sup>. The sample and sheath flow rates were set such that the measurement (diameter) range was nominally either 12-437nm or 14-670nm, with the dilution ratio set to 200:1 using a heated rotating disc diluter

(150°C). The temperature controlled dilution process minimised the possibility of any HC condensation and nucleation which can occur during sampling. The size distributions of the particles in the exhaust represented a mixture of fine, ultrafine, and nanoparticles based on their mobility diameter. The particle number and size distributions were converted to a particle mass distribution by using the effective particle density exponential function formulated by Lapuerta et al. (2003). This allowed an effective density value to be assigned to each particle diameter as a function of their size. Hence the diesel exhaust particle densities gradually decrease from smaller primary soot particles to larger agglomerate particles from 1.55-0.155g/cm<sup>3</sup> in the equivalent diameter interval 0.03-1.0µm.

H<sub>2</sub> concentrations were measured by sampling the gas-stream through a Hewlett-Packard (HP) gas chromatograph (GC) equipped with a thermal conductivity detector (TCD). Higher TCD sensitivity to H<sub>2</sub> was achieved by using argon as the carrier-gas flowing through two separation columns. The first column was 1m long with a 1/8-in. diameter Haysep Q, 80-100 mesh. The second column was a 2m long 1/8-in. diameter Molesieve 5Å (MS5A). The H<sub>2</sub> chromatogram area was measured using a HP 3395 integrator. In order to determine the concentration of H<sub>2</sub> present in the gas sample, the equipment was first calibrated using a certified gas mixture composed of 30% H<sub>2</sub> balance N<sub>2</sub>, thus giving an area plot from the integrator representative of 300,000 ppm H<sub>2</sub> (i.e. 30% by volume). Another area plot was then obtained once the actual gas sample was taken. Using these readings the actual H<sub>2</sub> concentration was determined by extrapolation. Several samples were taken and averaged before the final value of H<sub>2</sub> was used. Further, the sampling line to the various analysers was heated up to 191°C to avoid HC condensation in the line.

PM was collected on 47mm diameter glass micro-fibre filters (Whatman - without Teflon coating) using an in-house built venturi nozzle diluter with the dilution ratio set at

10:1. This involved drawing cooled diluted gas through the filter held in place by a filter holding plate and filter stopper (Figure 15) at 10 l/min for 1 hour. A PerkinElmer (Pyris 1 TGA) thermogravimetric analyser was used to analyse the PM composition (soot and VOF). The sample was heated in the TGA according to the method listed in Table 7. A slow 3°C/min ramp under an atmosphere of N<sub>2</sub> was employed to allow sufficient time for the vaporisation of the VOF. However before O<sub>2</sub> was introduced, the furnace temperature was cooled down to 350°C to broaden the soot oxidation window. The maximum temperature reached in air atmosphere to oxidise the remaining soot was set to 600°C as at higher temperatures (> 650°C) the filter itself began to decompose. Additional technical data of the TGA is given in Appendix A: Table 22.

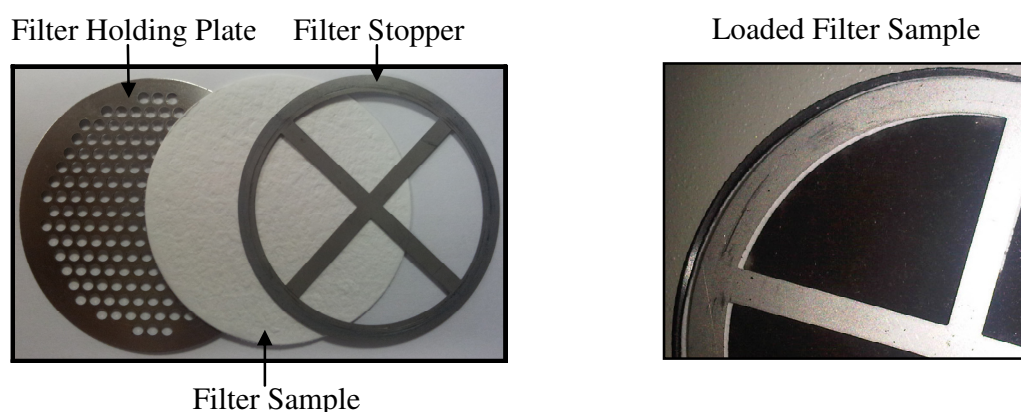


**Figure 15: Filter Set**

**Table 7: TGA Heating Programme**

1	Initial Atmosphere: Nitrogen
2	Hold for 10 min at 40°C
3	Heat from 40°C to 400°C at 3.00°C/min
4	Hold for 30 min at 400°C
5	Cool from 400°C to 350°C at 3.00°C/min
6	Changing Atmosphere: Air
7	Heat from 350°C to 600°C at 3.00°C/min
8	Hold for 60 min at 600°C

### **3.6 Other Parameters and Equipment**

The exhaust system aftertreatment devices are a source of engine back pressure and as a result can cause increased emissions, increased fuel consumption and have a negative impact on the performance of the engine. Therefore a system was implemented which enabled manual control of the exhaust back pressure. In order to study the low temperature passive regeneration and soot deposition (i.e. pressure drop and loading) across the DPF, two Cole-Parmer<sup>®</sup> high-accuracy pressure transducers (K-68074-02) were used in combination with PicoLog software (accuracy of  $\pm 0.13\%$  full scale) giving a real-time measurement of the pressure drop. These specific transducers were used as they offered resistance to electromagnetic interference and are capable of withstanding vibration and high shock applications.

# CHAPTER 4

## ENHANCING THE PERFORMANCE OF AN Ag-Al<sub>2</sub>O<sub>3</sub> CATALYST FOR LEAN NO<sub>x</sub> REDUCTION IN DIESEL ENGINE EXHAUSTS

### 4.1 Introduction

The key aim of this study is to observe the benefits of practical and viable methods for on-board vehicle H<sub>2</sub> production for low temperature lean NO<sub>x</sub> reduction over an Ag-Al<sub>2</sub>O<sub>3</sub> catalyst. The approach considers H<sub>2</sub> production through the dissociation of anhydrous NH<sub>3</sub> forming a gaseous mixture representative of 1-2%NH<sub>3</sub> + 75%H<sub>2</sub> + 23-24%N<sub>2</sub>. It is also known that NH<sub>3</sub> is readily available, as well as its storage, production, handling and distribution facilities already well established worldwide (Saika et al., 2006). The main focus of this approach was to observe any variations in the catalyst activity as a result of the residual NH<sub>3</sub> in the H<sub>2</sub> feed under passive HC-SCR (i.e. no externally added hydrocarbons into exhaust). This work also involves looking into a combined DPF-SCR system with the influence of H<sub>2</sub> and HC:NO<sub>x</sub> ratio.

All tests were steady state with an engine speed of 1500rpm used throughout the experiment; with an engine load of 3 bar IMEP. Two 25.4mm diameter HC-SCR catalysts were cored from a monolith and placed one after the other for a greater active site length in a reactor linked to the exhaust tailpipe of the engine; downstream of the H<sub>2</sub> addition point. An uncatalysed SiC-DPF was also positioned in front of the HC-SCR catalysts to trap the carbonaceous species from blocking the active sites. The reactor was placed in a tubular furnace with the temperature set to simulate that of the engine-out exhaust (i.e. 250°C unless

otherwise stated). The GHSV over the total catalyst length was approximately 30,000h<sup>-1</sup>. Thus under passive, low temperature conditions (< 250°C), earlier studies have indicated that the formation of surface soot will be more favourable than its oxidation resulting in fouling of the catalyst by coking (Theinnoi et al., 2007). The experimental apparatus is detailed and illustrated in Figure 16.

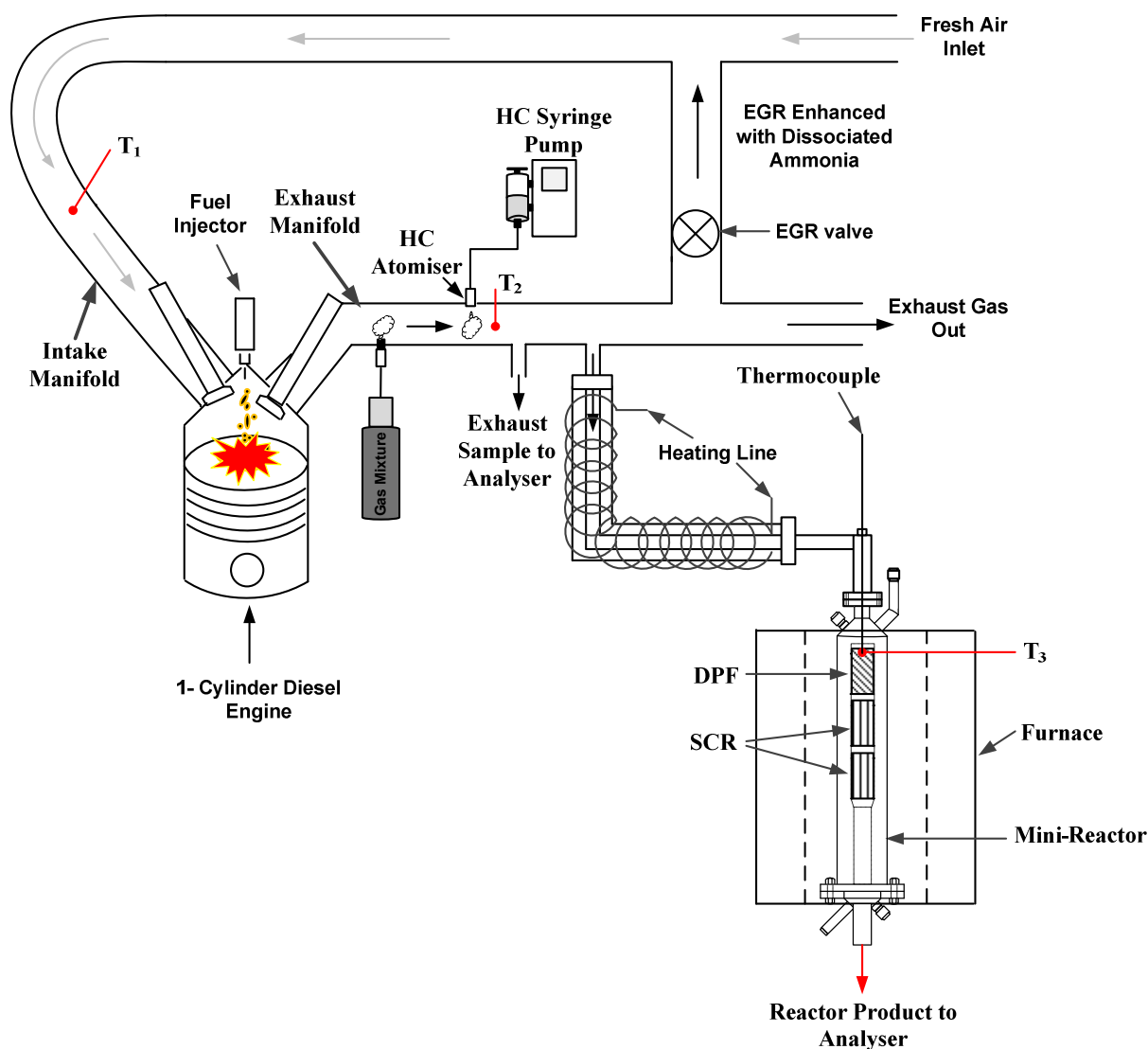


**Figure 16: Schematic of Dissociated NH<sub>3</sub> with HC-SCR System**

## **4.2 Results and Discussion**

The following section has been split up to give an overview of how the catalyst behaves in the presence of H<sub>2</sub> and an upstream DPF. Comparisons will be made with and without 20%Vol.EGR under both passive and active modes (i.e. HC injection). Once these preliminary tests have been presented, the main part of the work will follow showing the results of the 1% and 2% non-dissociated NH<sub>3</sub> mixtures.

### **4.2.1 The effect of a DPF on the overall passive-SCR activity and NO<sub>x</sub> reduction performance**

Before the catalytic tests were carried out all the catalysts were pre-treated at 550°C in air for 2 hours. In the presence of 20%Vol.EGR the engine-out NO<sub>x</sub> concentration is lower and is therefore partially responsible for the NO<sub>x</sub> conversion improvement over the catalyst and is not an accurate representation of the catalyst performance. Therefore in order to observe the actual catalyst performance, the effect of EGR on the overall system NO<sub>x</sub> reduction was omitted and a direct reflection of the catalyst activity was obtained.

Figure 17 gives a good overview of how an Ag-Al<sub>2</sub>O<sub>3</sub> lean NO<sub>x</sub> catalyst performs in the presence of actual diesel exhaust gas without the presence of an upstream DPF. As shown, the catalyst performance without any H<sub>2</sub> addition (i.e. illustrated as baseline) is approximately 15%. However, this activity soon decays over time indicating that the catalyst itself is deactivating. Incorporation of EGR technology can increase the HC:NO<sub>x</sub> ratio by increasing HC's and by significantly reducing the NO<sub>x</sub> concentration in the engine exhaust gas. However, this will result in an increase in engine-out soot. This has a significant impact on the catalyst performance as the activity further deteriorates to < 5%, highlighting that the catalyst has been subjected to coking with a very poor tolerance to EGR.

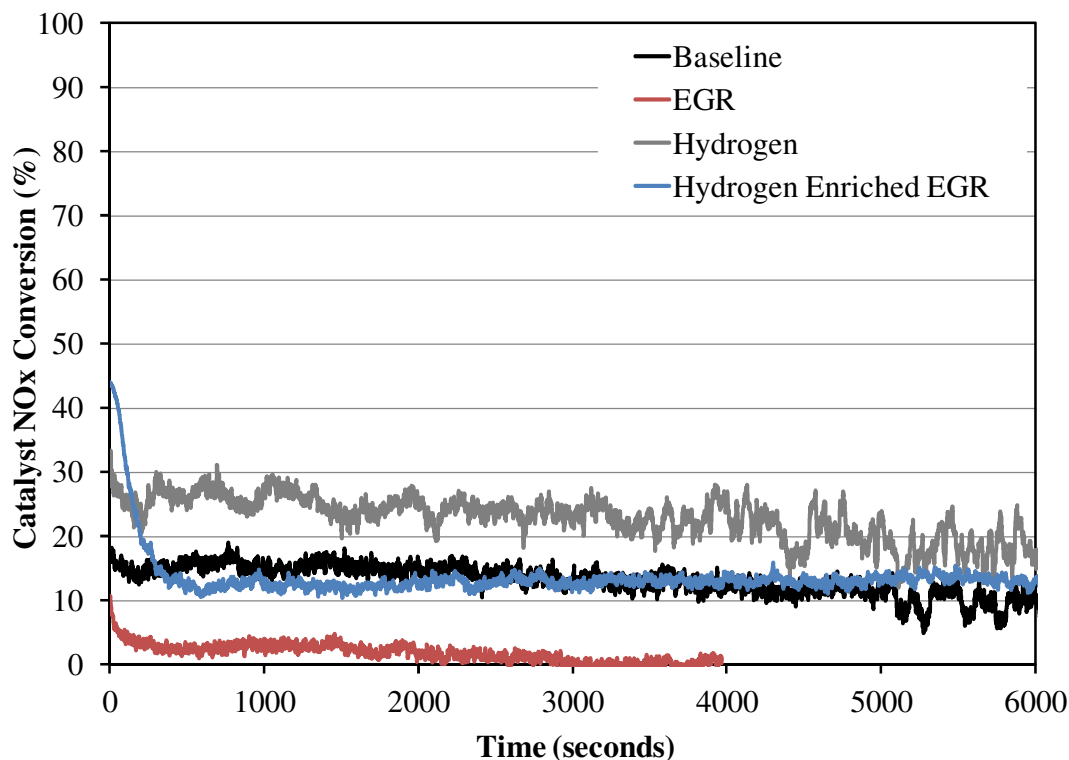
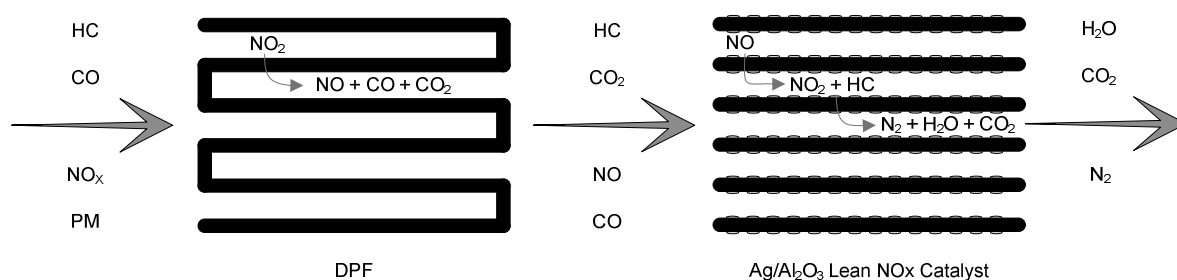


Figure 17: Enhancing Catalyst Performance with 8000ppm H<sub>2</sub>

Although the addition of H<sub>2</sub> (8000ppm) upstream the catalyst is promising, the beneficial impact is outweighed by the reduction in active sites as a result of catalyst coking. The choice of using 8000ppm H<sub>2</sub> is based on the results shown later in this study. Furthermore this will also allow a direct comparison to be made within the individual results. By introducing EGR in the presence of H<sub>2</sub> (i.e. hydrogen enriched EGR), the overall exhaust gas composition alters. As a result, the small concentration of H<sub>2</sub> (after dilution with the intake) will promote the diffusion phase combustion resulting in a higher NO<sub>2</sub>/NO<sub>x</sub> ratio while the lower in-cylinder temperatures will promote the HC:NO<sub>x</sub> ratio. As shown in Figure 17, the enhanced exhaust gas composition promotes a more stable catalyst, although the NO<sub>x</sub> conversion is lower than that of H<sub>2</sub> alone (without EGR). This could be a result of either the lower O<sub>2</sub> content or increased non-reactive unburned HC present in the exhaust. In both cases with and without EGR, the H<sub>2</sub> concentration available to the catalyst was 8000ppm. This

ensured the catalyst effect with EGR was the direct result of the engine-out emissions and not caused through a change in H<sub>2</sub> availability. Therefore in the presence of EGR the addition of H<sub>2</sub> was controlled to consider any H<sub>2</sub> left over from combustion.

In order to restrict some of the carbonaceous species from blocking the catalyst active sites, a DPF was positioned upstream the lean NO<sub>x</sub> catalyst. Figure 18 gives a model representation of the emission control over the combined aftertreatment system.



**Figure 18: Generalised Emission Conversion over a DPF-SCR System**

As shown in Figure 19, the NO<sub>x</sub> reduction activity remains more stable and consistent over time. This confirms that soot is a major participant in the catalyst deactivation. The influence of H<sub>2</sub> without EGR gives an overall 30% steady catalyst NO<sub>x</sub> conversion, while with EGR this conversion falls by approximately 5% resulting from the reduced exhaust O<sub>2</sub> concentration. This is also the case in the absence of H<sub>2</sub>. Therefore the catalyst performance has actually been reduced but to a lesser extent than without a DPF highlighting an improved tolerance to EGR.

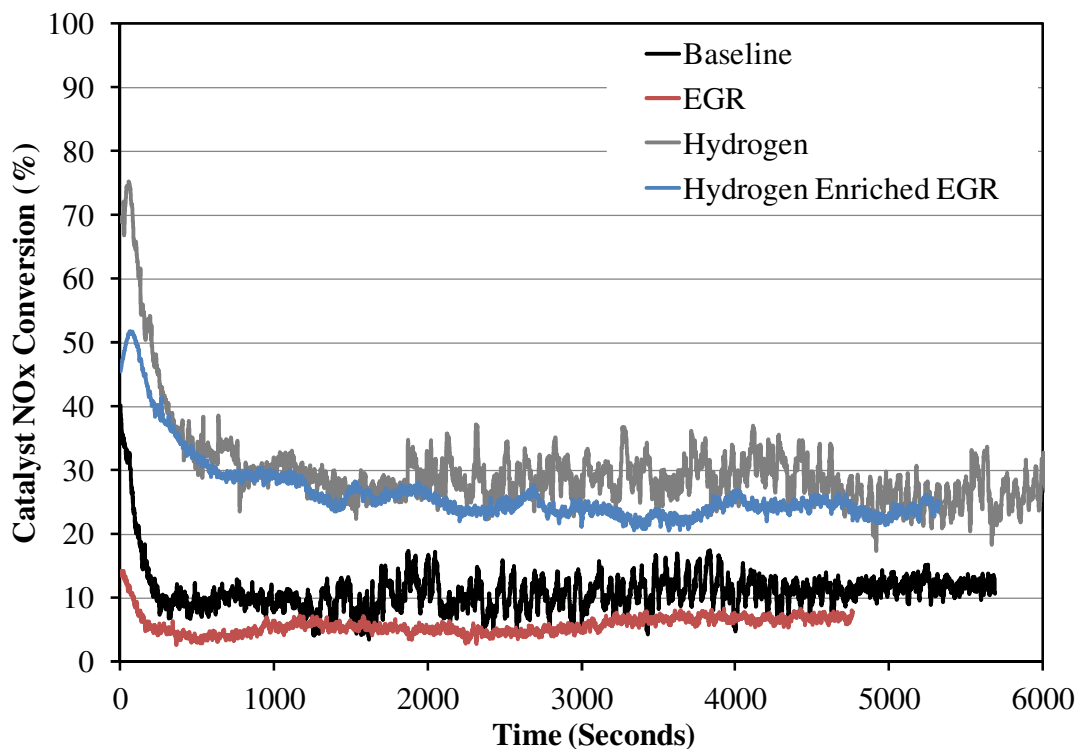


Figure 19: Enhancing Catalyst Performance with 8000ppm H<sub>2</sub> and Upstream DPF

Overall this indicates that the removal of agglomerated solid carbonaceous material (i.e. soot) promotes a clean catalyst. The implementation of both a DPF and lean NO<sub>x</sub> catalyst can combine effectively to promote a simultaneous PM and NO<sub>x</sub> reduction system. At this point we have observed the benefit of H<sub>2</sub> and to further investigate the impact of the HC:NO<sub>x</sub> ratio, an active approach needs to be investigated (i.e. the addition of external HC).

#### 4.2.2 Active mode HC-SCR in the presence of H<sub>2</sub> and a DPF

It has been previously reported that by using long-chained hydrocarbons the SCR reaction can proceed with a wider activity window under low exhaust temperatures in comparison to shorter hydrocarbons. It was suggested that the reason was related to the lower activation temperature of the longer hydrocarbons, thus the hydrocarbon activation is a key factor for NO reduction activity on Ag-Al<sub>2</sub>O<sub>3</sub> (Eränen et al., 2004, Shimizu et al., 2000, Shimizu et al., 2001). Although long chain alkanes such as diesel fuel improve the low

temperature catalyst activity, it has been reported that the catalyst can become poisoned under low exhaust temperatures as a result of deposited carbonaceous species (Theinnoi et al., 2007, Houel et al., 2007a). Further studies have also reported the deactivation is not only a result of the C-containing species but also the nitrate formation and accumulation. Therefore, the low temperature limitations need to be resolved before this NO<sub>x</sub> abatement system can become commercially viable (Lindfors et al., 2004).

The following section demonstrates how the catalyst is more active under HC injection and stable in the presence of the upstream DPF. In general, the diesel exhaust has a small quantity of HC which may not be sufficient for good NO<sub>x</sub> reduction activity (i.e. passive mode). Therefore additional HC, ideally injecting diesel fuel itself, will promote the HC:NO<sub>x</sub> ratio. However, it has also emerged that excess HC in the presence of H<sub>2</sub> at low exhaust gas temperatures can also accelerate the fouling of the catalyst as a result of carbonaceous species being unable to burn-off at such temperatures (Wichterlová et al., 2005). When diesel type fuels (long chain HC's) are used for the reduction of NO<sub>x</sub> emissions, both C-species and nitrate accumulation deactivation mechanisms can occur consecutively.

Figure 20 illustrates how the catalyst remains active in the presence of long chain diesel hydrocarbons with approximately 8000ppm H<sub>2</sub>. The concentration of H<sub>2</sub> was kept similar to the earlier results so a direct comparison could be made. The fuel control for the hydrocarbon injection consists of an electronic syringe pump (with regulated flow rate) and a fuel atomiser which creates a fine misted spray of the liquid fuel to allow better mixing with the exhaust gas. As the HC:NO<sub>x</sub> ratio was successively increased from a ratio HC:NO<sub>x</sub>=3 onwards there was no substantial benefit in the catalyst activity, as shown in Figure 20. However, further addition of HC began to have a negative impact on the overall NO<sub>x</sub> conversion reducing the catalyst activity closer to that observed during passive mode conditions in the presence of H<sub>2</sub>.

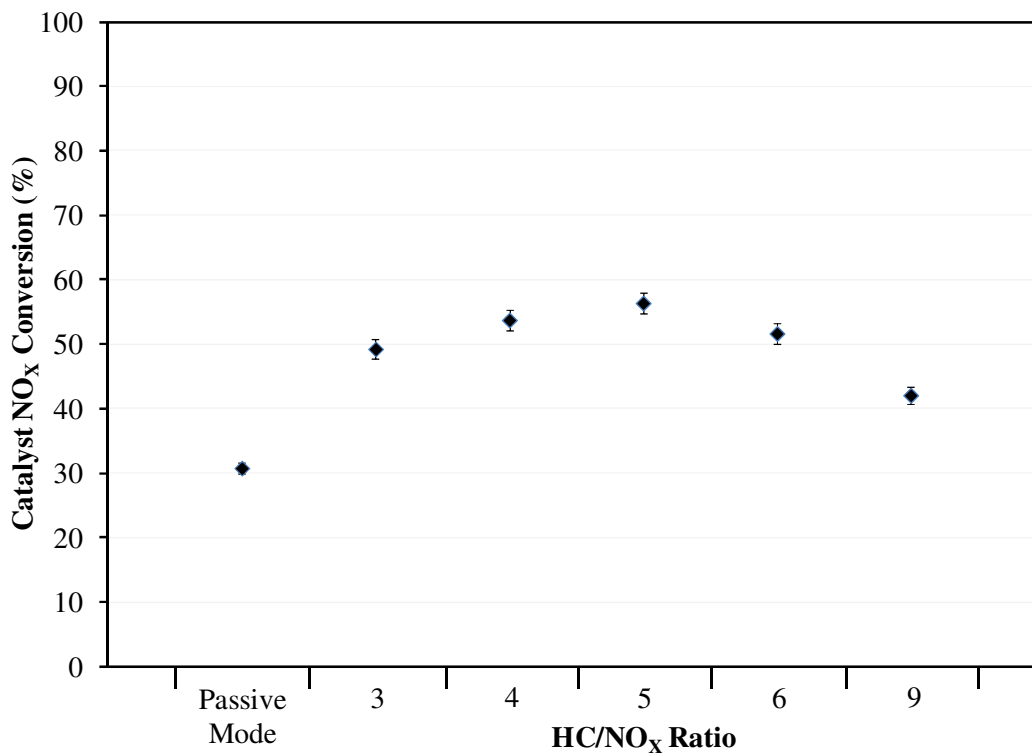


Figure 20: The Effect of HC:NO<sub>x</sub> Ratio on Catalyst Activity with 8000ppm H<sub>2</sub>

Increasing the HC:NO<sub>x</sub> ratio from a value of 3 onwards does not appear to have a significant influence on the catalyst activity and therefore choosing a ratio of 3 for instance can also reduce the overall fuel penalty. Keeping the HC:NO<sub>x</sub> ratio at approximately 3, as illustrated in Figure 21, the overall catalyst NO<sub>x</sub> reduction is improved by 20% compared to the passive mode condition in Figure 19. Under diesel HC addition, the catalyst remained stable without showing any signs of deactivation. Furthermore the stable HC utilisation over the SCR is also encouraging.

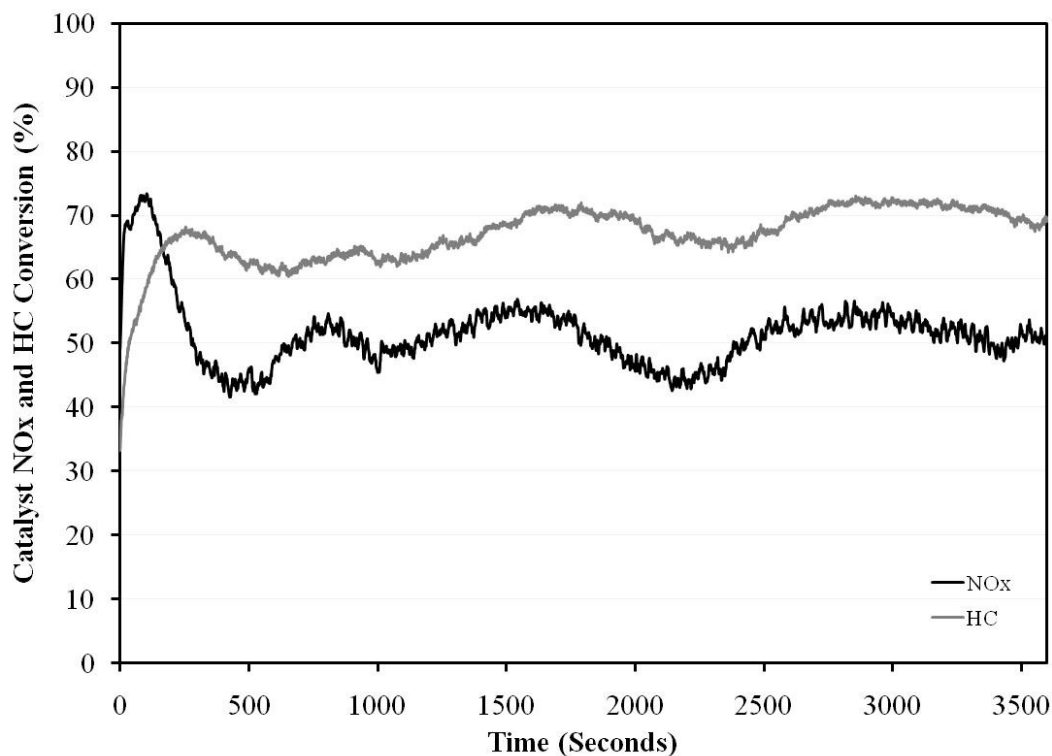
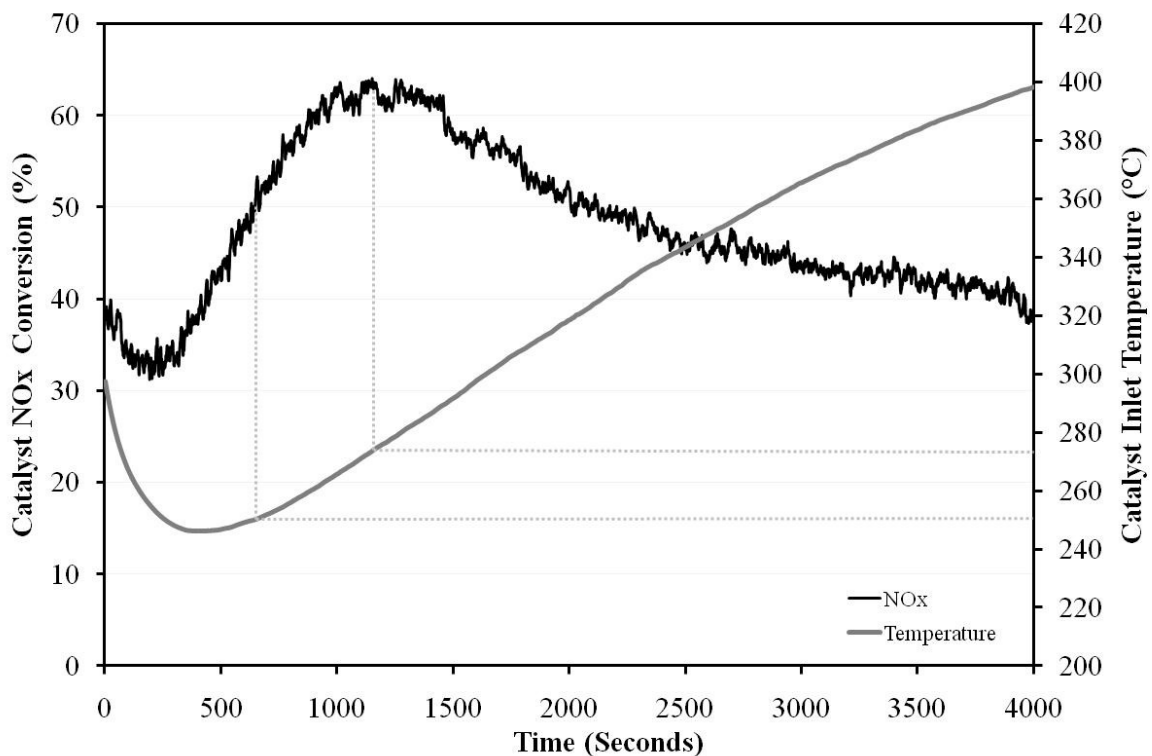


Figure 21: Catalyst NO<sub>x</sub> Reduction Activity at HC:NO<sub>x</sub> = 3 with 8000ppm H<sub>2</sub>

Overall this indicates that by removing the agglomerated solid carbonaceous material (i.e. soot) from settling on the catalyst sites the heavier HC can directly take part in the NO<sub>x</sub> reduction reaction rather than adsorb on to the dry carbon particles. Using the same catalyst as above (i.e. no regeneration), Figure 22 shows that the catalyst is still active and performing consistently. Thus a similar NO<sub>x</sub> conversion can be obtained at 250°C as before. From Figure 22 it can be observed that the catalyst activity varies with temperature. The peak catalyst performance was achieved at a temperature of approximately 270-280°C and declined thereafter. However, it is important to note that there is a possibility that some of the injected heavier HC may adsorb onto the trapped soot within the DPF under low temperature conditions hence making the soot oxidation over the DPF more challenging. An active mode can be achieved through the utilisation of the on-board fuel supply (i.e. using the existing fuel infrastructure); the supply and method of implementing H<sub>2</sub> on-board will also need to be

considered. At the moment there are two popular approaches that have been studied over the last decade. The first is on-board exhaust gas fuel reforming, a process essentially involving the catalytic cracking of the source feed into synthesis gas (H<sub>2</sub> + CO) or more specifically direct catalytic interaction of fuel with the engine exhaust gases. An alternative method is the dissociation of on-board NH<sub>3</sub>. This requires cracking anhydrous NH<sub>3</sub> in the presence of a nickel/alumina catalyst. According to Saika et al. (2006) the dissociation is an endothermic reaction requiring 45.7kJ/mol of energy at 298K (25°C). It is also understood that the dissociation can result in the presence of residual NH<sub>3</sub> thus resulting in a product mixture of 1-2%NH<sub>3</sub> + 75%H<sub>2</sub> + 23-24%N<sub>2</sub>. The following section focuses on the lean NO<sub>x</sub> reduction in the presence of dissociated NH<sub>3</sub>. This approach can be considered as passive mode as no additional HC are introduced in the exhaust stream.



**Figure 22: Temperature Effect on the Catalyst NO<sub>x</sub> Reduction Activity**

### 4.2.3 The influence of NH<sub>3</sub> on the activity of an Ag-Al<sub>2</sub>O<sub>3</sub> catalyst in H<sub>2</sub> and DPF assisted conditions

It is also understood that silver, for instance, is a very active catalyst for NH<sub>3</sub> oxidation under low temperatures (Gang et al., 2001). From the work of Richter et al. (2004b) it was also shown that the ‘H<sub>2</sub> effect’ works with not only hydrocarbons but also NH<sub>3</sub> over a Ag-Al<sub>2</sub>O<sub>3</sub> catalyst. Pure anhydrous NH<sub>3</sub> is generally an option for NH<sub>3</sub>-SCR and the main reaction was shown earlier in Reaction 21 (Koebel et al., 2000, Chatterjee et al., 2008). The gaseous mixtures of 1% and 2% non-dissociated NH<sub>3</sub> were premixed and supplied directly in to the exhaust manifold. The flow rates of the dissociated mixtures were chosen to ensure there was significant NH<sub>3</sub> presence in the exhaust. Figure 23 and Figure 24 give an overall perspective of how the flow rates of the mixtures affect the performance of the catalyst. In order to demonstrate this effect, a flow rate was chosen as a baseline (i.e. represented as 100%) and the corresponding flow rates were chosen as a percentage of this flow.

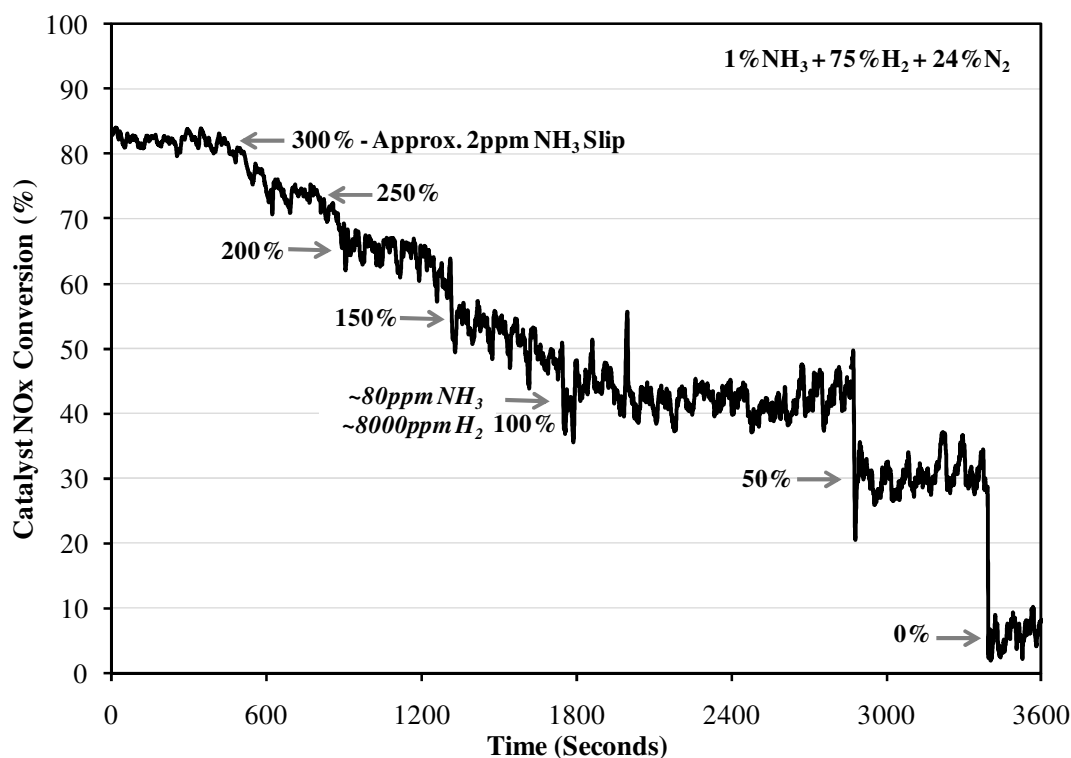


Figure 23: The Effect of 1% NH<sub>3</sub> Mixture over the Ag-Al<sub>2</sub>O<sub>3</sub> Catalyst

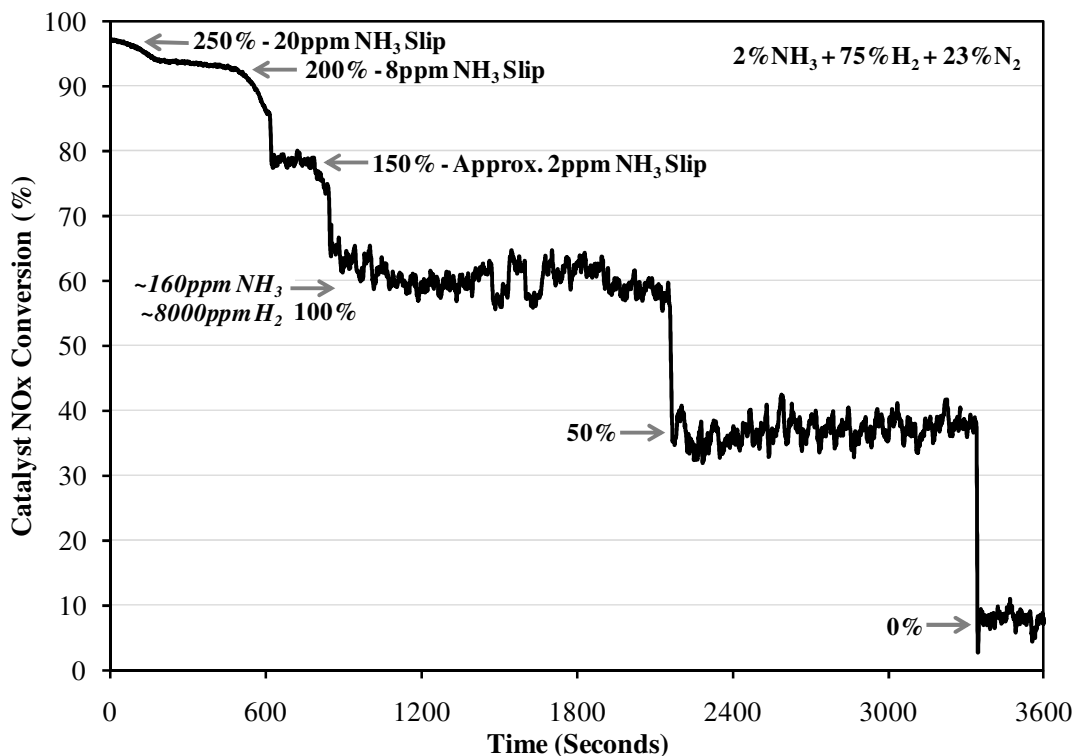


Figure 24: The Effect of 2% NH<sub>3</sub> Mixture over the Ag-Al<sub>2</sub>O<sub>3</sub> Catalyst

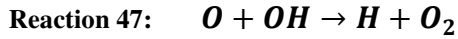
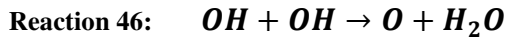
As shown in Figure 23, the baseline flow rate represented a mixture of 80ppm NH<sub>3</sub> and 8000ppm H<sub>2</sub> in the exhaust gas supplied to the catalyst, giving approximately 40-45% catalyst NO<sub>x</sub> reduction. However, when this flow was doubled (i.e. 200%) this promoted the catalyst performance to 65%, while a flow rate 3 times (i.e. 300%) of that chosen for the baseline gave a steady 80% NO<sub>x</sub> reduction. To determine whether NH<sub>3</sub> or H<sub>2</sub> is causing this improved catalyst activity, a comparison to 2% non-dissociated NH<sub>3</sub> mixture was also implemented. Comparing the baseline flows, Figure 24 shows under the same H<sub>2</sub> content as that in Figure 23, doubling the NH<sub>3</sub> content in the mixture resulted in a further NO<sub>x</sub> reduction of approximately 20%. Comparing 100% and 50% of the mixtures in Figure 23 and Figure 24 respectively, the 4000ppm increase in H<sub>2</sub> alone results in a 5% NO<sub>x</sub> improvement over the catalyst. Although adding H<sub>2</sub> as observed earlier promoted the catalyst performance by approximately 15-20%, further increasing the H<sub>2</sub> concentration does not have any significant

benefit. This suggests a lower H<sub>2</sub> concentration in the exhaust upstream the catalyst can be just as effective and efficient.

It is also important to note that although the baseline flow rate of the 2% mixture outperformed that of the 1% mixture, any further increase in flow (e.g. 150%, 250% and 300%) resulted in NH<sub>3</sub> slip. Therefore the flow rate of the dissociated mixture must be chosen carefully to ensure minimal NH<sub>3</sub> slip and fuel penalty. As the concentration of NH<sub>3</sub> in the total mixture is fairly small, it can be said that NH<sub>3</sub> as a reductant is more active over the Ag-Al<sub>2</sub>O<sub>3</sub> catalyst than HC. The NH<sub>3</sub>:NO<sub>x</sub> ratio is particularly low in comparison to the ratio of ~1 required for an NH<sub>3</sub>-SCR catalyst (DiMaggio et al., 2009).

Overall from the results it is possible to observe that a flow of mixture containing 160ppm NH<sub>3</sub> with 8000ppm H<sub>2</sub> is beneficial to maintain a significant NO<sub>x</sub> reduction over the lean NO<sub>x</sub> catalyst, while minimising H<sub>2</sub> waste and ammonia slip. Taking this into consideration, further work was undertaken to promote the catalyst activity. Figure 25 shows how the combustion can be enhanced through the use of EGR in the presence of dissociated NH<sub>3</sub>. When enhanced EGR was implemented, the diesel fuelling (i.e. amount of fuel injected per cycle) was adjusted to achieve the desired engine torque throughout the series of tests. As shown, EGR results in a lower combustion temperature reducing NO<sub>x</sub> in the premixed combustion phase. The reduced effective A/F ratio will also result in greater HC and CO emission formation as can be observed in Table 8 and as a result will promote the HC:NO<sub>x</sub> ratio. H<sub>2</sub> influences the combustion with a greater ROHR in the diffusion phase promoting the HO<sub>2</sub> radical for NO<sub>2</sub> production. As the concentration of H<sub>2</sub> is particularly low, the chemical effect will be more significant than the thermal effect. Hence the overall NO<sub>x</sub> will remain similar as observed in Table 8. It can be assumed that H<sub>2</sub> is continuously promoting the

generation of the HO<sub>2</sub> radical at low temperatures through the following reactions while finally prompting NO oxidation through Reaction 9 (Hori, 1988, Hargeaves et al., 1981):



As the concentration of NH<sub>3</sub> is particularly low, it will not play an important role in combustion as it is heavily diluted with the intake air. However, it can also be observed from Table 8 that there was a small CO<sub>2</sub> reduction indicating some diesel fuel replacement with the dissociated mixture under EGR conditions.

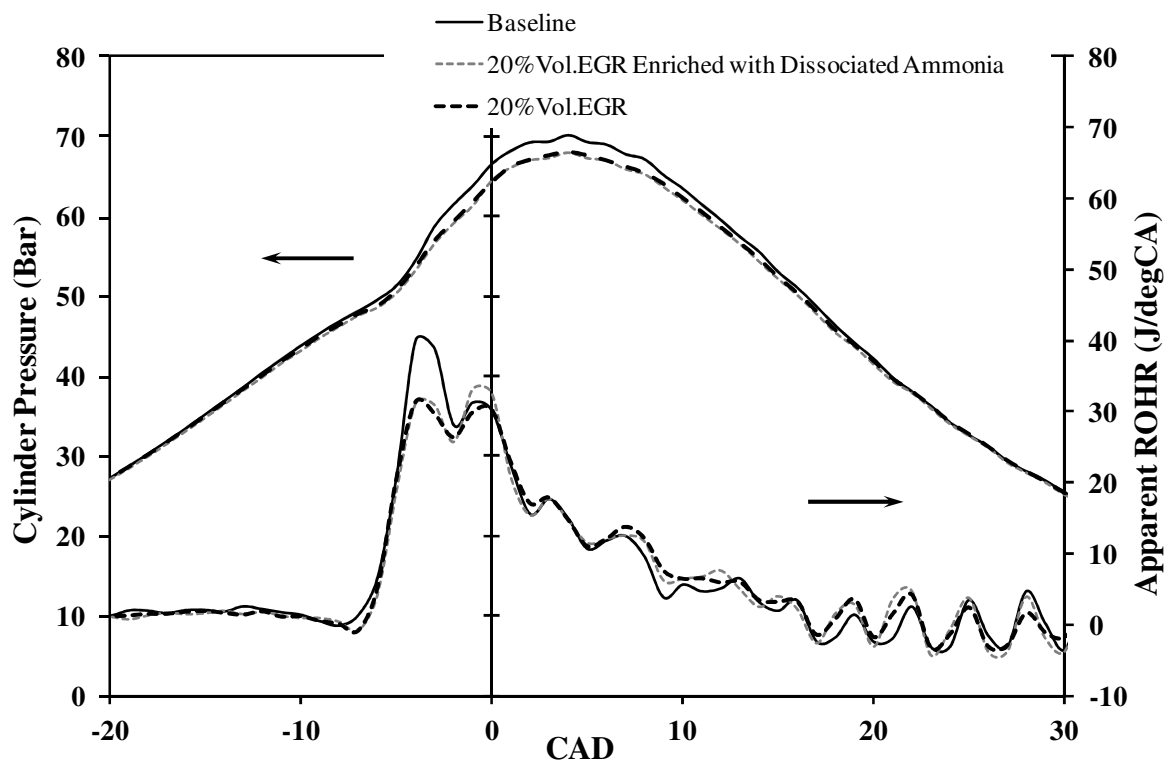


**Figure 25: Combustion Characteristics under EGR and Dissociated NH<sub>3</sub> Conditions**

**Table 8: Exhaust Gas Composition during Dissociated NH<sub>3</sub> Addition and/or EGR**

Engine Condition	CO ppm	CO <sub>2</sub> %	H <sub>2</sub> O %	HC ppm	NO ppm	NO <sub>2</sub> ppm	N <sub>2</sub> O ppm	NO <sub>x</sub> ppm	HC:NO <sub>x</sub> Ratio
Baseline	141.05	3.25	3.73	563.82	444.30	54.46	0.60	499.36	1.13
20% Vol.EGR	219.34	4.11	4.51	745.38	282.49	79.16	1.08	362.73	2.05
20% Vol.EGR Enriched with 2%NH <sub>3</sub> + 75%H <sub>2</sub> + 23%N <sub>2</sub>	197.31	4.01	4.52	711.80	242.42	111.32	1.68	355.42	2.00

The NO<sub>x</sub> reduction results in Figure 26 clearly show the benefit of the upstream DPF but also the implementation of EGR in the presence of the dissociated mixture. As observed previously, the catalyst has a better tolerance to EGR in the presence of a DPF. Although the catalyst NO<sub>x</sub> conversion reduces by approximately 10% with EGR, the overall NO<sub>x</sub> reduction of the system will be greater as the benefit from EGR is still yet to be included.

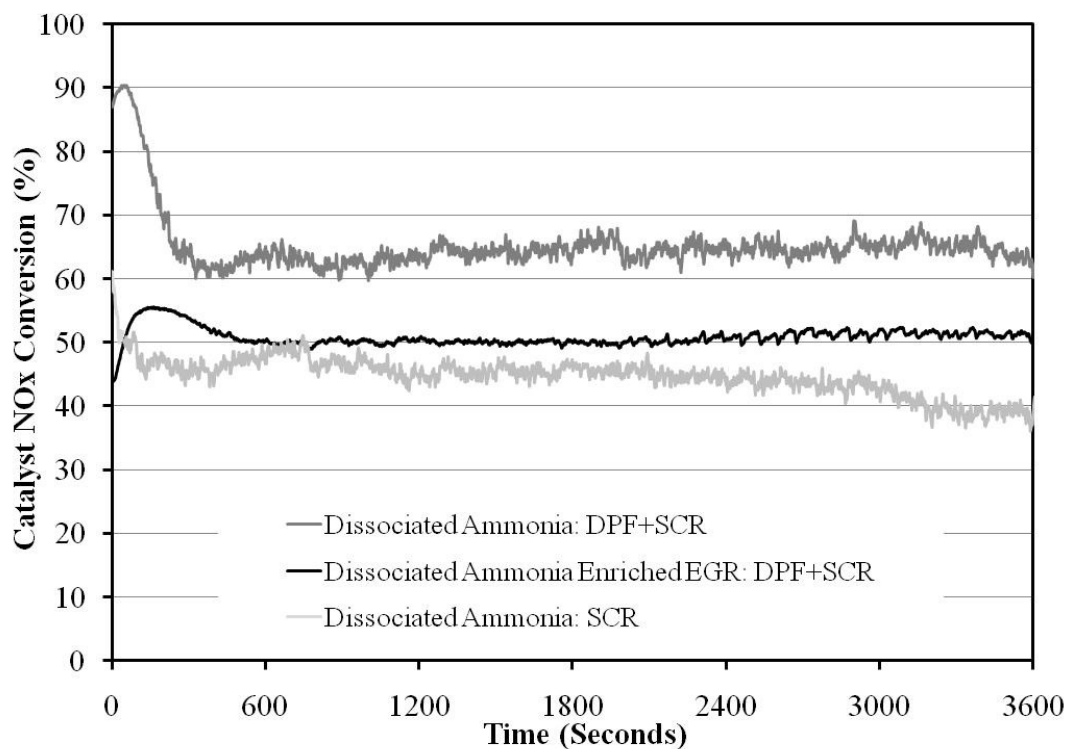


**Figure 26: The Influence of Dissociated NH<sub>3</sub> over an Ag-Al<sub>2</sub>O<sub>3</sub> Catalyst**

Figure 27 shows the composition of the product gas downstream the lean NO<sub>x</sub> catalyst. The initial reduction in HC indicates that some of these species are also being utilised simultaneously with NH<sub>3</sub> during the NO<sub>x</sub> reduction reactions over the silver catalyst in the presence of H<sub>2</sub>.

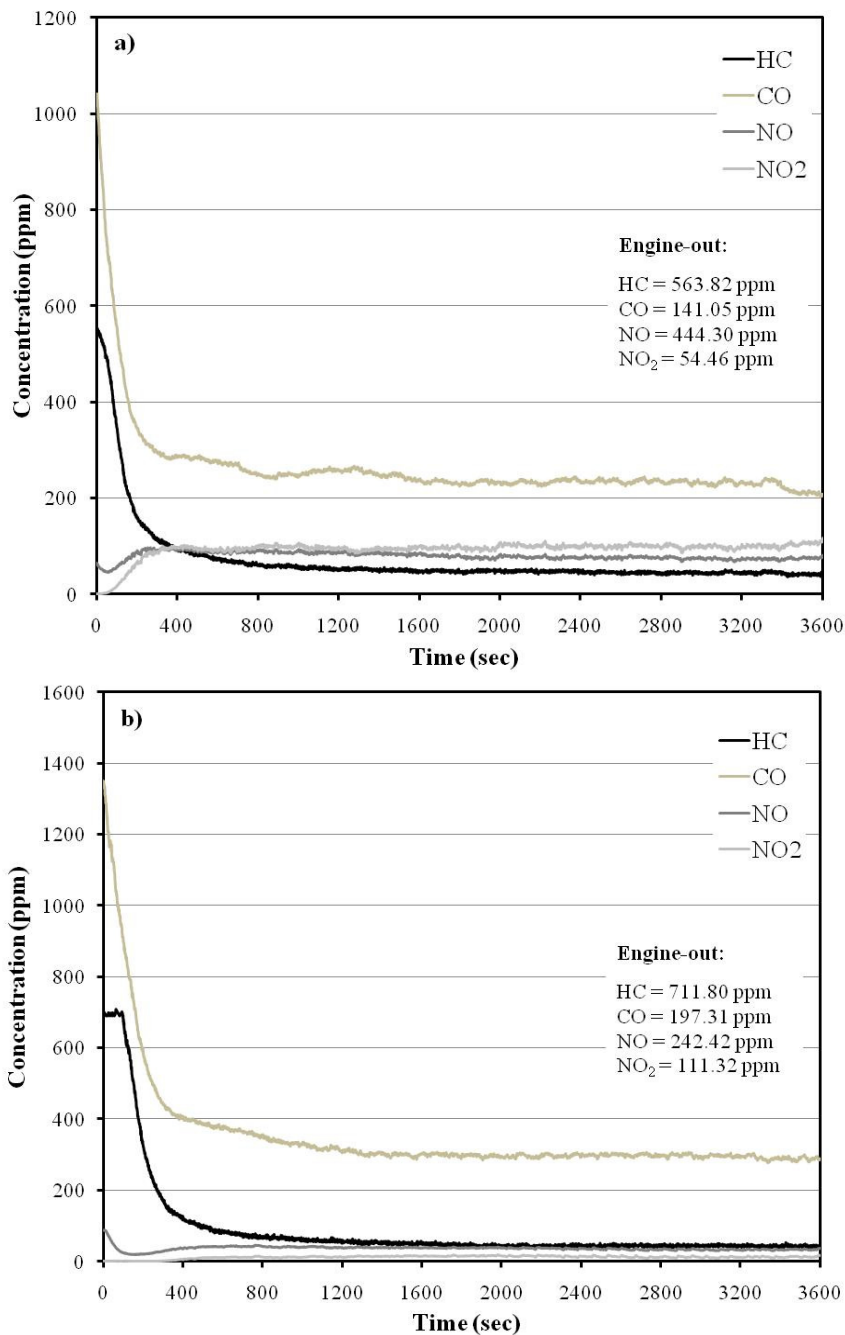


**Figure 27: Composition of Exhaust Emission during the Addition of, a) Dissociated Mixture and b) Dissociated Mixture with EGR**

The stability of the HC also indicates a more promising catalyst activity that is promoted by the addition of a DPF. An increased CO emission is also measured downstream of the aftertreatment system while the catalyst cools to the desired temperature (250°C). After this fall, the CO stabilises to a concentration greater than that of the engine-out. This shows the temperature is sufficient for passive DPF regeneration through the reaction shown earlier in Reaction 20. The use of dissociated NH<sub>3</sub> and in combination with passive HC-SCR seems to be a very effective approach. It was concluded by Richter et al. (2004b) that the presence of H<sub>2</sub> was not only to promote the reductant activation step but influence the activation of NO. In addition, it was believed that NH<sub>3</sub> was able to react directly in the gas phase as well as after activation on the Lewis acid sites of the alumina support.

Figure 28 gives an overview of the overall NO<sub>x</sub> reduction which can be achieved through the combined effect of EGR and a lean NO<sub>x</sub> catalyst. As shown, the overall NO<sub>x</sub> reduction performance of the system reaches 90%, where 50% as observed earlier in Figure 26 is due to the catalyst while approximately 40% is influenced through EGR. Referring back to Figure 24, it can be observed that in order to achieve the similar 90% conversion the flow rate of dissociated NH<sub>3</sub> needs to be doubled. Thus by choosing a smaller flow rate and implementing EGR a considerable fuel penalty has been avoided.

Further, to observe the effect of the GHSV, the exhaust flow rate over the DPF-SCR system was doubled reducing the reaction residence time over the catalyst. As shown in Figure 28 the NO<sub>x</sub> conversion over the catalyst reduces by approximately 10%, however the overall system NO<sub>x</sub> conversion remains in the region of 80%.

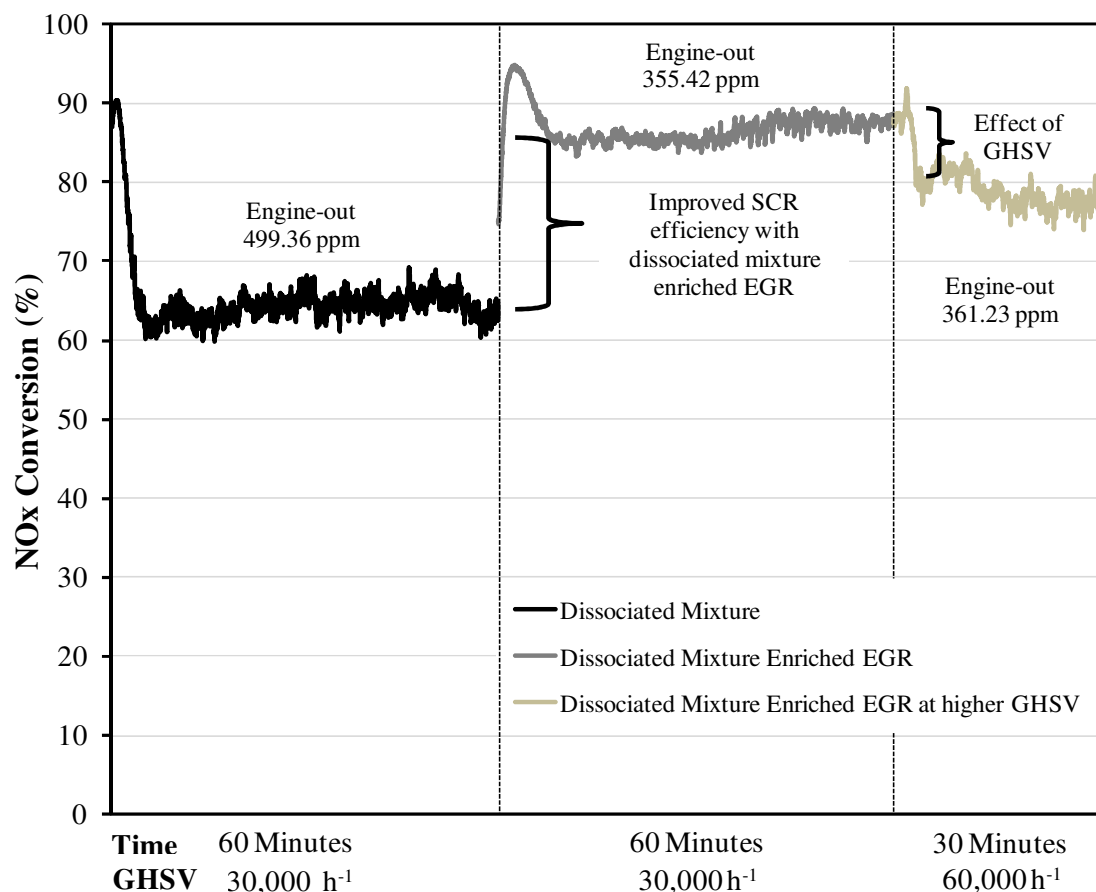
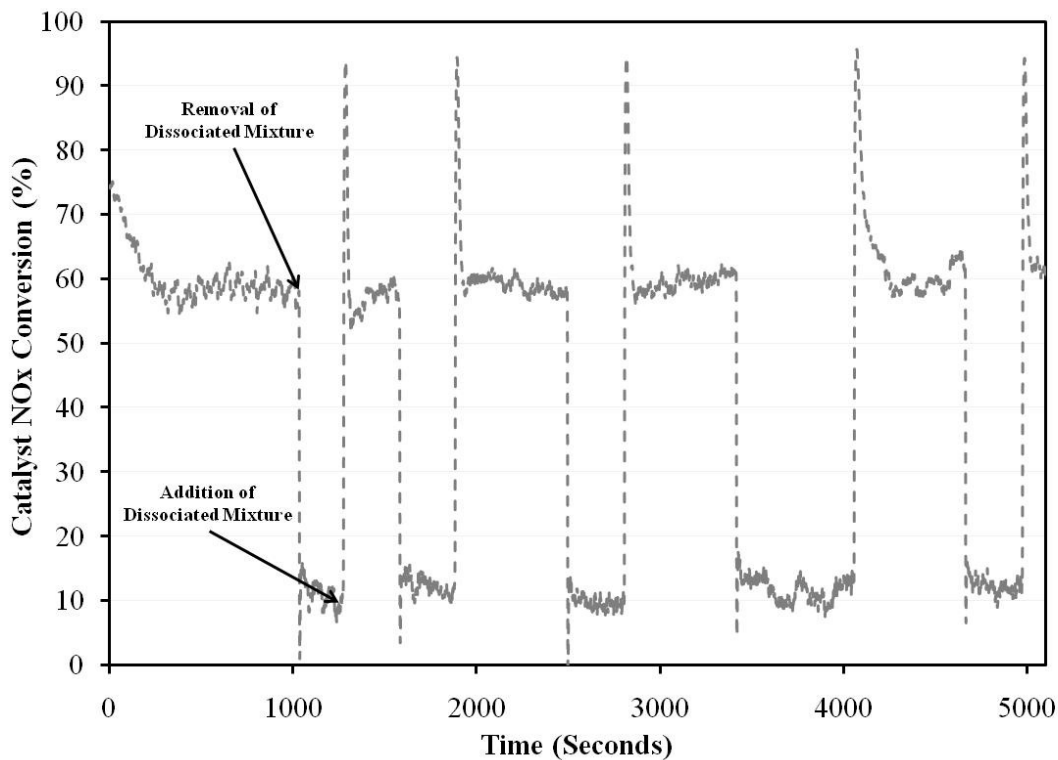


Figure 28: Observing the Influence of EGR and GHSV during the Addition of Dissociated NH<sub>3</sub>

To replicate the performance of the catalyst on-board a vehicle, the catalyst tolerance to a stop-start sequence representing the removal and addition of the dissociated mixture from the exhaust must be considered. This represents a scenario where the mixture may have depleted on-board a vehicle, significantly reducing the catalyst performance. Figure 29 shows that the overall NO<sub>x</sub> conversion of ~60% can be easily recovered when the mixture is re-introduced without any signs of catalyst deterioration. It was concluded by Kondratenko et al. (2006) that during the NH<sub>3</sub>-SCR reaction over Ag-Al<sub>2</sub>O<sub>3</sub>, the O<sub>2</sub> was found to regenerate the active catalytic sites through the decomposition of surface NH<sub>x</sub> and NO intermediate species, which could explain the positive catalyst activity observed in this study. Further, it was also suggested by Kondratenko et al. (2006) that in the presence of H<sub>2</sub> the N<sub>2</sub>O selectivity of the

NH<sub>3</sub>-SCR reaction decreased and as observed in this study the measured concentration of N<sub>2</sub>O downstream the lean NO<sub>x</sub> catalyst was negligible similar to that of NH<sub>3</sub>.



**Figure 29: Catalyst Performance during a Stop-Start Sequence**

Looking back to Figure 16, the aftertreatment system is positioned outside of the EGR loop with the gaseous mixture of dissociated ammonia added directly after engine-out, thus representing a modern vehicle. The low temperature approach considered in this study shows a method in which both H<sub>2</sub> and small concentrations of NH<sub>3</sub> can be made available on-board a vehicle. Thus additional HC injection at low temperatures is not required as simultaneous residual NH<sub>3</sub> and exhaust HC will act as reductants. The presence of H<sub>2</sub> and a DPF to filter majority of the carbonaceous PM species further promotes the catalyst activity and EGR tolerance. In order to meet future stringent regulations it is believed that current activities such as lean NO<sub>x</sub> catalyst combined with a DPF will need to be made practical in combination with EGR on-board light duty vehicles.

### **4.3 Summary**

The study has demonstrated an effective method of simultaneously controlling the emissions of NO<sub>x</sub> and PM. The activity of an Ag-Al<sub>2</sub>O<sub>3</sub> catalyst was promoted in the presence of H<sub>2</sub> and maintained by positioning a DPF upstream the catalyst.

The dissociation of NH<sub>3</sub> is very effective and a way to make available H<sub>2</sub> on-board the vehicle. As observed in this study, the residual NH<sub>3</sub> can be used in the presence of H<sub>2</sub> to promote the NO<sub>x</sub> reduction performance of the lean NO<sub>x</sub> catalyst, specifically an Ag-Al<sub>2</sub>O<sub>3</sub> catalyst. Implementing EGR in the presence of dissociated NH<sub>3</sub> resulted in dual-fuelling, where some of the H<sub>2</sub> replaced a portion of the diesel fuel resulting in a reduction in the CO<sub>2</sub> emissions, thus having a positive reflection on the overall fuel penalty gained from carrying NH<sub>3</sub>. Further the catalyst performed well under the removal and addition of the dissociated mixture during a stop-start sequence. However to maintain a significant NO<sub>x</sub> conversion a continuous supply of the dissociated mixture is required.

Overall there are many gains which can be brought from such a technique, especially when forthcoming regulations are becoming more stringent. The benefits of this technique lie in the fact that the unburned hydrocarbons from the combustion, combined with the residual NH<sub>3</sub>, can be used for the reduction of NO<sub>x</sub>. As current vehicles already implement a combined strategy of EGR for NO<sub>x</sub> reduction and a DPF for PM control, integrating the lean NO<sub>x</sub> system can be considered as a possible option. This will not only reduce the levels of EGR but also minimise the effect of the NO<sub>x</sub>/PM trade-off which can have a significant benefit towards the regeneration of the DPF.

# CHAPTER 5

## ENHANCING THE PERFORMANCE OF AN Ag-Al<sub>2</sub>O<sub>3</sub> LEAN NO<sub>x</sub> CATALYST USING ON-BOARD DIESEL EXHAUST GAS FUEL REFORMING

### 5.1 Introduction

Despite the large quantity of experimental studies on the effect of H<sub>2</sub> addition on Ag-Al<sub>2</sub>O<sub>3</sub>, only a small percentage use actual exhaust gas with catalysts coated on monolith substrates. This study, however, is a step towards a full-scale NO<sub>x</sub> reduction system using an actual Ag-Al<sub>2</sub>O<sub>3</sub> HC-SCR catalyst under real exhaust conditions with an integrated on-board exhaust gas fuel reformer. The key aim of this study is to observe the benefits of H<sub>2</sub> produced from onboard exhaust gas fuel reforming for low temperature lean NO<sub>x</sub> reduction. This involves identifying the conditions required for the on-board reformer to maintain sufficient H<sub>2</sub> production. The synthesis gas from the reformer or more commonly referred to as reformat contains generous quantities of H<sub>2</sub>, CO and HC, thus benefiting the HC:NO<sub>x</sub> ratio and eliminating the need for additional HC-dosing systems.

In this study the monolith aspect ratio of 3 was selected on the basis of the on-board reformer design and was loaded into the reformer, as shown in Figure 30. The GHSV of the reformer catalyst was kept constant at approximately 10,000h<sup>-1</sup> and was chosen based on previous studies (Tsolakis and Golunski, 2006). A lower GHSV resulted in an increased residence time, enabling an improved catalytic reaction between the gas feed and the catalyst itself.

Two 25.4mm diameter HC-SCR catalysts were cored from the monolith and placed one after the other for a greater active site length in a reactor linked to the exhaust tailpipe of the engine; downstream of the reformat addition point. The GHSV over the SCR catalyst was kept at approximately 30,000h<sup>-1</sup>, which is the actual GHSV that is obtained when two monolith HC-SCR catalysts are positioned in the main exhaust system and exposed to the full exhaust flow of the engine. A 25.4mm diameter DPF was also positioned in front of the HC-SCR catalysts to trap the majority of the carbonaceous species that can block the active sites of the catalyst. The reactor was placed in a tubular furnace with the temperature set to approximately 250°C, replicating the low end of a diesel exhaust temperature window. All tests were steady state under an engine speed of 1500rpm used throughout the experiment; with an engine load of either 5.3 or 3 bar IMEP.

The schematic in Figure 30 shows the on-board reformer integrated into the exhaust manifold taking only a portion of the exhaust for the reforming itself while bypassing the rest to the main exhaust. The product syngas is directly fed into the aftertreatment reactor alongside actual exhaust gas from the engine exhaust at a temperature of approximately 150°C to avoid water condensation. The reforming product and exhaust gas is mixed at the reactor entrance before passing through to the DPF. The temperature was measured and monitored using type-K thermocouples at various points. The exhaust and reformat samples were taken as shown in Figure 30 and the actual exhaust composition upstream the DPF was calculated taking dilution effects into account. Exhaust flow rates into the on-board reformer and aftertreatment reactor were controlled by using calibrated flow meters. The fuel control for the hydrocarbon injection to the on-board reformer consists of an electronic syringe pump (with regulated flow rate) and a fuel atomiser which creates a fine misted spray of the liquid fuel to allow better mixing with the exhaust gas.

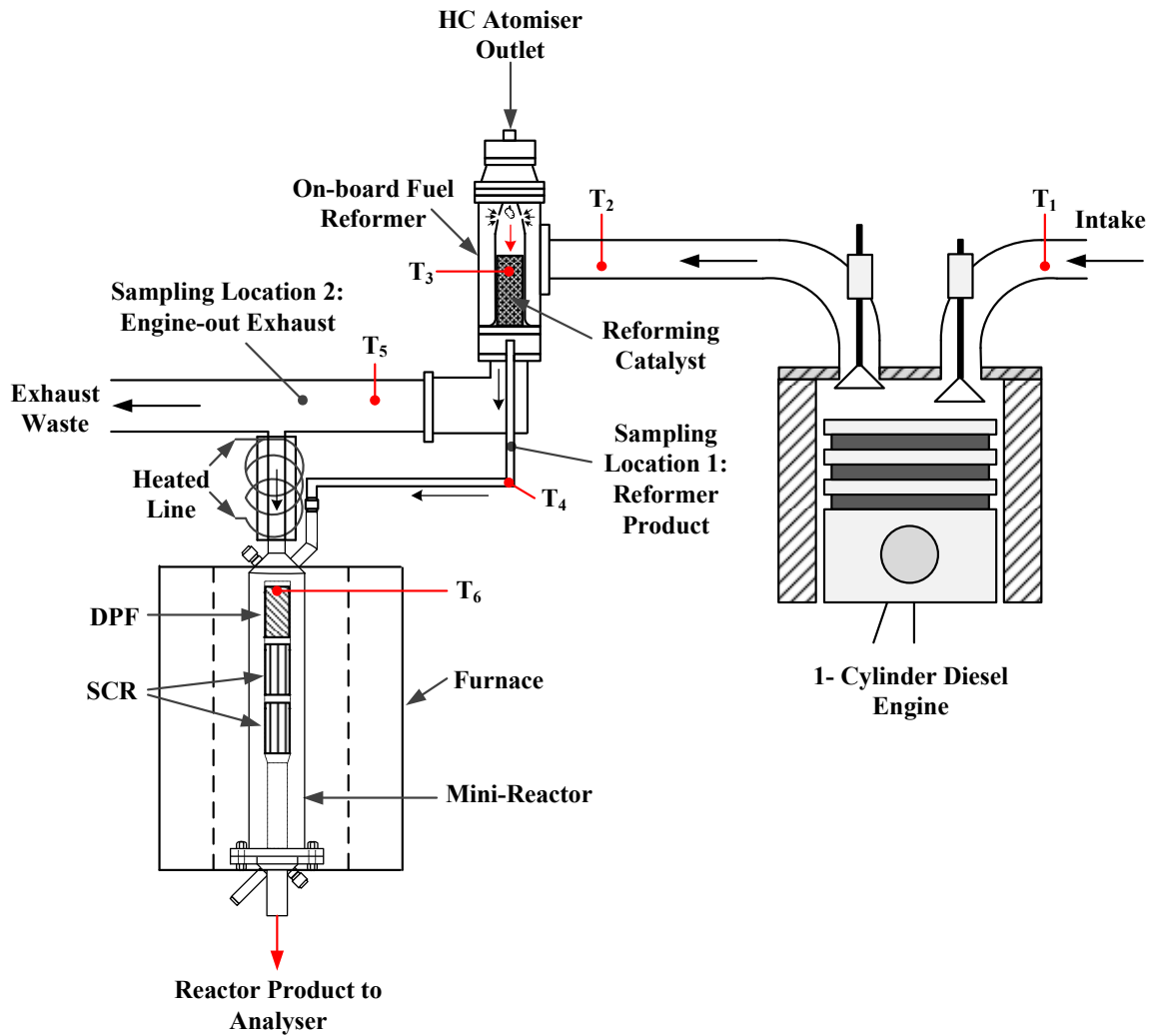


Figure 30: Schematic of an Integrated On-board Exhaust Gas Fuel Reformer with Aftertreatment Reactor

## 5.2 Results and Discussion

### 5.2.1 Performance of a HC-SCR with an on-board fuel reformer

For exhaust gas reforming to work effectively, a higher temperature than that of the exhaust is required to reach the catalyst light-off temperature. In this study, the temperature in the reforming reactor was achieved through partial or complete oxidation of part of the fuel supplied to the reactor while the rest of the fuel was then utilised in the endothermic SR reaction. However, to light-off the catalyst the engine was operated under high load until the

catalyst inlet temperature of approximately 320°C was achieved. The reforming conditions in this study have been chosen primarily for the H<sub>2</sub> production, which can promote the silver catalyst as observed in many earlier investigations (Theinnoi et al., 2008, Sitshebo et al., 2009, Houel et al., 2007b). The focus is not to optimise the reformer but to observe the benefits this can have on the aftertreatment system. Table 9 shows the various reformer conditions that were considered with the H<sub>2</sub> quantity that can be generated. Further the oxygen/carbon (O/C), steam/fuel (S/F) and oxygen/fuel (O<sub>2</sub>/F) ratios are also given. As shown in Table 9, reducing the O/C ratio by increasing the fuel flow (i.e. resulting in an increased fuel penalty) enhances the production of H<sub>2</sub> and the overall reforming efficiency (Leung et al., 2009). At lower engine loads, the increase in O<sub>2</sub> content and reduced exhaust temperature reduces the overall H<sub>2</sub> production. Therefore more fuel is required to decrease the O/C ratio to maintain a H<sub>2</sub> production similar to that at higher engine loads.

**Table 9: On-board Fuel Reformer Conditions and H<sub>2</sub> Production**

<b>Engine Speed (rpm)</b>	1500							
<b>Engine Load (bar)</b>	5.3				3.0			
<b>Exhaust Temperature (°C)</b>	331				224			
<b>Fuel Flow (ml/h)</b>	20	30	<b>35</b>	30	<b>40</b>	50	60	
<b>Equivalence Ratio (Based on O<sub>2</sub> and ATR)</b>	0.57	0.85	<b>0.99</b>	0.51	<b>0.68</b>	0.85	1.02	
<b>O/C (n/n)</b>	2.03	1.35	<b>1.16</b>	2.09	<b>1.57</b>	1.26	1.05	
<b>S/F (n/n)</b>	5.56	3.71	<b>3.18</b>	3.77	<b>2.83</b>	2.26	1.89	
<b>O<sub>2</sub>/F (n/n)</b>	11.44	7.63	<b>6.54</b>	12.76	<b>9.57</b>	7.65	6.38	
<b>H<sub>2</sub> (% Vol.)</b>	3.63	6.39	<b>8.02</b>	2.12	<b>7.12</b>	12.61	13.53	
<b>Reactor Exhaust Gas Flow (l/min)</b>	5							

## 5.2.2 High load HC-SCR catalyst performance – Engine load of 5.3 bar IMEP

### 5.2.2.1 On-board Reforming Tests

The engine conditions in this section were chosen to help light-off the catalyst, where therein the fuel can be utilised to promote the reformer temperature until the desired reforming reactions can take place for H<sub>2</sub> production. Choosing a high load engine condition can be seen as a worst case scenario (i.e. high NO<sub>x</sub> and soot emissions) where the HC-SCR catalyst deactivation is most prominent. The chosen engine, on-board reformer and aftertreatment reactor conditions are given in Table 10. The HC:NO<sub>x</sub> ratio was calculated to be in the range of 2.6-3.0, which from the work of DiMaggio et al. (2009) was believed to minimise fuel penalty without affecting the NO<sub>x</sub> reduction efficiency.

**Table 10: Summary of Test Conditions under an Engine Load of 5.3 bar IMEP**

<i>Engine Conditions</i>			<i>DPF-SCR System</i>		
Inlet	35	°C	SCR Inlet Temp	254	°C
Speed	1500	rpm	Space Velocity	30,000	h <sup>-1</sup>
Load	5.3	bar	HC:NO <sub>x</sub> Ratio	2.6 - 3.0	
Exhaust	331	°C	H <sub>2</sub>	0.8 - 1.0	%Vol.
<i>On-board Reformer</i>					
Reformer Inlet	297	°C			
Catalyst Inlet	866	°C			
Peak Reaction Temp	1030	°C			
Exhaust Flow Rate	5	l/min			
Space Velocity	10,000	h <sup>-1</sup>			
Fuel Flow Rate	35	ml/hr			
Equivalence Ratio	0.99				
O/C (n/n)	1.16				
S/F (n/n)	3.18				
O <sub>2</sub> /F (n/n)	6.54				

The engine-out exhaust emissions are presented in Table 11 alongside the product gas from the on-board fuel reformer. The measured emissions from the reformer show an increase in CO<sub>2</sub> emissions from complete oxidation (Reaction 41) of the fuel causing an exothermic reaction and raising the local catalyst temperature. The CO emission is approximately half of the corresponding H<sub>2</sub> content indicating that H<sub>2</sub> is mainly formed during the SR endothermic reactions (Reaction 36).

**Table 11: Average Engine-out Emissions and On-board Reformer Product Gas - Engine Load of 5.3 bar IMEP**

		<b>Engine-out</b>	<b>REGR Product Gas</b>
<i>NO</i>	<i>ppm</i>	901.61	1.82
<i>NO<sub>2</sub></i>	<i>ppm</i>	39.58	98.18
<i>NO<sub>x</sub></i>	<i>ppm</i>	941.20	100.00
<i>NH<sub>3</sub></i>	<i>ppm</i>	1.95	161.48
<i>Propylene</i>	<i>ppm</i>	1.27	199.58
<i>Ethylene</i>	<i>ppm</i>	4.00	387.73
<i>Methane</i>	<i>ppm</i>	4.25	2999.43
<i>Ethane</i>	<i>ppm</i>	0.00	421.56
<i>Total HC</i>	<i>ppm</i>	951.45	9254.94
<i>CO</i>	<i>ppm</i>	127.09	44041.79
<i>H<sub>2</sub>O</i>	<i>%Vol.</i>	6.68	5.54
<i>CO<sub>2</sub></i>	<i>%Vol.</i>	6.20	9.31
<i>O<sub>2</sub></i>	<i>%Vol.</i>	11.91	0.081

The SR reaction absorbs part of the heat generated by the oxidation reaction thus limiting the maximum temperature in the reformer, as shown in Table 10. It is also suggested that the WGS reaction (Reaction 39) has also taken place as there is reduced H<sub>2</sub>O in the product gas. Another secondary reaction of H<sub>2</sub> with NO<sub>x</sub> seems to have also taken place in the

reformer producing NH<sub>3</sub> or N<sub>2</sub> and H<sub>2</sub>O. This can be indicated by the reduction in NO<sub>x</sub> emissions and the presence of NH<sub>3</sub> in the reformer product gas (Tsolakis et al., 2004).

Since pyrolysis is assisted by catalysis, small olefins such as ethylene and propylene were also formed on the surface of the reforming catalyst. In reforming, it is believed that ethylene is a coke precursor. A high ethylene concentration generally means a severe carbon deposition is taking place on the catalyst (Rostrup-Nielsen et al., 1998, Yoon et al., 2008). At higher temperatures ( $\geq 650^{\circ}\text{C}$ ), the higher hydrocarbons may react by thermal cracking (i.e. pyrolysis or steam reforming) producing olefins which can easily form coke (Equation 12) as reported by Rostrup-Nielsen et al. (1993). As a result, this can have implications on the overall long-term performance of the reforming catalyst as the active surface sites will become blocked by various types of carbon deposits.

**Equation 12:**  $C_nH_m \rightarrow \text{Olefins} \rightarrow \text{Polymers} \rightarrow \text{Coke}$

In the study of Shimizu et al. (2000), it was concluded that short chain HC species are not active over the Ag-Al<sub>2</sub>O<sub>3</sub> catalyst under normal diesel exhaust temperatures unlike the longer-chained hydrocarbons. Studies have shown that the longer-chained hydrocarbons tend to have a lower activation (i.e. partial oxidation) temperature and therefore enabling the SCR reaction to proceed within a wider activity window under lower exhaust gas temperatures (Eränen et al., 2004, Shimizu et al., 2000, Shimizu et al., 2001, Lindfors et al., 2004).

Using the chosen reformer and engine conditions stated earlier, the HC-SCR catalyst was subjected to various exhaust/reformate ratios. Reducing the overall reformate flow rate had a significant impact on the NO<sub>x</sub> reduction performance. Figure 31 shows how the catalyst loses approximately 30% of its NO<sub>x</sub> reduction activity as the reformate flow rate is successively halved. However, the catalyst is able to regain its NO<sub>x</sub> performance of ~90%

when the exhaust/reformate ratio was brought back to 6, indicating either the amount of H<sub>2</sub> or HC were insufficient to promote the HC-SCR reaction. Therefore by controlling the reformate flow with respect to the exhaust gas flow rate over the catalyst; a significant NO<sub>x</sub> reduction can be achieved.

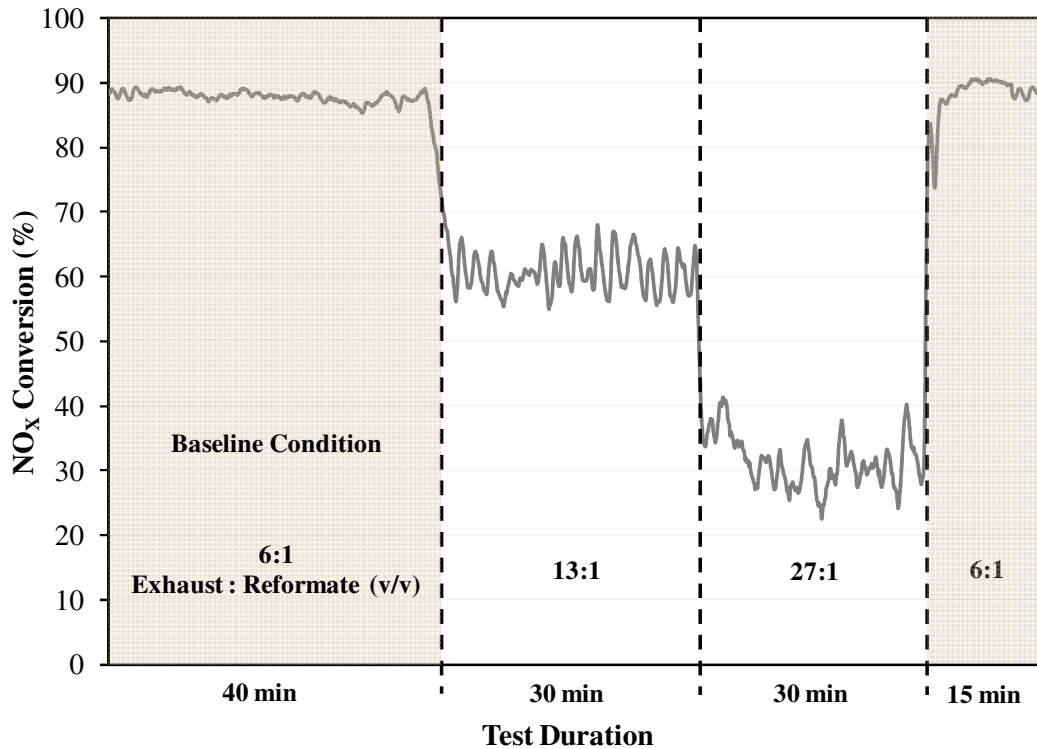


**Figure 31: The Effect of Reformate Addition on the Catalyst Performance**

Further, by altering the GHSV while keeping an exhaust/reformate ratio of 6 as shown in Figure 32, it was possible to maintain a high catalyst activity. Although lowering the GHSV resulted in an increased residence time, there was no further improvement in the catalyst performance. This suggests that the catalyst configuration used here may have been the ideal compromise to gain maximum NO<sub>x</sub> conversion (i.e. the result of a greater active site length).

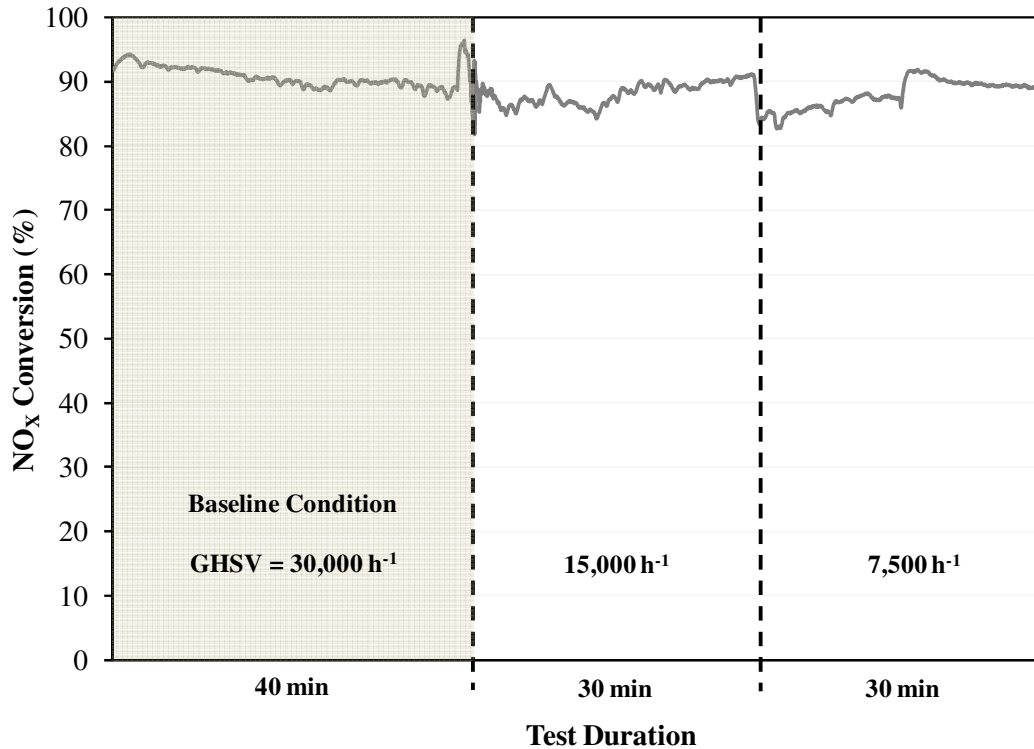
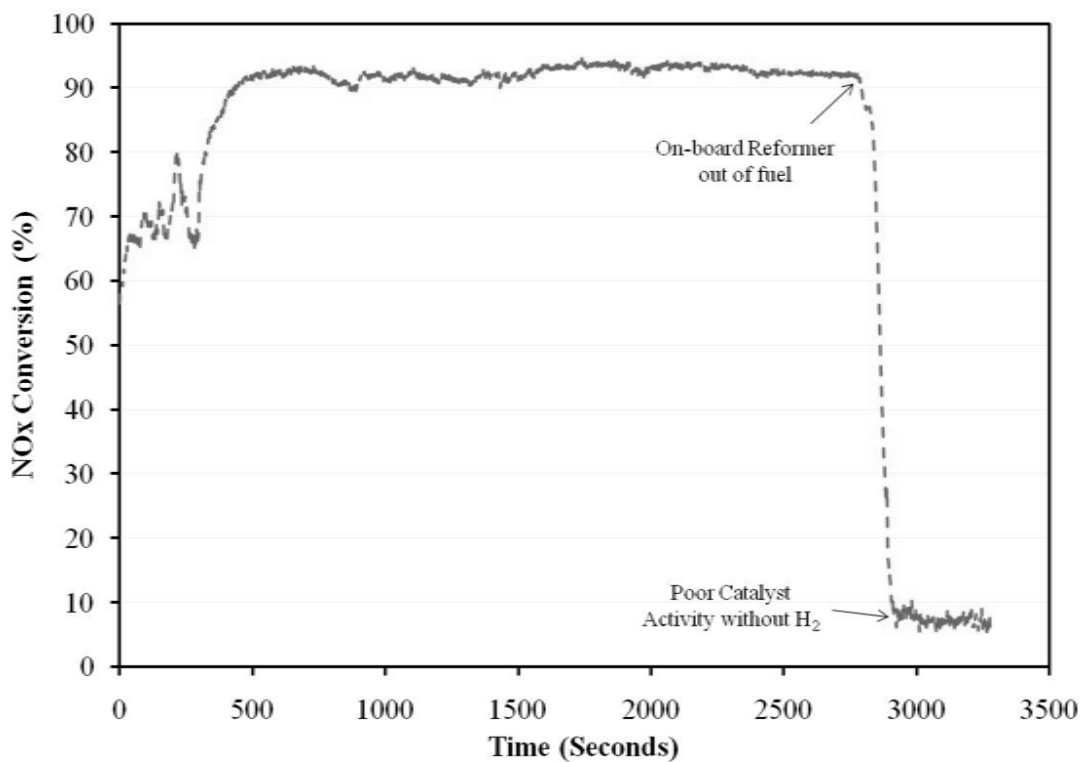


Figure 32: The Effect of GHSV on the Catalyst NO<sub>x</sub> Conversion Performance

Considering an exhaust/reformate ratio of 6, Figure 33 shows that a 90% NO<sub>x</sub> reduction can be achieved and maintained in the presence of an upstream DPF. Once the fuel to the reformer is stopped, the catalyst activity significantly falls as a result of the reduced HC:NO<sub>x</sub> ratio and the absence of H<sub>2</sub>. This highlights the substantial benefit that can be gained from the available HC species which can act as reductants as well as the H<sub>2</sub> produced from the on-board fuel reformer. As the reformer product itself contains a plentiful supply of HC species which are sufficient to provide a suitable HC:NO<sub>x</sub> ratio, additional reducing agents are not required (e.g. external fuel dosing system apart from the fuel supplied to the reformer). This therefore minimises the overall fuel penalty of the system. To achieve an efficient HC-SCR catalyst, oxidation sites that can partially oxidise the reductant are required as observed in the study of Shimizu et al. (2007). The lower amount of oxidation sites (i.e. metallic silver particles) in 2%Ag, as used in this study, can partially oxidise a higher fraction of the HC

compared to higher loaded silver catalysts which can result in complete oxidation of the HC as observed in the work of Kannisto et al. (2009). Figure 34 and Figure 35 show the total HC as well as some of the non-active species, with reference to Table 11, that are present in the exhaust gas downstream the HC-SCR catalyst. In order to prevent HC-slip, a clean-up catalyst will be required after the SCR unit. For example, a DOC can be utilised after the HC-SCR catalyst to oxidise any remaining HC and CO with the aid of any unused H<sub>2</sub>. As already well known, the oxidation reactions over the DOC can be enhanced in the presence of H<sub>2</sub> by promoting the catalyst light-off temperature as shown in the study by Katare and Laing (2009).



**Figure 33: Lean NO<sub>x</sub> Catalyst Performance with On-board Integrated Fuel Reformer**

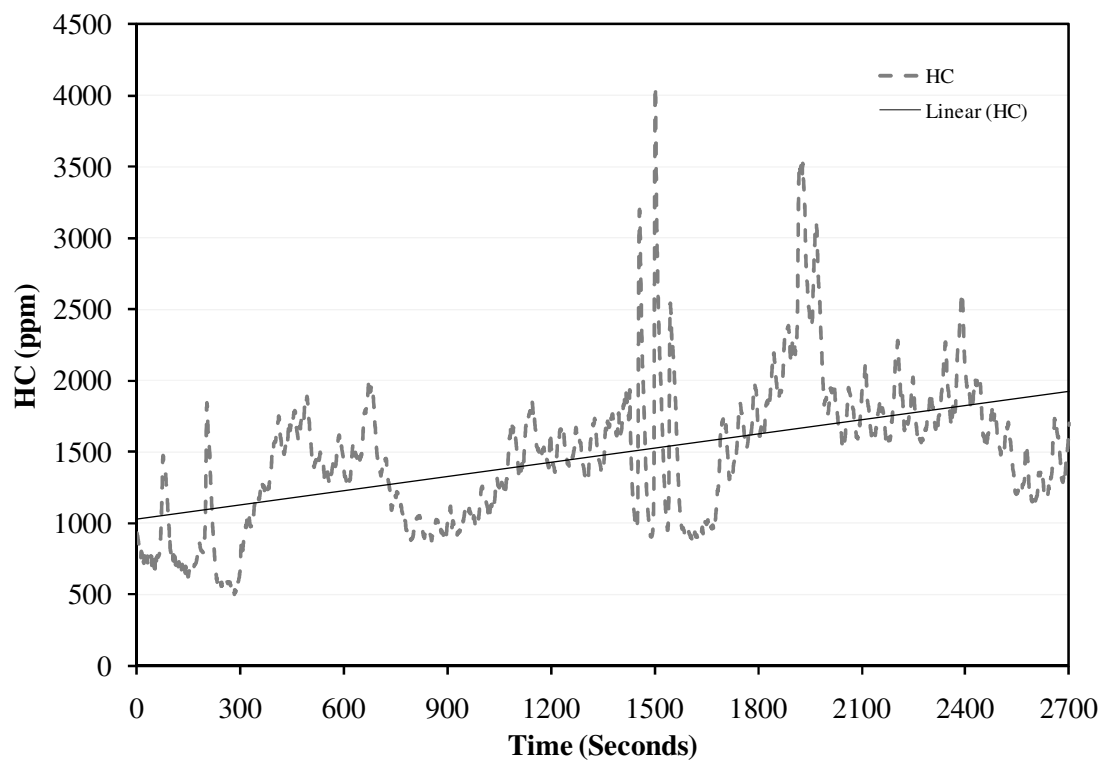


Figure 34: Hydrocarbon Concentration Downstream the Lean NO<sub>x</sub> Catalyst

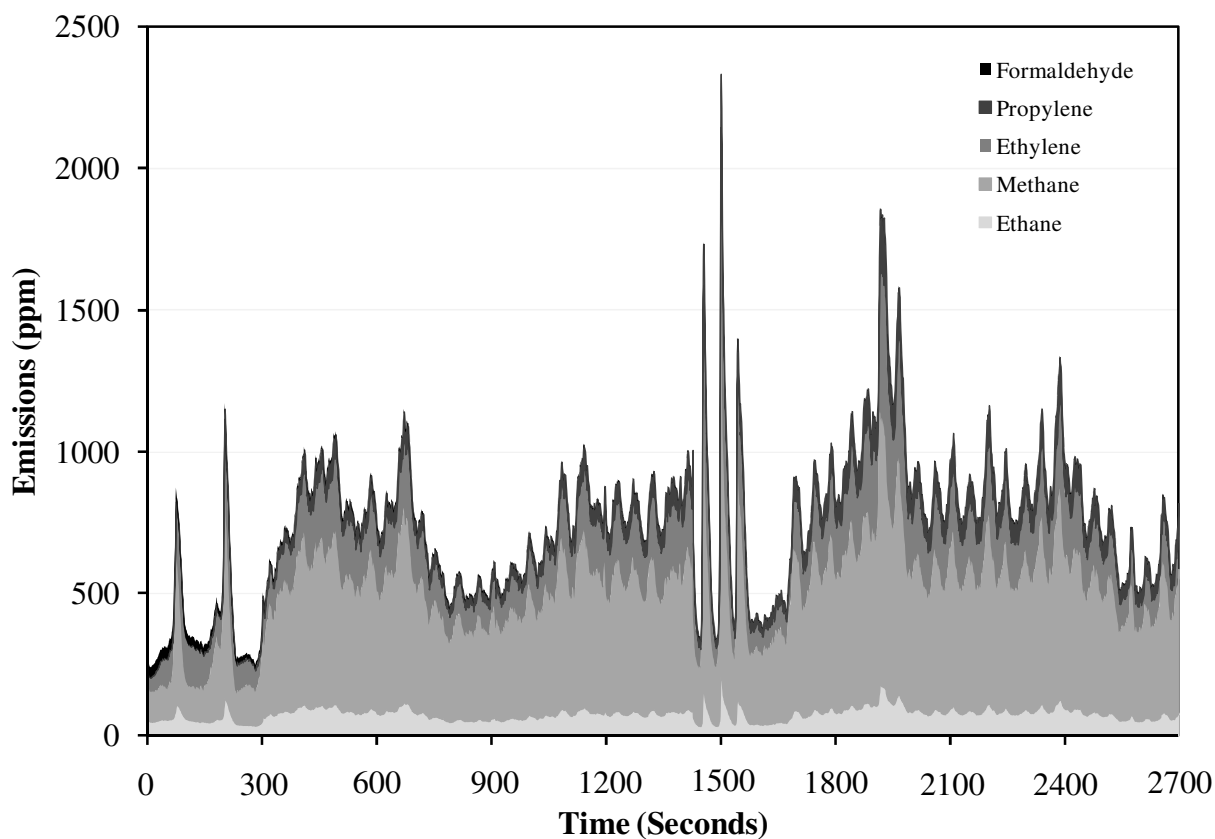
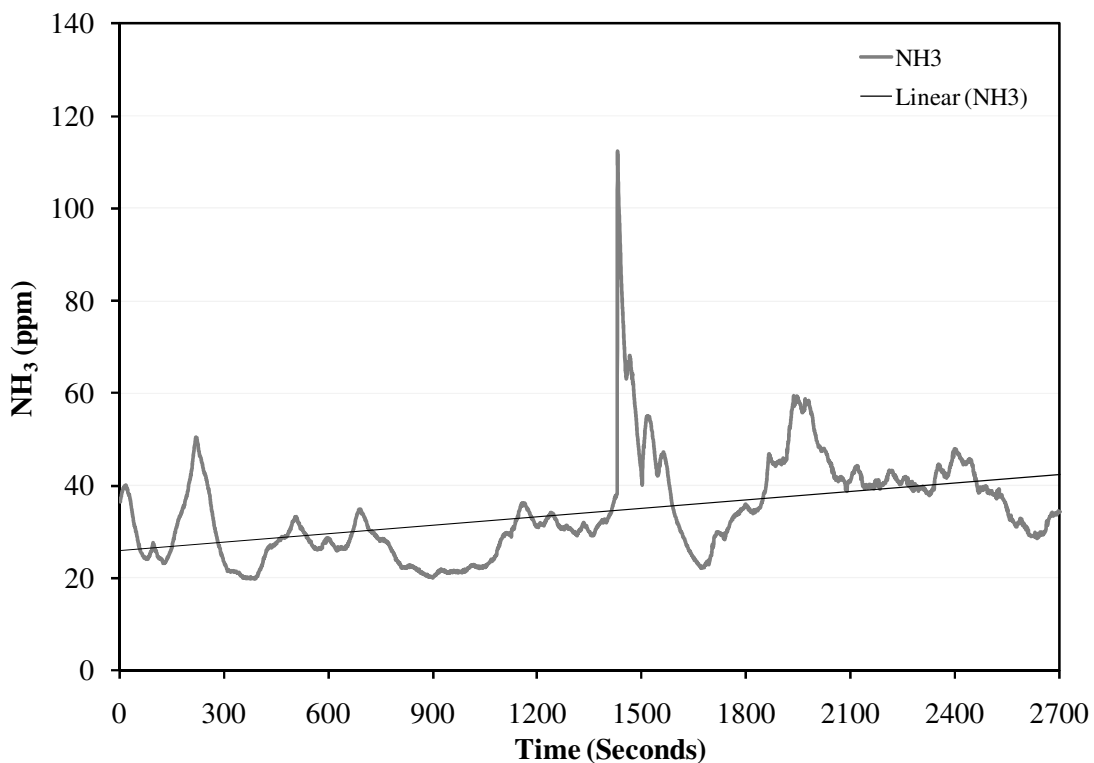


Figure 35: Measurable Non-active Hydrocarbon Species

The reformer product gas also consists of NH<sub>3</sub>, which can be beneficial over the HC-SCR catalyst. However from the work of Eränen et al. (2004), it was reported that NH<sub>3</sub> is also formed during the HC-SCR reaction via N<sub>2</sub> containing species such as isocyanate and isocyanide. The formation of such species is promoted by a high HC:NO<sub>x</sub> ratio, the presence of H<sub>2</sub> and/or increased temperature which has been extensively reported (Burch et al., 2004, Wichterlová et al., 2005, Sazama et al., 2005, Meunier et al., 2000, Breen et al., 2007). Figure 36 shows the combination of unused NH<sub>3</sub> from the reformer product as well as that produced over the HC-SCR catalyst. A clean-up catalyst will need to be considered to account for the NH<sub>3</sub> slip or, as shown in the work of DiMaggio et al. (2009), the remaining NO<sub>x</sub> species can be reduced by implementing an NH<sub>3</sub>-SCR downstream the HC-SCR.



**Figure 36: NH<sub>3</sub> Slip Downstream Lean NO<sub>x</sub> Catalyst**

From our ongoing investigation with NH<sub>3</sub> and H<sub>2</sub> over the Ag-Al<sub>2</sub>O<sub>3</sub> catalyst, the quantity of NH<sub>3</sub> present in the reformat, after considering the dilution with the exhaust gas

upstream the HC-SCR catalyst, is not enough to have solely promoted the high NO<sub>x</sub> conversion as observed in Figure 33. It is suggested that the NH<sub>3</sub> measured in Figure 36 is a combination of the unused reformat product and a small concentration produced over the HC-SCR catalyst under the high H<sub>2</sub> presence. As a result, there are particular HC species produced from the reformer that are highly active as a reductant and will need to be further investigated through the speciation of the reformat product. It is also believed that under the present conditions, the HC reaction is more dominant than the utilisation of NH<sub>3</sub> over the Ag-Al<sub>2</sub>O<sub>3</sub> catalyst.

It is also important to observe the influence temperature plays on the HC-SCR catalyst performance. Figure 37 shows a controlled temperature ramp with the reformer active and the results show how the peak NO<sub>x</sub> conversion is substantially affected within a narrow temperature window. The low activity at higher catalyst temperatures can be the result of combustion of the reductant (e.g. HC) as there is an increase in CO<sub>2</sub> emissions in the product gas (i.e. downstream HC-SCR catalyst). However, the amount of CO<sub>2</sub> already present in the feed makes it difficult to distinguish the amount of formed CO<sub>2</sub> from this combustion. At high engine loads (i.e. higher exhaust temperatures) the oxidation reaction becomes predominant and further HC is required. Thus this loss in catalyst activity can be alleviated by tuning the HC:NO<sub>x</sub> ratio as a function of the exhaust temperature. It is also important to note that the result in Figure 37 shows the effect of temperature under a constant engine exhaust composition where the O<sub>2</sub> availability does not change. In real engine operation conditions, a high exhaust temperature (i.e. corresponding to a high engine load) would result in a reduction in the O<sub>2</sub> availability.

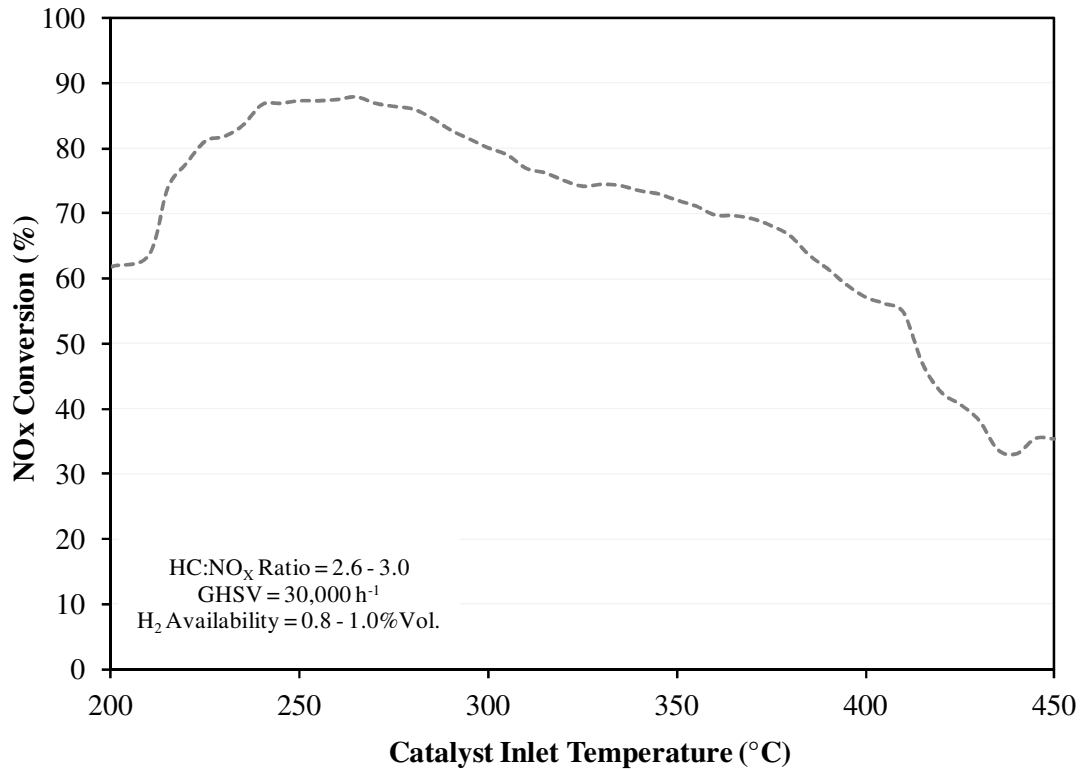


**Figure 37: Lean NO<sub>x</sub> Catalyst Performance over a Wide Diesel Exhaust Gas Temperature Window**

To observe the effect of a stop-start sequence, the reformer product gas was redirected away from the HC-SCR catalyst (while keeping the reformer itself active). This scenario demonstrates how the HC-SCR catalyst will behave if the reformat is suddenly stopped and then reintroduced. As shown in Figure 38, this specific test has a significant impact on the catalyst performance and the catalyst cannot regain its efficiency even though the same quantity of reformat is re-introduced each time. Soot which is effectively trapped within the upstream DPF cannot be the cause for the catalyst deterioration. Thus it is suggested that either the excessive CO or the longer chain HC species are having an impact.

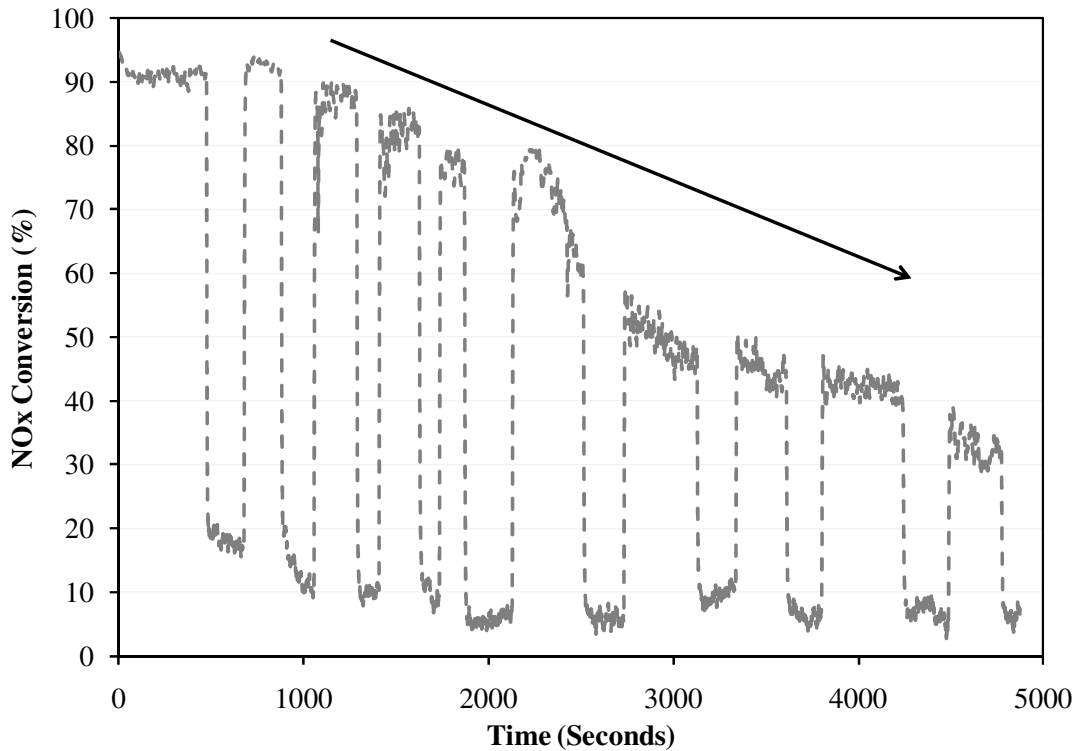


**Figure 38: The Effect of a Start-Stop Sequence on the Activity of a Lean NO<sub>x</sub> Catalyst**

In order to demonstrate the effectiveness of the upstream DPF, a similar stop-start sequence was carried out with only the HC-SCR catalysts present in the mini-reactor. As illustrated in Figure 39, the catalyst activity is again in the region of 90%. However, after stopping the reformat flow for a short period of time and following a similar stop-start sequence as before, the HC-SCR catalyst performance is significantly affected. In this case the presence of soot is also participating in the catalyst deactivation through the mechanism of coking. It is suggested that H<sub>2</sub> needs to be continuously available when the HC-SCR catalyst is subjected to the exhaust gas to promote a clean catalyst. Figure 31 as illustrated previously shows such an example. Although the quantity of reformat was significantly reduced, it was possible to return to a high NO<sub>x</sub> conversion activity as a result of having H<sub>2</sub> present in exhaust gas mixture.

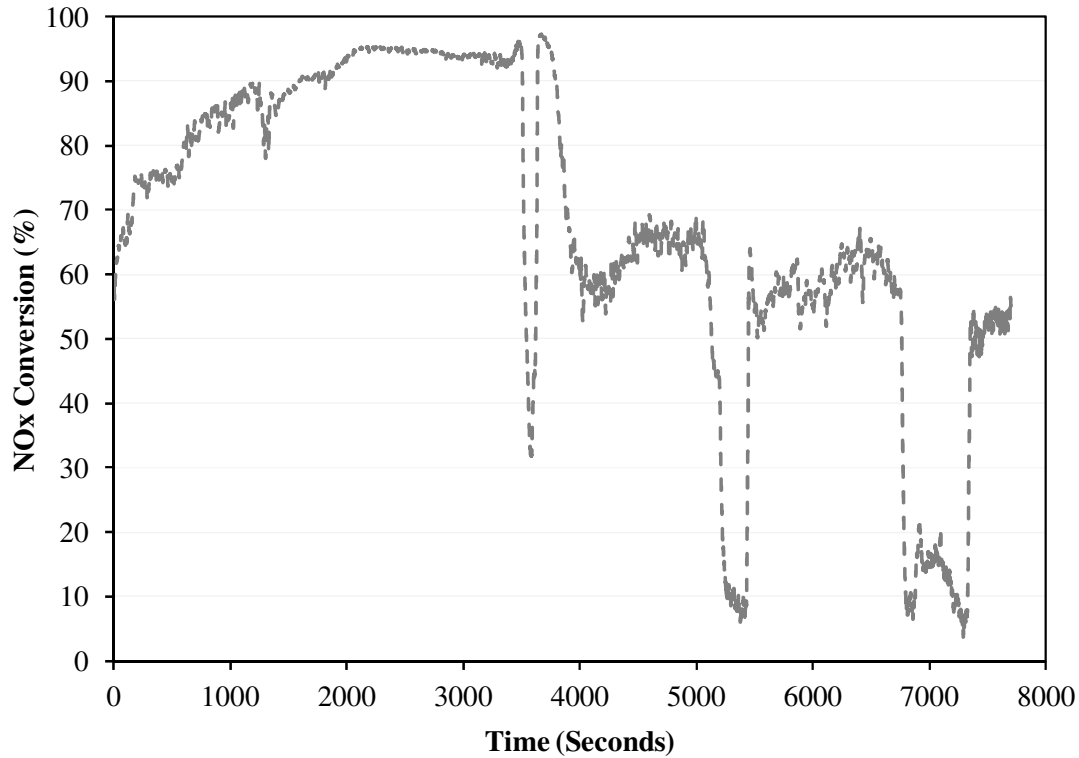


**Figure 39: The Effect of a Start-Stop Sequence on the Activity of a Lean NO<sub>x</sub> Catalyst without a DPF**

### **5.2.2.2 Simulated Reforming Tests**

To trace the cause of deactivation, a series of stop-start tests were implemented in the presence of various gaseous fuels which were introduced in the main exhaust before directed through to the mini-reactor. The first was a passive mode test with the HC-SCR catalyst positioned in the mini reactor and subjected to a homogeneous mixture of exhaust gas and pure H<sub>2</sub> (i.e. from bottled source). The concentration of H<sub>2</sub> was kept similar to that produced with the on-board fuel reformer using a calibrated needle valve. As shown in Figure 40, the addition and removal of H<sub>2</sub> through a stop-start sequence had no long term affect on the catalyst activity.

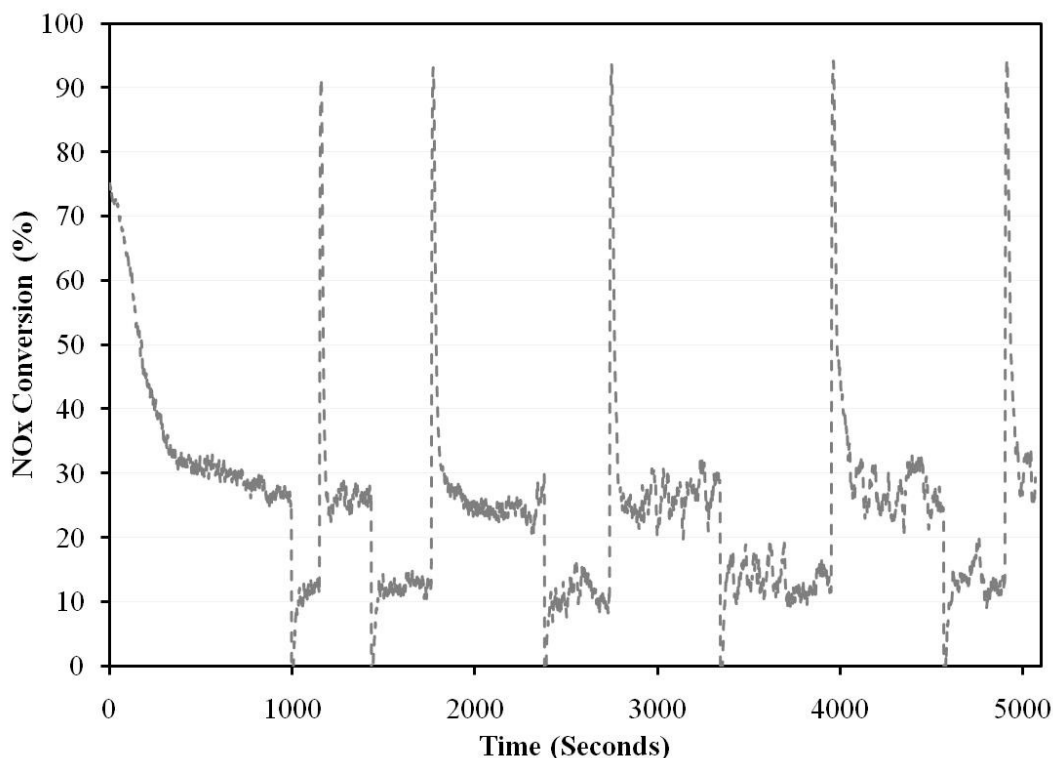
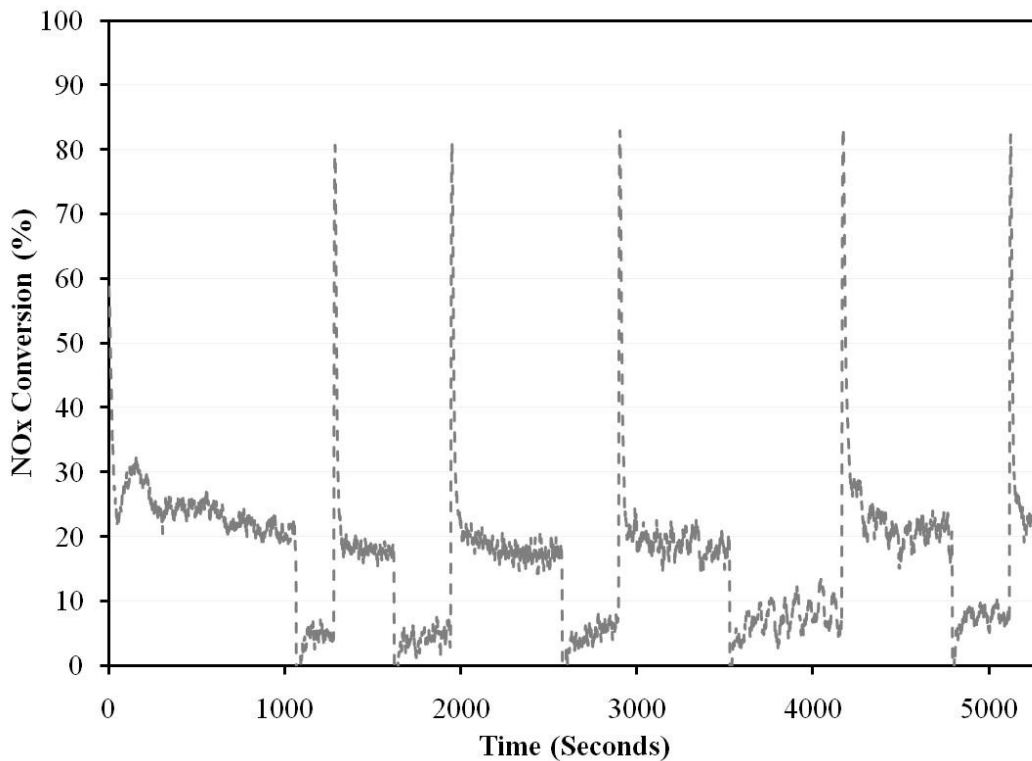


Figure 40: The Effect of Pure H<sub>2</sub> on the Activity of a Lean NO<sub>x</sub> Catalyst during a Start-Stop Sequence

The second test was to introduce CO into a mixture of exhaust gas and pure H<sub>2</sub>. Thus, the concentrations were chosen to replicate that of the on-board fuel reformer. As shown in Figure 41, the addition of CO reduces the overall NO<sub>x</sub> reduction performance of the catalyst by approximately 5% compared to Figure 40. However, the catalyst is able to regain its activity after a stop-start process. Several research groups have reported evidence suggesting that CO is not an effective coreductant over an Ag-Al<sub>2</sub>O<sub>3</sub> catalyst. The study by Wichterlová et al. (2005) showed that during HC-SCR the addition of CO into the H<sub>2</sub> feed resulted in an increased number of Ag clusters. However, there was no improvement in catalyst activity in terms of NO conversion. Similar observations were made by Breen et al. (2005), where CO replaced or substituted part of the H<sub>2</sub> feed. During this study it was found that the number of Ag clusters remained almost the same, although there was a significant loss in NO conversion. It was concluded by Shimizu et al. (2007) that CO can reduce Ag<sup>+</sup> species on Ag-

Al<sub>2</sub>O<sub>3</sub> to form Ag clusters but it does not yield protons. Hence the reactive oxygen species, which are formed by the reaction of O<sub>2</sub> with protons as seen with H<sub>2</sub>, are not formed. The study established that both protons and electrons with reduced Ag<sup>+</sup> species on Ag-Al<sub>2</sub>O<sub>3</sub> to form Ag clusters are extremely important for the reductive oxidation of O<sub>2</sub> to give way for reactive oxygen species (O<sub>2</sub><sup>-</sup>). In conjunction with fuel reforming, the WGS reaction can be promoted as a CO removal method, thus producing more H<sub>2</sub> in the product feed.



**Figure 41: The Effect of Pure H<sub>2</sub> and CO on the Activity of a Lean NO<sub>x</sub> Catalyst during a Start-Stop Sequence**

The final test was to introduce HC (i.e. diesel fuel) with a fuel atomiser into a mixture of exhaust gas and pure H<sub>2</sub> to promote the HC-SCR reaction through an active mode. Although the initial activity of the HC-SCR catalyst is relatively high as shown in Figure 42, the resulting stop-start sequence tends to have a similar negative impact as that observed earlier in Figure 38. It is also clear that the activity of the catalyst begins to stabilise similar to

that result obtained with pure H<sub>2</sub> in Figure 40. Although soot is a major contributor to the deactivation of the HC-SCR catalyst, the hydrocarbons can also have further implications as shown here.

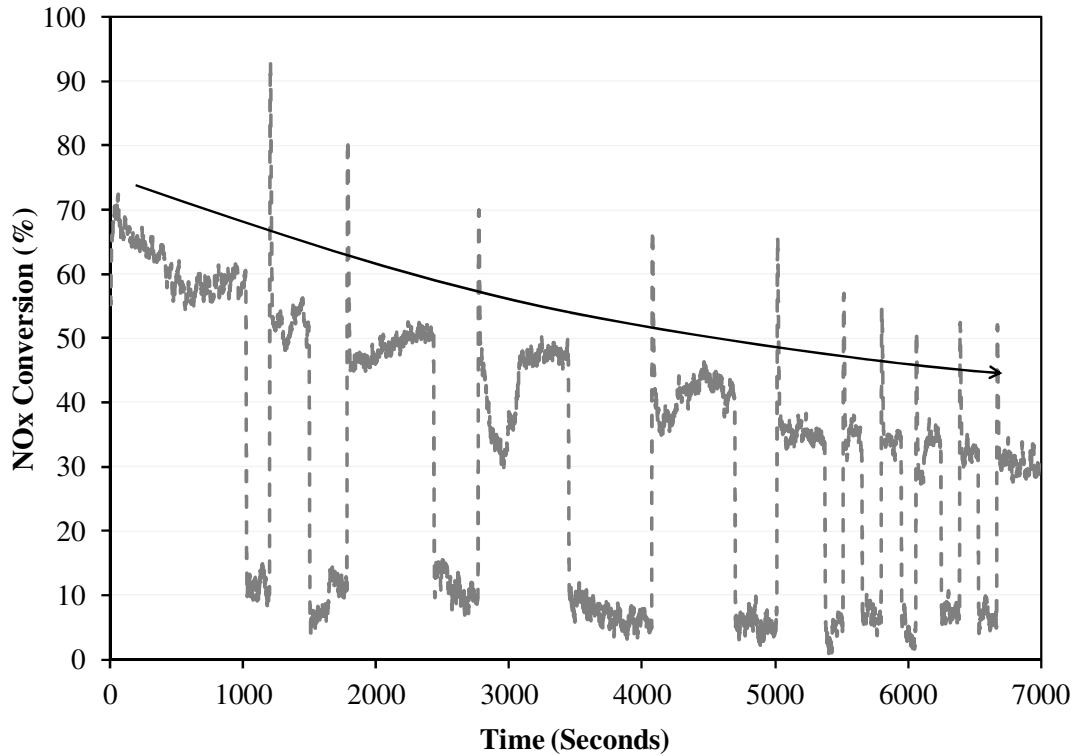


**Figure 42: The Effect of Pure H<sub>2</sub> and HC on the Activity of a Lean NO<sub>x</sub> Catalyst during a Start-Stop Sequence**

### **5.2.3 Low load HC-SCR catalyst performance – Engine load of 3 bar IMEP**

The following results demonstrate an actual low load condition where the exhaust temperature is the same as the inlet HC-SCR catalyst temperature. To ensure sufficient H<sub>2</sub> is available upstream the HC-SCR catalyst a fuel flow rate of 40ml/hr was chosen based on the quantity of H<sub>2</sub> that can be produced as explained earlier in this study. Table 12 gives an overall summary of the test conditions.

**Table 12: Summary of Test Conditions under an Engine Load of 3 bar IMEP**

<i>Engine Conditions</i>			<i>DPF-SCR System</i>		
Inlet	35	°C	SCR Inlet Temp	247	°C
Speed	1500	rpm	Space Velocity	30,000	h <sup>-1</sup>
Load	3	bar	HC:NO <sub>x</sub> Ratio	~ 3.5	
Exhaust	224	°C	H <sub>2</sub>	0.7 - 0.9	%Vol.
<i>On-board Reformer</i>					
Catalyst Inlet	~ 850	°C			
Exhaust Flow Rate	5.0	l/min			
Space Velocity	10,000	h <sup>-1</sup>			
Fuel Flow Rate	40	ml/h			
Equivalence Ratio	0.68				
O/C (n/n)	1.57				
S/F (n/n)	2.83				
O <sub>2</sub> /F (n/n)	9.57				

In contrast with the higher engine load operation, running at lower load resulted in more complete oxidation (Reaction 41) of the fuel increasing the CO<sub>2</sub> component of the reformate product, while simultaneously reducing the amount of unburnt HC. As the concentrations of CO and H<sub>2</sub>O are smaller than that at high load, it is suggested that the SR reaction (Reaction 36) is not as dominant, with the WGS reaction (Reaction 39) taking place to account for the lower CO and H<sub>2</sub>O concentrations. It is believed that in this study the WGS reaction was constrained thermodynamically by the relatively high temperatures of the reforming catalyst. In earlier studies it has been reported that the optimum WGS range for the same catalyst is 550-700°C, while a H<sub>2</sub>O/CO molar ratio  $\geq 1$  is theoretically required to utilise the entire CO at a point when all of the diesel fuel has been utilised for the endothermic reactions (Tsolakis and Golunski, 2006, Tsolakis et al., 2005). Table 13 shows the engine-out exhaust emissions alongside the product gas from the on-board fuel reformer.

**Table 13: Average Engine-out Emissions and On-board Reformer Product Gas - Engine Load of 3 bar IMEP**

		<b>Engine-out</b>	<b>REGR Product Gas</b>
<i>NO</i>	<i>ppm</i>	456.73	6.73
<i>NO<sub>2</sub></i>	<i>ppm</i>	61.49	144.58
<i>NO<sub>x</sub></i>	<i>ppm</i>	518.22	151.32
<i>NH<sub>3</sub></i>	<i>ppm</i>	0.69	13.43
<i>Propylene</i>	<i>ppm</i>	1.25	38.88
<i>Ethylene</i>	<i>ppm</i>	4.66	53.99
<i>Methane</i>	<i>ppm</i>	4.87	60.46
<i>Ethane</i>	<i>ppm</i>	0.00	30.64
<i>Total HC</i>	<i>ppm</i>	643.50	5856.93
<i>CO</i>	<i>ppm</i>	156.29	29064.38
<i>H<sub>2</sub>O</i>	<i>%Vol.</i>	4.58	5.12
<i>CO<sub>2</sub></i>	<i>%Vol.</i>	3.76	9.83
<i>O<sub>2</sub></i>	<i>%Vol.</i>	15.48	0.19

Figure 43 shows the activity of the HC-SCR catalyst during the low load stop-start sequence; however in this case the fuel to the reformer is switched off and then reintroduced rather than keeping the reformer active and only bypassing the reformat product. The effect is not as severe as observed earlier and could be because of the lower HC and CO emissions present in the reformer product. It can also be observed that by stopping the fuel to the reformer the activity of the HC-SCR catalyst first increases unlike that observed in any of the results presented earlier. This suggests that when the fuel to the reformer is stopped, the reduction in HC promotes the catalyst activity, indicating that either the HC:NO<sub>x</sub> ratio may be high for the specific condition or there are surplus amounts of non-active short chain HC species present in the reformat which can deposit on the surface of the HC-SCR catalyst at

such low temperatures. In order to minimise the HC-SCR catalyst deactivation, optimisation of the reformer is essential to control the HC concentration in the reformer product. Although reducing the fuel flow can be seen as the most practical solution, the resulting higher O/C ratio will have a negative impact on the production of H<sub>2</sub>.

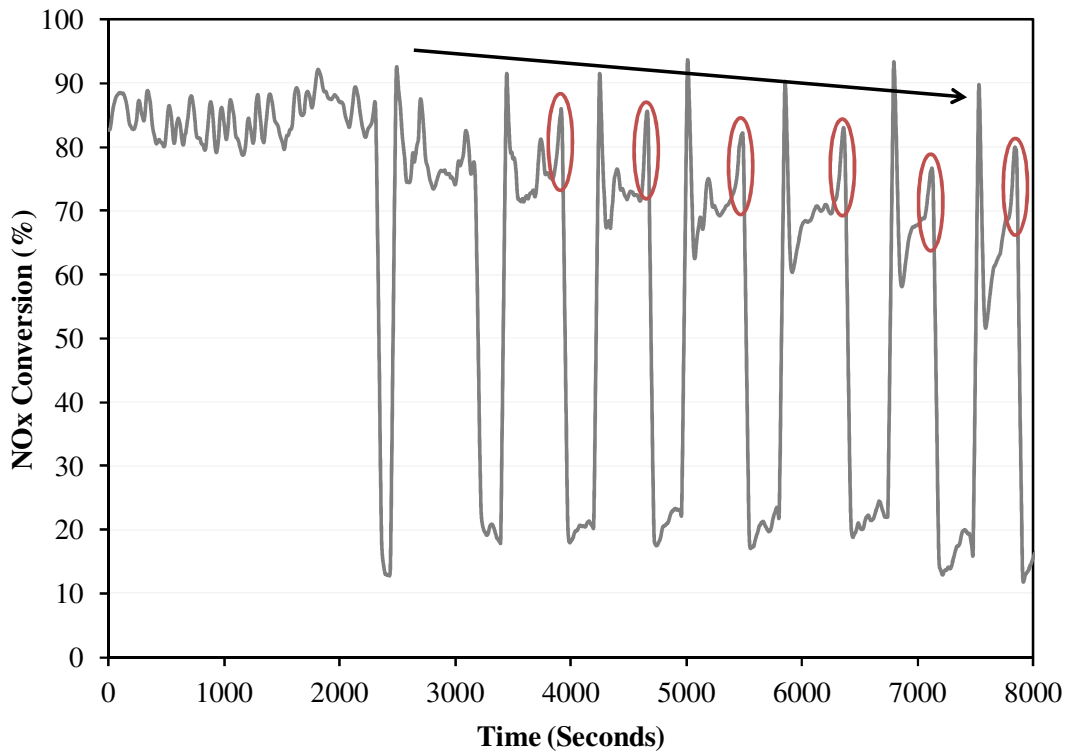


**Figure 43: The Effect of a Start-Stop Sequence during Low Load Operation on the Activity of a Lean NO<sub>x</sub> Catalyst**

#### **5.2.4 Reformer Activity**

After a series of tests it was observed that the reformer itself was becoming unstable as illustrated in Figure 44, suggesting the reforming catalyst may be heavily coked from the series of tests. This fluctuation can be observed by the changes in reformer temperature, hence finally affecting the performance of the HC-SCR catalyst. At low engine load (3 bar IMEP) the introduction of more fuel (i.e. heavy HC) as well as a lower exhaust temperature may also influence the reformer catalyst performance. The instability of the reforming could effectively

be looked at as a rapid stop-start towards the HC-SCR catalyst, where the reformate product is continuously present but in varying quantities of H<sub>2</sub> and/or active HC species.

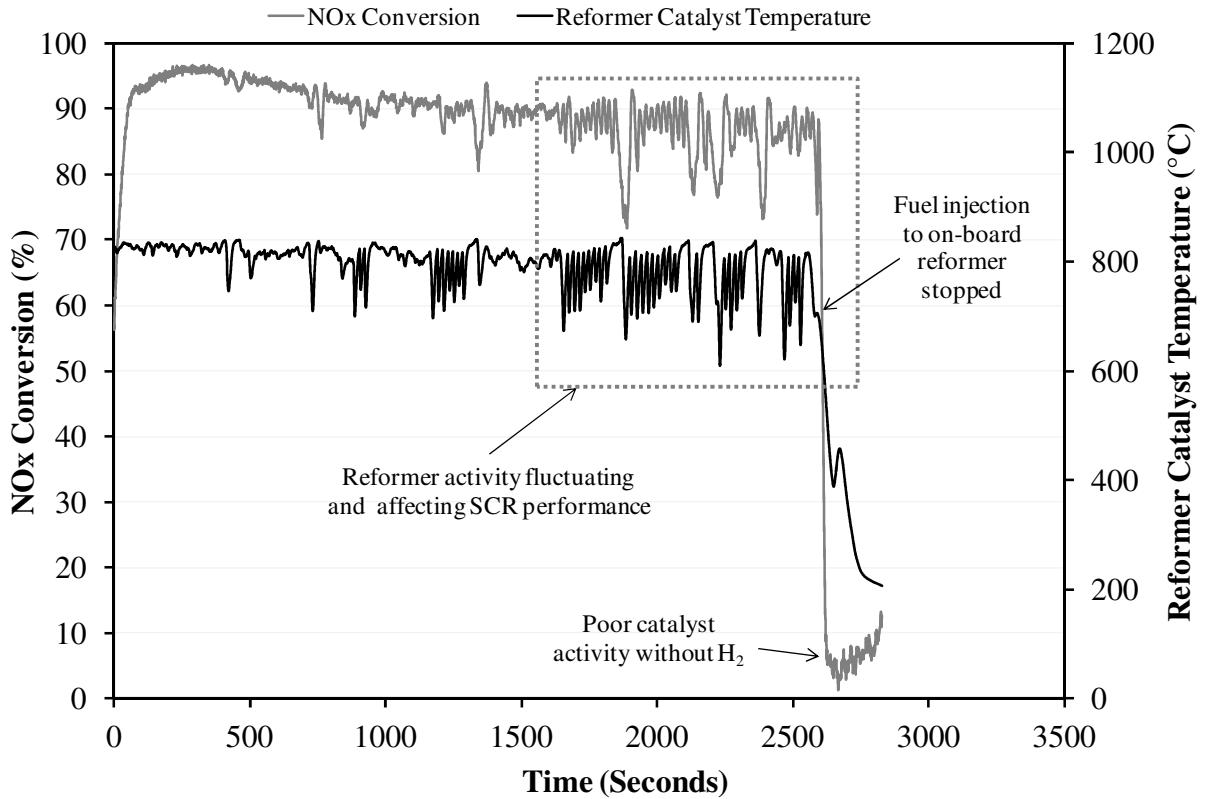


**Figure 44: On-board Fuel Reformer Affecting the Lean NO<sub>x</sub> Catalyst Performance during 3 bar IMEP**

Similarly, running at a higher engine load (5.3 bar IMEP) the coking becomes more severe, as shown in Figure 45. As mentioned earlier, a high ethylene concentration generally means a severe carbon deposition is taking place on the catalyst.

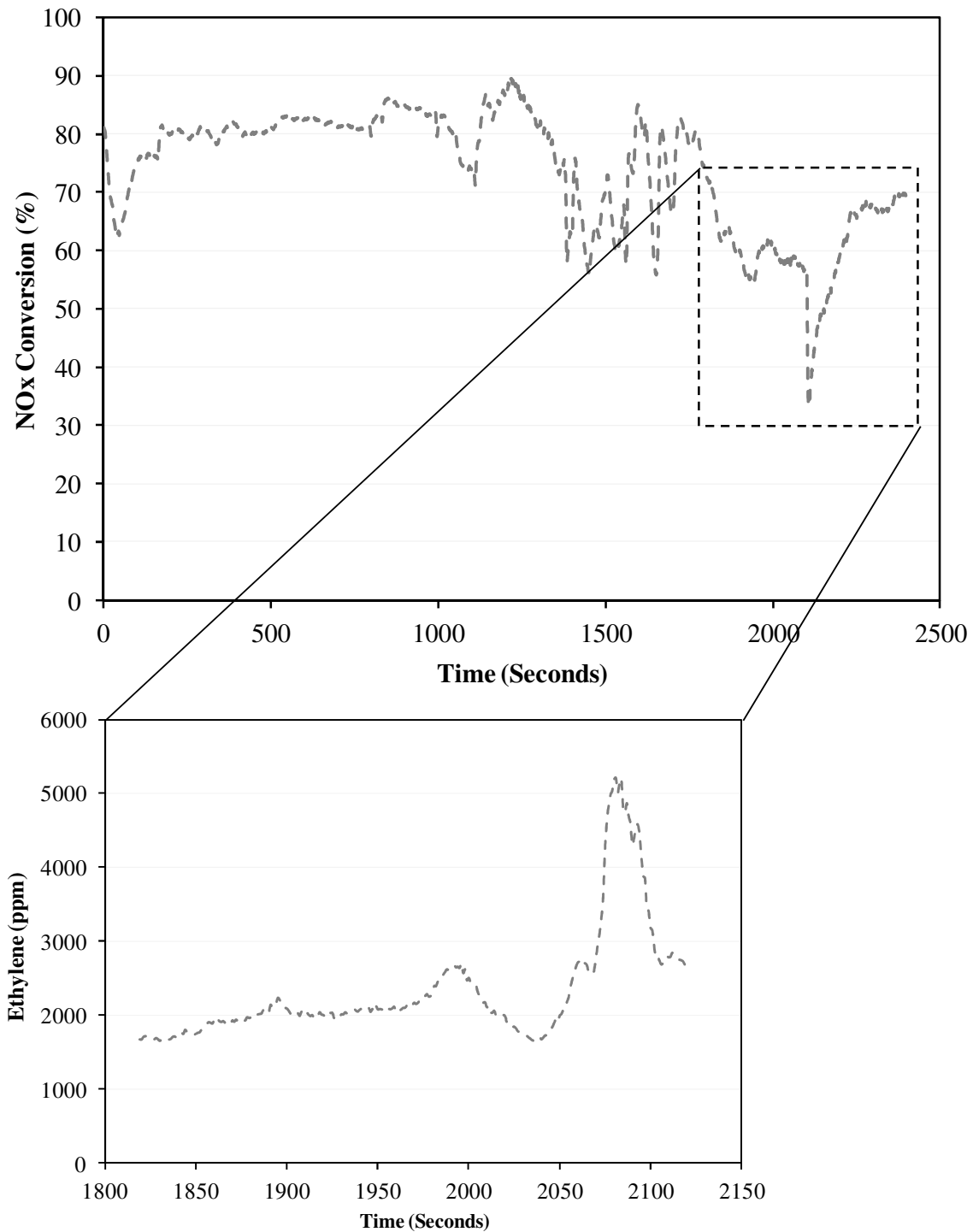
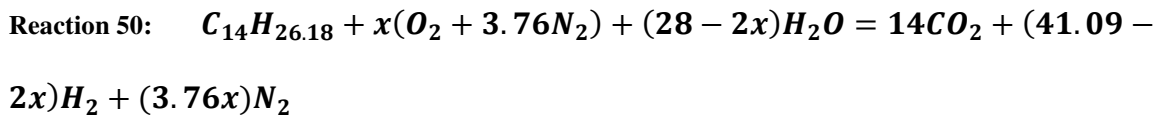


**Figure 45: Reformer Coking Affecting Lean NO<sub>x</sub> Catalyst Performance during 5.3 bar IMEP**

It is also known that steam reforming can also result in carbon formation (below a certain steam to carbon ratio) through the Boudouard reaction (Reaction 48) as well as by the decomposition (Reaction 49) of hydrocarbons (Rostrup-Nielsen, 1993).



However, one method to avoid coke formation is to use higher S/F ratios (or a higher O/C ratios) and high temperatures as reported by Rostrup-Nielsen (1993, 1997) and Ahmed and Krumpelt (2001). Using water as a source of O<sub>2</sub> lowers the temperature required to avoid coke formation. Considering the idealised reaction stoichiometry for the conversion of diesel fuel as shown in Reaction 50, where ‘x’ represents the O<sub>2</sub>/F ratio, the water required to convert the carbon in the fuel to CO<sub>2</sub> can be calculated.



Using the O<sub>2</sub>/F ratio from Table 9 for the reforming under high load conditions, the water present in the exhaust only accounted for 21% of that required for the ideal case to convert the carbon in the fuel to CO<sub>2</sub>. Also from the idealised reaction the maximum percentage of the H<sub>2</sub> in the product was calculated to be approximately 42%. Although this is an ideal case, the amount of H<sub>2</sub> achievable is still substantially higher than that achieved in this study. Using heavy hydrocarbons like diesel fuel with a boiling point higher than 300°C is partially responsible for the reduced efficiency (Tsolakis et al., 2004). Overall more water (i.e. steam) could have been added to increase the yield and concentration of H<sub>2</sub> in the product gas by promoting the endothermic reactions (i.e. ATR) especially under the higher O/C ratios which can also result in a minimised fuel penalty. It has also been reported in literature (Ahmed and Krumpelt, 2001) that the coking tendency is reduced at higher O/C ratios and is favoured that the O<sub>2</sub> feed to the reformer be in the form of water. However, introducing water will require additional heat for evaporation and will further add to a reduction in efficiency.

In this study it has been shown that there is potential for a combined integrated fuel reformer and HC-SCR system. However optimisation primarily of the reformer is required not only to control the self-coking but minimise the production of excessive HC species as well as CO.

### **5.3 Summary**

The results of this study have shown an approach of enhancing the activity of an Ag-Al<sub>2</sub>O<sub>3</sub> HC-SCR catalyst with reformat promoting the low temperature lean NO<sub>x</sub> reduction activity window. The lean NO<sub>x</sub> improvement can be observed without the need of external HC dosing systems, apart from the fuel supplied to the reformer, as well as the requirement of on-board H<sub>2</sub> storage. The exhaust gas fuel reforming of diesel fuel was able to supply the demand of H<sub>2</sub> and promote the HC:NO<sub>x</sub> ratio needed for the HC-SCR catalyst to work effectively. Further by controlling the exhaust/reformate ratio a 90% NO<sub>x</sub> conversion was achievable. Positioning a DPF upstream the HC-SCR catalyst was promising, especially in supporting the catalyst activity by filtering the exhaust of carbonaceous species (i.e. soot). However, as most lean NO<sub>x</sub> catalysts are susceptible to coking in the presence of excess HC's, optimisation of the reformer will need to be considered. The temperature ramp of the HC-SCR catalyst under steady state conditions showed that at higher engine loads (i.e. high exhaust gas temperatures), the oxidation reaction is more predominant and as a result further HC addition is necessary. However, under low exhaust temperatures excess HC has shown to lead to partial catalyst deactivation by the deposition of carbon-rich species, which are subsequently removed at higher temperatures.

In order to extend the practical aspects of the work, the behaviour of the aftertreatment catalyst under a start-stop sequence was carried out. The results showed that the HC-SCR

catalyst activity decreases after the reformat flow is stopped and re-introduced several times. As soot was controlled by implementing an upstream DPF, the reduction in catalyst activity was suggested to be directly linked to the large presence of hydrocarbons, possibly the non-active species, from the reforming process. Therefore better control of the HC:NO<sub>x</sub> ratio is required. In practice the rate of fuel flow addition to the reformer needs to be optimised to account for the different exhaust gas compositions and space velocities. It is also suggested that the operating parameters of the reformer have to be chosen to ensure the WGS reaction is part of the reforming process, not only to control the CO concentration but also effectively support the long term efficiency of the reforming catalyst by using a higher S/F ratio.

# CHAPTER 6

## ANALYSIS OF REFORMED EGR ON THE PERFORMANCE OF A DIESEL PARTICULATE FILTER

### 6.1 Introduction

The objective of this study is to investigate the low temperature passive regeneration and soot deposition (i.e. pressure drop and loading across the filter) between a combined DPF/DOC-DPF and cDPF/ DOC-cDPF systems, while utilising reformat to promote the NO<sub>2</sub> fraction either through combustion or catalyst interaction. This is to further understand the influence the different configurations may have on the performance of the CRT<sup>®</sup>. The crucial parameters recorded during regeneration were the local filter/catalyst temperatures, the residual NO<sub>2</sub> concentrations and the local filter soot loading/pressure drop within each system.

This study focuses primarily on the low temperature NO<sub>2</sub> passive regeneration under real loading conditions. Passive regeneration, also referred to as continuous regeneration, is based on the high reactivity of NO<sub>2</sub> for PM oxidation as shown by Reaction 19 and Reaction 20 previously. The reaction which uses the exhaust heat will occur at a temperature 200-300°C lower with NO<sub>2</sub> than with O<sub>2</sub>. This can be further improved by the addition of a catalyst promoting the lower DPF inlet temperatures. This is the basis of the CRT<sup>®</sup> which uses exhaust NO<sub>2</sub> (enhanced through the oxidation of NO over a DOC) to oxide soot continuously within relatively low temperatures (< 300°C) over a DPF (York et al., 2007,

Allansson et al., 2002). The amount of NO to NO<sub>2</sub> conversion is dependent on the hydrocarbon fuels and the exhaust gas temperature window (Hori et al., 2002).

A recent study by Shin et al. (2011) demonstrated the effectiveness of introducing H<sub>2</sub> into the combustion chamber through the intake manifold as considered in this study. It was concluded that low temperature NO<sub>x</sub> reduction improved as a result of the H<sub>2</sub> addition under high EGR ratios. It was observed that by replacing part of the intake charge with H<sub>2</sub> (i.e. reducing the O<sub>2</sub> concentration) there was an increased content of inert gasses in the exhaust stream and, as this was part of an EGR loop, it influenced the intake manifold gas concentrations. Overall it was suggested that H<sub>2</sub> promoted diesel combustion, reducing the engine-out emissions of unburned HC and CO emissions. Compared to diesel fuel, H<sub>2</sub> has a greater heating value, lower density and requires a higher auto-ignition temperature. Thus, once ignited H<sub>2</sub> is highly reactive.

An earlier study carried out by Abu-Jrai et al. (2009) also showed the benefits of H<sub>2</sub> through the use of REGR. It was observed greater REGR levels improved the emissions of smoke and NO<sub>x</sub> especially under low load conditions. However, there was a penalty in NO<sub>x</sub> emissions at high load with high REGR levels. The influence of H<sub>2</sub> for combustion and aftertreatment performance has been the focus of many researchers.

In this study tests were carried out under steady state operation with an engine speed of 1200rpm and an engine load of 3 bar IMEP used throughout the experiment, thus giving a GHSV of ~43,000h<sup>-1</sup> based on the DOC volume. These conditions were used as a preliminary starting point to replicate those used for the actual exhaust gas reforming studies implemented in the past by our research group. However, the aim here is to observe the effectiveness of on-board reformate in combustion and aftertreatment for passive regeneration over the DPF. The

original exhaust gas fuel reforming study was carried out under the low exhaust temperature window ( $< 300^{\circ}\text{C}$ ) of a typical diesel exhaust, where catalyst activity and filter regeneration are challenging. A passive approach was chosen rather than an active one because it is well known that the latter can lead to an additional fuel penalty and unconditional regeneration (i.e. which can cause DPF failure).

The experimental setup is illustrated in Figure 46, showing the arrangement of the aftertreatment devices as well as the locations of the simulated reformat addition. In this study the engine was fed with REGR, a reforming reactor product from diesel exhaust gas fuel reforming as implemented in an earlier study (Tsolakis et al., 2004). This was simulated by replacing part of the EGR with simulated reformat (consisting primarily of  $\text{H}_2$  and  $\text{CO}$ ) added directly into the exhaust upstream of the aftertreatment system. In addition to this, an alternative approach was also considered. This involved adding reformat directly into the intake manifold of the engine, replacing part of the intake air and keeping the full potential of EGR. The differences between the systems lie primarily on the quantity of reformat available in combustion and the overall  $\text{O}_2$  availability in the exhaust for aftertreatment performance.

A composition of REGR was simulated by mixing standard EGR with bottled pure  $\text{H}_2$  and  $\text{CO}$ , with the composition of these gases chosen based on previously published studies on exhaust gas fuel reforming using diesel fuels (Tsolakis et al., 2007a, Tsolakis et al., 2003, Tsolakis and Megaritis, 2004a). Therefore the final REGR composition contained 17%  $\text{H}_2$  (6000ppm  $\pm$  5% of the exhaust flow) and 15%  $\text{CO}$  (5300ppm  $\pm$  5% of the exhaust flow) balance  $\text{N}_2$  in 20% Vol.EGR. The  $\text{H}_2$  and  $\text{CO}$  volumetric flow rates were controlled and measured by separate flow meters. It was reported by Rodríguez-Fernández et al. (2009b) that such compositions correspond to a situation where the exothermic WGS reaction is not significantly promoted.

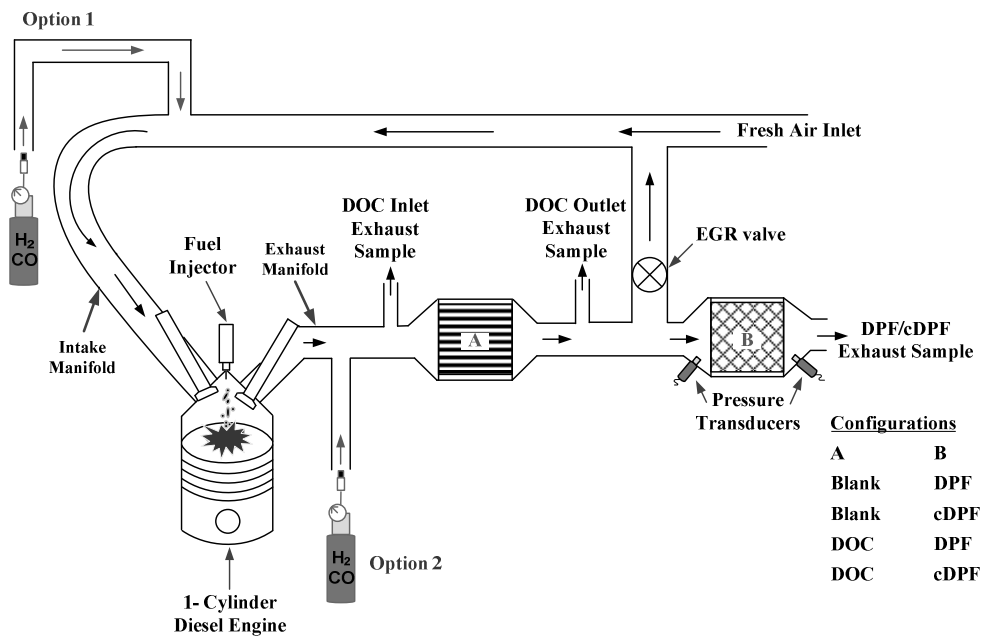


Figure 46: Schematic of Passive DPF Regeneration with Simulated Reformate

From Figure 46, the catalyst positioned at point A in the system is part of the EGR loop back into the engine inlet. Hence the EGR composition will differ with and without the DOC. Figure 47 shows the DOC and DPF models that have been studied individually or combined to simulate the CRT<sup>®</sup> and CCRT<sup>®</sup> systems (Schejbal et al., 2010).

As mentioned earlier the CRT<sup>®</sup> system is comprised of a DOC which oxidises the HC, CO and NO, followed by an uncatalysed DPF. The CCRT<sup>®</sup> system has a similar setup but replaces the standard DPF with one that is catalysed on the inlet channels, thus enabling some of the NO to be reoxidised back to NO<sub>2</sub> which then reacts with more trapped PM. As a result, this enables the system to regenerate in applications with very low exhaust temperatures or lower NO<sub>x</sub>/PM ratios present in the exhaust.

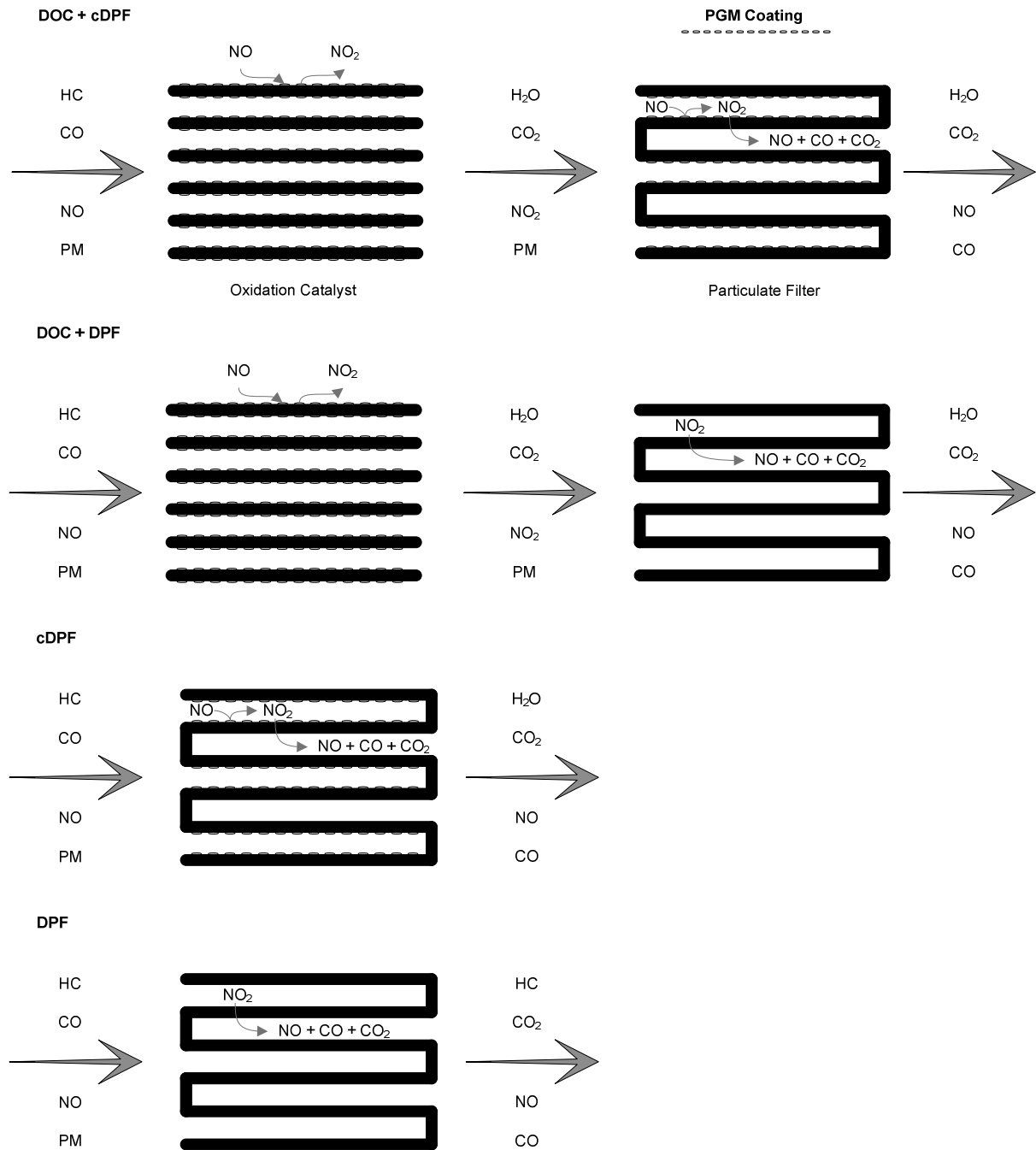


Figure 47: DOC, DPF and cDPF Systems with overall Emission Conversions

## 6.2 Results and Discussion

The results of the various individual tests have been compared and collated in the following sections. The first area is combustion, which links all the aspects of the proposed

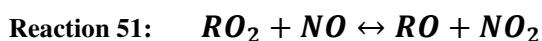
engine, REGR and aftertreatment system. The second focuses directly on the performance of the individual aftertreatment devices in the presence of simulated reformat.

### **6.2.1 Combustion Performance**

In all the tests presented in this study, especially those with reformat addition; the COVs were below 5%, well below the COV threshold of 10% whereby concerns arise.

#### **6.2.1.1 Effects of EGR**

The combustion temperature with EGR decreased, reducing the total engine-out NO<sub>x</sub> and increasing the NO<sub>2</sub> concentration (i.e. primarily the NO<sub>2</sub>/NO<sub>x</sub> ratio). The latter is associated with the production of the HO<sub>2</sub> radical which is suggested to be the most effective agent for promoting NO oxidation (Hargeaves et al., 1981). Several studies (Hori et al., 2002, Hargeaves et al., 1981, Hori, 1988) have suggested that the oxidation of NO to NO<sub>2</sub> is dependent on temperature and HC presence. At low temperatures, the formation of HO<sub>2</sub> and RO<sub>2</sub> peroxy radicals are essential for promoting NO oxidation as shown previously in Reaction 9 and through the following reaction:



Using EGR under the engine condition considered in this study, the indicated specific fuel consumption (ISFC) and the indicated engine thermal efficiency (IETE) are not substantially affected. Some increase in fuel consumption and reduction in thermal efficiency was seen as expected with the addition of EGR.

#### **6.2.1.2 Effects of REGR**

In earlier work, a mini catalytic exhaust gas fuel reformer was integrated within the engine exhaust. This mini reformer was primarily used to enhance the performance of the aftertreatment systems but also for combustion. The reformat combustion allowed lower fuel

usage for equal engine torque and speed while both  $\text{NO}_x$  and PM emissions were reduced simultaneously (Rodríguez-Fernández et al., 2009b, Bika et al., 2008, Pundir and Kumar, 2007). This was attributed to the decrease in the quantity of the in-cylinder injected diesel fuel,  $\text{O}_2$  concentration and shift of the combustion patterns from diffusion to premixed in addition to  $\text{H}_2$  combustion characteristics (Tsolakis et al., 2009, Abu-Jrai et al., 2007). Hence the addition of REGR reduces the volumetric A/F ratio as air is replaced with gaseous fuel.

The in-cylinder pressure with intake REGR (Figure 48) reduced by approximately 3% at 5CAD, reflecting the reduction in overall  $\text{NO}_x$  emission. Under intake REGR conditions, it was observed that reformat addition had an effect of increasing the ignition delay and shifted the combustion towards the expansion stroke resulting in a reduced in-cylinder pressure. It should be noted that the introduction of gases with a higher specific heat capacity during EGR (in this case  $\text{CO}_2$  and  $\text{H}_2\text{O}$ ), absorb part of the heat released and as a result decrease the combustion temperature (Hu et al., 2009). However, replacing part of the EGR with simulated reformat added directly into the exhaust (upstream of the aftertreatment systems) reduces the overall effectiveness of EGR. This is because the amounts of  $\text{CO}_2$ ,  $\text{H}_2\text{O}$  and  $\text{N}_2$  brought in by EGR absorbing energy released from combustion is reduced (Zheng et al., 2004, Ladommatos et al., 1998). Whereas, by directly replacing part of the air intake with reformat, a more efficient EGR can be maintained, further increasing the heat capacity of the cylinder charge while reducing the flame temperature. Although  $\text{H}_2$  has a high auto-ignition temperature, the ignition energies of  $\text{H}_2$ /air are significantly low in comparison to many hydrocarbon fuel/air mixtures (Heywood, 1988).

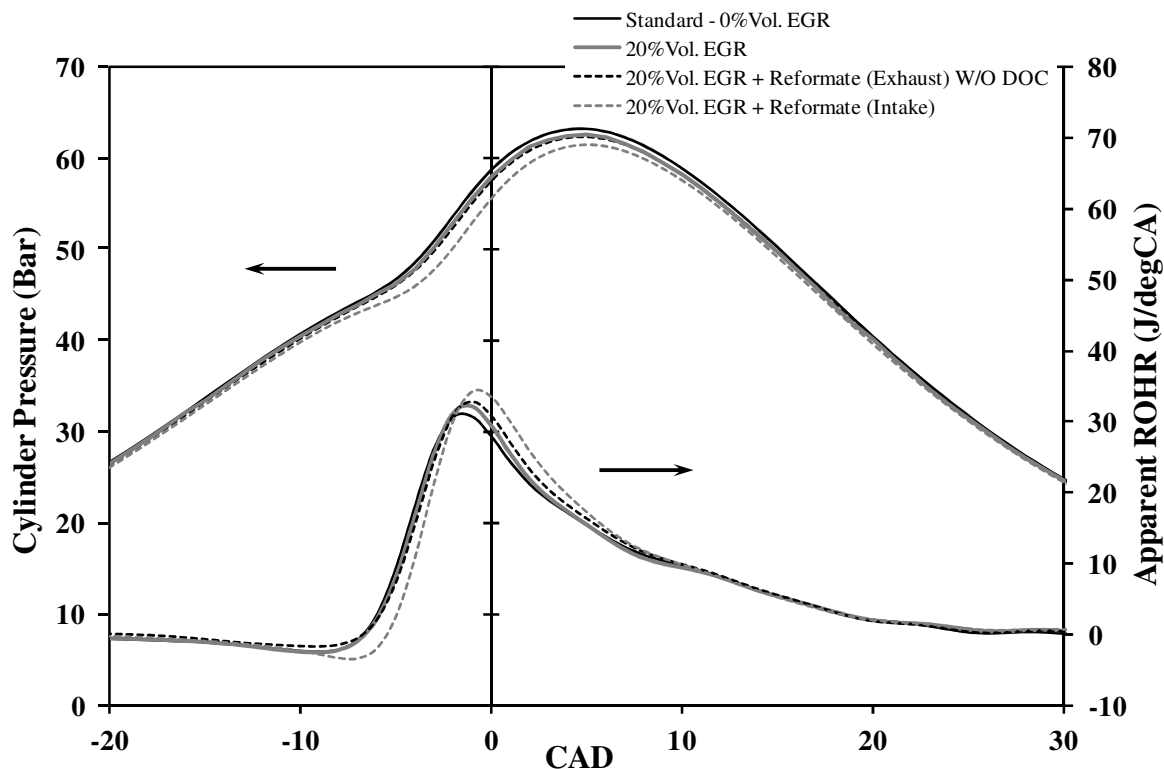
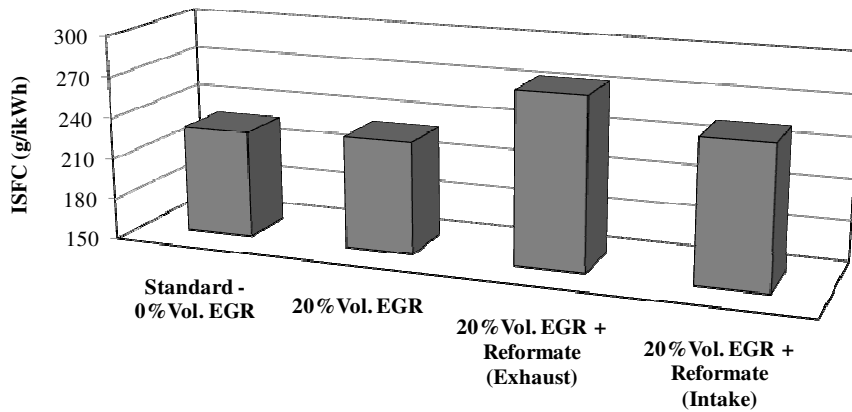


Figure 48: The Effect of REGR on Diesel Combustion

The effect of reformat addition on the ISFC and IETE are illustrated in Figure 49 and Figure 50 respectively. As expected, the addition of reformat increases the fuel consumption with an impact on engine thermal efficiency. This is not only directly related to the addition of reformat but also the reforming process efficiency itself. As the reformat concentrations were based on earlier exhaust gas reforming studies, the indicated fuel consumption takes into account the actual fuel required by the reformer to produce the required  $H_2$  concentration as well as that used during combustion. It is important to note that in this particular study we have considered a concentration of  $H_2$  that requires a substantial amount of diesel fuel through exhaust gas assisted fuel reforming. This approach can be referred to as a worst case scenario where the reformer was not optimised. There are numerous ways in which the fuel penalty can be improved and is currently still under investigation. For example, this can be achieved by either optimising the fuel reformer design and operation to convert the HC and CO into  $H_2$ ,

optimising the reactant ratios (i.e. process parameters such as GHSV and O/C ratios) or by optimisation of both the reforming processes using a prototype mini-fuel reformer integrated within the engine tailpipe system (Sitshebo et al., 2009).



**Figure 49: Indicated Specific Fuel Consumption**

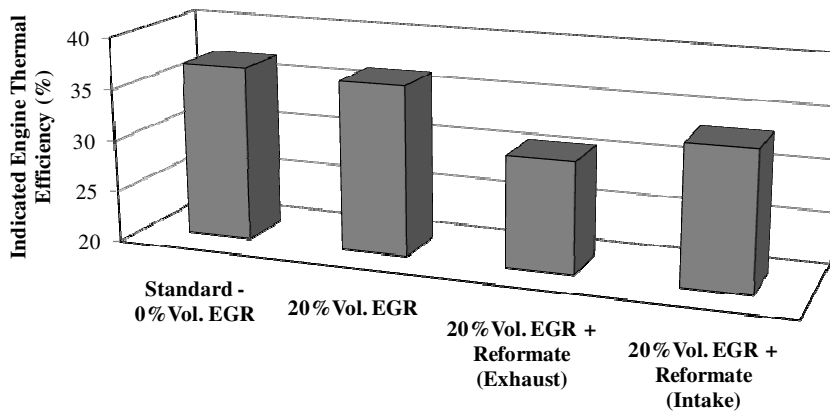


**Figure 50: Indicated Engine Thermal Efficiency**

## 6.2.2 Aftertreatment System Performance

### 6.2.2.1 Reformate Utilisation

As shown in Figure 51a both the cDPF and DOC utilised majority of the  $H_2$  while simultaneously oxidising the entire CO that was added with the  $H_2$ . Under intake REGR conditions as shown in Figure 51b, approximately 73.3% of  $H_2$  was utilised during the combustion, with a large portion consumed over the cDPF or DOC. However under these

specific conditions there was a larger portion of CO, approximately 20%, still unconverted downstream the cDPF suggesting there could be some soot oxidation taking place.

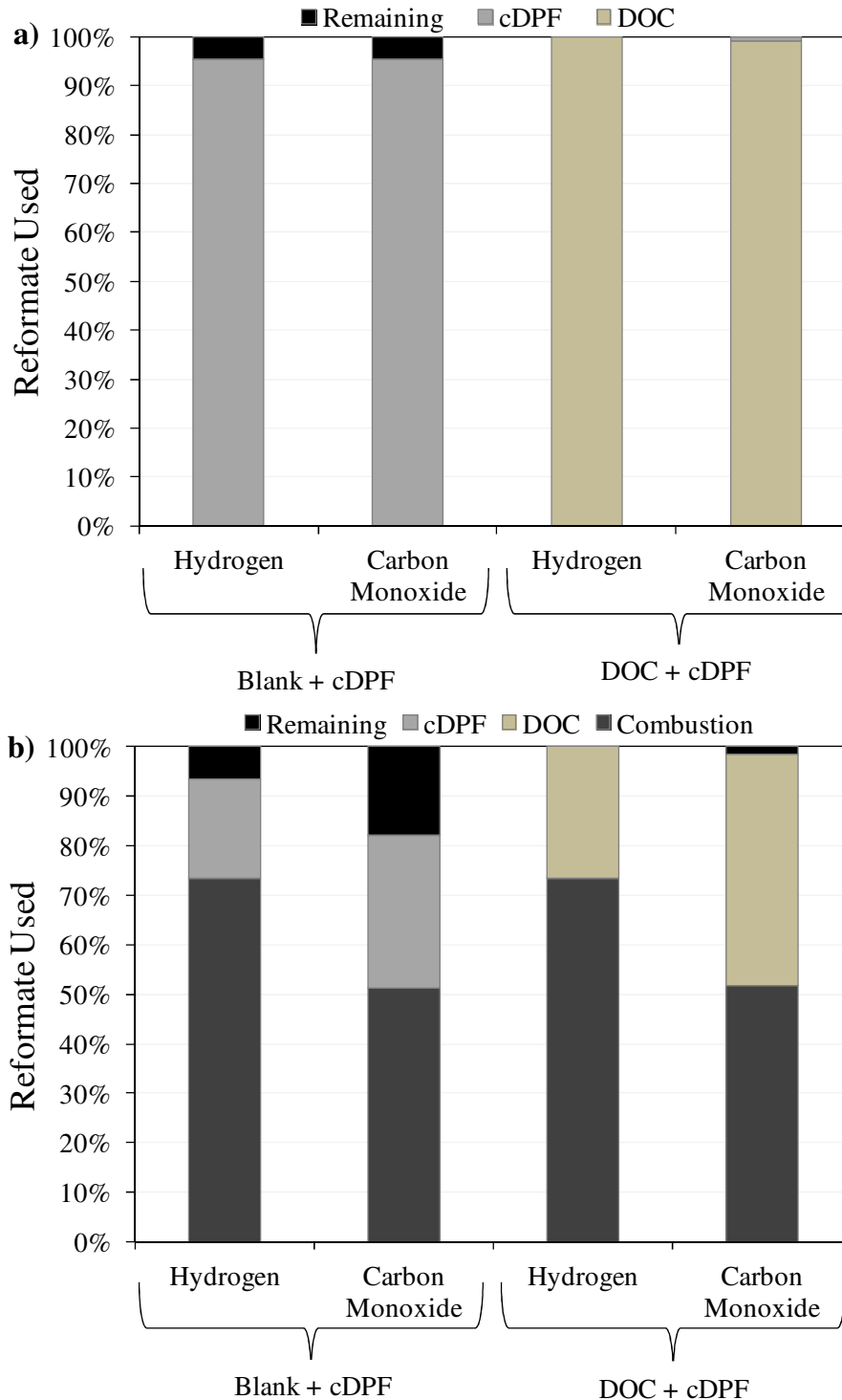
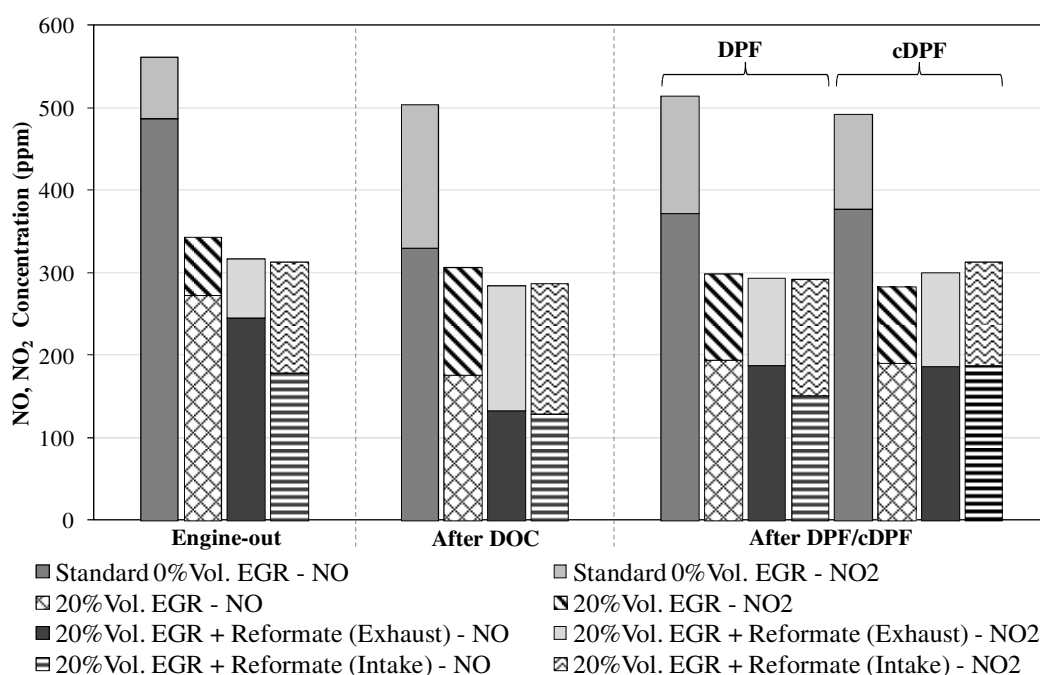


Figure 51: Reformat Oxidation during Combustion and over the DOC and cDPF: Reformat added to the a) Exhaust, b) Intake

Overall the results suggest that in the presence of H<sub>2</sub> a DOC is not necessary if there is a cDPF present in the system. It is important to note that in all conditions the DPF did not make use of any of the H<sub>2</sub> available in the exhaust.

### 6.2.2.2 Effects of EGR on the NO<sub>2</sub>/NO<sub>x</sub> ratio

The total engine-out NO<sub>x</sub> emissions reduce with the use of EGR (Figure 52 and Figure 53) while the overall NO<sub>2</sub>/NO<sub>x</sub> ratio increases as illustrated in Figure 54 and Figure 55. The reduction of global in-cylinder A/F ratio by EGR addition and /or reduced fuel concentration (due to a lower engine load) influences the in-cylinder temperatures and combustion efficiencies leading to inhibition of NO oxidation to NO<sub>2</sub> (Chong et al., 2010).



**Figure 52: Exhaust NO and NO<sub>2</sub> Concentrations in the Presence of a DOC**

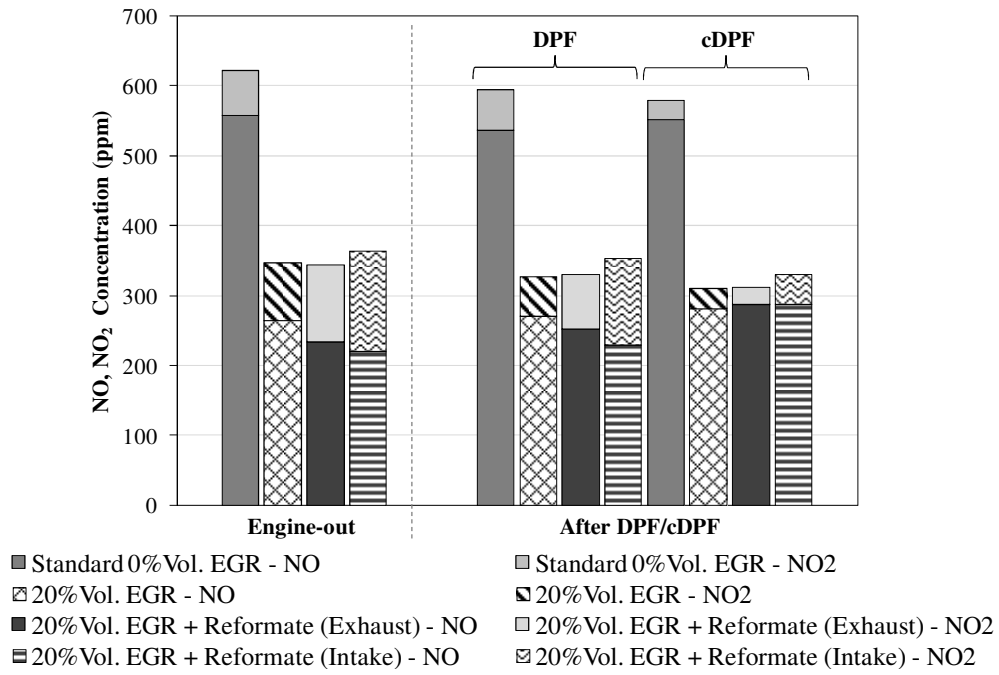


Figure 53: Exhaust NO and NO<sub>2</sub> Concentrations without a DOC

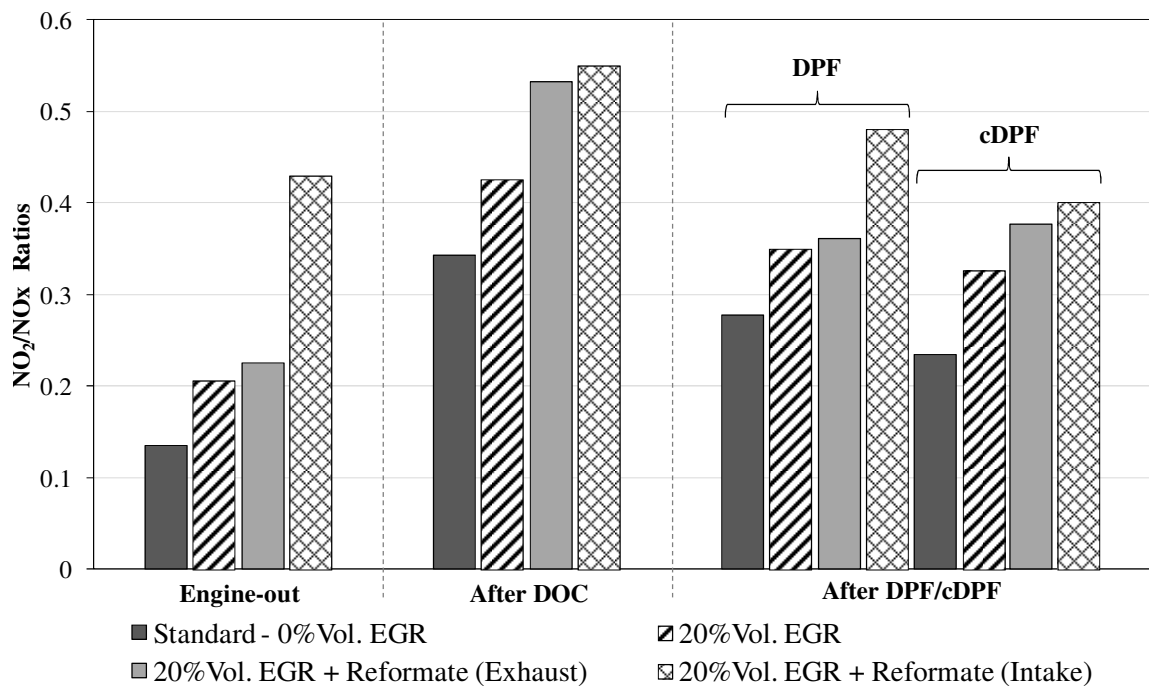


Figure 54: The Effect of the NO<sub>2</sub>/NO<sub>x</sub> Ratio in the Presence of a DOC

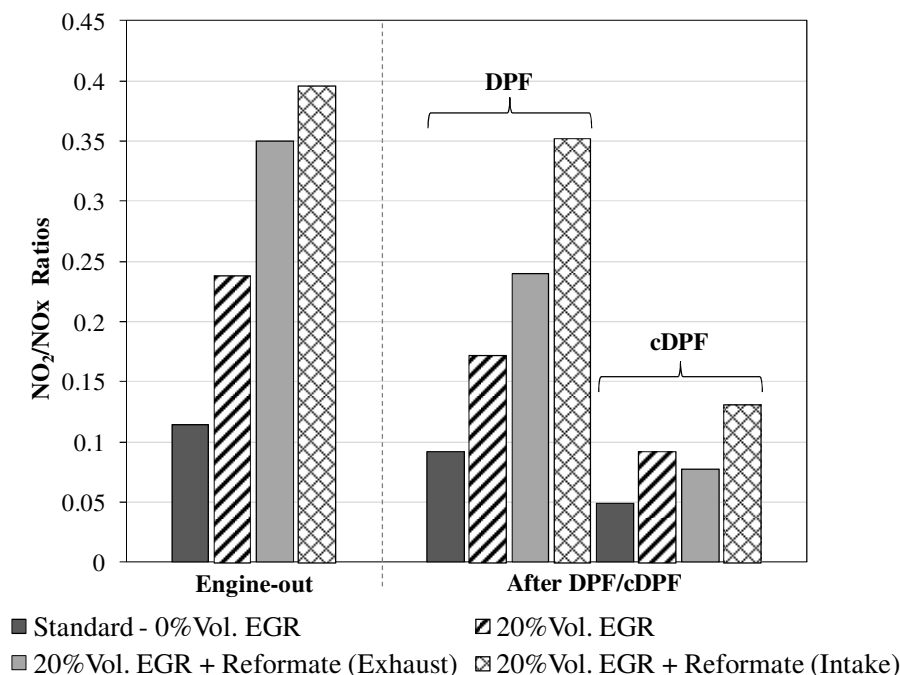


Figure 55: The Effect of the NO<sub>2</sub>/NO<sub>x</sub> Ratio without a DOC

### 6.2.2.3 Effects of REGR on NO<sub>2</sub>

The addition of REGR improved the NO<sub>2</sub> concentration in the exhaust, as also observed in an earlier study by Chong et al. (2010). The overall engine-out NO<sub>2</sub>/NO<sub>x</sub> ratio (Figure 54 and Figure 55) was approximately 35% greater with EGR and up to 70% when REGR was added. However, when adding REGR into the engine intake, the NO<sub>2</sub> engine-out concentration (see Figure 52 and Figure 53) was significantly increased. This could have been a result of the reformat presence (H<sub>2</sub>, CO and HC) supporting the generation of the HO<sub>2</sub> radical enhancing the NO<sub>2</sub> production. Thus, the presence of H<sub>2</sub> or CO may also be prominent in the following reaction:



### 6.2.2.4 Effect of the DOC

The NO<sub>x</sub> emission from a diesel engine exhaust typically consists of 85-95% NO and 5-15% NO<sub>2</sub> (Soltic and Weilenmann, 2003). A DOC is principally used to oxidise CO and HC

emissions under excess  $O_2$  but can also be vital for promoting  $NO_2$ , benefitting the DPF or cDPF regeneration performance. By looking at Figure 52 and Figure 53, the effect of a DOC on  $NO_2$  and  $NO$  contribution for total  $NO_x$  can be seen. It can also be observed that the DOC contributes to a small  $NO_x$  reduction which has been attributed to the utilisation of the HC through Reaction 29. It is important to note that under low exhaust temperatures, it is possible that platinum catalysts reduce  $NO_x$  to nitrous oxide ( $N_2O$ ), which is known as a harmful greenhouse gas promoter and responsible for ozone destruction (Yates et al., 2005). The effect of  $H_2$  on the  $N_2O$  formation over the DOC will be the focus of a subsequent study. With a DOC present in the exhaust (Figure 52), the  $NO_2$  concentration in some cases doubled, leaving approximately 150ppm  $NO_2$  available after the DOC for all conditions. This is clearly the result of  $NO$  oxidation, as shown in Reaction 14 previously (Schejbal et al., 2010).

Figure 54 shows that the  $NO_2/NO_x$  ratio doubles under standard conditions and during 20%Vol.EGR with the use of a DOC. Adding reformat under EGR, whether in the exhaust or intake, increases the  $NO_2/NO_x$  ratio over a DOC, with the reformat added in the exhaust showing the largest increase. It can also be seen that downstream of a DOC (Figure 52 and Figure 54) there is no significant beneficial difference between the amounts of  $NO_2$  concentration present, whether reformat is added directly into the exhaust or intake. Directly comparing both reformat conditions, benefits in fuel economy, engine thermal efficiency and engine-out  $NO_2$  concentration in a DOC absent system makes intake added reformat the most beneficial condition for overall combustion and aftertreatment performance.

By comparing the  $NO_2$  usage over a cDPF (i.e. with and without an upstream DOC) it can be seen from Figure 53 and Figure 55 the cDPF uses more of the  $NO_2$  that is available in the exhaust. This is seen by the greater reduction in  $NO_2/NO_x$  ratio when a DOC is not combined with a cDPF. This effect may be directly related to the reformat reaction on the

catalyst coat, raising the local temperature. As a result, this can either enhance the rate of oxidation and/or enable the soot to react more effectively with the incoming NO<sub>2</sub> (Nickolas et al., 2006). It is important to note that a DOC will utilise the majority if not all of available reformat if positioned upstream of a cDPF. Overall, reformat addition into the exhaust raised the DOC/cDPF temperature by 70°C in comparison to 25°C when added to the intake.

At low temperatures the NO oxidation activity of the DOC can be significantly reduced, especially in the presence of oil and fuel derived sulphur species in the exhaust stream. This is where the SO<sub>2</sub> competes very effectively for the active catalyst sites and strongly inhibits the NO oxidation activity (Allansson et al., 2002). This study has shown with reformat addition we can raise the local DOC temperature to minimise this effect. In addition, as REGR substantially promotes the engine-out NO<sub>2</sub> concentration, the loss of NO oxidation activity over the DOC may become insignificant.

#### **6.2.2.5 DPF and cDPF comparison**

From the results in earlier figures it is quite clear that the cDPF uses more NO<sub>2</sub> than an individual DPF. With a DOC to maximise the NO<sub>2</sub> content, the cDPF uses on average 30% of the NO<sub>2</sub> available compared to 16% over a DPF. When removing the DOC, the cDPF uses on average 70% of the NO<sub>2</sub> available compared to 24% over the DPF. A clearer picture of the NO<sub>2</sub>/NO<sub>x</sub> ratio is illustrated in Figure 54 and Figure 55. From these observations it seems to highlight that there is a greater NO<sub>2</sub> concentration downstream the DPF, therefore, a compromise between the optimal amounts of NO<sub>2</sub> to be promoted across the system with the lowest achievable NO<sub>2</sub>/NO<sub>x</sub> ratio may have to be considered.

### 6.2.2.6 Pressure drop and soot loading

Figure 56 illustrates the mass of soot accumulated on the DPF and cDPF when used in different configurations with and without a DOC. The filters were clean at the beginning of the loading and were removed directly after each test and weighed, taking approximately 5 minutes. It can be seen that EGR, while reducing overall NO<sub>x</sub> emission, can also increase the soot loading in each system configuration by increasing the engine-out PM. This is because of the NO<sub>x</sub>-PM trade-off coming into effect. This can also be observed in the DPF and cDPF pressure drop curves shown in Figure 57 and Figure 58, where the systems with EGR show a higher pressure drop indicating an increased soot loading.

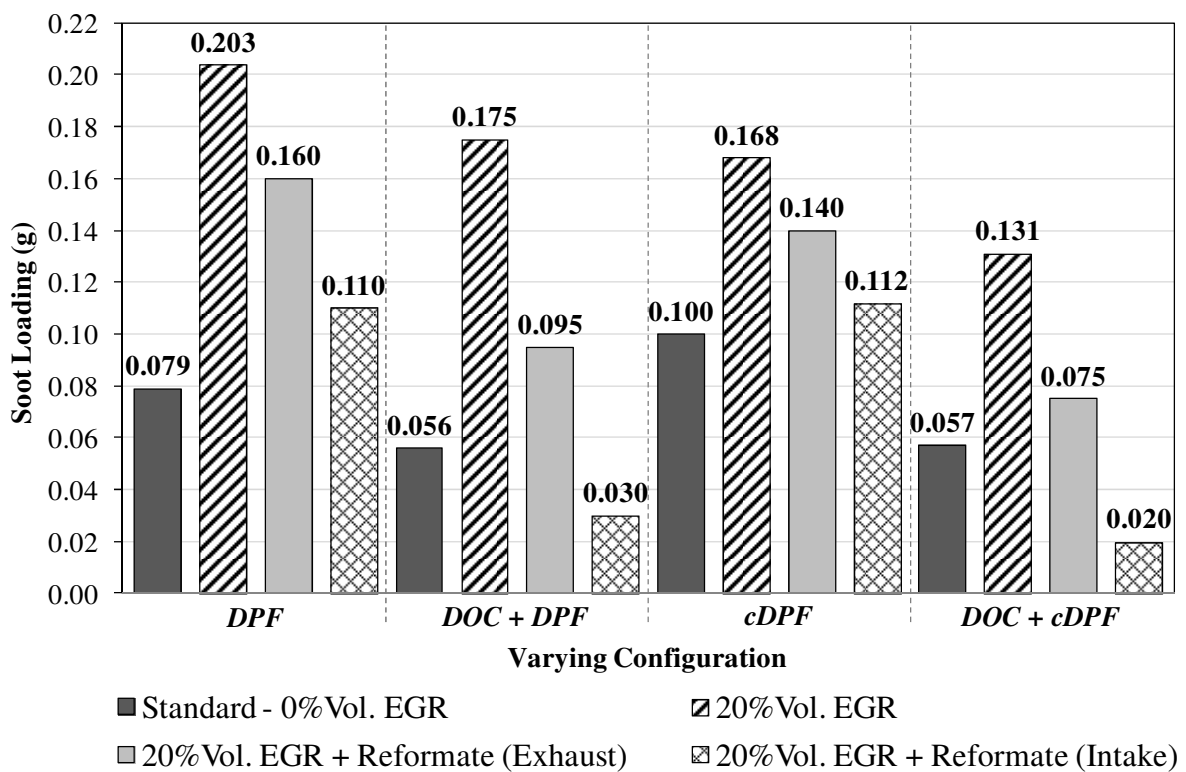


Figure 56: Filter Soot Loading for each Configuration Tested

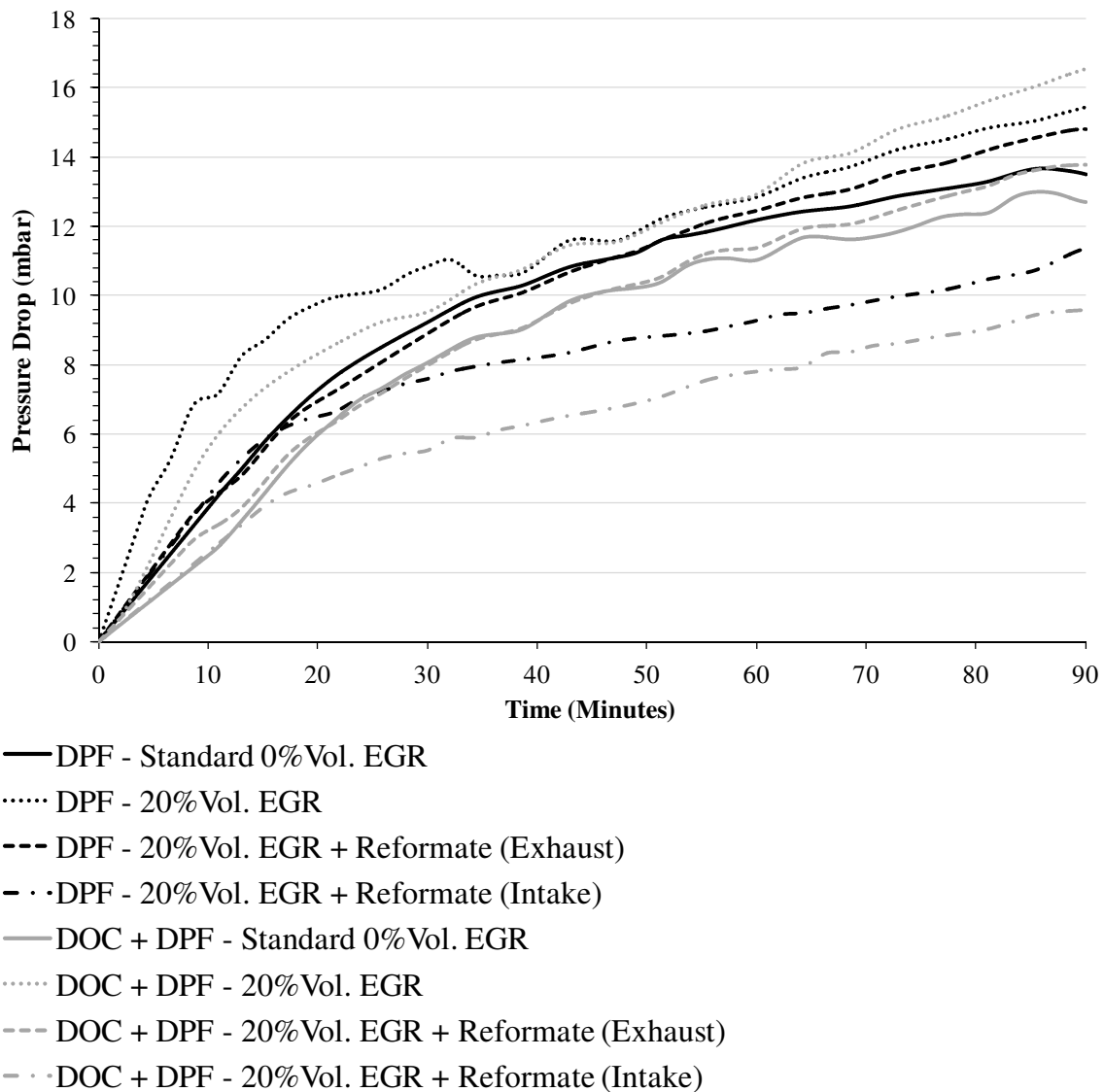
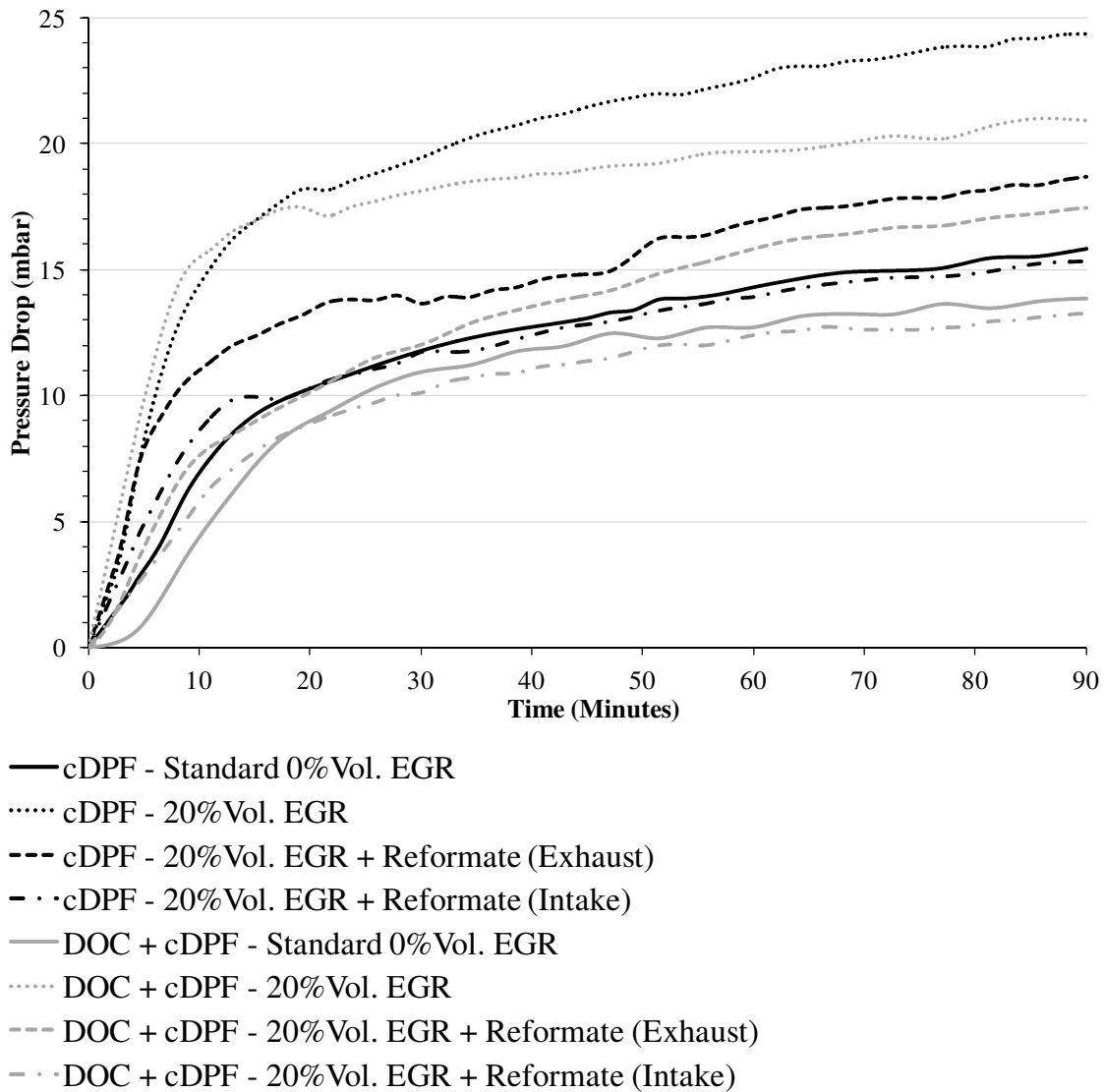


Figure 57: Pressure Drop across DOC-DPF and DPF Configurations

The engine operation under EGR or REGR led in the significant reduction of  $\text{NO}_x$  emissions as compared to standard engine operation, but resulted in the increased soot loading of the DPF (Figure 56). The test condition which produced the lowest pressure drop across the filter occurred with the addition of intake REGR. As illustrated in Figure 57, the DPF pressure drop was 20% less than compared to standard engine operation. The largest reduction in soot loading was experienced with the addition of intake REGR, a reduction in soot loading of 62% by using an upstream DOC. The DOC configured system with intake

REGR showed to be the most effective as the pressure drop across the DPF was reduced by 30%. It is also clear that for every condition with a DPF the use of a DOC will reduce the pressure drop across the filter, as shown by Figure 57.



**Figure 58: Pressure Drop across DOC-cDPF and cDPF Configurations**

The cDPF (Figure 56) loads faster than a DPF without an upstream DOC, except when EGR is used. However, the use of a combined upstream DOC (with a cDPF) has a positive impact by further reducing the soot loading to levels lower than a DOC-DPF configuration. By implementing intake REGR, this resulted in the lowest soot loading out of all the tests.

This condition also produced the lowest pressure drop across the cDPF (13 mbar), although not significantly lower than a simple cDPF system (16 mbar).

It can also be seen that a different loading profile is obtained between those systems with a cDPF compared to those with a DPF. Several studies (Bensaid et al., 2009, Schejbal et al., 2010) have shown that the pressure drop across a filter is divided into two approximate linear regions. This is due to the first region of soot loading gradually reducing the porosity and permeability of the filter (known as depth filtration). The second region begins when the filter pores are plugged (impermeable), thus leading to layers of soot building up on the filter surface (known as cake formation). Results from this paper agree with earlier published work as well as the observed differences between the loading profile of a cDPF and DPF. By examining Figure 57 and Figure 58, the initial region of loading (depth filtration) for a catalysed filter occurs more rapidly than that of a non-catalysed and is a result of the pores of the cDPF being smaller due to the catalyst coating. This leads to the pores clogging faster at this low exhaust temperature and being responsible for the sharper pressure drop in the first near linear region of loading.

The study has shown the effectiveness of having an on-board H<sub>2</sub> system by simulating the main constituents of the reformer product. As observed earlier, this can promote substantial benefits in the performance and activity of the aftertreatment systems. It is believed that the fuel penalty associated with the reforming process can be balanced out by the benefits that can be brought from having on-board H<sub>2</sub> availability. The addition of H<sub>2</sub> in combustion can replace part of the diesel fuel, as observed in a more recent study by Lilik et al. (2010), thus reducing further the CO<sub>2</sub> content in the exhaust stream. It was concluded that the substitution of the diesel fuel with H<sub>2</sub> can be implemented successfully without having significant detrimental effects. Generally H<sub>2</sub> tends to enhance the ROHR, resulting in more

complete combustion favouring NO<sub>x</sub> formation; on the other hand the total PM would reduce as a result of the NO<sub>x</sub>/PM trade-off. Overall in terms of combustion the addition of reformat allows lower fuel usage for equal engine torque and speed while reducing simultaneously the NO<sub>x</sub> and PM emissions. In terms of emission control, H<sub>2</sub> promotes the oxidation reactions over the DOC, which will further benefit the DPF for passive regeneration as observed in this study.

### **6.3 Extended Work – The effect of H<sub>2</sub> over the DOC**

The influence of H<sub>2</sub> over a platinum DOC was investigated with the key focus being on the lean oxidation kinetics of CO, HC and NO. Although it is well known that H<sub>2</sub> has a positive effect on NO<sub>2</sub> formation, there is still uncertainty whether this is due to the temperature rise caused by H<sub>2</sub> oxidation or if it is really influencing the reaction kinetics of NO oxidation.

Two mini DOC's referred to as catalysts A and B, cored from the same monolith, were positioned consecutively inside a mini-reactor specifically designed to study the effects of catalyst performance under real diesel exhaust gas compositions. The reactor was placed in a tubular furnace with the temperature successively increased from 150-450°C in intervals of 50°C. A steady state low temperature (220-230°C) exhaust composition (i.e. engine speed of 1500rpm and engine load of 3 bar IMEP reflecting approximately 40% of full load) was chosen for this study. Pure H<sub>2</sub> was mixed with the exhaust gas before passing it over the DOC. In this study 20%Vol.EGR was also introduced giving approximately 40% engine-out NO<sub>x</sub> reduction. Table 14 highlights the differences between the two mini DOC catalysts as well as the engine operating conditions. It can also be observed that by implementing H<sub>2</sub> with EGR there is an improved NO<sub>2</sub>/NO<sub>x</sub> ratio resulting from the formation of the HO<sub>2</sub> radicals as

discussed earlier. It is also important to note that the exhaust gas volumetric flow rate over the DOC was controlled to ensure consistency between all tests.

**Table 14: Operating Conditions and Engine-out NO<sub>2</sub> Concentrations**

Catalyst	Size	Test Condition	Engine-out NO <sub>2</sub> Concentration (ppm)
A	1" x 2.5" (GHSV = 37,000h <sup>-1</sup> )	0H <sub>2</sub> , 0%Vol.EGR	53.09
		5000ppm H <sub>2</sub> , 0%Vol.EGR	56.93
		0H <sub>2</sub> , 20%Vol.EGR	69.18
		5000ppm H <sub>2</sub> , 20%Vol.EGR	92.19
B	1" x 3.5" (GHSV = 26,000h <sup>-1</sup> )	0H <sub>2</sub> , 0%Vol.EGR	63.77
		5000ppm H <sub>2</sub> , 0%Vol.EGR	62.48

As shown in Figure 59, the NO-NO<sub>2</sub> oxidation ability of the DOC is illustrated over a wide temperature window showing the direct influence of temperature and H<sub>2</sub> addition. From these results the following conclusions can be drawn:

- A limit is placed on the NO-NO<sub>2</sub> oxidation over the DOC at higher temperatures. After this limit the NO<sub>2</sub> concentration reduces similar to the rate at which it increased. The decrease in NO<sub>2</sub> is related directly to the thermodynamic equilibrium of the reaction.
- H<sub>2</sub> promotes the rate of NO-NO<sub>2</sub> oxidation by improving the catalyst light-off performance, thus greater NO<sub>2</sub> can be obtained under lower exhaust gas temperatures.
- Smaller H<sub>2</sub> concentrations are more beneficial for NO oxidation, thus suggesting that the oxidation of H<sub>2</sub> may be more predominant than the oxidation of NO.
- EGR reduces the O<sub>2</sub> availability in the exhaust, thus the NO-NO<sub>2</sub> oxidation significantly reduces.

- Reducing the GHSV (i.e. using a larger catalyst) improves the oxidation rate of NO as a result of the longer residence time.

Overall, the benefit of H<sub>2</sub> addition for NO<sub>2</sub> production is a result of not only the exothermic reactions increasing the localised temperature but also the H<sub>2</sub> increasing the rate of reaction thus reducing the catalyst light-off temperature so further NO oxidation can occur at low exhaust gas temperatures. However, this is dependent on the H<sub>2</sub> concentration, with smaller concentrations being more advantageous. Similar observations were found in the study by Katare and Laing (2009), where H<sub>2</sub> promoted the catalyst light-off temperature.

Figure 60 shows that as the temperature increases so does the oxidation rate of CO and HC. Under higher exhaust gas temperatures the catalyst performance stabilises forming a plateau. The conversion rate of CO is higher than that of HC, which depends on the mass transfer conditions, thus higher conversion rates can be achieved with the use of larger catalysts (giving the gas a greater residence time within the catalyst) or a higher cell density substrate (i.e. smaller cells). The addition of H<sub>2</sub> significantly promotes the low temperature CO and HC oxidation which is dependent on the O<sub>2</sub> availability. Under low temperatures, platinum catalysts reduce NO<sub>x</sub> to N<sub>2</sub>O. The effect of H<sub>2</sub> on the N<sub>2</sub>O formation can be observed in Figure 61, where the presence of H<sub>2</sub> and its oxidation result in a dilution effect rather than affecting the kinetics of the reaction as observed previously with NO<sub>2</sub>.

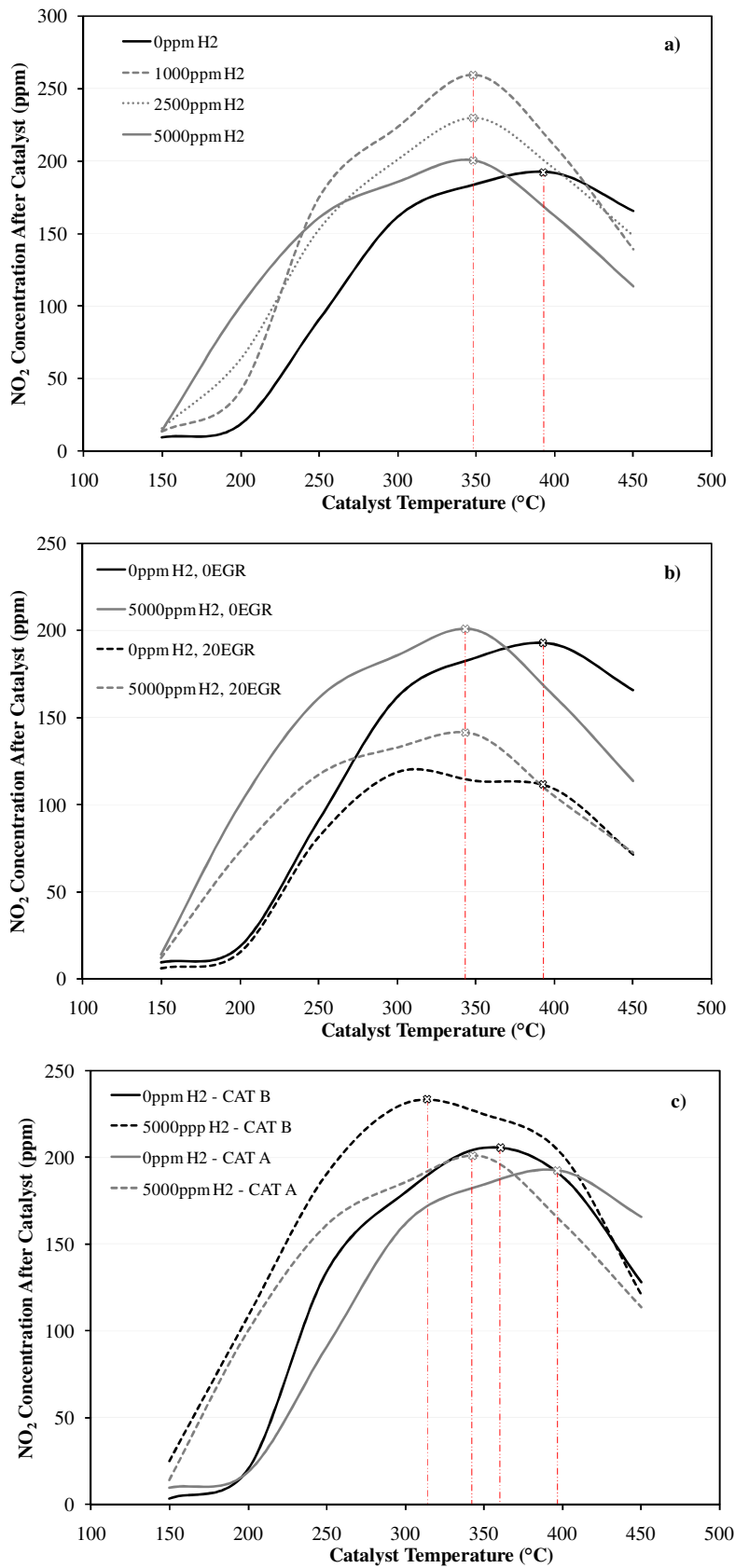


Figure 59: NO<sub>2</sub> Formation Over DOC: a) Effect of H<sub>2</sub> over Catalyst A, b) Effect of EGR and H<sub>2</sub> over Catalyst A and c) Effect of GHSV

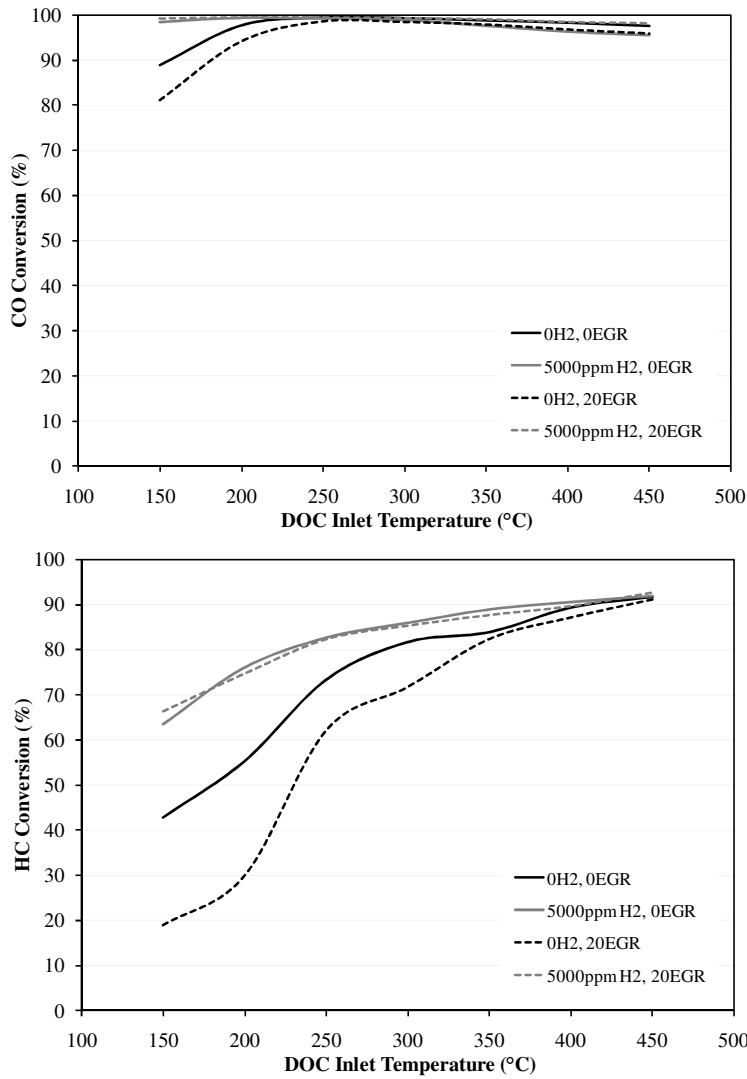


Figure 60: CO and HC Oxidation - Catalyst A

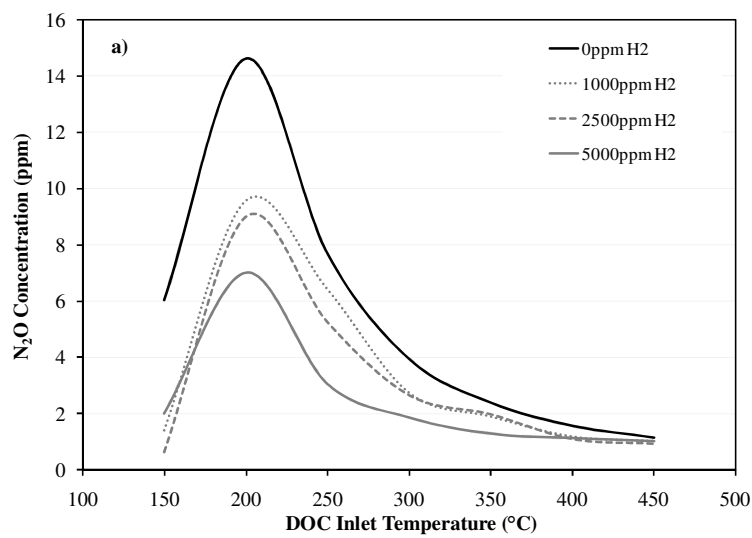
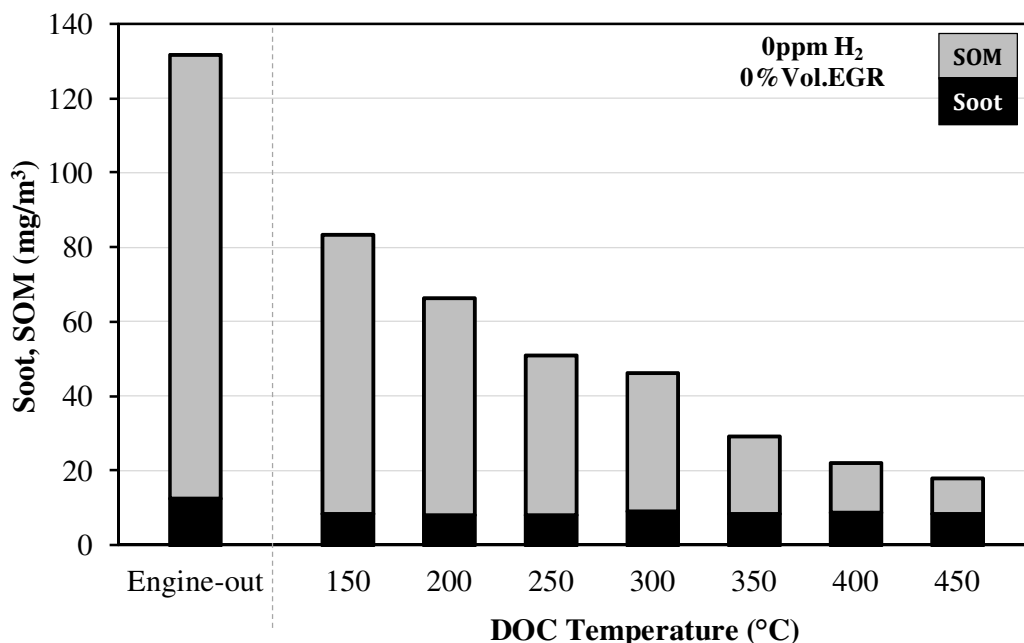


Figure 61: N<sub>2</sub>O Formation over DOC - Catalyst A

The DOC is effective in controlling the CO and gaseous HC emissions from the exhaust stream, with the possibility of soot oxidation and deposition on the surface of the DOC (Katara and Laing, 2009). Figure 62 shows the direct influence of temperature on the oxidation ability of PM over the catalyst. Although there is a reduction in soot, the level is consistent over the whole temperature range, thus increasing the catalyst temperature has no direct influence in the removal of the soot particles. This suggests the reduction in soot in our system and under these conditions was simply the result of deposition on the surface of the catalyst rather than reactions with solid particulates, which would require a catalyst support/substrate which exhibits some PM holding capacity or a longer residence time within the catalyst.

It can also be observed from Figure 60 and Figure 62 that there is a good correlation between the reduction in SOM and gas phase HC conversion (i.e. oxidation), which are both directly influenced by the inlet catalyst temperature. The reduction in SOM is suggested to be the result of the oxidation of the gas phase HC which will eventually form SOM during the dilution process, rather than the oxidation of the adsorbed or condensed HC already present on the particles upstream the DOC. As the sample needs to be cooled and diluted according to the definition of PM, there will be condensation or adsorption of the vapour compounds (i.e. adsorption of HC onto the soot cores) resulting in the growth of the PM and shifting the particulate size distribution to larger particulate sizes (an increase in emitted particle mass). The higher the catalyst temperature, the greater the oxidation rate of gaseous HC until the catalyst reaches its optimum achievable performance, reducing the amount of HC that can be adsorbed onto the particulates. It was suggested by Klein et al. (1998), that the reduction in SOM was likely to be a reduction in the gas phase HC rather than the oxidation of adsorbed HC. Thus, the DOC had no influence on the primary particulates (soot cores) as well as the

aggregates of primary particles as illustrated in Figure 63. Therefore, using a DOC it is difficult to oxidise the SOM already adsorbed or condensed onto the soot particles, however it is possible to control the recirculation of the gaseous HC which may form SOM during the cooler parts of the exhaust.



**Figure 62: Influence of Temperature on the Oxidation Ability of PM - Catalyst A**

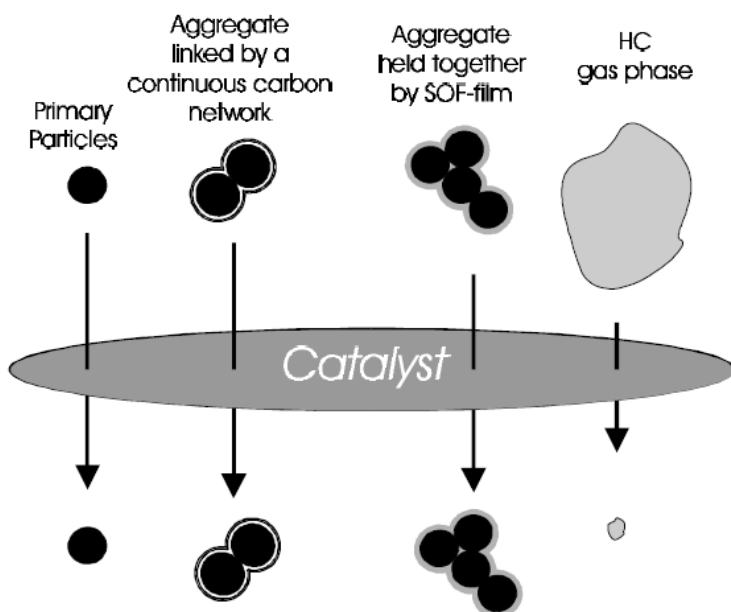


**Figure 63: The Effect of a DOC on the Particulate Matter**

## **6.4 Summary**

The addition of REGR into the engine intake showed to be the most efficient approach in reducing the soot loading and pressure drop across the combined DOC-DPF/cDPF systems while enhancing the  $\text{NO}_2/\text{NO}_x$  ratio. It was observed that by positioning the DOC upstream of the filter, the  $\text{NO}_2/\text{NO}$  ratio can be promoted, further resulting in a lower pressure drop across both the DPF and cDPF individual configurations. However, the cDPF washcoat layer (or PGM coating) causes a pressure drop increase and strongly influences the loading curve. This is given by the structural difference between the washcoat and the wall material. Overall, using REGR and implementing this with a DOC-cDPF system, the total engine-out  $\text{NO}_x$  and PM concentrations are considerably reduced, while simultaneously improving the filter efficiency under passive regeneration.

As a preliminary study, we have observed a technique in which simulated exhaust gas fuel reforming can be implemented alongside EGR to promote the combustion and aftertreatment performance; thus lowering both  $\text{NO}_x$  and PM emissions simultaneously.

The extended work has shown that smaller  $\text{H}_2$  concentrations are more effective in promoting the NO oxidation as well as improving the catalyst light-off temperature. Thus the increase in NO oxidation is a result of not only the exothermic reactions, which in turn increase the local catalyst temperature, but also the  $\text{H}_2$  increasing the rate of reaction hence further NO oxidation can occur at lower catalyst temperatures. As the temperature increases so does the oxidation rate of gaseous CO and HC, while at higher temperatures the catalyst performance stabilises forming a plateau. The temperature profile under steady state conditions has also given an insight into the thermodynamic equilibrium of the NO- $\text{NO}_2$  reaction over a diesel temperature window of 150-450°C highlighting the peak conversion

attainable in the presence of H<sub>2</sub>. Thus we can achieve greater NO<sub>2</sub> concentrations under lower exhaust gas temperatures, ideal for low temperature passive DPF regeneration.

## CHAPTER 7

# CONTROLLING SOOT FORMATION WITH FILTERED EGR FOR DIESEL AND BIODIESEL FUELLED ENGINES

### 7.1 Introduction

The work presented here is part of a research study with the overall aim of understanding the influence of PM and gaseous hydrocarbon recycled back into the combustion chamber as part of EGR on total PM formation and concentration. Thus the focus will be on observing the effect of engine-out PM when using untreated and filtered engine exhaust gas as EGR into the combustion chamber. FEGR will be implemented by recirculating exhaust gas downstream an aftertreatment system replicating a low pressure loop system (LPL-EGR). Unlike the LPL-EGR scheme, a high pressure loop EGR (HPL-EGR) utilises the exhaust at a point upstream the turbocharger (i.e. where exhaust pressure is significantly higher than that of the intake manifold) and as a result can reduce the overall performance of the turbocharger (Psaras et al., 1997). In addition, as the exhaust gas downstream of the DPF is cooler than that provided upstream the turbocharger, the LPL-EGR system would reduce the EGR cooling requirements and have a higher heat absorbing capacity for similar flow rates to those of the HPL-EGR system.

### 7.2 Filtered EGR – Filtering the EGR Loop

In this work all tests were examined under steady state conditions, at a constant engine speed of 1500rpm with an engine load of 5 bar IMEP reflecting ~70% of full load. The test conditions were chosen to illustrate a high PM emission scenario implementing EGR under

high load. The exhaust gas was recycled from the engine exhaust to the inlet (with the temperature controlled to 120°C using a heated line and furnace to avoid condensation in the loop and enhance the heat absorbing capacity to further reduce NO<sub>x</sub>). For the engine operation without EGR, the inlet temperature was 30°C and increased to approximately 35°C when 20%Vol.EGR was added.

In this particular study there was no attempt to match the filtering performance of the two filters, thus two filters of the same size with one coated with PGM and denoted as a cDPF in this study were chosen based on the same packaging requirements. The DPF/cDPF was integrated within the EGR loop which required only slight modification to implement an in-line reactor to house the filters. The SiC-DPF/cDPF of size 25.4mm diameter and 177.8mm length was positioned inside a mini-reactor and heated by a tubular furnace set at 120°C, hence avoiding water condensation and keeping the exhaust gas just above its dew point temperature. The experimental apparatus is illustrated in Figure 64. As the temperature of the DPF is well below the temperature required for soot oxidation with NO<sub>2</sub>, it is suggested that the reaction rates within the DPF will be significantly reduced. The temperature of the DPF was measured using K-type thermocouples positioned at mid-bed of the DPF.

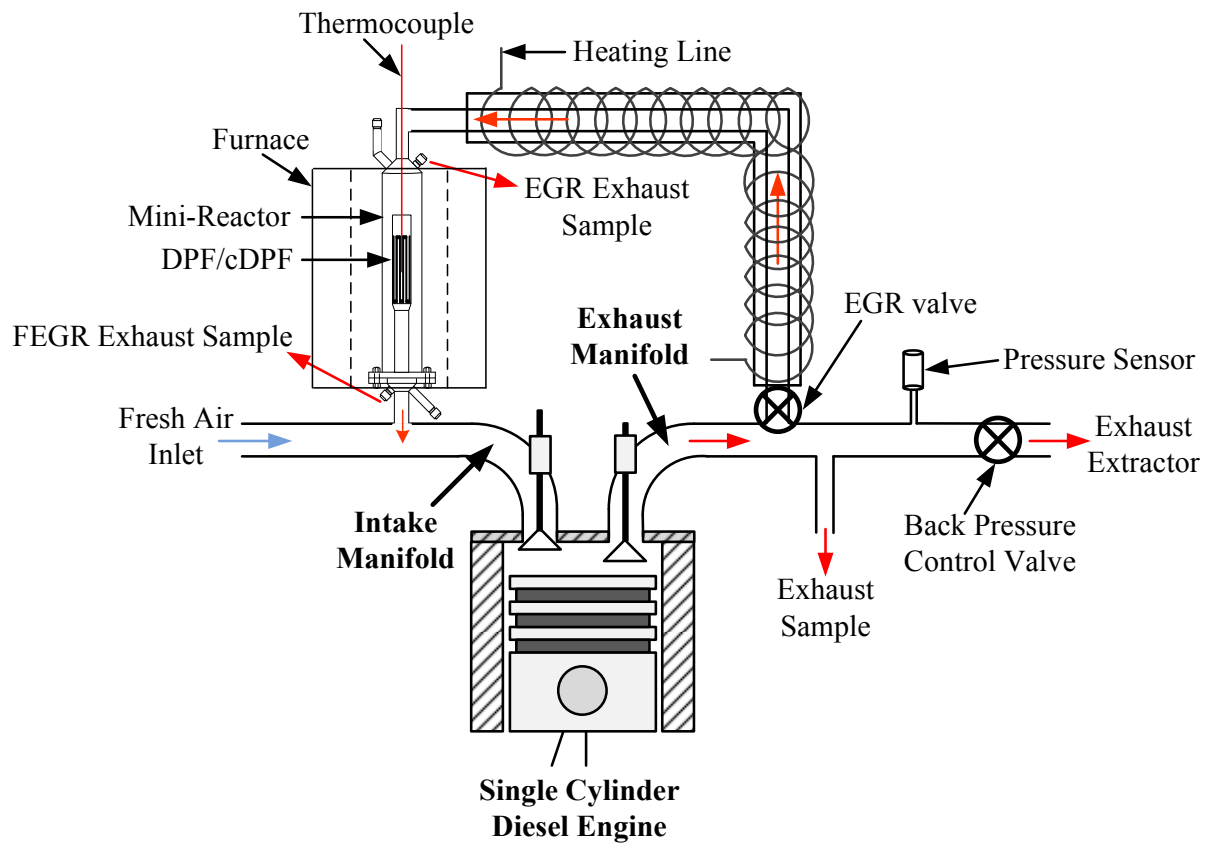


**Figure 64: Schematic of FEGR Setup and Sampling Locations**

## **7.2.1 Results and Discussion**

### **7.2.1.1 Combustion and emissions performance of diesel and biodiesel (RME)**

The in-cylinder pressure and heat release patterns for diesel and RME are presented in Figure 65 representing an average of 100 cycles. While it is well known that excessive EGR rates can substantially reduce  $\text{NO}_x$  emissions, the resulting engine operation can approach zones of higher cyclic variation. The heat capacity of the cylinder charge increases, while the flame temperature reduces (Zheng et al., 2004, Abd-Alla, 2002, Ladommatos et al., 1998). The increase in  $\text{CO}_2$  and the reduction of  $\text{O}_2$  causes a prolonged ignition delay as well as incomplete combustion (Zheng et al., 2004). Hence the heat release rates during premixed combustion are suppressed, thus significantly controlling  $\text{NO}_x$  formation. Some of these effects can be observed under 20% Vol.EGR as illustrated in Figure 65.

Biodiesel combustion, such as with RME, has been reported to show a reduction in fuel pyrolysis and an increase in oxidation as a result of higher oxygen concentrations in the spray, hence shortening the combustion duration. In comparison to diesel fuel, biodiesel exhibits numerous differences in fuel properties which influence the engine performance and emissions characteristics. As well as having inherent oxygen availability, it has a higher viscosity and density than diesel fuel. Many studies have observed one or more of the following effects; an increased injection pressure, reduced ignition delay and/or advanced combustion with an increased premixed combustion phase. The induced higher rate of heat release results in increased levels of NO<sub>x</sub> while reducing the overall CO and HC emissions simultaneously. In addition, it has also been reported that RME combustion in comparison to diesel fuel tends to reduce the formation of soot while increasing the relative portion of the SOF (Krahl et al., 2003, Schröder et al., 1999, Mueller et al., 2003, Tsolakis et al., 2007b). In comparison to diesel fuel, RME resulted in a 43.3% and 39.7% reduction in engine-out soot emissions under 0 and 20%Vol.EGR conditions respectively. This improvement is attributed to the oxygen content available in the fuel molecule and its physical properties that influence the injection process. Hence soot derived from oxygenated fuels possess higher reactivity than soot from conventional diesel fuels (Song et al., 2006). In addition it has been reported that combustion of oxygenate fuels, such as biodiesel, allow a greater engine tolerance to EGR as a result of the oxygen enrichment which leads to reduced PM/smoke recycled back into combustion chamber (Tsolakis, 2006).

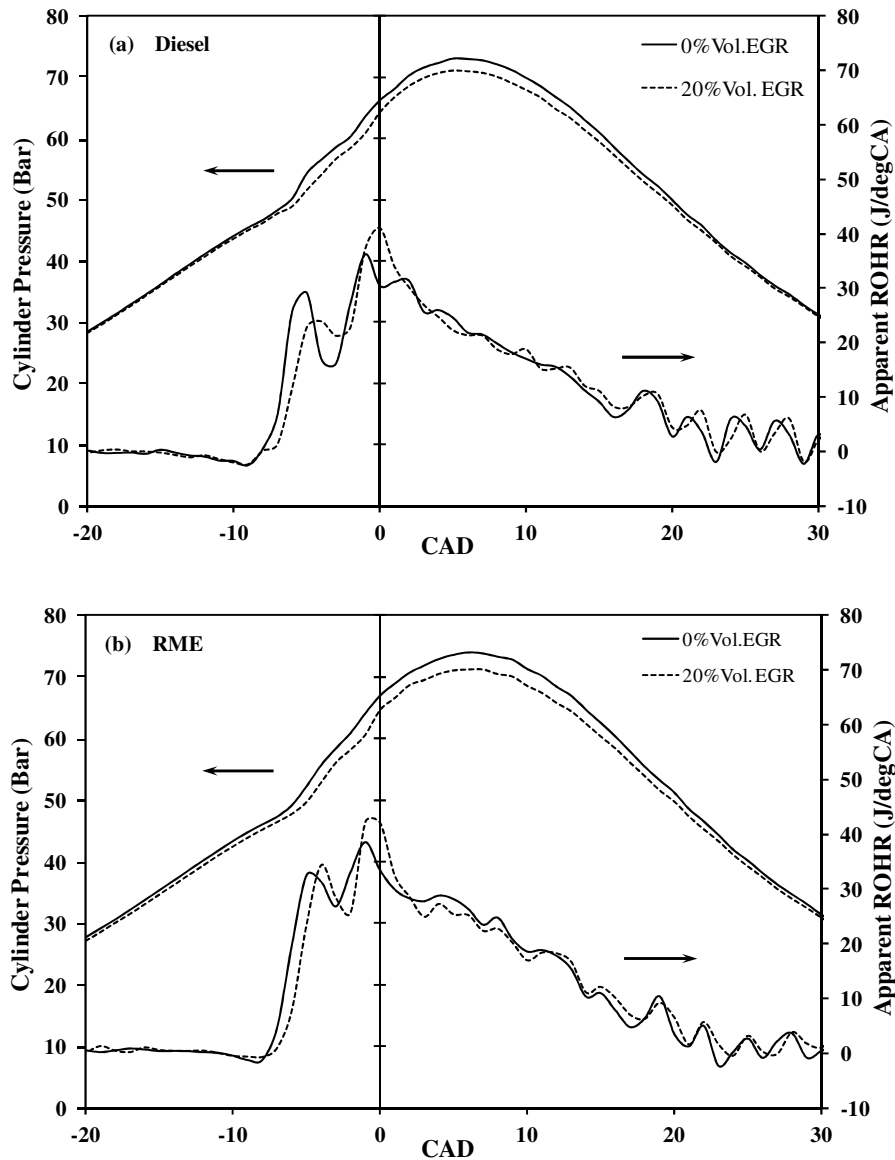
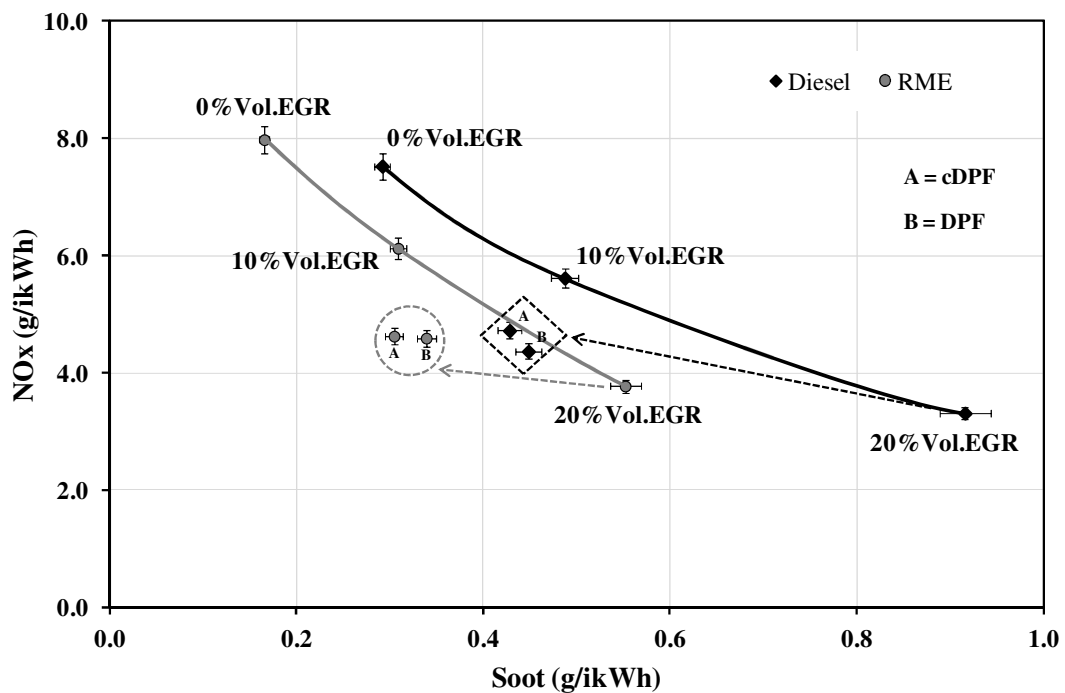


Figure 65: Combustion Characteristics of Diesel and Biodiesel Fuel (RME)

Figure 66 shows the benefits associated with RME and the effect of EGR on the  $\text{NO}_x$ /soot trade-off, with  $\text{NO}_x$  increasing by 6% and 14% with RME under 0 and 20% Vol. EGR conditions. The lower combustion temperatures with EGR result in an increase in the rate of PM formation from unsaturated species such as acetylene and ethylene (Mueller et al., 2003). It is important to note that the PM reductions associated with RME were not significant when compared with diesel fuel. With RME, it was observed that the SOM of the total PM increased, while the soot portion reduced as a direct effect of the local oxygen

availability during combustion. This is illustrated in Figure 67, which gives a plot of the total PM distinguishing between soot and SOM for both diesel and RME fuels. This has been attributed to the lower volatility of the unburned HC, thus favouring their condensation and adsorption onto the particles' surface (Lapuerta et al., 2008a). It was reported by Knothe et al. (2005) and Bagley et al. (1998) that this is the effect of the higher boiling point, higher viscosity and higher density leading to a poor air/fuel mixture and incomplete combustion, hence resulting in an increased portion of SOF.



**Figure 66: The Effect of Fuel Types and EGR/FEGR on the NO<sub>x</sub>/Soot Trade-off**

### 7.2.1.2 Effect of filtered EGR on engine-out emissions

The engine-out specific emissions are illustrated in Figure 67 and Figure 68, presenting the key regulated emissions. The large SOM content for both diesel and RME can be attributed to the large engine-out gaseous HC concentration measured during both low and high engine loads which will result in greater HC adsorption and condensation onto the soot particles. However, by controlling the temperature of the EGR loop and the DPF it is possible

to minimise the adsorption or condensation of the gaseous HC on to the recirculated soot particles.

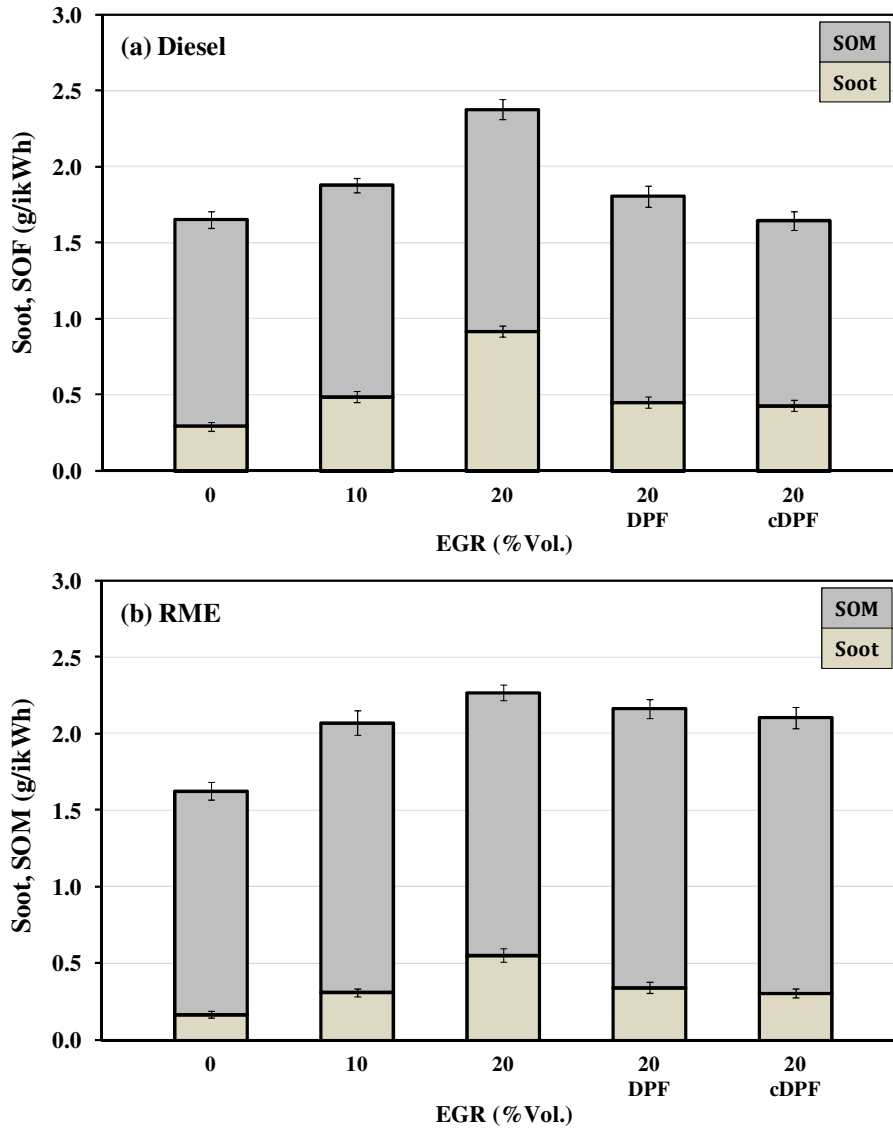


**Figure 67: The Effect of EGR and FEGR on Engine-out Total PM Emissions with a) Diesel and b) RME**

In the worst case scenario (i.e. high HC adsorption and condensation) a proportion of the recirculated adsorbed HC will form species that will participate in the soot surface growth mechanism. Therefore, further investigation will be required to determine the influence of these recirculated HC species.

In order to demonstrate the effectiveness of filtered EGR, emission results for 10%Vol.EGR have also been recorded for completeness. From the results in Figure 68, the use of FEGR also resulted in a reduction in engine-out CO and HC emissions. This suggests that the lower soot recirculation will result in less soot-NO<sub>2</sub>/O<sub>2</sub> interaction, resulting in a reduced CO formation. However as this effect may be small, it is suggested that the removal of soot improved the combustion itself which could account for the reduced CO and HC emission. This benefit is clearer under diesel combustion where these specific emissions were reduced to a similar level as those measured during 10%Vol.EGR.

It must be noted that the filter tests were only carried out with the use of 20%Vol.EGR and it was not possible to achieve greater EGR rates with this particular system design. However, the key benefit of the system used in this study is that the increased backpressure caused by the loading of the DPF can be isolated and as a result will not affect the engine performance. It was observed that the mini filter positioned directly in the EGR loop was heavily loaded during 30%Vol.EGR, which resulted in a significant loss in the EGR flow rate and thus has not been included in the results. In addition, there was no measured benefit when the test was run with 10%Vol.FEGR suggesting that the level of soot in the exhaust is not enough to observe the benefits of this technique.

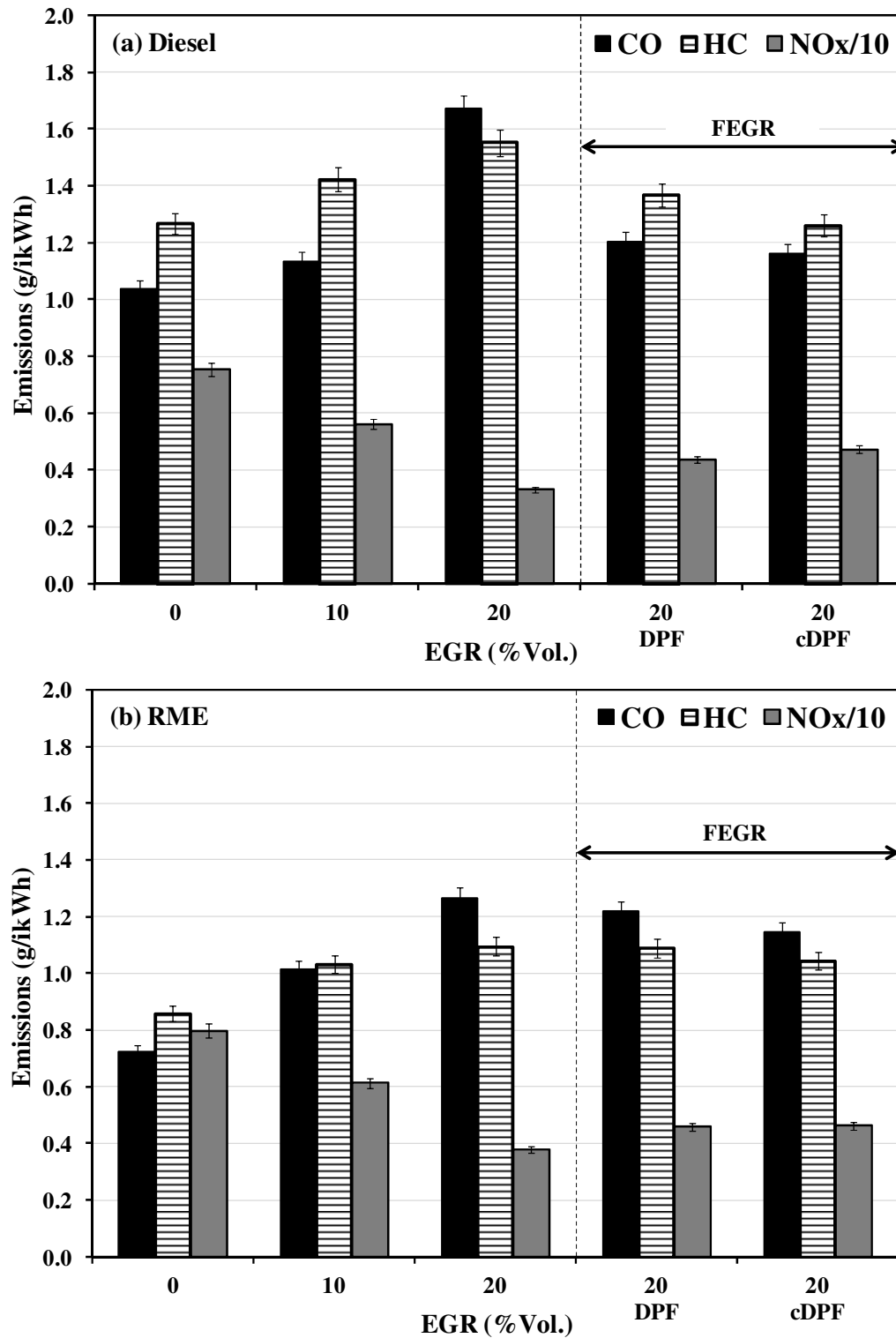


Figure 68: The Effect of EGR and FEGR on the Engine-out Specific Emissions with a) Diesel and b) RME

With diesel fuel it was observed that by using 20%Vol.DPF-FEGR and 20%Vol.cDPF-FEGR there was a reduction in soot of approximately 50% compared to unfiltered

20%Vol.EGR, improving the overall engine-out NO<sub>x</sub>/soot ratio. However, by filtering the EGR loop it was noticed that this had an influence on the NO<sub>x</sub> reduction efficiency of EGR. As shown previously in Figure 66, 20%Vol.EGR was able to reduce the NO<sub>x</sub> emission by 55%. However, this reduced to 43% and 38% when 20%Vol.DPF-FEGR and 20%Vol.cDPF-FEGR were implemented respectively. Although there is a NO<sub>x</sub> penalty, the results have shown that this is outweighed by the substantial reduction in the engine-out soot emissions. In comparison to diesel fuel, the overall soot reduction with RME using 20%Vol.DPF-FEGR and 20%Vol.cDPF-FEGR was approximately 40-45% compared to unfiltered 20%Vol.EGR. Although this again demonstrates the benefit of filtered EGR in terms of soot reduction, using RME resulted in an increase in the proportion of SOM (~ 5%) of the total PM. In addition, when 20%Vol.EGR was introduced there was a NO<sub>x</sub> reduction of 50%, similar to that achieved with diesel fuel; however this reduced to 42% when 20%Vol.DPF-FEGR and 20%Vol.cDPF-FEGR were implemented.

The NO<sub>x</sub>/soot trade-off given in Figure 66 also shows the influence of filtering the EGR loop. This not only shows the potential benefit in terms of soot reduction but also an overall benefit towards the NO<sub>x</sub>/soot trade-off, especially when implementing EGR. It can be seen that there are some differences between the two filters used in this study and this is more apparent when RME is used as the combustion fuel. As the cDPF is below its light-off temperature, the differences between the two filters lie primarily on the structural differences rather than any chemical influence that will influence the total NO<sub>x</sub> levels (Suresh et al., 2001). This includes oxidation of particulate SOM, which can reduce the HC pyrolysis in the combustion chamber (Kennedy, 1997). The cDPF appears to be more effective than the uncoated DPF at reducing the recycled particulates and soot precursors. The main reason for

this is considered to be the smaller pores, arising from the PGM coating resulting in higher filtration efficiencies than for the uncoated DPF (Bensaid et al., 2009, Schejbal et al., 2010).

Overall with 20%Vol.FEGR, lower NO<sub>x</sub> emissions can be maintained while keeping the levels of engine-out soot in the region of that produced with 10%Vol.EGR. With RME, the results are fairly similar to that of diesel fuel; however the benefits are clearer under diesel combustion. This is most likely attributed to the fact that engine-out soot with RME is much lower and more reactive than that of diesel, as explained earlier in this study. It is expected that the composition of the EGR remained similar with the use of a DPF/cDPF as the filter only traps the soot and possibly a small amount of HC, which may have been adsorbed or condensed onto the soot. Therefore it is unlikely for the local air/fuel ratio to be affected.

Numerous authors have concluded biodiesel gives a lower accumulation mode particle concentration than diesel fuel. Jung et al. (2006) concluded the reduction was based around the oxygen content resulting in reduced soot formation and hence reducing the cores for accumulation mode formation. Di et al. (2009) thought the heavier compounds of biodiesel could self nucleate and condense into particles in the exhaust and increase the nucleation mode particles. Moreover, the higher oxygen content of biodiesel could simply improve the locally rich diffusion combustion phase and result in a direct reduction in larger diameter particles.

As soot particles are reintroduced into the combustion chamber through EGR, some of the particles can either go through the process of coagulation (collisions between particles which does not affect the total particle mass but only the particle concentration), surface growth (the addition of gas phase HC increasing the net mass of particles) or become partially (reducing the size of the agglomerate) or fully re-oxidised (resulting in no soot recirculation

penalty). It is suggested that the particles which are reintroduced during EGR can serve as particle nuclei, which can undergo surface growth both in the primary reaction zone and cooler parts of the combustion chamber as well as in the cooler parts of the exhaust. As a result there will be a net increase in engine-out particle mass.

By analysis of the EGR and exhaust flow rates under steady state operating conditions, it was possible to determine the mass per cycle of soot recirculated through EGR and the global effect of combustion on both the newly and recirculated soot particles. This includes the growth and re-oxidation of the recirculated particles and the formation, growth and oxidation of the newly formed particles. The analysis in Table 15 compares EGR with FEGR and shows that the effect of particulate growth through combustion (taking into consideration the re-oxidation of recirculated soot) on the engine-out mass per cycle of soot is greater than the mass per cycle of soot recirculated through EGR. Therefore by introducing a filter in the EGR loop there is a benefit not only from the obvious removal of the particles but also their participation in further soot formation and growth in the combustion chamber.

**Table 15: Calculated Mass per Cycle of Soot (Under Diesel Combustion)**

		<b>Unfiltered EGR</b>	<b>Filtered EGR</b>
<b>EGR</b>	mg/cycle	0.0163	0.0004
<b>Exhaust</b>	mg/cycle	0.0926	0.0475
<b>Combustion</b>	mg/cycle	0.0763	0.0471

Looking back at the NO<sub>x</sub>/soot trade-off results in Figure 66, it can be observed that the two filters have different trapping efficiencies. The effect of the combustion fuel on the behaviour of the filters is clear. Therefore this highlights that further improvements can be

made through more optimised or efficient filters, especially when considering biodiesels or biofuels. In this work, it was concluded that there was a soot recirculation penalty with EGR, and this could effectively be controlled by using a DPF in a FEGR configuration. However, it is believed that there may be some additional penalties, for example, from the recirculation of HC species which may also participate in particulate growth and hence put a limit to the amount of EGR that can be introduced to a diesel engine before reaching smoke limited conditions.

### **7.3 Full Scale Filtered EGR – Taking the EGR Loop Downstream the Aftertreatment System**

In order to further assess the FEGR technique, a LPL-EGR system consisting of a DOC and DPF (as illustrated in Figure 69) was implemented to not only filter the soot particles but also oxidise the gas phase HC species from re-entering the combustion chamber through EGR. Particular focus with the filtered system was placed on the exhaust gas back-pressure, ensuring this remained consistent between the FEGR and EGR conditions to allow for a direct comparison.

In this work all tests were examined under steady state conditions, at a constant engine speed of 1500rpm with an engine load of 5 bar IMEP reflecting approximately 70% of full load. This condition was chosen so that the concentration of soot in the exhaust is large enough to show a soot recirculation penalty as observed in our earlier study. The GHSV was  $60,000\text{h}^{-1}$  based on the DOC volume and exhaust flow rate. The main differences between EGR and FEGR are the levels of soot and HC species being reintroduced to the combustion chamber. The system allows for passive oxidation of the HC and CO emissions while filtering the soot species. Filtration efficiencies are known to reach as high as 95-98%, therefore, by

knowing the oxygen concentrations present in the combustion chamber (Equation 13) during this process the soot recirculation effect can be isolated within FEGR. It is also important to note that during each individual test the filter was preloaded to ensure maximum performance and filtration efficiency.

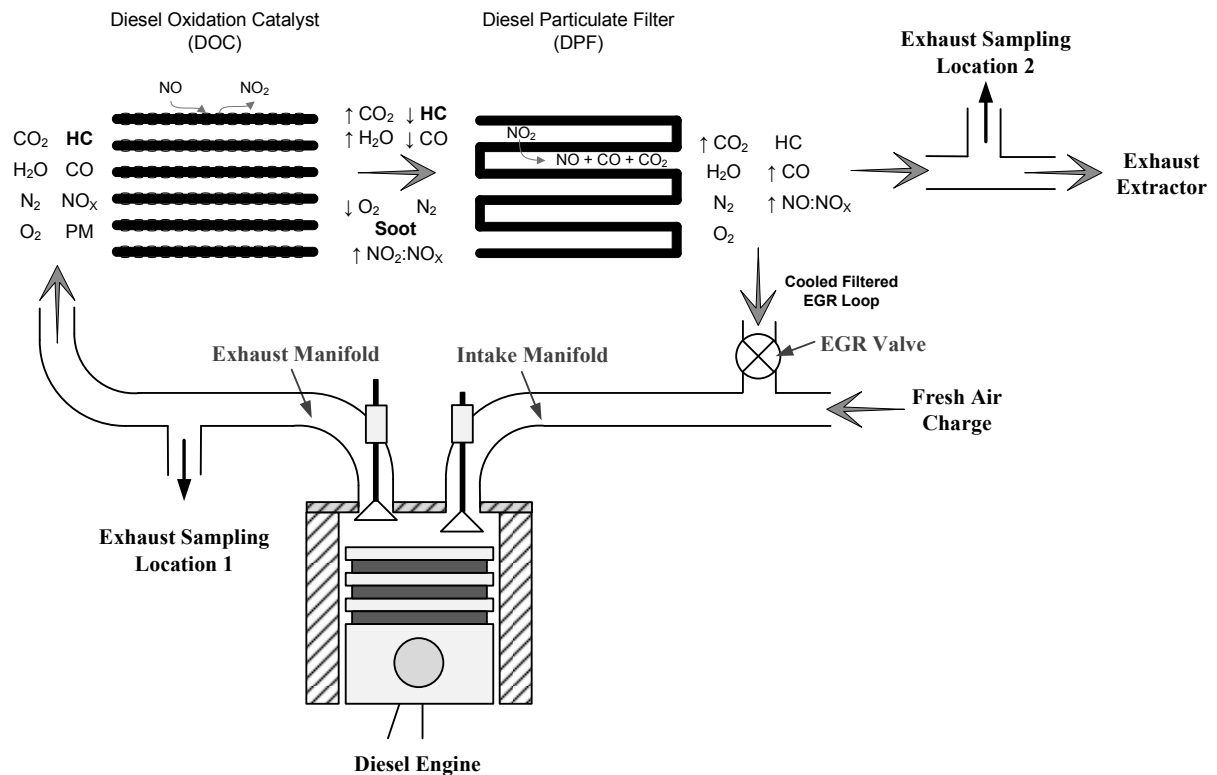


**Figure 69: FEGR Schematic with Emission Control**

**Equation 13:**  $Mass O_{2Intake} = Mass O_{2Air} + Mass O_{2EGR}$

**7.3.1 The Effectiveness of Combining a DOC and DPF for FEGR**

To observe the effects of EGR and FEGR (with and without the presence of the DOC), comparisons were made to pure N<sub>2</sub> as a benchmark. During the addition of pure N<sub>2</sub>, the DPF and DOC were removed and the EGR modified allowing the connection of a pure N<sub>2</sub> gas bottle. The amount of N<sub>2</sub> addition was determined based on the intake O<sub>2</sub> availability, ensuring this was consistent with that of the EGR tests. The results of engine-out NO<sub>x</sub> and soot emissions have been collated and presented in Figure 70 and Figure 71 respectively. The

primary focus switches to the dilution effect and its impact on diesel particulate formation and  $\text{NO}_x$  emissions. By directly isolating the dilution effect (i.e. comparing at the same  $\text{O}_2$  intake concentration), it was possible to distinguish a relationship with regards to the recirculation of the soot, gaseous HC and different  $\text{CO}_2$  and  $\text{H}_2\text{O}$  concentrations with an increasing EGR ratio. Results are given at 5 bar IMEP, mainly as the concentration of soot in the exhaust is large enough to show a soot recirculation penalty as observed in our earlier study.

The difference between introducing pure  $\text{N}_2$  to unfiltered EGR (for the same mass of intake  $\text{O}_2$ ) lies primarily on the mass of soot present in the EGR loop, presence of HC and the composition of  $\text{H}_2\text{O}$  and  $\text{CO}_2$  which can play a role in the thermal and chemical effects during combustion. Introducing  $\text{N}_2$  provides an example of clean EGR with no recirculated soot and gaseous HC occurring from the earlier cycle and thus reducing particulate growth. However, if the dilution was the main effect of EGR, the emissions of soot and  $\text{NO}_x$  for both unfiltered EGR and  $\text{N}_2$  should be comparable for a given intake oxygen concentration. It was observed that the removal of these specific emissions during the addition of  $\text{N}_2$  resulted in a substantial reduction in engine-out mass of soot, although there was an increase in engine-out  $\text{NO}_x$  emissions. This effect is more visible as the EGR ratio is increased and shows the influence  $\text{CO}_2$ ,  $\text{H}_2\text{O}$  and soot (which tends to play a role in absorbing heat, thus reducing the combustion temperature) have on the reduction of  $\text{NO}_x$ .

Comparing  $\text{N}_2$  to FEGR (without DOC) there was a small reduction in engine-out  $\text{NO}_x$  emissions, which can be attributed to the presence of  $\text{CO}_2$  and  $\text{H}_2\text{O}$  within the EGR gas. However, the  $\text{NO}_x$  emissions of FEGR are higher than that of unfiltered EGR and can be directly linked to the absence of soot, which again suggests soot exhibits some radiative heat absorption capacity. In Figure 71 it can also be observed that there is an increase in engine-out soot emissions with respect to  $\text{N}_2$ , resulting directly from the recirculation of HC even though

the presence of H<sub>2</sub>O and CO<sub>2</sub> effectively have an opposing influence. Comparing to unfiltered EGR, the removal of soot plays a substantial role in reducing the engine-out soot emissions, again indicating its potential towards particulate growth. The effectiveness of the FEGR system can be further improved with the addition of a DOC upstream the DPF. The oxidation of HC and CO gives a further benefit in terms of its thermal and chemical abilities towards NO<sub>x</sub> and soot control; with the removal of HC also limiting soot formation and surface growth. The DOC inlet temperature ranged between 330-340°C, resulting in 99% oxidation of CO and 80% oxidation of gas phase HC emissions present in the exhaust

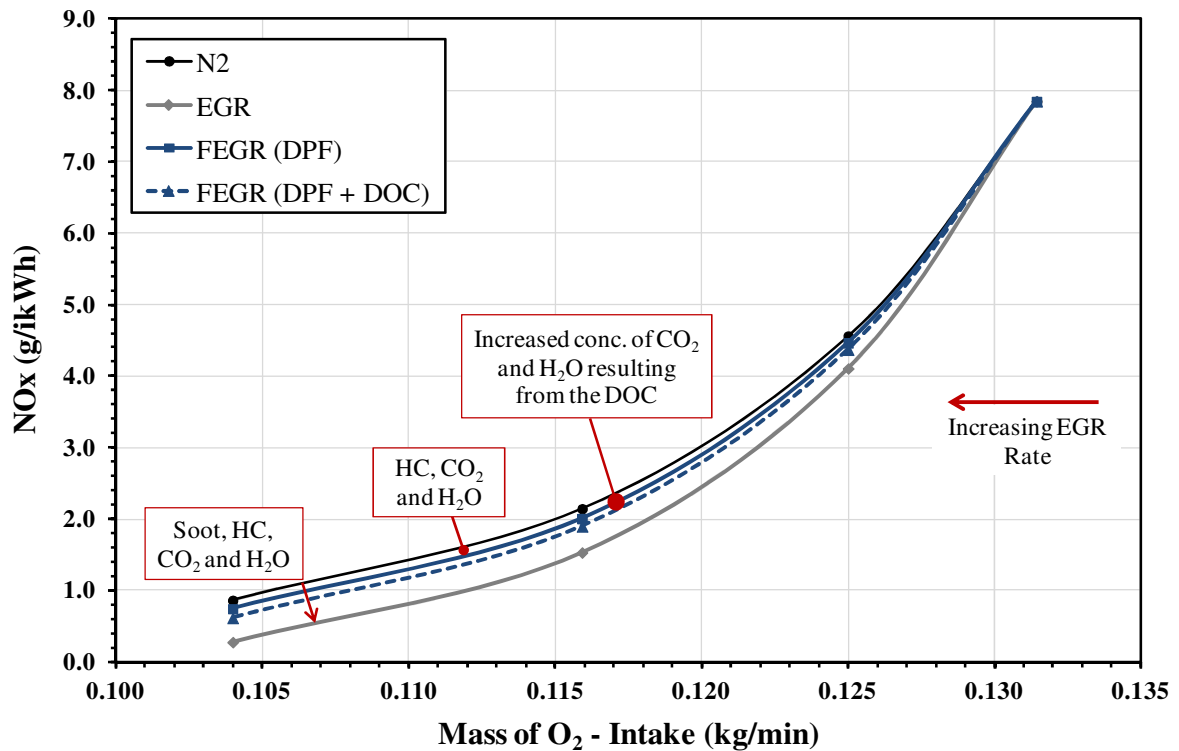


**Figure 70: Effect of NO<sub>x</sub> Emissions during EGR and FEGR Compared to Pure N<sub>2</sub> EGR**

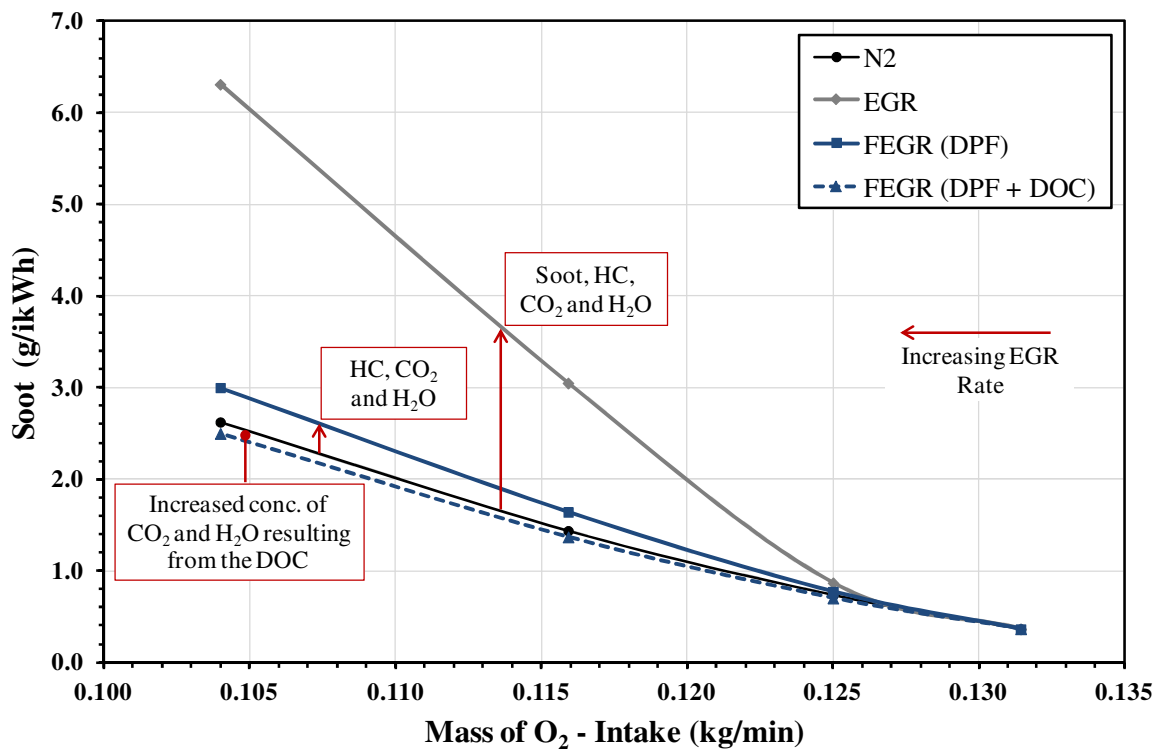


Figure 71: Effect of Soot Emissions during EGR and FEGR Compared to Pure N<sub>2</sub> EGR

Overall it can be observed that the presence of H<sub>2</sub>O and CO<sub>2</sub> have a positive impact on the reduction of both engine-out NO<sub>x</sub> and soot emissions through the chemical and thermal effects as previously illustrated in Table 1. However, the greatest impact comes from the soot recirculation penalty significantly favouring particulate growth, which is also supported by the recirculation of HC emissions. It is suggested that these recirculated HC emissions condense onto the soot when the exhaust gas and the fresh inlet charge meet within the intake manifold, resulting in an increased surface mass. Therefore, in order to obtain the best possible NO<sub>x</sub>/soot trade-off, soot recirculation must be controlled while promoting the oxidation of CO and HC emissions to promote the presence of H<sub>2</sub>O and CO<sub>2</sub>.

### 7.3.2 Assessing the Potential of FEGR

The main benefit of FEGR (with DOC) is that there are fewer gaseous HC's and particles with which agglomerates can form and undergo surface growth during their time in

the primary reaction zone and cooler parts of the combustion chamber and exhaust. This can be observed in Figure 72 where the engine-out particle mass concentration during FEGR is reduced considerably for particles with diameters over 100nm suggesting particle growth has been reduced in comparison to unfiltered EGR.

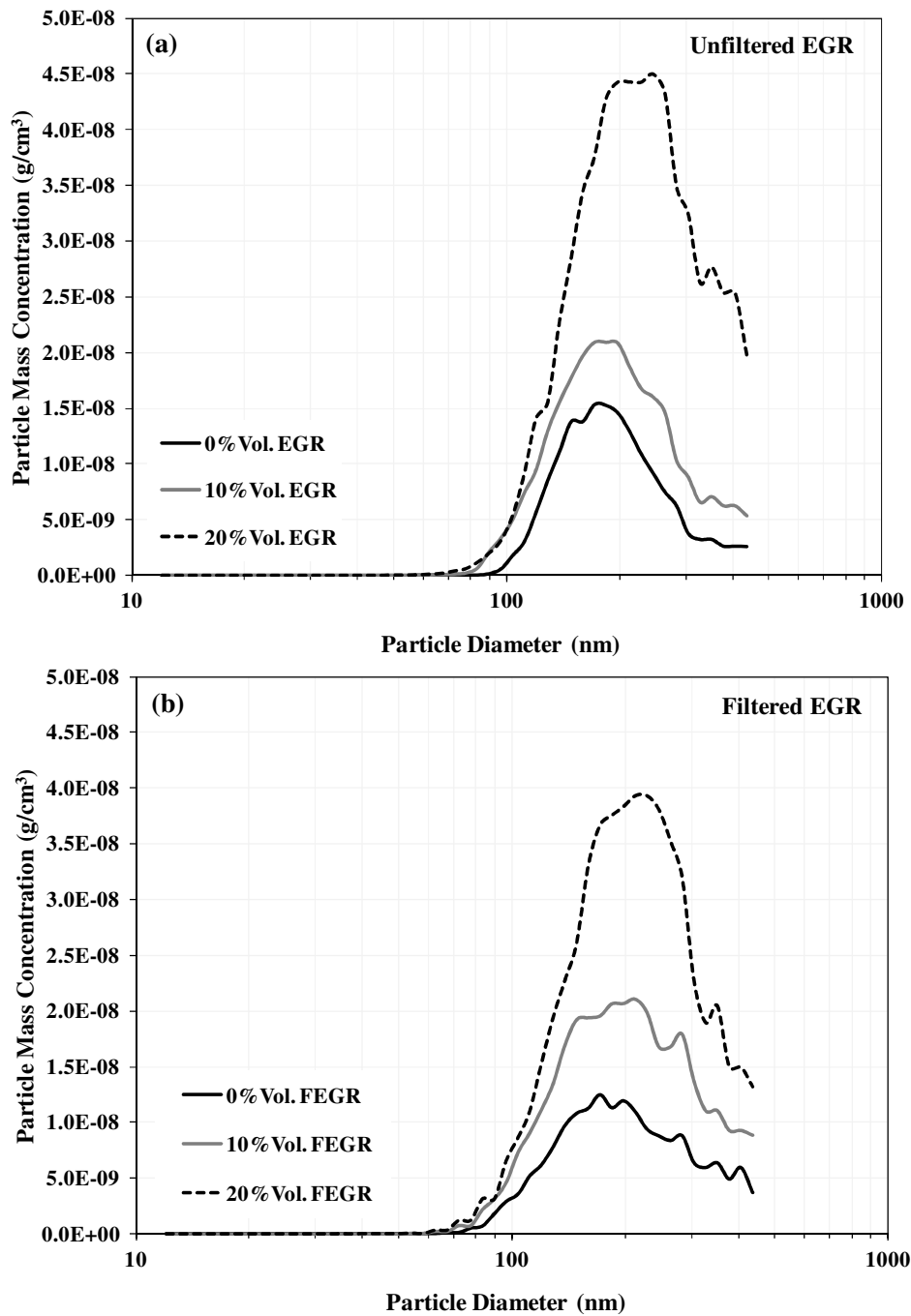


**Figure 72: Particulate Mass Distribution: a) EGR and b) FEGR with DOC**

However, it is important to note that there is no significant influence or increase in the nanoparticles (< 50nm) during FEGR, although when the EGR rate is increased the particulate mass concentration increases for every particle size diameter. The results of the particulate mass distributions have a good correlation with the results of the soot presented earlier, further showing the benefit of FEGR on the overall NO<sub>x</sub>/soot trade-off.

Table 16 shows a similar analysis as implemented earlier. Comparisons with N<sub>2</sub> and FEGR have been made based on the same intake O<sub>2</sub> availability. This again shows the mass per cycle of soot recirculated through EGR and the global effect of combustion on both the newly and recirculated soot particles. However, the analysis now compares unfiltered EGR with N<sub>2</sub> as well as FEGR. As observed in our previous investigation, the effect of particulate growth through combustion (taking into consideration the re-oxidation of recirculated soot) on the engine-out mass per cycle of soot is greater than the mass per cycle of soot recirculated through EGR.

**Table 16: Calculated Mass per Cycle of Soot (FEGR with DOC)**

		<b>Unfiltered EGR</b>	<b>Pure N<sub>2</sub> EGR</b>	<b>FEGR (DPF + DOC)</b>
<b>EGR</b>	mg/cycle	0.0385	0	0.0009
<b>Exhaust</b>	mg/cycle	0.3096	0.1498	0.1372
<b>Net Combustion</b>	mg/cycle	0.2711	0.1498	0.1363

Although a benefit can be gained from the obvious removal of the soot particles, it is also evident from Figure 71 that the gas phase HC emissions also play an important role. The removal of both soot and HC emissions therefore cannot participate in further soot formation and growth in the combustion chamber. It is also known that the main difference between the

addition of  $N_2$  and FEGR is the presence of  $H_2O$  and  $CO_2$ , with some recirculated HC emissions. Therefore, if the entire HC emission could be oxidised upstream the EGR loop during FEGR, the benefit of this system would be greater.

As there is a greater mass flow rate of exhaust being filtrated by the DPF when using the LPL-EGR compared to the HPL-EGR configuration, calculations have shown this is outweighed by the benefit of a lower engine-out soot concentration brought about from controlling the soot and HC recirculation. By calculating the mass flow rates of soot for both HPL and LPL-EGR configurations, based on the same intake  $O_2$  availability (corresponding to 20%Vol.EGR), it was observed that there is approximately 50% less mass of soot present in the exhaust when the LPL-EGR system is used. It is important to note that this takes into consideration the greater exhaust gas flow being filtered through the DPF during a LPL-EGR configuration. Therefore, this shows that the resulting reduction in engine-out soot emissions through the control of the soot and HC recirculation penalty is far more beneficial compared to a HPL-EGR system. Thus, the final result would be a lower rate of DPF soot loading and hence a reduced level of active regeneration intervals. It also seems that by controlling the HC recirculation we have gained a further benefit compared to our previous investigation which was focused primarily on soot emissions.

The results presented in this study have given an insight into how a cooled EGR system can be enhanced, allowing further control of the engine-out soot emissions with an improved  $NO_x$ /soot trade-off.

## **7.4 Summary**

The results presented in this study have demonstrated a potential of extending the EGR limits (i.e. controlling the formation of engine-out soot during EGR) by significantly reducing

the soot particles present in EGR and further the removal of soot particle nuclei that are recycled back into the cylinder. The likely mechanism for engine-out particle growth through the use of EGR is the reintroduction of soot particle nuclei into the combustion chamber, thus serving as sites for further condensation and accumulation promoting larger and greater number of particles. A similar hypothesis was made by Wagner et al. (2000) in an earlier study. As a result, a similar soot concentration with an improved NO<sub>x</sub> reduction of up to 25% can be achieved compared to 10%Vol.EGR. It was also observed that removing the recirculated soot affected the overall NO<sub>x</sub> emissions. With the filter in place, it was believed that the flame temperature increased as a result and that soot may be a chemical participant in the reduction of such pollutants as well as having a role of promoting the heat transfer during combustion (Kennedy, 1997). Further it is suggested that by limiting the amount of soot back into the combustion chamber there will be less soot-NO<sub>2</sub> interaction, hence resulting in an overall increase in engine-out NO<sub>x</sub> emissions.

Consequently, with the addition of a DPF in the exhaust, the flow rate will become restricted as the soot begins to accumulate within the filter. Therefore the filter will need to be actively or passively regenerated to ensure the maximum EGR potential can be achieved at all times. However, by using the LPL-EGR configuration there will be a higher exhaust flow rate being filtrated by the DPF with respect to the usual HPL-EGR configuration. Calculations have shown that although there is a greater mass flow rate of exhaust being passed through the DPF when using the LPL-EGR configuration, it is outweighed by the substantial benefit gained from controlling the soot recirculation penalty. By calculating the mass flow rates of soot for both 20%Vol. HPL and LPL-EGR configurations it was observed that there is approximately 40% less mass of soot present in the exhaust when the LPL-EGR system is used. As a result this will decrease the loading of the DPF and thus reduce the frequency of

regenerations. However, it is important to note that if the soot recirculation penalty is small (e.g. when operating under a low engine load or low EGR ratios), the LPL-EGR system may not be as beneficial.

As the initial study primarily focused on controlling the soot emissions, further work was carried out to control the recirculation of organic and polyaromatic unburned hydrocarbons (PM precursors) back into the combustion chamber during EGR. This involved using a LPL-EGR downstream a combined DPF and DOC system, paying significant attention to the exhaust back pressure. The results again showed the recirculated soot particles (especially at high load and high EGR ratios) playing an important role in promoting the growth of further particles within the combustion chamber. However, by isolating the dilution effect and introducing N<sub>2</sub> as the exhaust gas it was possible to correlate the increase in soot mass with EGR to the recirculation of these particles as well as the presence of unburned HC emissions. The findings from this report particularly highlight the possibility of extending the EGR tolerance at high engine loads, giving the potential to further reduce NO<sub>x</sub> before reaching smoke limited conditions in order to meet future regulations that are likely to dominate future engine designs. The key advantages of this system is that FEGR can be implemented in current EGR systems to reduce engine-out soot emissions, thus reducing the DPF loading and regeneration intervals, or used as an approach to extend the current EGR limits for further NO<sub>x</sub> control. In both cases this technique will also result in an improved NO<sub>x</sub>/soot ratio which can help promote passive DPF regeneration.

# **CHAPTER 8**

## **DIESEL EMISSIONS IMPROVEMENTS THROUGH THE USE OF BIODIESEL OR OXYGENATED BLENDING COMPONENTS**

### **8.1 Introduction**

Reformulation of diesel fuels including the reduction in sulphur, aromatics and potentially introducing oxygen within the fuel by using fuel components such as alcohols, esters and ethers have been the focus of many researchers. The influence of fuel oxygen content on soot reduction in diesel engines is well known. According to Ren et al. (2008), addition of oxygenates did not influence the NO<sub>x</sub> emissions and had no impact on the engine thermal efficiency. Increasing the oxygen content of diesel by adding oxygenate will improve the PM emissions of a diesel exhaust. Similar results were obtained by Miyamoto et al. (1998) where the amount of soot reduction depended on the total amount of oxygen added to the diesel fuel. It was discovered that soot emissions decreased as the concentration of oxygenated component increased and once the oxygen content of the fuel reached 25-30% almost all the soot emissions were practically removed. The reason for such benefits have been associated with the improvement in diffusive combustion as well as the promotion of post-flame oxidation of soot in the late expansion and exhaust processes (Ren et al., 2008). With diesel-oxygenated blends, the trade-off curve between the NO<sub>x</sub> and soot emissions is much flatter; indicating more oxygenate components can be added in diesel fuel without raising the NO<sub>x</sub> emissions. In addition, oxygenate fuels have a greater EGR tolerance as a

result of the oxygen enrichment (Ren et al., 2008). The method of adding liquid oxygenates into diesel fuel to reduce engine-out emissions seems to be a practical approach, requiring no modifications to the fuel system itself.

The primary objective of this study is to investigate the influence of a diesel-diglyme and a diesel-biodiesel blend on the performance of combustion and emissions. A blend of each was chosen based on the inherent oxygen content and were compared to pure diesel and biodiesel fuels. The aim of this study was primarily to observe the benefits of diglyme over conventional biodiesel-diesel fuel blends, using numerous emission monitoring methods. Bis (2-methoxyethyl) ether commonly known as Diglyme or DGM was chosen as the high cetane number and oxygenated component, with lower carbon content by wt.% than diesel fuel. DGM is a clear, colourless liquid with an ethereal odour. It is miscible with water, alcohols, diethyl ether and hydrocarbon solvents. The choice of an ether as an oxygenated blending component was due to its performance in terms of combustion behaviour and soot reduction as observed in previous studies (Ren et al., 2008, Beatrice et al., 1999). The high cetane number associated with DGM will affect the engine performance and emissions through the chemical ignition delay and thus improve the ignition quality of the oxygenate-diesel fuel blend. A high cetane number tends to reduce the ignition delay, thus the fraction of injected fuel that is burnt under premixed conditions is reduced (Ying et al., 2006).

Two distinct blends of 50%ULSD + 50%RME (represented as B50) and 15%DGM + 85%ULSD (represented as 15DGM) were investigated and compared to the base fuels. A 15% blend of DGM was chosen based on earlier investigations. From the work of Di et al. (2010), it was shown that the combustion deteriorated when a 20% blend was tested, reducing the brake thermal efficiency (BTE) by more than 3% while increasing the brake specific fuel consumption (BSFC) by around 15%. The volumetric blending ratio for the ULSD-RME was

prepared to match the oxygen content of the 15DGM blend. The lower heating value of each blend was calculated based on the mass fractions of each component in the fuel and the measured higher heating value using a calorimeter. It is important to note that the density of the blends was calculated based on the volumetric fraction and density of the neat fuels. Although the cetane number is not given in Table 17, it can be assumed that it will be higher for the 15DGM blend than for the other fuels, as neat DGM has an exceptionally high cetane number.

**Table 17: Fuel Properties**

Abbreviation	% Volumetric Make-up				
ULSD	100 Ultra Low Sulphur Diesel				
RME	100 Rapeseed Methyl Ester				
B50	50 ULSD + 50 RME				
15DGM	15 Diglyme + 85 ULSD				

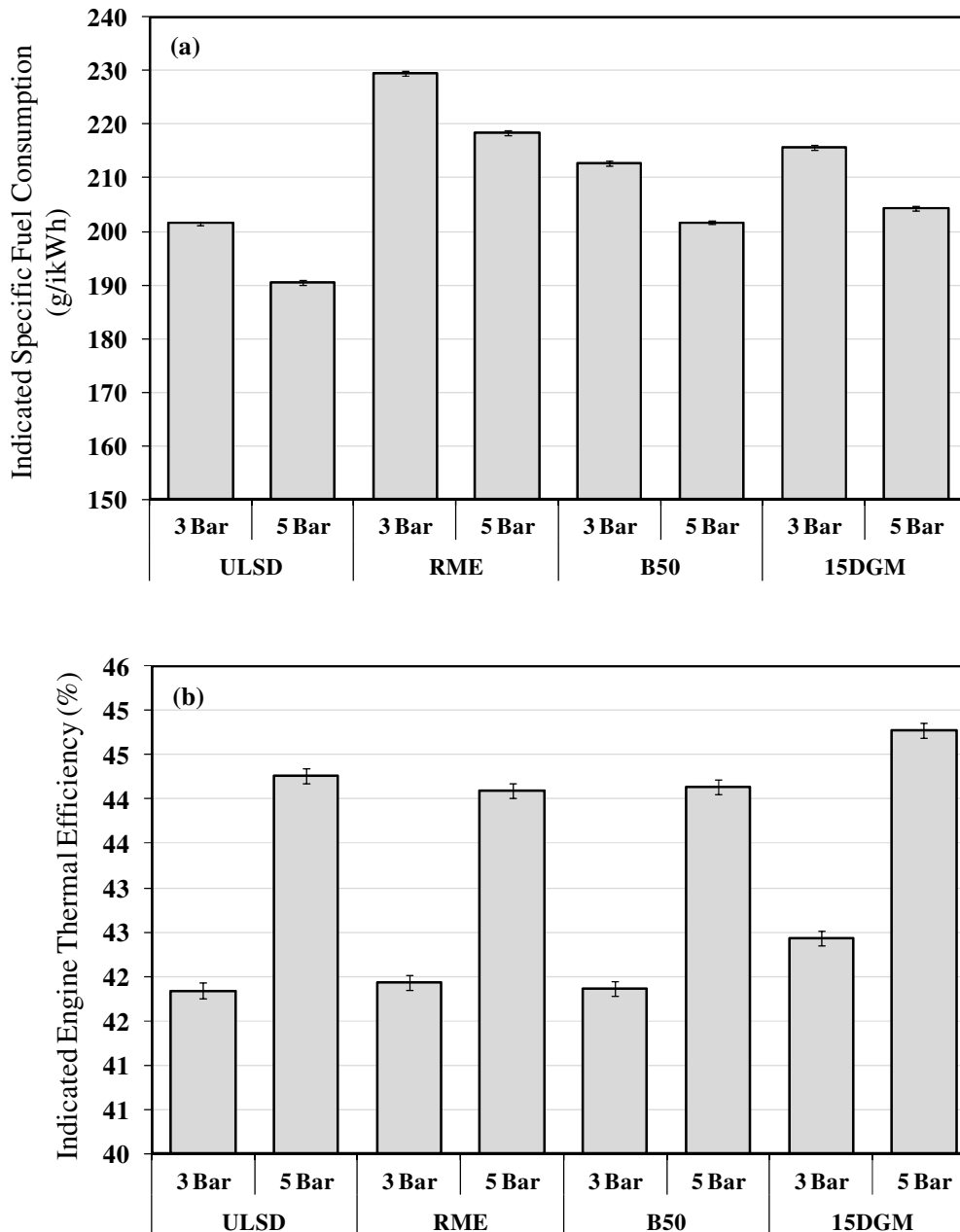
  

Fuel Analysis	Diesel (ULSD)	Biodiesel (RME)	Diglyme (DGM)	B50	15DGM
Chemical Formula	$C_{14}H_{26.18}$	$C_{18.96}H_{35.29}O_2$	$C_6H_{14}O_3$	$C_{16.76}H_{31.26}O_{0.86}$	$C_{12.54}H_{24.04}O_{0.64}$
Cetane Number	53.9	54.7	126	-	-
Density at 15°C (kg/m <sup>3</sup> )	827.1	882.54	937.0	854.8	843.6
Viscosity at 40°C (cSt)	2.467	4.478	-	-	-
Lubricity at 60°C (µm)	274	205	519	211	292
LCV (MJ/kg)	43.3	37.4	26.4	40.4	39.3
Sulphur (mg/kg)	46	5	-	-	-
Total Aromatics (% wt)	24.4	-	-	-	-
C (wt.%)	86.44	77.12	53.71	81.63	81.34
H (wt.%)	13.56	12.04	10.52	12.78	13.09
O (wt.%)	0	10.84	35.77	5.59	5.57

All tests were performed under steady-state conditions at a controlled engine speed of 1500rpm throughout. Two engine loads of 3 bar ( $\lambda = 4.28$ ) and 5 bar ( $\lambda = 2.65$ ) IMEP were used, representing ~40% and ~70% of the maximum load respectively. The overall lambda (i.e. actual air/fuel ratio over the stoichiometric air/fuel ratio) was calculated to be similar for all the fuels tested in this study at each operating condition. This indicates that the difference between the fuels (i.e. in terms of emission and combustion performance) was the direct result of the fuel composition.

## **8.2 Results and Discussion**

The increase in RME percentage in the fuel blend increases the ISFC, as shown in Figure 73a. The lower calorific value of RME compared to ULSD resulted in an increased fuel mass used and hence a higher ISFC to gain the same power output. A similar observation was made with the addition of the DGM. This behaviour can be explained by the fact that the lower heating value of the blend decreases as a result of adding oxygenates (Ren et al., 2008). The improved thermal combustion efficiency as shown in Figure 73b with 15DGM blend highlights the benefit of oxygen enrichment and an improved cetane number due to the properties of neat DGM. The improved thermal efficiency with DGM was also observed by Miyamoto et al. (1998).



**Figure 73: a) Indicated Specific Fuel Consumption and b) Indicated Engine Thermal Efficiency**

In comparison to diesel fuel, RME has inherent oxygen availability with a higher viscosity and density. It has previously been reported (Ren et al., 2008, Lapuerta et al., 2008a) that a higher oxygen concentration in the spray will result in a reduction in pyrolysis and an increase in oxidation, hence shortening the combustion duration. Others have also observed (Tsolakis, 2006, Lapuerta et al., 2008a, Mathis et al., 2005) an increase in injection pressure,

an advance in combustion and an increase in the premixed combustion phase. The resulting higher rate of heat release increases the  $\text{NO}_x$  emissions while reducing the HC and CO emissions simultaneously (Tsolakis et al., 2007b). Although the increased maximum temperature during combustion reduces the formation of soot (Tree and Svensson, 2007), the relative portion of SOM tends to increase because of the lower volatility of biodiesel (Krahl et al., 2003, Schröder et al., 1999, Mueller et al., 2003). According to Tree and Svensson (2007), as the temperature is increased the rate of soot oxidation increases more rapidly than the rate of soot formation. The effect of thermal  $\text{NO}_x$  reduction with 15DGM can be confirmed by the heat release rate analysis shown in Figure 74, where the reduction in premixed burn peak can be observed.

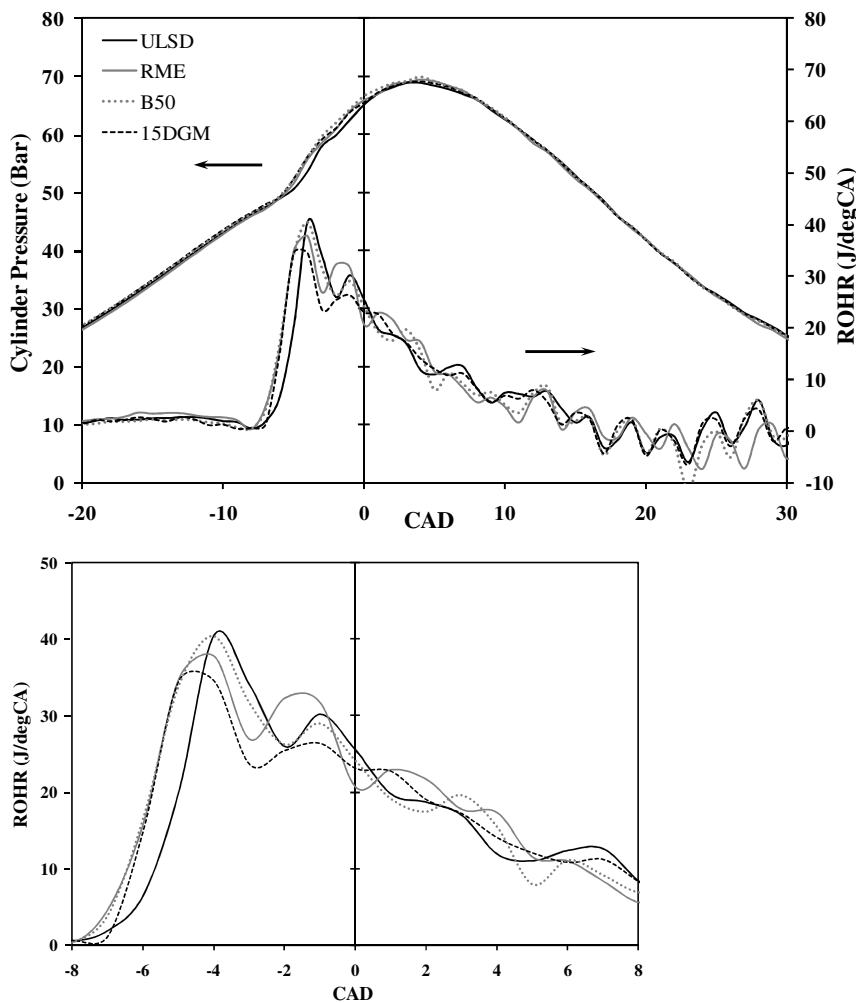


**Figure 74: Combustion Characteristics of Neat and Blended Fuels - 3 bar IMEP**

A slight reduction in HC and CO from Figure 75 also indicates an improvement in combustion efficiency with the inclusion of oxygen. The DGM-diesel blend reduces the peak of the premixed combustion rate and as a consequence the diffusion controlled phase of combustion is extended. Thus according to Ren et al. (2008), the combustion phase and the heat release rates are strongly influenced by the cetane number of the oxygenate fuel. A larger cetane number extends the diffusion controlled combustion phase, resulting in a reduced in-cylinder peak pressure and temperature by spreading the heat release over a later CAD (Gill et al., 2011b). The ignition delay also strongly depends on the cetane number of the fuel and as the cetane number increases the ignition delay decreases. The advance in injection timing with RME and B50 is thought to have been due to the increased bulk modulus of compressibility (i.e. resistance to compression) as a result of the higher polarity of the oxygen content and density of the fuel causing a greater rate of pressure rise within the fuel pump and an earlier injection into the cylinder than diesel, even at the same nominal pump timing (Boehman et al., 2004, Tsolakis et al., 2007b, Szybist and Boehman, 2003). Thus this results in an overall advance in combustion. With 15DGM there was also a combustion advance, however this was thought to have been a direct result of a lower ignition delay brought about from the higher cetane number of the blend rather than an advance in injection as observed with RME.

During the late combustion phase (from 15CAD after TDC), there still remains a small fraction of fuel which is present in the form of soot or as fuel-rich combustion products. It is known that these species can release a small amount of energy, resulting in a lower rate of ROHR into the expansion stroke (Heywood, 1988). Thus it is suggested to be responsible, together with background noise, for the fluctuations in the combustion pattern after the diffusion phase.

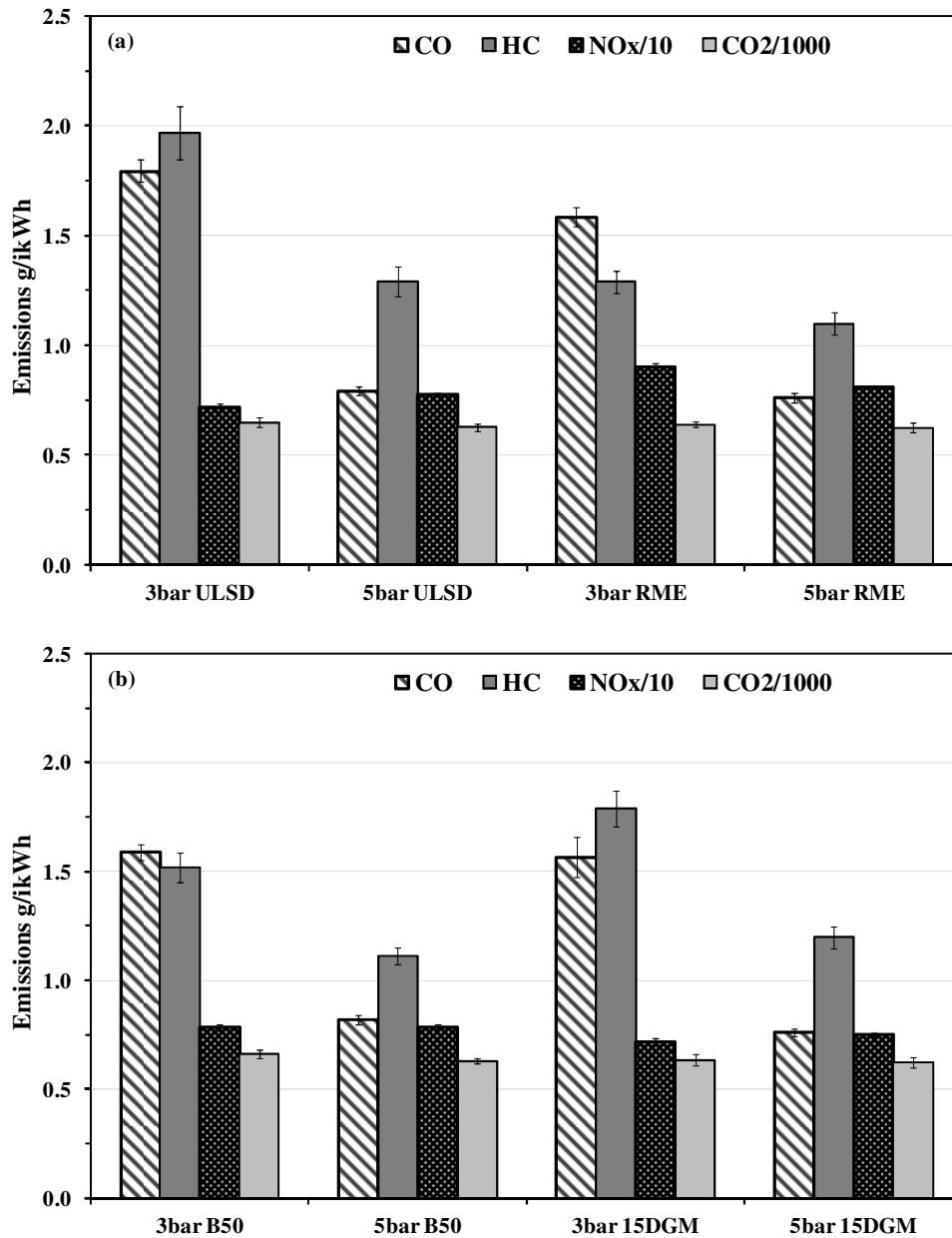


Figure 75: Engine-out Specific Emissions of Neat and Blended Fuels

It is also well-known (Lapuerta et al., 2008a, Song et al., 2004, Monyem and H. Van Gerpen, 2001) that the advanced combustion (as in the case for RME and B50) can cause an increase in the NO<sub>x</sub> emissions from a diesel engine. The reduced NO<sub>x</sub> emissions with 15DGM reflect the lower in-cylinder temperatures as a result of the reduced heat of combustion. However, Song et al. (2002) also referred to this being a result of a leaner overall mixture in the premixed-dominated combustion. As the engine load is increased from 3 to 5

bar IMEP, the combustion efficiency increases. Thus it is suggested that the oxygen present in the fuel would promote the reduction in HC and CO emissions as a result of an increase in oxidation of combustion intermediates. Further the oxygen enrichment will also favour the oxidation of HC in the expansion and exhaust processes (Song et al., 2002, Ren et al., 2008). As observed in Figure 75, the HC and CO emissions decreased in comparison to the diesel base fuel with a much smaller change at higher engine load.

Oxygenated fuel components, such as the blend of 15DGM, can significantly reduce PM emissions whilst keeping the NO<sub>x</sub> emissions similar to that of diesel fuel. This impact varies with engine operating conditions as observed in Figure 76 where at 5 bar IMEP a simultaneous NO<sub>x</sub> and PM reduction can be obtained. Miyamoto et al. (1998) also observed benefits in NO<sub>x</sub> emissions with DGM and concluded it was because of the inherent lower adiabatic flame temperature and milder first stage combustion compared to diesel fuel. The numerical study by Cheng et al. (2002) gives a broader explanation to how the oxygenates affect the soot formation. In summary it was found that the key factor affecting soot formation was the nature and relative concentrations of the fuel-rich premixed flame products, which subsequently control the processes of aromatic ring formation, PAH growth and soot particle inception. It was suggested that the increase in radical concentrations (e.g. O, OH, etc produced by oxygenates) promoted the carbon oxidation to CO and CO<sub>2</sub> within the premixed flame zone, thus limiting the carbon available for the formation of soot precursor species.

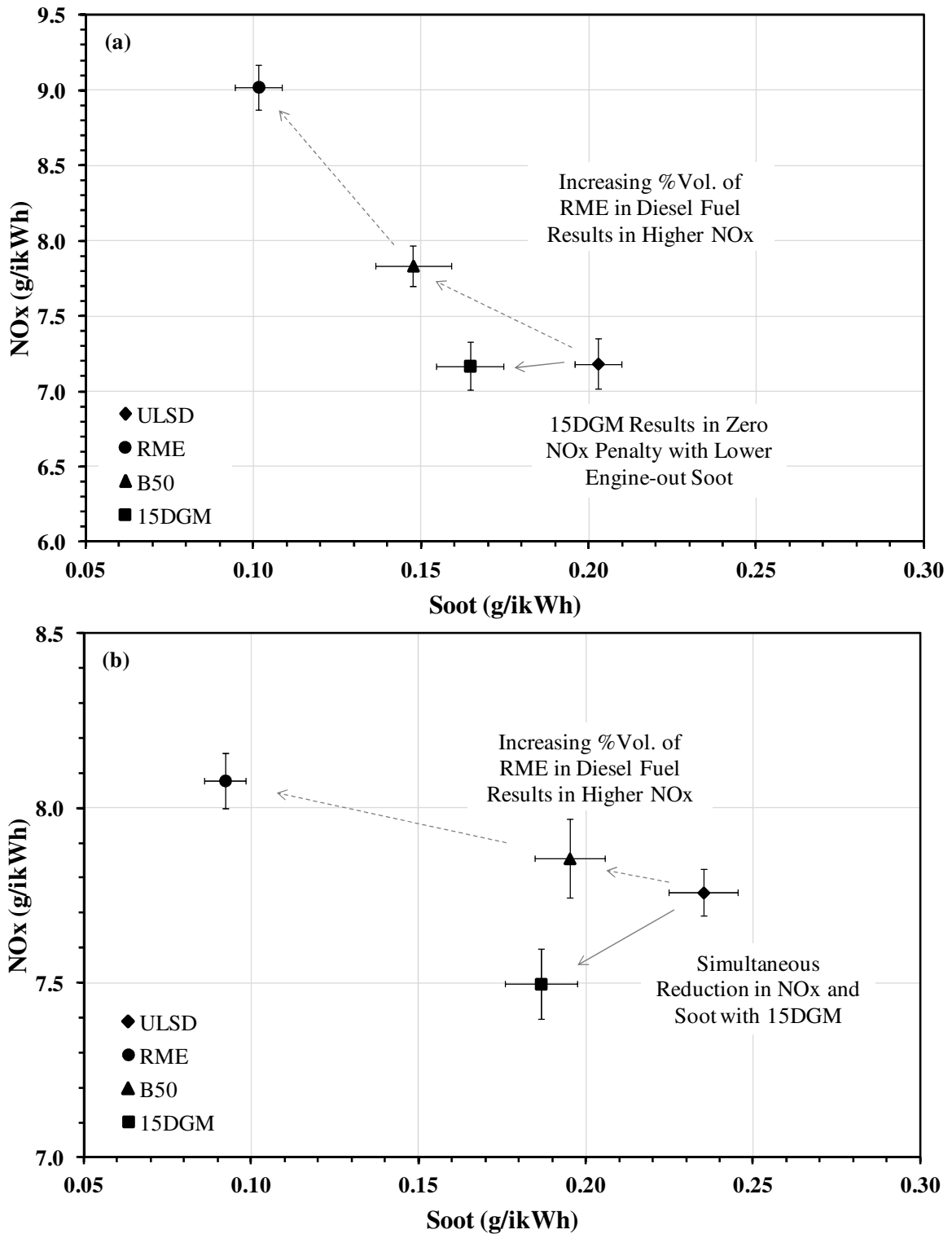


Figure 76: The Effect of the NO<sub>x</sub>/Soot Trade-off: a) 3Bar IMEP, b) 5Bar IMEP

Further the kinetic work of Westbrook et al. (2006) showed ether type oxygenates exhibiting an oxygen (O) atom bonded to two carbon (C) atoms. During combustion one C-O

bond is broken and the O atom remains bonded to another C atom, leading to the formation of CO. As a result, the strong CO bond remains intact preventing it from becoming available for soot production. In terms of 15DGM, the oxygenated species displace the C atoms in the diesel fuel with C atoms that are bonded to O atoms. This displacement according to Westbrook et al. (2006) exchanges the C atoms that can produce soot with C atoms that cannot contribute to soot production as a result of the bonded O atoms. As the ester group has two O atoms bonded to a single C atom, the ether is seen to be more effective than the ester in reducing the total level of soot precursors (Boot et al., 2008, Westbrook et al., 2006).

According to Boot et al. (2008), the use of a cetane booster had a negative influence on the soot emissions. It was suggested to be because of a reduced non-sooting premixed burn duration brought about by the shorter ignition delay. Although the ether should in theory be more effective than the ester, the effect of a higher cetane number may result in an overall diminished benefit. Thus, depending on the engine operating conditions, the ester may outperform the ether in terms of soot control, as observed in Figure 76, highlighting the  $\text{NO}_x$ /soot trade-off. At lower load (i.e. 3 bar IMEP) an increase in RME content in diesel fuel resulted in a significant increase in engine-out  $\text{NO}_x$  emissions, while the blend of 15DGM kept the  $\text{NO}_x$  emissions at the same level as ULSD. This trend is similar for RME at a higher engine load (i.e. 5 bar IMEP); however the blend of 15DGM was able to promote a simultaneous reduction in engine-out  $\text{NO}_x$  and soot emissions. It is suggested to be the result of the combined effect of an increased fuel cetane number (e.g. reduced ignition delay) and oxygen content resulting in lower premixed combustion and higher soot oxidation in the diffusion combustion phase.

All oxygenated fuels gave a lower particle number and mass concentration with a shift in the size distribution to smaller mean diameter particles. The reason for a significantly

reduced mean particle size can be explained by not only a reduction in the soot formation (i.e. due to increased in-cylinder temperatures) but also suppression in particle collision. The control of the latter can prevent the formation of larger particles through agglomeration as the combustion gases cool. Therefore with both oxygen enrichment and reduced carbon content in the fuel blends, there is a greater possibility for oxidation of primary particles. Hence this will decrease the particle number concentrations as observed in Figure 77 and Figure 78 in comparison to diesel fuel.

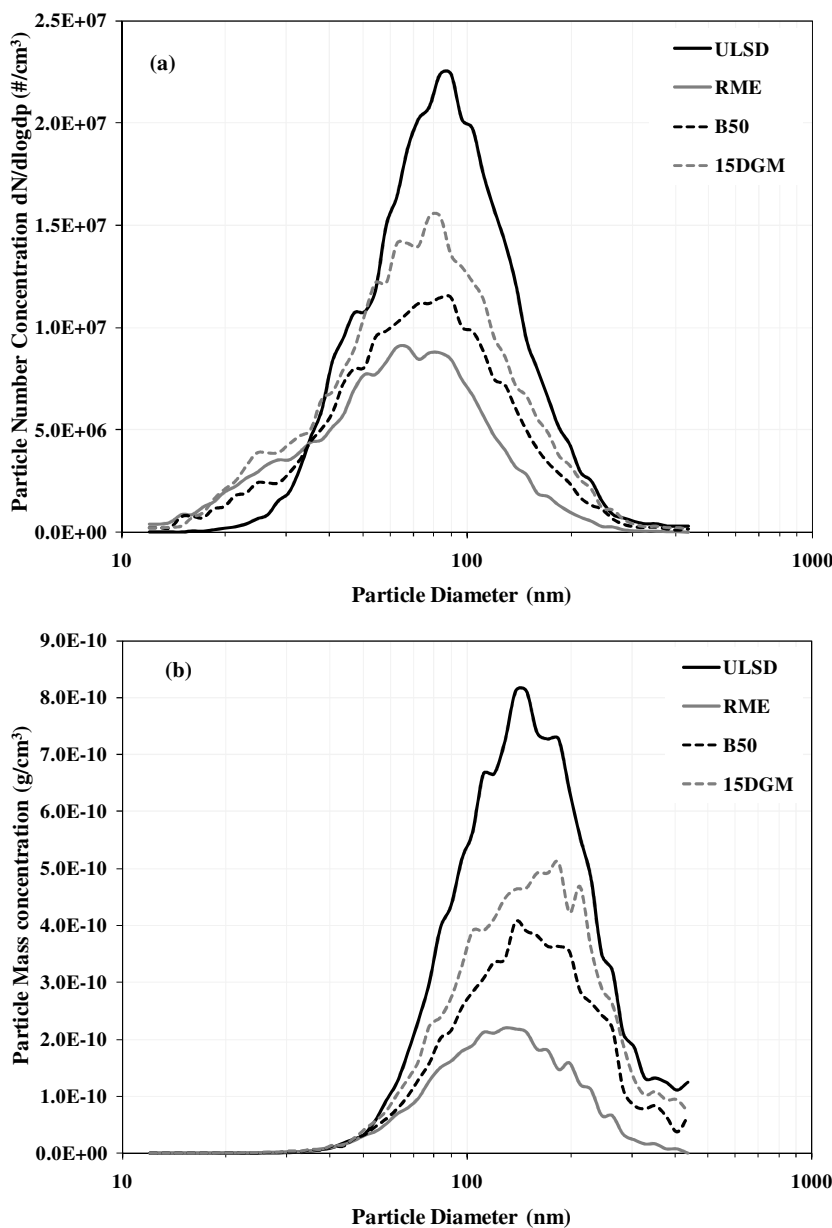


**Figure 77: Particulate Size Distributions at 3 bar IMEP: a) Particulate Number, b) Particulate Mass**

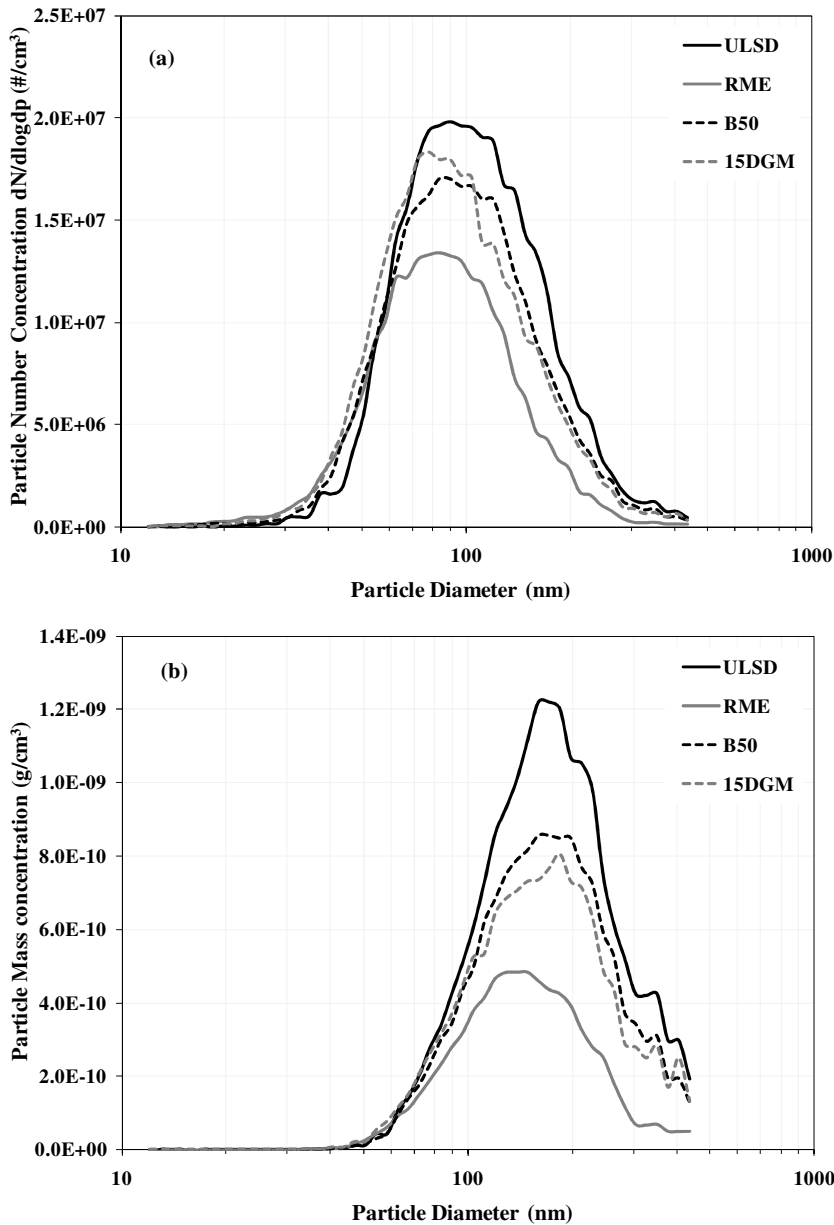


Figure 78: Particulate Size Distributions at 5 bar IMEP: a) Particulate Number, b) Particulate Mass

As the number of particles and the rate of agglomeration are decreased, the corresponding smaller particles will lead to a decrease in mean diameter. It can also be observed from particularly Figure 77 (low load), the quantity of particles bigger than 40nm are significantly lower with RME, B50 and 15DGM compared to ULSD. The reduction in accumulation mode particles of diesel particulate mass with biodiesel is consistent with other studies (Jung et al., 2006, Cheng et al., 2008, Di et al., 2009). Under both load conditions, the

results in Figure 77a and Figure 78a show a similar particulate number concentration, however there is a reduction in the number of smaller diameter particles under high load conditions. The significant difference between the two engine loads can be observed from the mass concentration distributions which are in fact the difference in mean particle diameter. Thus smaller mean diameter is thought to have been due to either the agglomerates consisting of lower primary particles or the aggregate itself consists of smaller primary particles. In the work of Lapuerta et al. (2008b), it was also observed that the mean particle diameter reduced with biodiesel blends with respect to diesel fuel. In addition there was a slight shift in the whole size distribution towards smaller particles as observed in this study and others (Bagley et al., 1998, Cheng et al., 2008). This can be seen as a drawback of not only biodiesel blends but also oxygenated blends.

The smaller particles are considered to be more difficult to trap and more severe than the larger particles in terms of their impact on health and the environment. The smaller particles are more reactive and can take part in atmospheric chemistry resulting from a higher surface/volume ratio. The larger particles are removed quickly from the atmosphere by settling, while the smaller ones take longer (greater atmospheric residence time) and are removed by coagulating and diffusing with the larger particles (Kittelson, 1998). However, from Figure 77 and Figure 78 it can also be seen that the particle number concentration for RME, B50 and 15DGM are all reduced. This suggests that the smaller mean size of the emitted particles is not caused by an increase in the number of smaller particles but a significant reduction of the number of larger particles.

Figure 79 shows that the total particle number concentration, mean particle diameter and total particle mass concentration decrease linearly with oxygen concentration. This is again the similar trend observed with the particle size distributions earlier. It is generally

known that with RME the benefit in PM is a direct result of the reduction in soot (the insoluble fraction); however the overall benefit is reduced by the increase in SOM. The reason for the increase has been attributed to the lower volatility of the unburned HC, thus favouring their condensation and adsorption onto the particles' surface (Lapuerta et al., 2008a). The work of Knothe et al. (2005) and Bagley et al. (1998) were a few of many who concluded that this was the effect of the higher boiling point, higher viscosity and higher density, thus leading to a poor air/fuel mixture and incomplete combustion.

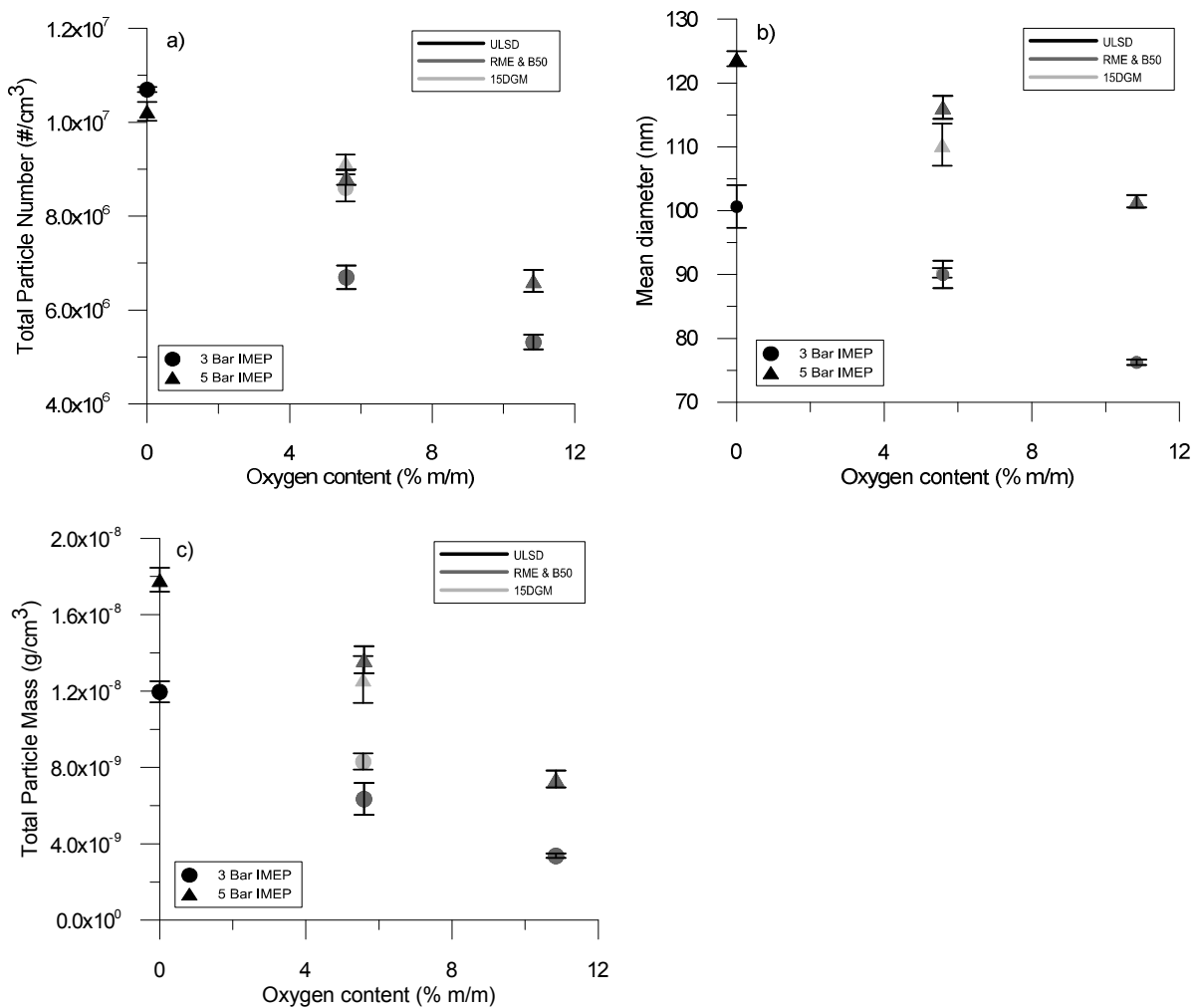


**Figure 79: a) Total particle Number, b) Mean Diameter and c) Total Particle Mass**

Figure 80 highlights a good correlation between the SOF (Soxhlet extraction method) and VOF (TGA method). The fractions are a measure of the SOM over the PM in the exhaust.

However, it is important to note that some volatile particulate components can remain after the solvent extraction and thus result in differences between the SOF and VOF (Lapuerta et al., 2007). Increasing the biodiesel percentage within ULSD (i.e. 0, 50 and 100%Vol. replacement) both the soluble and volatile compounds in the particulate matter increase. This was also observed in the work of Lapuerta et al. (2007). The joint effect of soot reduction and an increase in SOM result in a higher SOF as shown in Figure 80.

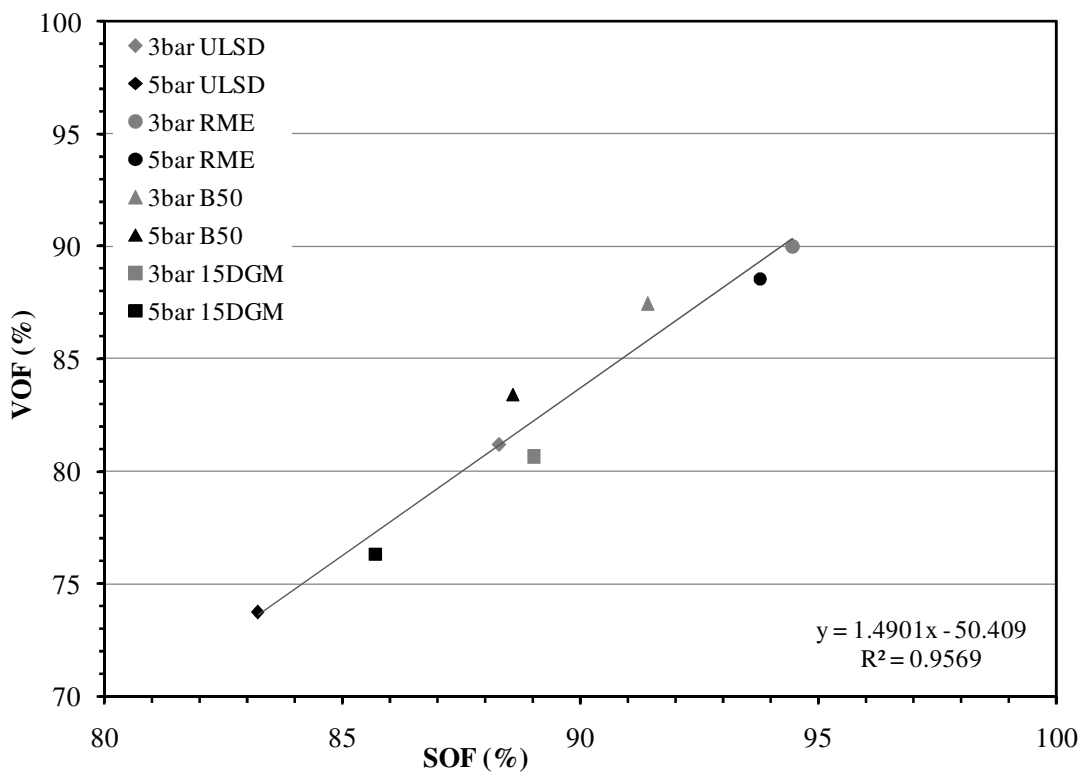


**Figure 80: Correlation between VOF and SOF**

The effect of engine load on SOF formation was explained in the work of Tan et al. (2007). It was suggested that soot was the most dominant player in the PM formation process while SOM only had a greater influence at low load conditions, where the equivalence ratio of fuel-air is lower and the ignition delay is longer. During this period the more over-lean mixture regions are beyond the lean flammability limit and with lower in-cylinder temperatures, slower rate of soot oxidation, more HC and their partial oxidation products

leave as SOM adsorbed on the soot particles. At higher loads the effect is vice versa and the influence of SOM on the PM reduces. PAH present in the SOF have a mutagenic action and are known to cause health and environmental hazards (Tan et al., 2007). These concerns have led to more stringent forthcoming emission regulations such as those imposed by Euro 5, forcing manufacturers to reduce PM emissions significantly. In the case of Euro 6, which comes into effect in 2014, the PM emissions will remain similar to those set for Euro 5 but the latter has already forced the manufacturers to introduce a DPF to their diesel vehicles (2009a). Taking this into consideration, 15DGM seems to be more favourable than the B50 fuel blend, reducing not only the soot fraction of the PM but also keeping the SOM lower than biodiesel itself. However, it is important to note that as aromatics and PAH are soot precursors, the absence of aromatic content in RME and DGM may assist in the reduction of PM emission (Di et al., 2009).

In this study it was assumed that the volatile organic material (VOM) will remain adsorbed on the dry soot accumulated on the filter and once the filter temperature exceeded approximately 380-400°C most of the VOM will be vaporised and only the dry soot will remain. Further increasing the furnace temperature in an atmosphere of air, the soot will begin to oxidise, and the derivative weight loss curve in Figure 81 identifies the point at which weight loss due to soot oxidation is most evident, i.e. the peak oxidation temperature. Thus there are inherent differences in the reactivity of the particulate, as shown in Figure 82. RME shows a greater lower temperature peak indicating a greater VOF in comparison to diesel fuel.

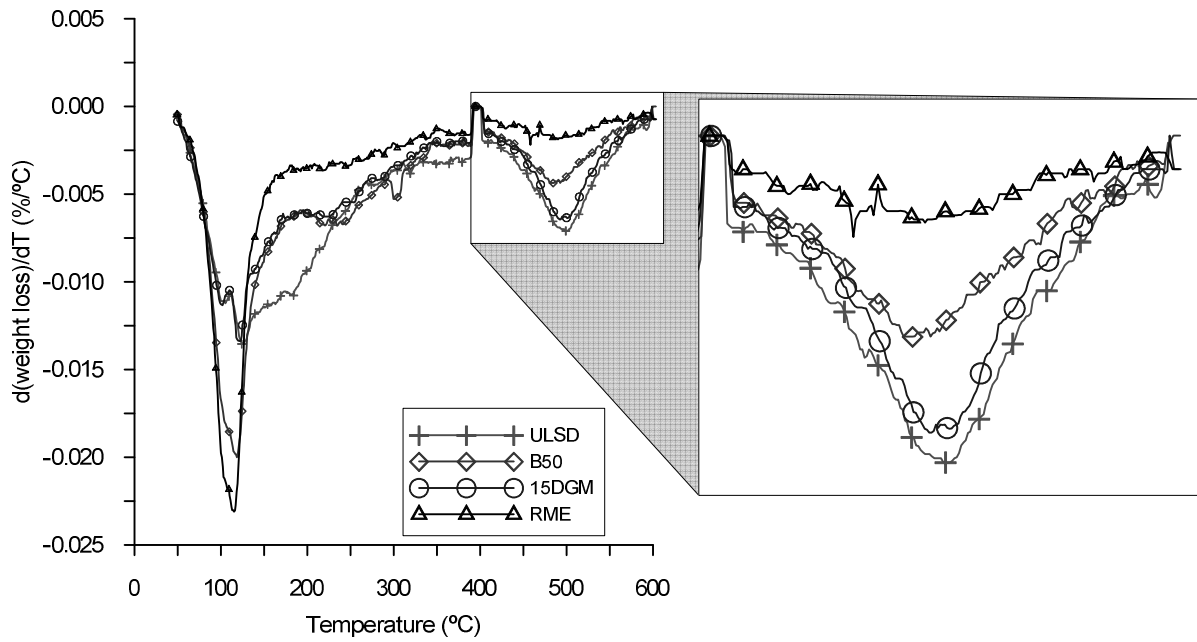


Figure 81: TGA Analysis from a Loaded Filter Paper at 5 bar IMEP

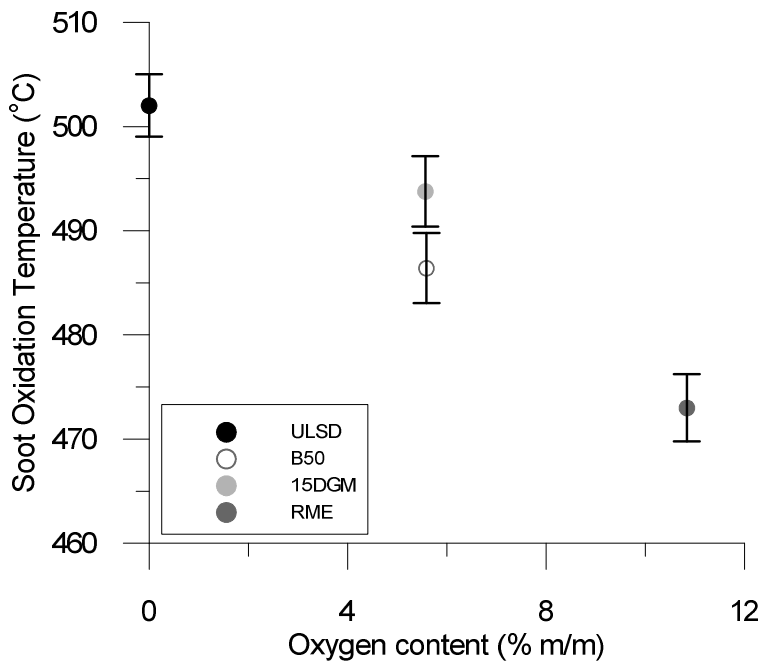


Figure 82: Peak Soot Oxidation Temperature at 5 bar IMEP

According to Boehman et al. (2005), biodiesel fuelling alters the nanostructure and oxidation reactivity of the primary soot particles. As a result, this leads to a more amorphous soot structure which enhances the rate of soot oxidation, easing the regeneration of DPF's.

The combined effect of a lower soot oxidation temperature and a reduced rate of soot loading over the DPF can have a positive impact on the overall fuel penalty during active regeneration. A less frequent regeneration and a reduced fuel injection can further benefit the long term performance of the DPF (Gill et al., 2011a).

### **8.3 Summary**

Fuel blending components such as DGM have demonstrated to be as effective and comparable to biodiesel fuel blends in suppressing the formation of soot. However, the DGM-diesel blend (15DGM) has proven to attain further benefits as a result of influenced combustion characteristics giving a simultaneous NO<sub>x</sub> and PM reduction in comparison to RME blends. As mentioned previously there are several factors that can contribute to the reduction in soot and a few of them have been summarised below:

- Although the diffusion phase is extended favouring soot formation (higher cetane number of DGM), the oxygen present in the fuel molecule counteracts this penalty, not only inhibiting soot formation but also enhancing the soot oxidation.
- Increased diffusion phase temperature will promote soot oxidation.
- An increase in oxygen content means a decrease in the carbon content of the blended fuel.
- A reduction in aromatic compounds results in the decrease of soot precursors.

15DGM demonstrated to be just as effective as the B50 blend even though the volumetric composition of DGM was smaller than that of RME. However, by keeping the same oxygen content in the fuel blends, it was possible to observe the benefit of the higher cetane number of DGM. The reduced ignition delay combined with a reduction in the premixed combustion further leads to the reduction in NO<sub>x</sub> emissions. Although similar trends were observed between the two blends, 15DGM showed to be a better blend in terms of

combustion efficiency. However, the emissions performance was dependent on the engine conditions as 15DGM outperformed B50 in the overall NO<sub>x</sub>/PM trade-off at higher engine loads. The peak soot oxidation temperature of the fuels tested are illustrated in Figure 82 and it can be seen that although the two blends exhibit a similar oxygen content, the chemical properties such as the cetane number also influence the soot oxidation properties of the fuel through combustion.

As with aftertreatment systems, control of engine-out PM can be advantageous. For example, a regeneration method for a DPF is another parameter that affects filter performance, and the selection of a regeneration strategy is important to extend the useful life of the DPF. In order to further extend the filter performance, reformulation of diesel fuels as demonstrated in this study can play a significant role. A reduction in engine-out soot and an improved soot oxidation temperature can result in reduced and more effective regeneration cycles.

# CHAPTER 9

## CONCLUSIONS

### 9.1 Concluding Remarks

The most practical reductant for the HC-SCR system is considered to be either reformed diesel fuel or dissociated ammonia. The work presented here has shown diesel exhaust gas fuel reforming to be effective in producing active HC species as well as H<sub>2</sub> for the reduction of NO<sub>x</sub> over an Ag catalyst. Although some deactivation of the active sites as well as physical blockage from soot can be avoided with the use of an upstream DPF, excessive HC production from reforming can lead to a loss in catalyst activity resulting from the deposition/adsorption onto the surface of the catalyst. Thus better control of the HC:NO<sub>x</sub> ratio is required to minimise catalyst deactivation. Although the HC-SCR is highly susceptible to HC deactivation when H<sub>2</sub> is removed, it is suggested that this activity can be regained during the high temperature active regeneration of the DPF. Thus the heat generated during the oxidation of the fuel can be used not only to promote soot oxidation within the DPF but also support the oxidation of the HC species that remain on the surface of the HC-SCR catalyst. An alternative solution to reforming is to introduce NH<sub>3</sub> on-board the vehicle and through its dissociation can be very effective over the Ag catalyst. The overall result is both HC (i.e. unburnt HC from combustion) and NH<sub>3</sub> can take part in the surface reactions of the Ag-Al<sub>2</sub>O<sub>3</sub> HC-SCR catalyst which is enhanced in the presence of H<sub>2</sub>. An overall summary of the HC-SCR results using Ag-Al<sub>2</sub>O<sub>3</sub> catalysts is given in Figure 83.

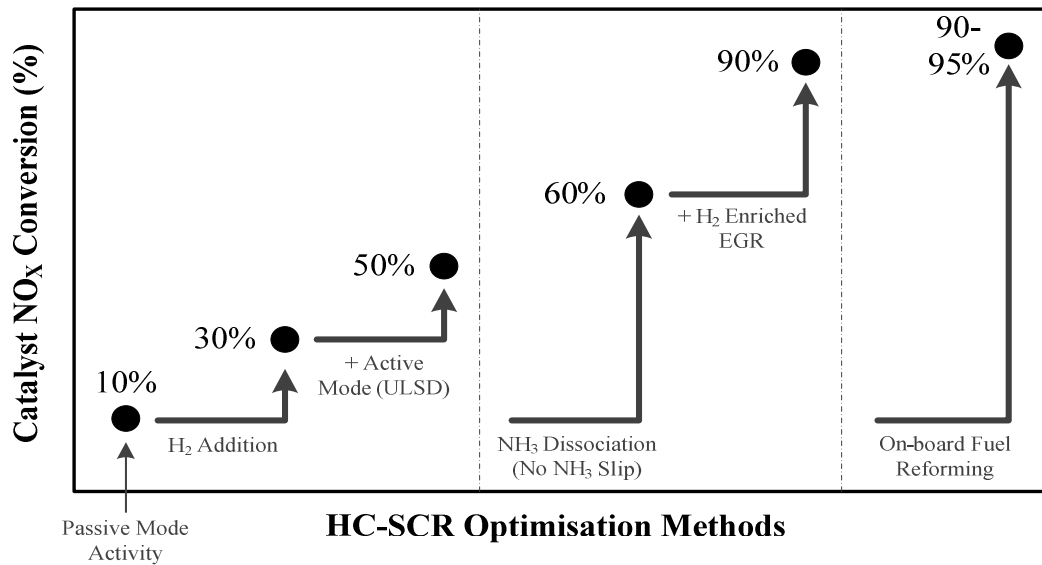


**Figure 83: Ag-Al<sub>2</sub>O<sub>3</sub> Optimisation Methods: In the Presence of a DPF at 250°C, GHSV of 30,000 h<sup>-1</sup>**

The benefit of H<sub>2</sub> was also observed when the engine was fed with simulated REGR, not only improving CO<sub>2</sub> emissions but also useful for promoting the NO<sub>2</sub> emission during combustion, especially for passive DPF regeneration. It was also observed that by introducing H<sub>2</sub> upstream the DOC it was possible to further increase the NO<sub>2</sub> emissions, resulting from not only an improved catalyst light-off temperature (improving the low temperature oxidation activity), thus increasing the rate of NO-NO<sub>2</sub> oxidation, but also the result of H<sub>2</sub> oxidation increasing the local temperature (thermal effect). This increase in exhaust temperature can also be advantageous for both DPF regeneration and lean NO<sub>x</sub> catalysts.

Although the NO<sub>x</sub>/soot trade-off can be effectively controlled using aftertreatment devices alone, techniques such as FEGR and the blending of fuel components can also be implemented simultaneously not only to help control the regulated emissions (i.e. enhance combustion) but reduce the stress currently placed on the aftertreatment devices. As presented earlier, by simply controlling the recirculation of HC and soot back into the combustion chamber through FEGR it is possible to improve the overall NO<sub>x</sub>/soot ratio compared to unfiltered EGR, where the HC and soot recirculation penalty has a detrimental impact on the

engine-out soot emissions. However, this particular technique is more beneficial under high EGR or high engine load conditions where the concentration of soot in the exhaust is large enough to result in a soot recirculation penalty during EGR. On the other hand, by introducing fuel components to oxygenate the fuel and improve the overall cetane number it is possible to enhance the diesel combustion and gain better control of the NO<sub>x</sub>/soot trade-off, especially at lower exhaust gas temperatures. Further a reduction in engine-out soot and an improved soot oxidation temperature can result in reduced and more effective regeneration cycles.

Figure 84 shows the results of each individual study and how they can be linked to give the most effective aftertreatment system as illustrated in Figure 85. This particular system comprises of a lean NO<sub>x</sub> catalyst downstream a CCRT<sup>®</sup> system with H<sub>2</sub> implemented on-board through the dissociation of NH<sub>3</sub>. The H<sub>2</sub> rich mixture is introduced directly upstream the DOC to increase the local temperature, enhance the rate of NO-NO<sub>2</sub> oxidation and reduce the SOM primarily through the oxidation of gas phase HC improving the passive regeneration strategy. It is important that the DOC produces enough NO<sub>2</sub> to oxidise the soot stoichiometrically. This, as well as the temperature within the DPF, is important to enable the NO<sub>2</sub>-soot reaction to proceed. If the temperature entering the DPF is too low, the soot will not react with incoming NO<sub>2</sub> and the DPF will not regenerate. The mixture is also added upstream the HC-SCR catalysts improving the NO<sub>x</sub> reduction performance of the catalysts. In addition, the presence of the upstream DOC and cDPF will effectively remove the carbonaceous species (e.g. HC and soot) present in the exhaust gas mixture, reducing the possibility of catalyst coking, especially at low temperatures. In order to make use of any unused H<sub>2</sub> downstream the HC-SCR, controlled levels of EGR are introduced to allow for H<sub>2</sub> combustion promoting further the NO<sub>2</sub> emission as well giving the opportunity for a CO<sub>2</sub> reduction. As this resembles a LPL-FEGR system, any associated soot and HC recirculation

penalty will be reduced. The benefit of this particular aftertreatment design is that the combustion of diesel fuel (i.e. ULSD) enhanced with the addition of DGM reduces the emission of soot without any NO<sub>x</sub> penalty at low exhaust temperatures, improving the overall NO<sub>x</sub>/PM ratio for passive regeneration.

Another system design is represented in Figure 86, an alternative option to that of using RME as the combustion fuel is believed to be the combination of FEGR with fuel components (i.e. DGM) under diesel fuelling, which may provide the ideal compromise for a simultaneous reduction in engine-out NO<sub>x</sub> and PM emissions. Although fuelling with RME results in an engine-out soot reduction, there is an associated NO<sub>x</sub> penalty arising from a reduced injection delay, an advance in combustion and a higher rate of heat release. The resulting advance in combustion is thought to have been a result of the advance in injection timing which is influenced by the increased bulk modulus of compressibility and not a reduction in the injection delay (i.e. as the cetane number of RME and ULSD are similar). Therefore the addition of DGM would not only result in a reduction in engine-out soot but a simultaneous reduction in NO<sub>x</sub>, especially at high engine loads. As a result, less NO<sub>x</sub> would need to be controlled through the use of EGR to meet forthcoming emission legislation. An overall benefit of this particular system is no additional lean NO<sub>x</sub> catalyst would be required, minimising any associated cost and fuel penalty. However, further attention would need to be given to the DPF regeneration strategy, which to some extent is improved through the addition of DGM resulting in a lower soot oxidation temperature. In comparison to the earlier aftertreatment design, the lack of NO<sub>2</sub> formation in this system will not favour passive regeneration, thus the HC content in the exhaust would need to be periodically enriched by either in-cylinder post injection or by direct injection of fuel into the exhaust stream to raise the temperature of the DPF to combust the collected PM.

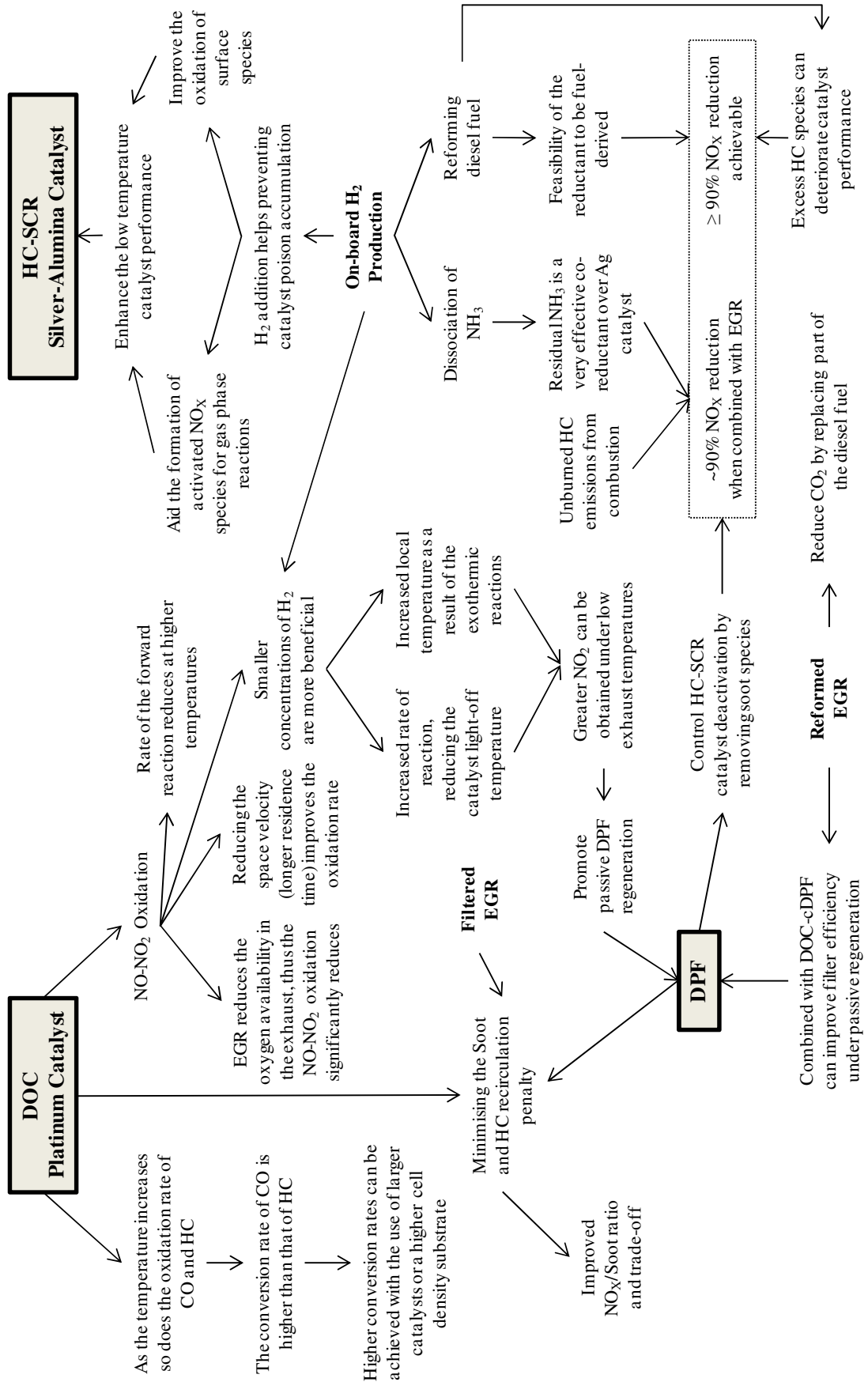


Figure 84: Optimising the Aftertreatment System

**SYSTEM 1**  
Control of NO<sub>x</sub>/soot trade-off with  
aftertreatment optimisation

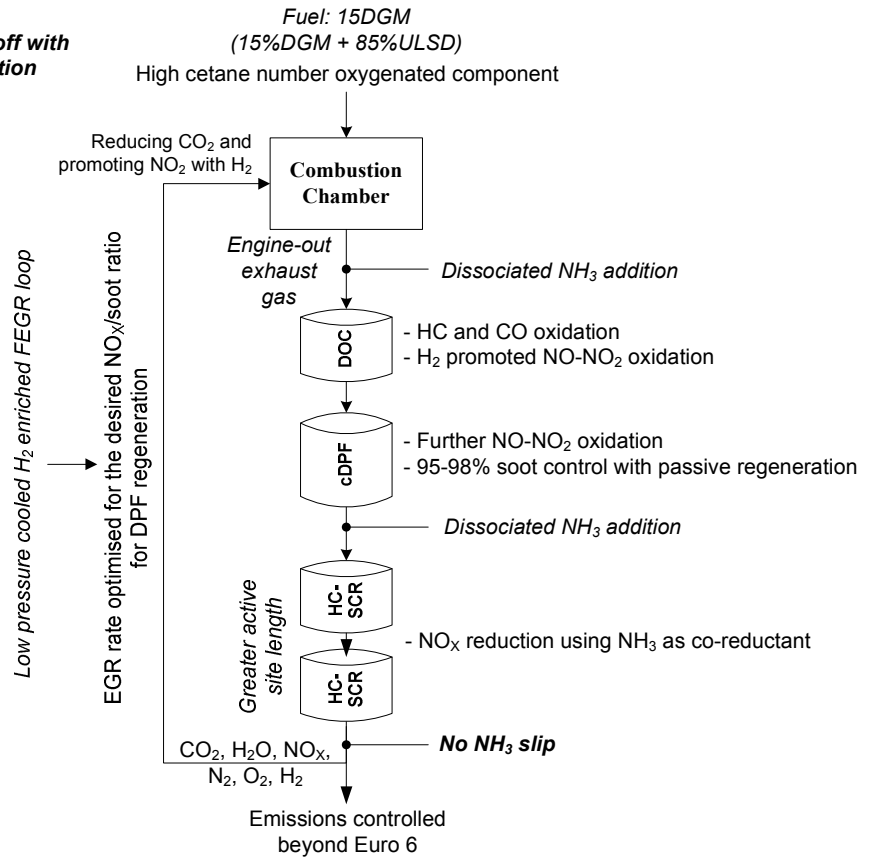


Figure 85: Optimised Aftertreatment System 1

**SYSTEM 2**  
Control of NO<sub>x</sub>/Soot trade-off by  
implementing the CCRT system with FEGR

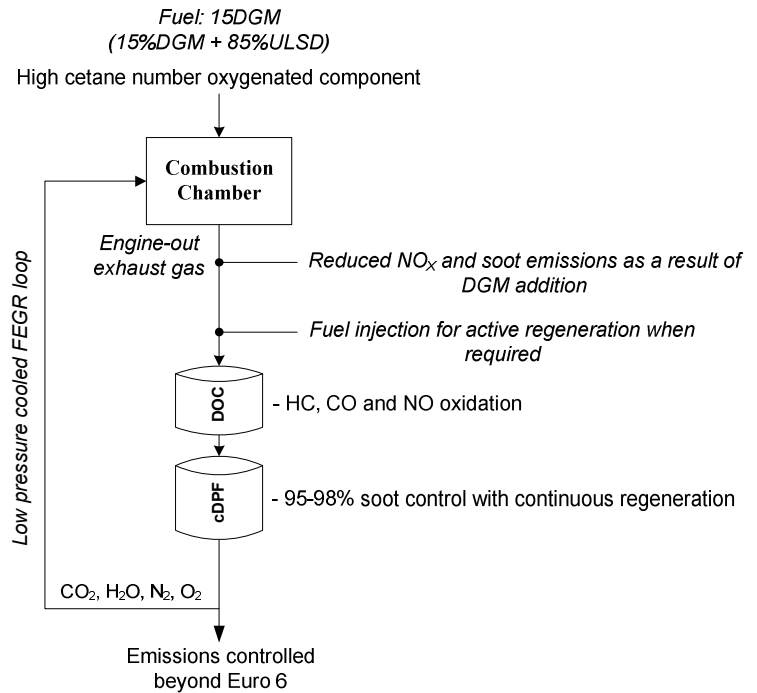


Figure 86: Optimised Aftertreatment System 2

## **9.2 Future Work**

As  $\text{NH}_3$  is a very effective co-reductant over the Ag catalyst, it is suggested that it may be possible to operate and optimise the reformer under certain conditions (e.g. high  $\text{NO}_x$  engine operation coupled with high catalyst inlet temperature) to generate not only  $\text{H}_2$  but also  $\text{NH}_3$ . The HC-SCR reaction can then be promoted in the presence  $\text{H}_2$  while using  $\text{NH}_3$  as the co-reductant with unburnt HC. However, the aim would be to minimise the concentration of HC in the reformer product gas by optimising the rate of fuel addition to the reformer (more specifically the reactant ratios at the reformer inlet) for different exhaust gas compositions and space velocities. This could also involve studying the effect of alternative renewable fuels (e.g. ethanol blends) for the reforming process, which may prove to have some benefit due to the presence of oxygen within the fuel itself.

The dissociation of  $\text{NH}_3$  seems to be very effective, especially in promoting the activity of a silver lean  $\text{NO}_x$  catalyst. As the work presented in this thesis focuses primarily on the  $\text{NO}_x$  reduction performance, the dissociation process itself would need to be investigated and how efficiently this can be implemented on-board the vehicle. Possible catalyst for this investigation is ruthenium, which is known to be the most active catalyst.

Further research into light duty  $\text{NO}_x$  control technology (either this be SCR or NAC) should be undertaken, thus allowing the possibility for diesel engines to be calibrated for lower PM emissions. This will reduce the need for active regeneration at high soot loadings, reducing the associated fuel penalty and favour passive oxidation of soot using  $\text{NO}_2$ . In addition it can be assumed that a less thermal mass is required in the DPF (usually used as a precaution for active regeneration), hence allowing a faster heat-up of a downstream SCR catalyst, especially during cold start.

As current engines are becoming more efficient through the use of various engine calibration techniques (i.e. injection strategies), it is envisaged that partial flow filters will become popular, especially due to the nature of its design which prevent clogging of the channels. It is suggested that investigations in combining a partial flow filter with a lean NO<sub>x</sub> catalyst should be considered and whether this could eventually replace the need for EGR techniques. It may also be useful to incorporate some fuel borne catalyst to this particular system (e.g. ceria or iron based) to promote a regeneration process independent of the NO<sub>x</sub>/PM ratio (i.e. natural soot combustion without the need for post injection), significantly reduce the soot oxidation temperature and reduce the production of secondary emissions (e.g. NO<sub>2</sub>). Alternatively, methods or options to lower the activation energy of soot oxidation with active oxygen species should be investigated; this will allow passive low temperature oxidation with oxygen species through a higher reaction rate.

Although there are numerous studies which can follow from the work presented in this thesis, it is important that work should also involve tuning of the system to an operating drive cycle and introducing cold starts, monitoring also the performance of the catalysts or filters outside their optimal temperature windows. Ideally, future tests should be run on a modern engine, equipped with a high pressure common rail fuel injection system (with injection flexibility) and turbocharger.

## LIST OF REFERENCES

2003. *Diglyme - U.S. EPA HPV Challenge Program* [Online]. Available: <http://www.epa.gov/hpv/pubs/summaries/diglyme/c15023.pdf> [Accessed November 2010].
- 2009a. *Euro 5 and Euro 6 standards: Reduction of pollutant emissions from light vehicles* [Online]. Available: [http://europa.eu/legislation\\_summaries/internal\\_market/single\\_market\\_for\\_goods/mot\\_or\\_vehicles/interactions\\_industry\\_policies/l28186\\_en.htm](http://europa.eu/legislation_summaries/internal_market/single_market_for_goods/mot_or_vehicles/interactions_industry_policies/l28186_en.htm) [Accessed November 2009].
- 2009b. *Euro 5 to Euro 6 standards* [Online]. Available: <http://www.euractiv.com/en/transport/euro-5-emissions-standards-cars/article-133325> [Accessed November 2009].
2010. *Fuel Regulations - European Union* [Online]. Available: <http://www.dieseln.net.com/standards/eu/fuel.php> [Accessed January 2011].
- EC 2009a. Amending Directive 98/70/EC as regards the specification of petrol, diesel and gas-oil and introducing a mechanism to monitor and reduce greenhouse gas emissions and amending Council Directive 1999/32/EC as regards the specification of fuel used by inland waterway vessels and repealing Directive 93/12/EEC. *Directive 2009/30/EC of the European Parliament and of the Council of 23 April 2009*. Official Journal of the European Union.
- EC 2009b. Setting emission performance standards for new light commercial vehicles as part of the Community's integrated approach to reduce CO<sub>2</sub> emissions from light-duty vehicles. *COM(2009) 593 Final*. Regulation of the European Parliament and of the Council.
- EC 2009c. Setting emission performance standards for new passenger cars as part of the Community's integrated approach to reduce CO<sub>2</sub> emissions from light-duty vehicles. *Regulation (EC) No. 443/2009 of the European Parliament and of the Council*. Official Journal of the European Union.
- RES 2009. Department of Energy and Climate Change - The Renewable Energy Strategy (RES). Department of Energy and Climate Change.
- ABD-ALLA, G. H. 2002. Using exhaust gas recirculation in internal combustion engines: a review. *Energy Conversion and Management*, 43, 1027-1042.
- ABU-JRAI, A., RODRÍGUEZ-FERNÁNDEZ, J., TSOLAKIS, A., MEGARITIS, A., THEINNOI, K., CRACKNELL, R. F. & CLARK, R. H. 2009. Performance, combustion and emissions of a diesel engine operated with reformed EGR. Comparison of diesel and GTL fuelling. *Fuel*, 88, 1031-1041.
- ABU-JRAI, A. & TSOLAKIS, A. 2007. The effect of H<sub>2</sub> and CO on the selective catalytic reduction of NO<sub>x</sub> under real diesel engine exhaust conditions over Pt/Al<sub>2</sub>O<sub>3</sub>. *International Journal of Hydrogen Energy*, 32, 2073 – 2080.

- ABU-JRAI, A., TSOLAKIS, A. & MEGARITIS, A. 2007. The influence of H<sub>2</sub> and CO on diesel engine combustion characteristics, exhaust gas emissions, and after treatment selective catalytic NO<sub>x</sub> reduction. *International Journal of Hydrogen Energy*, 32, 3565-3571.
- ABU-JRAI, A., TSOLAKIS, A., THEINNOI, K., CRACKNELL, R., MEGARITIS, A., WYSZYNSKI, M. L. & GOLUNSKI, S. E. 2006. Effect of Gas-to-Liquid Diesel Fuels on Combustion Characteristics, Engine Emissions, and Exhaust Gas Fuel Reforming. Comparative Study. *Energy & Fuels*, 20, 2377-2384.
- ABU-JRAI, A., TSOLAKIS, A., THEINNOI, K., MEGARITIS, A. & GOLUNSKI, S. E. 2008. Diesel exhaust-gas reforming for H<sub>2</sub> addition to an aftertreatment unit. *Chemical Engineering Journal*, 141, 290-297.
- AGARWAL, A. K. 2007. Biofuels (alcohols and biodiesel) applications as fuels for internal combustion engines. *Progress in Energy and Combustion Science*, 33, 233–271.
- AHMED, S. & KRUMPELT, M. 2001. Hydrogen from hydrocarbon fuels for fuel cells. *International Journal of Hydrogen Energy*, 26, 291-301.
- ALLANSSON, R., BLAKEMAN, P. G., COOPER, B. J., PHILLIPS, P. R., THOSS, J. E. & WALKER, A. P. 2002. The Use of the Continuously Regenerating Trap (CRT<sup>TM</sup>) to Control Particulate Emissions: Minimising the Impact of Sulfur Poisoning. *SAE Paper*
- ALLEMAN, T. L. & MCCORMICK, R. L. 2003. Fischer-Tropsch Diesel Fuels – Properties and Exhaust Emissions: A Literature Review. *SAE Paper*
- ARGACHOY, C. & PIMENTA, A. P. 2005. Phenomenological Model of Particulate Matter Emission from Direct Injection Diesel Engines. *Journal of the Brazilian Society of Mechanical Sciences and Engineering*, 27, 266-273.
- BABU, A. K. & DEVARADJANE, G. 2003. Vegetable Oils And Their Derivatives As Fuels For CI Engines: An Overview. *SAE Paper*
- BACKMAN, H., ARVE, K., KLINGSTEDT, F. & MURZIN, D. Y. 2006. Kinetic considerations of H<sub>2</sub> assisted hydrocarbon selective catalytic reduction of NO over Ag/Al<sub>2</sub>O<sub>3</sub>: II. Kinetic modelling. *Applied Catalysis A: General*, 304, 86-92.
- BAGLEY, S. T., GRATZ, L. D., JOHNSON, J. H. & MCDONALD, J. F. 1998. Effects of an Oxidation Catalytic Converter and a Biodiesel Fuel on the Chemical, Mutagenic, and Particle Size Characteristics of Emissions from a Diesel Engine. *Environmental Science & Technology*, 32, 1183-1191.
- BAUMGARTEN, C. 2006. *Mixture formation in internal combustion engines*, Springer.
- BEATRICE, C., BERTOLI, C., GIACOMO, N. D. & MIGLIACCIO, M. N. 1999. Potentiality of Oxygenated Synthetic Fuel and Reformulated Fuel on Emissions from a Modern DI Diesel Engine. *SAE Paper*
- BENSAID, S., MARCHISIO, D. L., RUSSO, N. & FINO, D. 2009. Experimental investigation of soot deposition in diesel particulate filters. *Catalysis Today*, 147, S295-S300.
- BIKA, A. S., FRANKLIN, L. M. & KITTELSON, D. B. 2008. Emissions Effects of Hydrogen as a Supplemental Fuel With Diesel and Biodiesel. *SAE Paper*

- BOEHMAN, A. L., MORRIS, D., SZYBIST, J. & ESEN, E. 2004. The Impact of the Bulk Modulus of Diesel Fuels on Fuel Injection Timing. *Energy & Fuels*, 18, 1877-1882.
- BOEHMAN, A. L., SONG, J. & ALAM, M. 2005. Impact of Biodiesel Blending on Diesel Soot and the Regeneration of Particulate Filters. *Energy & Fuels*, 19, 1857-1864.
- BOOT, M., FRIJTERS, P., LUIJTEN, C., SOMERS, B., BAERT, R., DONKERBROEK, A., KLEIN-DOUWEL, R. J. H. & DAM, N. 2008. Cyclic Oxygenates: A New Class of Second-Generation Biofuels for Diesel Engines? *Energy & Fuels*, 23, 1808-1817.
- BORMAN, G. L. & RAGLAND, K. W. 1998. *Combustion engineering*, McGraw-Hill.
- BOWMAN, C. T. 1975. Kinetics of pollutant formation and destruction in combustion. *Progress in Energy and Combustion Science*, 1, 33-45.
- BREEN, J. P., BURCH, R., HARDACRE, C. & HILL, C. J. 2005. Structural Investigation of the Promotional Effect of Hydrogen during the Selective Catalytic Reduction of NO<sub>x</sub> with Hydrocarbons over Ag/Al<sub>2</sub>O<sub>3</sub> Catalysts. *Journal of Physical Chemistry B*, 109, 4805-4807.
- BREEN, J. P., BURCH, R., HARDACRE, C., HILL, C. J. & RIOCHE, C. 2007. A fast transient kinetic study of the effect of H<sub>2</sub> on the selective catalytic reduction of NO<sub>x</sub> with octane using isotopically labelled <sup>15</sup>NO. *Journal of Catalysis*, 246, 1-9.
- BROGAN, M. S., CLARK, A. D. & BRISLEY, R. J. 1998. Recent Progress in NO<sub>x</sub> Trap Technology. *SAE Paper*
- BROSIUS, R., ARVE, K., GROOHAERT, M. H. & MARTENS, J. A. 2005. Adsorption chemistry of NO<sub>x</sub> on Ag/Al<sub>2</sub>O<sub>3</sub> catalyst for selective catalytic reduction of NO<sub>x</sub> using hydrocarbons. *Journal of Catalysis*, 231, 344-353.
- BURCH, R., BREEN, J., HILL, C., KRUTZSCH, B., KONRAD, B., JOBSON, E., CIDER, L., ERÄNEN, K., KLINGSTEDT, F. & LINDFORS, L. E. 2004. Exceptional activity for NO<sub>x</sub> reduction at low temperatures using combinations of hydrogen and higher hydrocarbons on Ag/Al<sub>2</sub>O<sub>3</sub> catalysts. *Topics in Catalysis*, 30-31, 19-25.
- CHANG, S. L. & RHEE, K. T. 1983. Computation of radiation heat transfer in diesel combustion. *SAE Paper*
- CHATTERJEE, S., WALKER, A. P. & BLAKEMAN, P. G. 2008. Emission Control Options to Achieve Euro IV and Euro V on Heavy-Duty Diesel Engines. *SAE Paper*
- CHENG, A. S., DIBBLE, R. W. & BUCHHOLZ, B. A. 2002. The effect of oxygenates on diesel engine particulate matter. *SAE Paper*
- CHENG, C. H., CHEUNG, C. S., CHAN, T. L., LEE, S. C., YAO, C. D. & TSANG, K. S. 2008. Comparison of emissions of a direct injection diesel engine operating on biodiesel with emulsified and fumigated methanol. *Fuel*, 87, 1870-1879.
- CHONG, J. J., TSOLAKIS, A., GILL, S. S., THEINNOI, K. & GOLUNSKI, S. E. 2010. Enhancing the NO<sub>2</sub>/NO<sub>x</sub> ratio in compression ignition engines by hydrogen and reformat combustion, for improved aftertreatment performance. *International Journal of Hydrogen Energy*, 35, 8723-8732.

- COOPER, B. J. & THOSS, J. E. 1989. Role of NO in Diesel Particulate Emission Control. *SAE Paper*
- DEC, J. E. 1997. A Conceptual Model of DI Diesel Combustion Based on Laser-Sheet Imaging. *SAE Paper*
- DI, Y., CHEUNG, C. S. & HUANG, Z. 2009. Experimental investigation on regulated and unregulated emissions of a diesel engine fueled with ultra-low sulfur diesel fuel blended with biodiesel from waste cooking oil. *Science of the Total Environment*, 407, 835-846.
- DI, Y., CHEUNG, C. S. & HUANG, Z. 2010. Experimental investigation of particulate emissions from a diesel engine fueled with ultralow-sulfur diesel fuel blended with diglyme. *Atmospheric Environment*, 44, 55-63.
- DIMAGGIO, C. L., FISHER, G. B., RAHMOELLER, K. M. & SELLNAU, M. 2009. Dual SCR Aftertreatment for Lean NO<sub>x</sub> Reduction. *SAE Paper*
- DRY, M. 2002. The Fischer–Tropsch process: 1950–2000. *Catalysis Today*, 71, 227-241
- DUIJM, N. J., MARKERT, F. & PAULSEN, J. L. 2005. Risø-R-1504(EN) - Safety assessment of ammonia as a transport fuel.
- EHRBURGER, P., BRILHAC, J. F., DROUILLOT, Y., LOGIE, V. & GILOT, P. 2002. Reactivity of Soot With Nitrogen Oxides in Exhaust Stream. *SAE Paper*
- EPLING, W. S., CAMPBELL, L. E., YEZERETS, A., CURRIER, N. W. & PARKS, J. E. 2004. Overview of the Fundamental Reactions and Degradation Mechanisms of NO<sub>x</sub> Storage/Reduction Catalysts. *Catalysis Reviews*, 46, 163-245.
- ERÄNEN, K., KLINGSTEDT, F., ARVE, K., LINDFORS, L.-E. & MURZIN, D. Y. 2004. On the mechanism of the selective catalytic reduction of NO with higher hydrocarbons over a silver/alumina catalyst. *Journal of Catalysis*, 227, 328-343.
- ERÄNEN, K., LINDFORS, L.-E., KLINGSTEDT, F. & MURZIN, D. Y. 2003. Continuous reduction of NO with octane over a silver/alumina catalyst in oxygen-rich exhaust gases: combined heterogeneous and surface-mediated homogeneous reactions. *Journal of Catalysis*, 219, 25-40.
- EU 2006. Well-to-Wheels analysis of future automotive fuels and power-trains in the European context, Well-to-Wheels Report Version 2b. EUCAR, CONCAWE and JRC (The Joint Research Centre of the EU Commission).
- FALESCHINI, G., HACKER, V., MUHR, M., KORDESCH, K. & ARONSSON, R. R. 2000. Ammonia for High Density Hydrogen Storage. *Fuel Cell Seminar Abstracts*, 336-339.
- FARIAS, T. L., CARVALHO, M. G. & KÖYLÜ, Ü. Ö. 1998. Radiative heat transfer in soot-containing combustion systems with aggregation. *International Journal of Heat and Mass Transfer*, 41, 2581-2587.
- FARRAUTO, R. J. & VOSS, K. E. 1996. Monolithic diesel oxidation catalysts. *Applied Catalysis B: Environmental*, 10, 29-51.

- FUKUSHIMA, H., ASANO, I., NAKAMURA, S., ISHIDA, K. & GREGORY, D. 2000. Signal Processing and Practical Performance of a Real-Time PM Analyzer Using Fast FIDs. *SAE Paper*
- GANESAN, V. 2008. *Internal combustion engines*, McGraw-Hill Education (India) Pvt Ltd.
- GANG, L., ANDERSON, B. G., VAN GRONDELLE, J. & VAN SANTEN, R. A. 2001. Intermediate Species and Reaction Pathways for the Oxidation of Ammonia on Powdered Catalysts. *Journal of Catalysis*, 199, 107-114.
- GILL, L. J., BLAKEMAN, P. G., TWIGG, M. V. & WALKER, A. P. 2004. The Use of NO<sub>x</sub> Adsorber Catalysts on Diesel Engines. *Topics in Catalysis*, 28, 157-164.
- GILL, S. S., CHATHA, G. S. & TSOLAKIS, A. 2011a. Analysis of reformed EGR on the performance of a diesel particulate filter. *International Journal of Hydrogen Energy*, 36, 10089-10099.
- GILL, S. S., TSOLAKIS, A., DEARN, K. D. & RODRÍGUEZ-FERNÁNDEZ, J. 2011b. Combustion characteristics and emissions of Fischer-Tropsch diesel fuels in IC engines. *Progress in Energy and Combustion Science*, 37, 503-523.
- GLAUDE, P.-A., FOURNET, R., BOUNACEUR, R. & MOLIÈRE, M. 2010. Adiabatic flame temperature from biofuels and fossil fuels and derived effect on NO<sub>x</sub> emissions. *Fuel Processing Technology*, 91, 229-235.
- GRABOSKI, M. S. & MCCORMICK, R. L. 1998. Combustion of fat and vegetable oil derived fuels in diesel engines. *Progress in Energy and Combustion Science*, 24, 125-164.
- GRASKOW, B. R., KITTELSON, D. B., ABDUL-KHALEK, I. S., AHMADI, M. R. & MORRIS, J. E. 1998. Characterization of exhaust particulate emissions from a spark-ignition engine. *SAE Paper*
- GRAY, J. T., DIMITROFF, E., MECKEL, N. T. & QUILLIUM, J. R. D. 1966. Ammonia Fuel - Engine Compatibility and Combustion. *SAE Paper*
- HALL-ROBERTS, V. J., HAYHURST, A. N., KNIGHT, D. E. & TAYLOR, S. G. 2000. The origin of soot in flames: is the nucleus an ion? *Combustion and Flame*, 120, 578-584.
- HARGEAVES, K. J. A., HARVEY, R., ROPER, F. G. & SMITH, D. B. 1981. Formation of NO<sub>2</sub> by laminar flames. *Symposium (International) on Combustion* 18, 133-142.
- HEYWOOD, J. B. 1988. *Internal combustion engine fundamentals*, Mc Graw-Hill.
- HÖÖK, M. & ALEKLETT, K. 2009. A review on coal-to-liquid fuels and its coal consumption. *International Journal of Energy Research*.
- HORI, M. 1988. Experimental study of nitrogen dioxide formation in combustion systems. *Symposium (International) on Combustion*, 21, 1181-1188.
- HORI, M., KOSHIISHI, Y., MATSUNAGA, N., GLAUDE, P. & MARINOV, N. 2002. Temperature dependence of NO to NO<sub>2</sub> conversion by n-butane and n-pentane oxidation. *Proceedings of the Combustion Institute*, 29, 2219-2226.

- HOUEL, V., MILLINGTON, P., RAJARAM, R. & TSOLAKIS, A. 2007a. Fuel effects on the activity of silver hydrocarbon-SCR catalysts. *Applied Catalysis B: Environmental*, 73, 203-207.
- HOUEL, V., MILLINGTON, P., RAJARAM, R. & TSOLAKIS, A. 2007b. Promoting functions of H<sub>2</sub> in diesel-SCR over silver catalysts. *Applied Catalysis B: Environmental*, 77, 29-34.
- HU, E., HUANG, Z., LIU, B., ZHENG, J. & GU, X. 2009. Experimental study on combustion characteristics of a spark-ignition engine fueled with natural gas-hydrogen blends combining with EGR. *International Journal of Hydrogen Energy*, 34, 1035-1044.
- ILIOPOULOU, E. F., EVDUO, A. P., LEMONIDOU, A. A. & VASALOS, I. A. 2004. Ag/alumina catalysts for the selective catalytic reduction of NO<sub>x</sub> using various reductants. *Applied Catalysis A: General*, 274, 179-189.
- INFINEUM. 2012. *Fuel Additives* [Online]. Available: <http://www.infineum.com/Pages/fuel.aspx> [Accessed 2012].
- JEGUIRIM, M., TSCHAMBER, V., BRILHAC, J. F. & EHRBURGER, P. 2005. Oxidation mechanism of carbon black by NO<sub>2</sub>: Effect of water vapour. *Fuel*, 84, 1949-1956.
- JELLES, S. J., MAKKEE, M. & MOULIJN, J. A. 2001. Ultra Low Dosage of Platinum and Cerium Fuel Additives in Diesel Particulate Control. *Topics in Catalysis*, 16-17, 269-273.
- JOHANSEN, K., DAHL, S., MOGENSEN, G., PEHRSON, S., SCHRAMM, J. & IVARSSON, A. 2007. Novel base metal-palladium catalytic diesel filter coating with NO<sub>2</sub> reducing properties. *SAE Paper*
- JOHNSON, T. 2008. Diesel Engine Emissions and Their Control. 53.
- JOHNSON, T. V. 2012. SAE 2011 World Congress - Vehicular emissions control highlights of the annual Society of Automotive Engineers (SAE) international congress. *Platinum Metals Review*, 56, 75-82.
- JORGENSEN, W. L. & IBRAHIM, M. 1980. Structure and properties of liquid ammonia. *Journal of the American Chemical Society*, 102, 3309-3315.
- JUNG, H., KITTELSON, D. B. & ZACHARIAH, M. R. 2006. Characteristics of SME Biodiesel-Fueled Diesel Particle Emissions and the Kinetics of Oxidation. *Environmental Science & Technology*, 40, 4949-4955.
- KAMIMOTO, T. & BAE, M.-H. 1988. High Combustion Temperature for the Reduction of Particulate in Diesel Engines. *SAE Paper*
- KANNISTO, H., INGELSTEN, H. H. & SKOGLUNDH, M. 2009. Aspects of the Role of Hydrogen in H<sub>2</sub>-Assisted HC-SCR Over Ag-Al<sub>2</sub>O<sub>3</sub>. *Topics in Catalysis*, 52, 1817-1820.
- KASPER, M., SATTLER, K., SIEGMANN, K., MATTER, U. & SIEGMANN, H. C. 1999. The influence of fuel additives on the formation of carbon during combustion. *Journal of Aerosol Science*, 30, 217-225.

- KASS, M., THOMAS, J., LEWIS, S., STOREY, J., DOMINGO, N., GRAVES, R. & PANOV, A. 2003. Selective catalytic reduction of diesel engine NO<sub>x</sub> emissions using ethanol as a reductant. Oak Ridge National Laboratory and Caterpillar, Inc.
- KATARE, S. R. & LAING, P. M. 2009. Hydrogen in Diesel Exhaust: Effect on Diesel Oxidation Catalyst Flow Reactor Experiments and Model Predictions. *SAE Paper*
- KENNEDY, I. M. 1997. Models of soot formation and oxidation. *Progress in Energy and Combustion Science*, 23, 95-132.
- KESKIN, A., GÜRÜB, M. & ALTIPARMAK, D. 2011. Influence of metallic based fuel additives on performance and exhaust emissions of diesel engine. *Energy Conversion and Management*, 52, 60-65.
- KIDOGUCHI, Y., YANG, C. & MIWA, K. 2000. Effects of fuel properties on combustion and emission characteristics of a direct-injection diesel engine. *SAE Paper*
- KIM, H.-J., KANG, B.-S., KIM, M.-J., PARK, Y. M., KIM, D.-K., LEE, J.-S. & LEE, K.-Y. 2004. Transesterification of vegetable oil to biodiesel using heterogeneous base catalyst. *Catalysis Today*, 93-95, 315-320.
- KIM, M. H., NAM, I.-S. & SPIVEY, J. J. 2005. New opportunity for HC-SCR technology to control NO<sub>x</sub> emission from advanced internal combustion engines. *Catalysis*. The Royal Society of Chemistry.
- KITAMURA, T., ITO, T., SENDA, J. & FUJIMOTO, H. 2002. Mechanism of smokeless diesel combustion with oxygenated fuels based on the dependence of the equivalence ration and temperature on soot particle formation. *International Journal of Engine Research*, 3, 223-248.
- KITANO, K., MISAWA, S., MORI, M., SAKATA, I. & CLARK, R. H. 2007. GTL Fuel Impact on DI Diesel Emissions. *SAE Paper*
- KITANO, K., SAKATA, I. & CLARK, R. 2005. Effects of GTL Fuel Properties on DI Diesel Combustion. *SAE Paper*
- KITTELSON, D. B. 1998. Engines and nanoparticles: a review. *Journal of Aerosol Science*, 29, 575-588.
- KLEIN, H., LOX, E., KREUZER, T., KAWANAMI, M., RIED, T. & BÄCHMANN, K. 1998. Diesel Particulate Emissions of Passenger Cars - New Insights into Structural Changes During the Process of Exhaust Aftertreatment Using Diesel Oxidation Catalysts. *SAE Paper*
- KLERKE, A., CHRISTENSEN, C. H., NØRSKOV, J. K. & VEGGE, T. 2008. Ammonia for hydrogen storage: challenges and opportunities. *Journal of Materials Chemistry*, 18, 2304-2310.
- KNOTHE, G., SHARP, C. A. & RYAN, T. W. 2005. Exhaust Emissions of Biodiesel, Petrodiesel, Neat Methyl Esters, and Alkanes in a New Technology Engine *Energy & Fuels*, 20, 403-408.
- KOEBEL, M., ELSENER, M. & KLEEMANN, M. 2000. Urea-SCR: a promising technique to reduce NO<sub>x</sub> emissions from automotive diesel engines. *Catalysis Today*, 59, 335-345.

- KONDRATENKO, E. V., KONDRATENKO, V. A., RICHTER, M. & FRICKE, R. 2006. Influence of O<sub>2</sub> and H<sub>2</sub> on NO reduction by NH<sub>3</sub> over Ag/Al<sub>2</sub>O<sub>3</sub>: A transient isotopic approach. *Journal of Catalysis*, 239, 23-33.
- KRAHL, J., MUNACK, A., SCHRÖDER, O., STEIN, H. & BÜNGER, J. 2003. Influence of biodiesel and different designed diesel fuels on the exhaust gas emissions and health effects. *SAE Paper*
- KROCH, E. 1945. Ammonia - A Fuel for Motor Buses. *Journal of the Institute of Petroleum*, 31, 213-223.
- LADOMMATOS, N., ABDELHALIM, S. & ZHAO, H. 2000. The effects of exhaust gas recirculation on diesel combustion and emissions. *International Journal of Engine Research*, 1, 107-126.
- LADOMMATOS, N., ABDELHALIM, S. M., ZHAO, H. & HU, Z. 1996a. The Dilution, Chemical, and Thermal Effects of Exhaust Gas Recirculation on Diesel Engine Emissions - Part 2: Effects of Carbon Dioxide. *SAE Paper*
- LADOMMATOS, N., ABDELHALIM, S. M., ZHAO, H. & HU, Z. 1998. The effects of carbon dioxide in exhaust gas recirculation on diesel engine emissions *Proceedings of the Institution of Mechanical Engineers - Part D: Journal of Automobile Engineering*, 212, 25-42.
- LAMBERT, C., HAMMERLE, R., MCGILL, R., KHAIR, M. & SHARP, C. 2004. Technical Advantages of Urea SCR for Light-Duty and Heavy-Duty Diesel Vehicle Applications. *SAE Paper*
- LAPUERTA, M., ARMAS, O. & GÓMEZ, A. 2003. Diesel Particle Size Distribution Estimation from Digital Image Analysis. *Aerosol Science and Technology*, 37, 369 - 381.
- LAPUERTA, M., ARMAS, O. & RODRÍGUEZ-FERNÁNDEZ, J. 2008a. Effect of biodiesel fuels on diesel engine emissions. *Progress in Energy and Combustion Science*, 34, 198-223.
- LAPUERTA, M., BALLESTEROS, R. & RODRÍGUEZ-FERNÁNDEZ, J. 2007. Thermogravimetric analysis of diesel particulate matter. *Measurement Science and Technology*, 18, 650-658.
- LAPUERTA, M., HERREROS, J. M., LYONS, L. L., GARCÍA-CONTRERAS, R. & BRICEÑO, Y. 2008b. Effect of the alcohol type used in the production of waste cooking oil biodiesel on diesel performance and emissions. *Fuel*, 87, 3161-3169.
- LAPUERTA, M. N., ARMAS, O. & GARCÍA-CONTRERAS, R. 2009. Effect of Ethanol on Blending Stability and Diesel Engine Emissions. *Energy & Fuels*, 23, 4343-4354.
- LARSSON, M. & DENBRATT, I. 2007. An Experimental Investigation of Fischer-Tropsch Fuels in a Light-Duty Diesel Engine. *SAE Paper*
- LAVOIE, G. A., HEYWOOD, J. B. & KECK, J. C. 1970. Experimental and Theoretical Study of Nitric Oxide Formation in Internal Combustion Engines. *Combustion Science and Technology* 1, 313-326.

- LAWRENCE, C. 2006. *Biomass Research and Development: Department of Defence Seeks to Explore the Use of Biofuels* [Online]. Available: <http://www.brdisolutions.com/web%20pages/News%20Center/Feature%20Articles/December%202006.aspx> [Accessed 2011].
- LECKEL, D. 2009. Diesel Production from Fischer-Tropsch: The Past, the Present, and New Concepts. *Energy & Fuels*, 23, 2342-2358.
- LEE, S. J., YI, H. S. & KIM, E. S. 1995. Combustion characteristics of intake port injection type hydrogen fueled engine. *International Journal of Hydrogen Energy*, 20, 317-322.
- LEUNG, P., TSOLAKIS, A., WYSZYNSKI, M. L., RODRÍGUEZ-FERNÁNDEZ, J. & MEGARITIS, A. 2009. Performance, Emissions and Exhaust-Gas Reforming of an Emulsified Fuel: A Comparative Study with Conventional Diesel Fuel. *SAE Paper*
- LEVENDIS, Y., PAVLATOS, I. & ABRAMS, R. 1994. Control of Diesel Soot, Hydrocarbon and NO<sub>x</sub> Emissions with a Particulate Trap and EGR. *SAE Paper*
- LEWIS, B. & VON ELBE, G. 1961. *Combustion, flames and explosions of gases*, Academic Press.
- LIEW, C., LI, H., NUSZKOWSKI, J., LIU, S., GATTS, T., ATKINSON, R. & CLARK, N. 2010. An experimental investigation of the combustion process of a heavy-duty diesel engine enriched with H<sub>2</sub>. *International Journal of Hydrogen Energy*, 35, 11357-11365.
- LILIK, G. K., ZHANG, H., HERREROS, J. M., HAWORTH, D. C. & BOEHMAN, A. L. 2010. Hydrogen assisted diesel combustion. *International Journal of Hydrogen Energy*, 35, 4382-4398.
- LINDFORS, L. E., ERÄNEN, K., KLINGSTEDT, F. & MURZIN, D. Y. 2004. Silver/alumina catalyst for selective catalytic reduction of NO<sub>x</sub> to N<sub>2</sub> by hydrocarbons in diesel powered vehicles. *Topics in Catalysis*, 28, 185-189.
- MAJEWSKI, W. A. Revised 2010.04. *Diesel Oxidation Catalyst* [Online]. DieselNet. Available: [www.DieselNet.com](http://www.DieselNet.com) [Accessed 7th November 2010].
- MAJEWSKI, W. A. & KHAIR, M. K. 2006. *Diesel emissions and their control*, SAE International.
- MARCHAL, C., DELFAU, J.-L., VOVELLE, C., MORÉAC, G., MOUNAÏM-ROUSSELLE, C. & MAUSS, F. 2009. Modelling of aromatics and soot formation from large fuel molecules. *Proceedings of the Combustion Institute*, 32, 753-759.
- MARCHETTI, A. A., KNIZE, M. G., CHIARAPPA-ZUCCA, M. L., PLETCHER, R. J. & LAYTON, D. W. 2003. Biodegradation of potential diesel oxygenate additives: dibutyl maleate (DBM), and tripropylene glycol methyl ether (TGME). *Chemosphere*, 52, 861-868.
- MARTIROSYAN, K. S., CHEN, K. & LUSS, D. 2010. Behavior features of soot combustion in diesel particulate filter. *Chemical Engineering Science*, 65, 42-46.
- MASUDA, K., TSUJIMURA, K., SHINODA, K. & KATO, T. 1996. Silver-promoted catalyst for removal of nitrogen oxides from emission of diesel engines. *Applied Catalysis B: Environmental*, 8, 33-40.

- MATHIS, U., MOHR, M., KAEGI, R., BERTOLA, A. & BOULOUCHOS, K. 2005. Influence of Diesel Engine Combustion Parameters on Primary Soot Particle Diameter. *Environmental Science & Technology*, 39, 1887-1892.
- MATTI MARICQ, M. 2007. Chemical characterization of particulate emissions from diesel engines: A review. *Journal of Aerosol Science*, 38, 1079-1118.
- MCGEEHAN, J. A., YEH, S., COUCH, M., HINZ, A., OTTERHOLM, B., WALKER, A. P. & BLAKEMAN, P. G. 2005. On the Road to 2010 Emissions: Field Test Results and Analysis with DPF-SCR System and Ultra Low Sulfur Diesel Fuel. *SAE Paper*
- MCMILLIAN, M. H. & GAUTAM, M. 2001. Combustion and Emission Characteristics of Fischer-Tropsch and Standard Diesel Fuel in a Single - Cylinder Diesel Engine. *SAE Paper*
- MEUNIER, F. C., ZUZANIUK, V., BREEN, J. P., OLSSON, M. & ROSS, J. R. H. 2000. Mechanistic differences in the selective reduction of NO by propene over cobalt- and silver-promoted alumina catalysts: kinetic and in situ DRIFTS study. *Catalysis Today*, 59, 287-304.
- MIYAMOTO, N., HOU, Z., HARADA, A., OGAWA, H. & MURAYAMA, T. 1987. Characteristics of Diesel Soot Suppression with Soluble Fuel Additives. *SAE Paper*
- MIYAMOTO, N., OGAWA, H., NURUN, N. M., OBATA, K. & ARIMA, T. 1998. Smokeless, low NO<sub>x</sub>, high thermal efficiency, and low noise diesel combustion with oxygenated agents as main fuel. *SAE Paper*
- MONYEM, A. & H. VAN GERPEN, J. 2001. The effect of biodiesel oxidation on engine performance and emissions. *Biomass and Bioenergy*, 20, 317-325.
- MUELLER, C. J., PITZ, W. J., PICKETT, L. M., MARTIN, G. C., SIEBERS, D. L. & WESTBROOK, C. K. 2003. Effects of oxygenates on soot processes in DI diesel engines: Experiments and numerical simulations. *SAE Paper*
- MURPHY, M. J., TAYLOR, J. D. & MCCORMICK, R. L. 2004. Compendium of Experimental Cetane Number Data. National Renewable Energy Laboratory.
- NEEFT, J. P. A., VAN PRUISSSEN, O. P., MAKKEE, M. & MOULIJN, J. A. 1997. Catalysts for the oxidation of soot from diesel exhaust gases II. Contact between soot and catalyst under practical conditions. *Applied Catalysis B: Environmental*, 12, 21-31.
- NICKOLAS, S. G., WHITE, A. D., KOTRBA, A. J. & YETKIN, A. 2006. Engine Tests of an Active Diesel Particulate Filter Regeneration System. *SAE Paper*
- NIGAM, P. S. & SINGH, A. 2010. Production of liquid biofuels from renewable resources. *Progress in Energy and Combustion Science*, 37, 52-68.
- NILSSON, M., KARATZAS, X., LINDSTRÖM, B. & PETTERSSON, L. J. 2008. Assessing the adaptability to varying fuel supply of an autothermal reformer. *Chemical Engineering Journal*, 142, 309-317.
- NISHIUMI, R., YASUDA, A., TSUKASAKI, Y. & TANAKA, T. 2004. Effects of Cetane Number and Distillation Characteristics of Paraffinic Diesel Fuels on PM Emission from a DI Diesel Engine. *SAE Paper*

- PEARSALL, T. J. & GARABEDIAN, C. G. 1967. Combustion of Anhydrous Ammonia in Diesel Engines. *SAE Paper*
- PICKETT, L. M., CATON, J. A., MUSCULUS, M. P. B. & LUTZ, A. E. 2006. Evaluation of the equivalence ratio-temperature region of diesel soot precursor formation using a two-stage Lagrangian model. *International Journal of Engine Research*, 7, 349-370.
- PSARAS, D., SUMMERS, J. C., DAS, P. K., CEYNOW, K., KHAIR, M. K. & DISILVERIO, W. D. 1997. Achieving the 2004 Heavy-Duty Diesel Emissions Using Electronic EGR and a Cerium Based Fuel Borne Catalyst. *SAE Paper*
- PUNDIR, B. P. & KUMAR, R. 2007. Combustion and Smoke Emission Studies on a Hydrogen Fuel-Supplemented DI Diesel Engine. *SAE Paper*
- REITER, A. J. & KONG, S.-C. 2008. Demonstration of Compression-Ignition Engine Combustion Using Ammonia in Reducing Greenhouse Gas Emissions. *Energy & Fuels*, 22, 2963-2971.
- REITER, A. J. & KONG, S.-C. 2011. Combustion and emissions characteristics of compression-ignition engine using dual ammonia-diesel fuel. *Fuel*, 90, 87-97.
- REN, Y., HUANG, Z., MIAO, H., DI, Y., JIANG, D., ZENG, K., LIU, B. & WANG, X. 2008. Combustion and emissions of a DI diesel engine fuelled with diesel-oxygenate blends. *Fuel*, 87, 2691-2697.
- RIBEIRO, N. M., PINTO, A. C., QUINTELLA, C. M., DA ROCHA, G. O., TEIXEIRA, L. S. G., GUARIEIRO, L. L. N., DO CARMO RANGEL, M., VELOSO, M. C. C., REZENDE, M. J. C., SERPA DA CRUZ, R., DE OLIVEIRA, A. M., TORRES, E. A. & DE ANDRADE, J. B. 2007. The Role of Additives for Diesel and Diesel Blended (Ethanol or Biodiesel) Fuels: A Review. *Energy & Fuels*, 21, 2433-2445.
- RICHTER, H. & HOWARD, J. B. 2000. Formation of polycyclic aromatic hydrocarbons and their growth to soot - a review of chemical reaction pathways. *Progress in Energy and Combustion Science*, 26, 565-608.
- RICHTER, M., BENTRUP, U., ECKELT, R., SCHNEIDER, M., POHL, M. M. & FRICKE, R. 2004a. The effect of hydrogen on the selective catalytic reduction of NO in excess oxygen over Ag/Al<sub>2</sub>O<sub>3</sub>. *Applied Catalysis B: Environmental*, 51, 261-274.
- RICHTER, M., FRICKE, R. & ECKELT, R. 2004b. Unusual Activity Enhancement of NO Conversion over Ag/Al<sub>2</sub>O<sub>3</sub> by Using a Mixed NH<sub>3</sub>/H<sub>2</sub> Reductant Under Lean Conditions *Catalysis Letters*, 94, 115-118.
- RISTOVSKI, Z. D., MORAWSKA, L., HITCHINS, J., THOMAS, S., GREENAWAY, C. & GILBERT, D. 2000. Particle emissions from compressed natural gas engines. *Journal of Aerosol Science*, 31, 403-413.
- RODRÍGUEZ-FERNÁNDEZ, J., TSOLAKIS, A., AHMADINEJAD, M. & SITSHEBO, S. 2009a. Investigation of the Deactivation of a NO<sub>x</sub>-Reducing Hydrocarbon-Selective Catalytic Reduction (HC-SCR) Catalyst by Thermogravimetric Analysis: Effect of the Fuel and Prototype Catalyst. *Energy & Fuels*, 24, 992-1000.
- RODRÍGUEZ-FERNÁNDEZ, J., TSOLAKIS, A., CRACKNELL, R. F. & CLARK, R. H. 2009b. Combining GTL fuel, reformed EGR and HC-SCR after treatment system to

- reduce diesel NO<sub>x</sub> emissions. A statistical approach. *International Journal of Hydrogen Energy*, 34, 2789-2799.
- ROESLER, J. F., MARTINOT, S., MCENALLY, C. S., PFEFFERLE, L. D., DELFAU, J. L. & VOVELLE, C. 2003. Investigating the role of methane on the growth of aromatic hydrocarbons and soot in fundamental combustion processes. *Combustion and Flame*, 134, 249-260.
- ROLLINSON, A. N., JONES, J., DUPONT, V. & TWIGG, M. V. 2011. Urea as a hydrogen carrier: a perspective on its potential for safe, sustainable and long-term energy supply. *Energy & Environmental Science*, 4, 1216-1224.
- ROSTRUP-NIELSEN, J. R. 1993. Production of synthesis gas. *Catalysis Today*, 18, 305-324.
- ROSTRUP-NIELSEN, J. R. 1997. Industrial relevance of coking. *Catalysis Today*, 37, 225-232.
- ROSTRUP-NIELSEN, J. R., CHRISTENSEN, T. S., DYBKJAER, I., RAO, T. S. R. P. & DHAR, G. M. 1998. Steam reforming of liquid hydrocarbons. *Studies in Surface Science and Catalysis*. Elsevier.
- ROUNCE, P., TSOLAKIS, A., RODRÍGUEZ-FERNÁNDEZ, J., YORK, A. P. E., CRACKNELL, R. F. & CLARK, R. H. 2009. Diesel Engine Performance and Emissions when First Generation Meets Next Generation Biodiesel. *SAE Paper*
- SAIKA, T., NAKAMURA, M., NOHARA, T. & ISHIMATSU, S. 2006. Study of hydrogen supply system with ammonia fuel. *JSME International Journal Series B*, 49, 78-83.
- SARAVANAN, N. & NAGARAJAN, G. 2010. Performance and emission studies on port injection of hydrogen with varied flow rates with Diesel as an ignition source. *Applied Energy*, 87, 2218-2229.
- SATOKAWA, S., SHIBATA, J., SHIMIZU, K.-I., SATSUMA, A. & HATTORI, T. 2003. Promotion effect of H<sub>2</sub> on the low temperature activity of the selective reduction of NO by light hydrocarbons over Ag/Al<sub>2</sub>O<sub>3</sub>. *Applied Catalysis B: Environmental*, 42, 179-186.
- SAZAMA, P., ČAPEK, L., DROBNÁ, H., SOBALÍK, Z., DĚDEČEK, J., ARVE, K. & WICHTERLOVÁ, B. 2005. Enhancement of decane-SCR-NO<sub>x</sub> over Ag/alumina by hydrogen. Reaction kinetics and in situ FTIR and UV-vis study. *Journal of Catalysis*, 232, 302-317.
- SCHEJBAL, M., STEPÁNEK, J., MAREK, M., KOCÍ, P. & KUBÍČEK, M. 2010. Modelling of soot oxidation by NO<sub>2</sub> in various types of diesel particulate filters. *Fuel*, 89, 2365-2375.
- SCHENK, C., MCDONALD, J. & OLSON, B. 2001. High-Efficiency NO<sub>x</sub> and PM Exhaust Emission Control for Heavy-Duty On-Highway Diesel Engines. *SAE Paper*
- SCHMIEG, S. J., BLINT, R. J. & DENG, L. 2008. Control Strategy for the Removal of NO<sub>x</sub> from Diesel Engine Exhaust using Hydrocarbon Selective Catalytic Reduction. *SAE Paper*
- SCHRÖDER, O., KRAHL, J., MUNACK, A., KRAHL, J. & BÜNGER, J. 1999. Environmental and health effects caused by the use of biodiesel. *SAE Paper*

- SHIBATA, J., SHIMIZU, K.-I., SATSUMA, A. & HATTORI, T. 2002. Influence of hydrocarbon structure on selective catalytic reduction of NO by hydrocarbons over Cu-Al<sub>2</sub>O<sub>3</sub>. *Applied Catalysis B: Environmental*, 37, 197-204.
- SHIBATA, J., SHIMIZU, K.-I., TAKADA, Y., SHICHI, A., YOSHIDA, H., SATOKAWA, S., SATSUMA, A. & HATTORI, T. 2004a. Structure of active Ag clusters in Ag zeolites for SCR of NO by propane in the presence of hydrogen. *Journal of Catalysis*, 227, 367-374.
- SHIBATA, J., TAKADA, Y., SHICHI, A., SATOKAWA, S., SATSUMA, A. & HATTORI, T. 2004b. Ag cluster as active species for SCR of NO by propane in the presence of hydrogen over Ag-MFI. *Journal of Catalysis*, 222, 368-376.
- SHIMIZU, K.-I. & SATSUMA, A. 2007. Reaction Mechanism of H<sub>2</sub>-Promoted Selective Catalytic Reduction of NO with NH<sub>3</sub> over Ag/Al<sub>2</sub>O<sub>3</sub>. *Journal of Physical Chemistry C*, 111, 2259-2264.
- SHIMIZU, K.-I., SATSUMA, A. & HATTORI, T. 2000. Catalytic performance of Ag-Al<sub>2</sub>O<sub>3</sub> catalyst for the selective catalytic reduction of NO by higher hydrocarbons. *Applied Catalysis B: Environmental*, 25, 239-247.
- SHIMIZU, K.-I., SHIBATA, J., YOSHIDA, H., SATSUMA, A. & HATTORI, T. 2001. Silver-alumina catalysts for selective reduction of NO by higher hydrocarbons: structure of active sites and reaction mechanism. *Applied Catalysis B: Environmental*, 30, 151-162.
- SHIMIZU, K.-I., TSUZUKI, M., KATO, K., YOKOTA, S., OKUMURA, K. & SATSUMA, A. 2007. Reductive Activation of O<sub>2</sub> with H<sub>2</sub>-Reduced Silver Clusters as a Key Step in the H<sub>2</sub>-Promoted Selective Catalytic Reduction of NO with C<sub>3</sub>H<sub>8</sub> over Ag/Al<sub>2</sub>O<sub>3</sub>. *Journal of Physical Chemistry C*, 111, 950-959.
- SHIN, B., CHO, Y., HAN, D., SONG, S. & CHUN, K. M. 2011. Hydrogen effects on NO<sub>x</sub> emissions and brake thermal efficiency in a diesel engine under low-temperature and heavy-EGR conditions. *International Journal of Hydrogen Energy*, 36, 6281-6291.
- SHUDO, T. 2007. Improving thermal efficiency by reducing cooling losses in hydrogen combustion engines. *International Journal of Hydrogen Energy*, 32, 4285-4293.
- SHUDO, T., NSBETANI, S. & NAKAJIMA, Y. 2001. Analysis of the degree of constant volume and cooling loss in a spark ignition engine fuelled with hydrogen. *International Journal of Engine Research*, 2, 81-92.
- SITSHEBO, S., TSOLAKIS, A. & THEINNOI, K. 2009. Promoting hydrocarbon-SCR of NO<sub>x</sub> in diesel engine exhaust by hydrogen and fuel reforming. *International Journal of Hydrogen Energy*, 34, 7842-7850.
- SOLTIC, P. & WEILENMANN, M. 2003. NO<sub>2</sub>/NO emissions of gasoline passenger cars and light-duty trucks with Euro-2 emission standard. *Atmospheric Environment*, 37, 5207-5216.
- SONG, J., ALAM, M., BOEHMAN, A. L. & KIM, U. 2006. Examination of the oxidation behavior of biodiesel soot. *Combustion and Flame*, 146, 589-604.

- SONG, J., CHEENKACHORN, K., WANG, J., PEREZ, J., BOEHMAN, A. L., YOUNG, P. J. & WALLER, F. J. 2002. Effect of Oxygenated Fuel on Combustion and Emissions in a Light-Duty Turbo Diesel Engine. *Energy & Fuels*, 16, 294-301.
- SONG, J., ZELLO, V., BOEHMAN, A. L. & WALLER, F. J. 2004. Comparison of the Impact of Intake Oxygen Enrichment and Fuel Oxygenation on Diesel Combustion and Emissions. *Energy & Fuels*, 18, 1282-1290.
- STANMORE, B. R., BRILHAC, J. F. & GILOT, P. 2001. The oxidation of soot: a review of experiments, mechanisms and models. *Carbon*, 39, 2247-2268.
- STONE, R. 1999. *Introduction to internal combustion engines*, Macmillan.
- SUPPES, G. J., GOFF, M., BURKHART, M. L., BOCKWINKEL, K., MASON, M. H., BOTTS, J. B. & HEPPERT, J. A. 2000. Multifunctional Diesel Fuel Additives from Triglycerides. *Energy & Fuels*, 15, 151-157.
- SURESH, A., JOHNSON, J. H., BAGLEY, S. T. & LEDDY, D. G. 2001. A Study of the Effect of a Catalyzed Particulate Filter on the Emissions from a Heavy-Duty Diesel Engine with EGR. *SAE Paper*
- SZWAJA, S. & GRAB-ROGALINSKI, K. 2009. Hydrogen combustion in a compression ignition diesel engine. *International Journal of Hydrogen Energy*, 34, 4413-4421.
- SZYBIST, J. P. & BOEHMAN, A. L. 2003. Behavior of a diesel injection system with biodiesel fuel. *SAE Paper*
- SZYBIST, J. P., KIRBY, S. R. & BOEHMAN, A. L. 2005. NO<sub>x</sub> Emissions of Alternative Diesel Fuels: A Comparative Analysis of Biodiesel and FT Diesel. *Energy & Fuels*, 19, 1484-1492.
- TAN, P. Q., HU, Z. Y., DENG, K. Y., LU, J. X., LOU, D. M. & WAN, G. 2007. Particulate matter emission modelling based on soot and SOF from direct injection diesel engines. *Energy Conversion and Management*, 48, 510-518.
- THEINNOI, K., SITSHEBO, S., HOUEL, V., RAJARAM, R. R. & TSOLAKIS, A. 2008. Hydrogen Promotion of Low-Temperature Passive Hydrocarbon-Selective Catalytic Reduction (SCR) over a Silver Catalyst. *Energy & Fuels*, 22, 4109-4114.
- THEINNOI, K., TSOLAKIS, A., HOUEL, V. & RAJARAM, R. R. 2007. Passive NO<sub>x</sub> Reduction Activity of a Silver Catalyst Under Real Diesel-Engine Exhaust Conditions. *SAE Paper*
- THOMAS, J. F., LEWIS, S. A., BUNTING, B. G., STOREY, J. M., GRAVES, R. L. & PARK, P. W. 2005. Hydrocarbon Selective Catalytic Reduction Using a Silver-Alumina Catalyst with Light Alcohols and Other Reductants. *SAE Paper*
- TREE, D. R. & SVENSSON, K. I. 2007. Soot processes in compression ignition engines. *Progress in Energy and Combustion Science*, 33, 272-309.
- TSOLAKIS, A. 2006. Effects on Particle Size Distribution from the Diesel Engine Operating on RME-Biodiesel with EGR. *Energy & Fuels*, 20, 1418-1424.

- TSOLAKIS, A., ABU-JRAI, A., THEINNOI, K., WYSZYNSKI, M. L., XU, H. M., MEGARITIS, A., CRACKNELL, R., GOLUNSKI, S. E. & PEUCHERET, S. M. 2007a. Exhaust gas fuel reforming for IC Engines using diesel type fuels. *SAE Paper*.
- TSOLAKIS, A. & GOLUNSKI, S. E. 2006. Sensitivity of process efficiency to reaction routes in exhaust-gas reforming of diesel fuel. *Chemical Engineering Journal*, 117, 131-136.
- TSOLAKIS, A. & MEGARITIS, A. 2004a. Catalytic exhaust gas fuel reforming for diesel engines - effects of water addition on hydrogen production and fuel conversion efficiency. *International Journal of Hydrogen Energy*, 29, 1409-1419.
- TSOLAKIS, A. & MEGARITIS, A. 2004b. Exhaust gas assisted reforming of rapeseed methyl ester for reduced exhaust emissions of CI engines. *Biomass and Bioenergy*, 27, 493-505.
- TSOLAKIS, A., MEGARITIS, A. & GOLUNSKI, S. E. 2005. Reaction Profiles during Exhaust-Assisted Reforming of Diesel Engine Fuels. *Energy & Fuels*, 19, 744-752.
- TSOLAKIS, A., MEGARITIS, A. & WYSZYNSKI, M. L. 2003. Application of Exhaust Gas Fuel Reforming in Compression Ignition Engines Fueled by Diesel and Biodiesel Fuel Mixtures. *Energy & Fuels*, 17, 1464-1473.
- TSOLAKIS, A., MEGARITIS, A. & WYSZYNSKI, M. L. 2004. Low temperature exhaust gas fuel reforming of diesel fuel. *Fuel*, 83, 1837-1845.
- TSOLAKIS, A., MEGARITIS, A., WYSZYNSKI, M. L. & THEINNOI, K. 2007b. Engine performance and emissions of a diesel engine operating on diesel-RME (rapeseed methyl ester) blends with EGR (exhaust gas recirculation). *Energy*, 32, 2072-2080.
- TSOLAKIS, A., TORBATI, R., MEGARITIS, A. & ABU-JRAI, A. 2009. Low-Load Dual-Fuel Compression Ignition (CI) Engine Operation with an On-Board Reformer and a Diesel Oxidation Catalyst: Effects on Engine Performance and Emissions. *Energy & Fuels*, 24, 302-308.
- URNS, S. R. 2000. *An Introduction to Combustion: Concepts and Applications*, McGraw-Hill Education.
- TWIGG, M. V. 2007. Progress and future challenges in controlling automotive exhaust gas emissions. *Applied Catalysis B: Environmental*, 70, 2-15.
- ULRICH, A. & WICHSER, A. 2003. Analysis of additive metals in fuel and emission aerosols of diesel vehicles with and without particle traps. *Analytical and Bioanalytical Chemistry*, 377, 71-81.
- VAARASLAHTI, K., RISTIMÄKI, J., VIRTANEN, A., KESKINEN, J., GIECHASKIEL, B. & SOLLA, A. 2006. Effect of Oxidation Catalysts on Diesel Soot Particles. *Environmental Science & Technology*, 40, 4776-4781.
- VARDE, K. S. & FRAME, G. A. 1983. Hydrogen aspiration in a direct injection type diesel engine-its effects on smoke and other engine performance parameters. *International Journal of Hydrogen Energy*, 8, 549-555.
- VERHELST, S. & WALLNER, T. 2009. Hydrogen-fueled internal combustion engines. *Progress in Energy and Combustion Science*, 35, 490-527.

- WAGNER, R. M., GREEN JR, J. B., STOREY, J. M. & DAW, C. S. 2000. Extending Exhaust Gas Recirculation Limits in Diesel Engines. *A&WMA 93rd Annual Conference and Exposition Salt Lake City, UT*.
- WEST, B., HUFF, S., PARKS, J., LEWIS, S., CHOI, J.-S., PARTRIDGE, W. & STOREY, J. 2004. Assessing Reductant Chemistry During In-Cylinder Regeneration of Diesel Lean NO<sub>x</sub> Traps. *SAE Paper*
- WESTBROOK, C. K., PITZ, W. J. & CURRAN, H. J. 2006. Chemical Kinetic Modeling Study of the Effects of Oxygenated Hydrocarbons on Soot Emissions from Diesel Engines. *Journal of Physical Chemistry A*, 110, 6912-6922.
- WHITTINGTON, B. I., JIANG, C. J. & TRIMM, D. L. 1995. Vehicle exhaust catalysis: I. The relative importance of catalytic oxidation, steam reforming and water-gas shift reactions. *Catalysis Today*, 26, 41-45.
- WICHTERLOVÁ, B., SAZAMA, P., BREEN, J. P., BURCH, R., HILL, C. J., CAPEK, L. & SOBALÍK, Z. 2005. An in situ UV-vis and FTIR spectroscopy study of the effect of H<sub>2</sub> and CO during the selective catalytic reduction of nitrogen oxides over a silver alumina catalyst. *Journal of Catalysis*, 235, 195-200.
- YAMAMOTO, K., OOHORI, S., YAMASHITA, H. & DAIDO, S. 2009. Simulation on soot deposition and combustion in diesel particulate filter. *Proceedings of the Combustion Institute*, 32, 1965-1972.
- YAMANE, K., UETA, A. & SHIMAMOTO, Y. 2001. Influence of physical and chemical properties of biodiesel fuels on injection, combustion and exhaust emission characteristics in a direct injection compression ignition engine. *International Journal of Engine Research*, 2, 249-261.
- YANG, H.-H., LEE, W.-J., MI, H.-H., WONG, C.-H. & CHEN, C.-B. 1998. PAH emissions influenced by Mn-based additive and turbocharging from a heavy-duty diesel engine. *Environment International*, 24, 389-403.
- YATES, M., MARTÍN, J. A., MARTÍN-LUENGO, M. Á., SUÁREZ, S. & BLANCO, J. 2005. N<sub>2</sub>O formation in the ammonia oxidation and in the SCR process with V<sub>2</sub>O<sub>5</sub>-WO<sub>3</sub> catalysts. *Catalysis Today*, 107-108, 120-125.
- YING, W., LONGBAO, Z. & HEWU, W. 2006. Diesel emission improvements by the use of oxygenated DME/diesel blend fuels. *Atmospheric Environment*, 40, 2313-2320.
- YOON, S., KANG, I. & BAE, J. 2008. Effects of ethylene on carbon formation in diesel autothermal reforming. *International Journal of Hydrogen Energy*, 33, 4780-4788.
- YORK, A. P. E., AHMADINEJAD, M., WATLING, T. C., WALKER, A. P., COX, J. P., GAST, J., BLAKEMAN, P. G. & ALLANSSON, R. 2007. Modeling of the Catalyzed Continuously Regenerating Diesel Particulate Filter (CCR-DPF) System: Model Development and Passive Regeneration Studies. *SAE Paper*
- YORK, A. P. E., TSOLAKIS, A., BUSCHOW, K. H. J., ROBERT, W. C., MERTON, C. F., BERNARD, I., EDWARD, J. K., SUBHASH, M. & PATRICK, V. 2010. Cleaner Vehicle Emissions. *Encyclopedia of Materials: Science and Technology*. Oxford: Elsevier.

- ZHANG, W. 2009. Automotive fuels from biomass via gasification. *Fuel Processing Technology*.
- ZHAO, H., HU, J. & LADOMMATOS, N. 2000. In-cylinder studies of the effects of CO<sub>2</sub> in exhaust gas recirculation on diesel combustion and emissions. *Proceedings of the Institution of Mechanical Engineers - Part D: Journal of Automobile Engineering*, 214, 405-419.
- ZHENG, M., READER, G. T. & HAWLEY, J. G. 2004. Diesel engine exhaust gas recirculation - a review on advanced and novel concepts. *Energy Conversion and Management*, 45, 883-900.
- ZUTTEL, A., REMHOF, A., BORGSCHULTE, A. & FRIEDRICHS, O. 2010. Hydrogen: the future energy carrier. *Philosophical Transactions of the Royal Society A*, 368, 3329-3342.

## APPENDICES

### Appendix A: Measuring Equipment Technical Data

**Table 18: Technical data for Horiba MEXA 7100 Analyser**

Species	Range	Resolution	Noise* (peak to peak width in 5min)
<b>CO</b>	Min. range 0 – 100ppm	1 ppm	± 1% FS
	Max. range 0 – 12% vol	0.01%	
<b>CO<sub>2</sub></b>	Min. range 0 – 5000ppm	1 ppm	± 1% FS
	Max. range 0 – 20% vol	0.01%	
<b>THC</b>	Min. range 0 – 10ppm C <sub>1</sub>	1 ppm	± 1% FS
	Max. range 0 – 50000ppm C <sub>1</sub>		
<b>O<sub>2</sub></b>	Min. range 0 – 5% vol	0.01%	± 1% FS for zero
	Max. range 0 – 25% vol		± 1.5% FS in measurement
<b>NO/NO<sub>x</sub></b>	Min. range 0 – 10ppm	1 ppm	< 20 ppm: ± 1.5% FS
	Max. range 0 – 10000ppm		> 20 ppm: ± 1.0% FS

**Table 19: Other technical data for Horiba MEXA 7100 Analyser**

Specification	Value*
<b>Zero/Span Drift</b>	Zero: ± 1% FS per 8hrs
	Span: ± 1% FS per 8hrs (ambient temp. fluctuation within ± 5°C)
<b>Linearity</b>	± 1% FS or 2% ind. val. (whichever is smaller)
<b>Repeatability</b>	± 0.5% FS

\* FS = Full Scale Measurement

Table 20: Measurements Specifications for MKS Type MultiGas Analyser

Specification	Comment
Gas Analyser	MKS MG-2030
Measurement Technique	FT-IR Spectroscopy
Range	Concentrations between high ppb and 100% full scale
Spectral Resolution	0.5-128cm <sup>-1</sup>
Scan Time/ Speed	1-300sec / 1 scans per sec @ 0.5cm <sup>-1</sup>
Gas Cell	MKS 5.11 Meter fixed pathlength heated cell
Detector	Infrared Analysis 0.25mm Liquid Nitrogen cooled MCT, digitally linearised
Pressure Transducer	± 1% uncertainty

Table 21: Technical data for Horiba MEXA 1230PM Real-time Analyser

Specification	Value*
Zero Noise (peak to peak width in 5 min)	Soot analyser: within 0.3mg/m <sup>3</sup> HFID: within 0.2ppC
Zero Drift	Soot analyser: within 0.3mg/m <sup>3</sup> per 8hrs HFID: within 0.2ppC per 8hrs
Linearity	± 1% FS
Repeatability	± 1% FS

\* FS = Full Scale Measurement

Table 22: Perkin Elmer Pyris 1 TGA Instrument Technical Data

Specification	Value
<b>Balance</b>	Tare: Reproducible to $\pm 2\mu\text{g}$
	Sensitivity: $0.1\mu\text{g}$
	Accuracy: Better than $0.02\%$
	Precision: $0.001\%$
<b>Standard Temperature Furnace</b>	Temperature Precision: $\pm 2^\circ\text{C}$

## Appendix B: Publications and Awards to Date

### Author Publications

1. **Gill, S.S.**; Chatha, G.S.; Tsolakis, A., Analysis of reformed EGR on the performance of a diesel particulate filter. *International Journal of Hydrogen Energy* 2011, 36, (16), 10089-10099.
2. **Gill, S.S.**; Tsolakis, A.; Dearn, K.D.; Rodríguez-Fernández, J., Combustion characteristics and emissions of Fischer-Tropsch diesel fuels in IC engines. *Progress in Energy and Combustion Science* 2011, 37, (4), 503-523.
3. **Gill, S.S.**; Turner, D.; Tsolakis, A.; York, A.P.E., Understanding the Role of Filtered EGR on PM Emissions. *JSAE Technical Paper No. 20119248*.
4. **Gill, S.S.**; Tsolakis, A.; Herreros, J.M.; York, A.P.E., Diesel emissions improvements through the use of biodiesel or oxygenated blending components. *Fuel* 2012, 95, 578-586.
5. **Gill, S.S.**; Chatha, G.S.; Tsolakis, A.; Golunski, S.E.; York, A.P.E., Assessing the effects of partially decarbonising a diesel engine by co-fuelling with dissociated ammonia. *International Journal of Hydrogen Energy* 2012, 37, (7), 6074-6083.

6. **Gill, S.S.**; Turner, D.; Tsolakis, A.; York, A.P.E., Controlling Soot Formation with Filtered EGR for Diesel and Biodiesel Fuelled Engines. *Environmental Science & Technology* 2012, 46, (7), 4215-4222.
7. Chong, J.J.; Tsolakis, A.; **Gill, S.S.**; Theinnoi, K.; Golunski, S.E., Enhancing the NO<sub>2</sub>/NO<sub>x</sub> ratio in compression ignition engines by hydrogen and reformat combustion, for improved aftertreatment performance. *International Journal of Hydrogen Energy* 2010, 35, (16), 8723-8732.
8. Theinnoi, K.; **Gill, S.S.**; Tsolakis, A.; Wyszynski, M.L.; Megaritis, A.; Yang, C.; Harrison, R., Fuel Efficient, Continuously Regenerating Diesel Particulate Filter with On-board Hydrogen Production: Towards a Fuel Reformer – Diesel Engine Aftertreatment System. FISITA 2010 World Automotive Congress, Paper F2010-A-125.
9. Theinnoi, K.; **Gill, S.S.**; Tsolakis, A.; York, A .P. E.; Megaritis, A.; Harrison, R. M., Diesel Particulate Filter Regeneration Strategies: Study of Hydrogen Addition on Biodiesel Fuelled Engines. *Energy & Fuels* 2012, 26, (2), 1192-1201.

### **Awards**

- University Postgraduate School Scholarship (Mechanical Engineering) 2009-2012
- Guest, Keen and Nettlefolds Postgraduate Scholarship 2010
- Austin Rover Prize 2010
- Joseph Chamberlain Postgraduate Scholarship 2010-11
- Ratcliffe Prize 2011
- Hufton PG Scholarship 2011
- Joseph Chamberlain Postgraduate Scholarship 2011-12
- David Brewster Cobb Prize 2011
- Dudley Docker Research Scholarship 2012